EPA

ESTIMATION OF SEASONAL AND ANNUAL ACIDIC DEPO
THROUGH AGGREGATION OF THREE-DAY EPISODIC PE

by

Perry J. Samson, Jeffrey R. Brook and Sanford Sillman
Department of Atmospheric, Oceanic and Space Sciences
University of Michigan
Ann Arbor, Michigan 48109-2143

EPA Cooperative Agreement CR-814854-01

Project Officer

John F. Clarke
Atmospheric Sciences Modeling Division
Atmospheric Research and Exposure Assessment Lab
Research Triangle Park, North Carolina 27709

ATMOSPHERIC RESEARCH AND EXPOSURE ASSESSMENT LAB
OFFICE OF RESEARCH AND DEVELOPMENT
U.S. ENVIRONMENTAL PROTECTION AGENCY
RESEARCH TRIANGLE PARK, NORTH CAROLINA 27709

DISCLAIMER

The information in this document has been funded wholly or in part by the U.S. Environmental Protection Agency under Cooperative Agreement CR-814854-01 to the Department of Atmospheric, Oceanic and Space Sciences, University of Michigan, Ann Arbor, Michigan. It has been subjected to Agency peer and administrative review, and has been approved for publication as an EPA document.

ABSTRACT

The Regional Acid Deposition Model (RADM) simulates the complex physical and chemical processes involved in the formation of acidic deposition. However, because of the complexity of RADM it has only been applied to selected episodes of a few days duration. While the detail provided by RADM is highly desirable to understand the interactions between emissions and deposition on a storm-by-storm basis there is also a need for understanding the probable long-term relationship between changing emissions patterns and deposition. The cost of simulating and interpreting seasonal or annual deposition patterns using RADM directly would be high.

A method for aggregating episodic deposition estimates has been developed and used to identify which meteorological situations merit simulation by RADM based on their likelihood of producing sulfate ($SO_4^=$) wet deposition at multiple locations across eastern North America, their frequency of occurrence, and their seasonality. The aggregation approach is based on four years (1982-1985) of meteorological and precipitation chemistry data.

The aggregation approach is based on the stratification of three-day periods into categories of similar 850 mb wind flow across eastern North America and subsequent selection of 30 RADM simulation periods from this stratification which represent the range pf storm patterns present over eastern North America. The program has also provided the RADM project with scaling factors for use in weighing episodic simulation results to seasonal and annual deposition. The approach is shown to improve upon the use of a random selection process in reproducing seasonal and annual wet deposition patterns.

CONTENTS

SECTION PAGE

DISCLAIMER ii

ABSTRACT iii

LIST OF FIGURES viii

LIST OF TABLES xv

EXECUTIVE SUMMARY xvii

1. INTRODUCTION 1

1.1 Goals and Purposes 1

1.2 History 2

1.3 Conceptual Approach 3

2. METHODS 6

2.1 Aggregation Approach 6

2.1.1 Meteorological Stratification 6

2.1.2 Selection of Stratification Parameters 8

2.1.3 Categorization for Other Years 10

2.1.4 Aggregation Procedures 10

2.1.5 Selection Process 13

2.1.6 Source/Receptor Relationships 15

2.1.6.1 Trajectory Calculations 15

2.1.6.2 Quantitative Transport Analysis 16

2.1.6.3 The Potential Source Contribution Function 18

2.2 Description of Data Base 19

2.2.1 Meteorological Data 19

2.2.2 Precipitation Chemistry Data 20

SECTION PAGE

2.3 Testing 24

2.3.1 Aggregation Versus Random Selection 24

2.3.2 Statistical Regression 25

2.3.3 Source-Receptor Relationships 27

3. RESULTS 29

3.1 Meteorological Categories 29

3.1.1 Choice of Stratification Parameters 29

3.1.2 Description of Categories 30

3.1.2.1 Wind Flow Patterns 31

3.1.2.2 Deposition Patterns 36

3.1.3 Statistical correlations between category and observed deposition 51

3.1.3.1 Three alternative statistical approaches 51

3.1.3.2 Time-of-Year Term 52

3.1.3.3 Results 53

3.1.4 Interannual variability 60

3.1.5 Evaluation of the category-based aggregation method 67

3.2 Selection of Cases 69

3.3 Comparison of Aggregate Estimate with Long-Term Deposition 70

3.3.1 Annual Wet Deposition 70

3.3.1.1 Sulfate Wet Deposition 71

3.3.1.2 Nitrate Wet Deposition 74

3.3.1.3 Acidity Wet Deposition 77

3.3.2 Seasonal Wet Deposition 77

3.3.2.1 Sulfate Wet Deposition 77

3.3.2.2 Nitrate Wet Deposition 77

3.3.2.3 Acidity Wet Deposition 88

3.3.3 Uncertainties in the Aggregate Estimates 88

3.4 Source-Receptor Relationships 99

3.4.1 Climatological Wind Flow Patterns during Precipitation 99

3.4.2 Wind Flow Associated with Sulfate Wet Deposition 100

3.4.3 Potential Source Contribution Functions 107

SECTION PAGE

3.5 The Variation in Source-Receptor Relationships between Categories 112

3.6 Selecting episodes to estimate source-receptor relationships 125

3.7 Source-receptor relationships with the 30 episodes 128

4. SUMMARY 138

4.1 Accomplishments 138

4.2 Recommendations for Future Work 139

4.2.1 Evaluation of the 30 Episodes and the Meteorological Categories 139

4.2.1.1 Source-Receptor Relationships 140

4.2.1.2 Chemical and Meteorological Behavior of the Categories 140

4.2.2 Application of aggregation to other atmospheric phenomena 141

4.2.2.1 Dry Deposition 141

4.2.2.2 Visibility 142

4.2.3 Quantification of Aggregation Sensitivity 143

5. REFERENCES 144

APPENDIX A: MEAN 850 MB WIND FLOW PATTERNS FOR THE 19 CATEGORIES ..... A - 1

APPENDIX B: 85TH PERCENTILE WET SULFATE DEPOSITION PLOTS FOR THE 19 CATEGORIES ..... B - 1

APPENDIX C: SITE SPECIFIC TABLES OF TOTAL AND PERCENT OF TOTAL WET SULFATE DEPOSITION ..... C - 1

APPENDIX D: SITE SPECIFIC TABLES OF TOTAL AND PERCENT OF TOTAL PRECIPITATION ..... D - 1

LIST OF FIGURES

NUMBER		PAGE
1	Illustration of the aggregation concept.	5
2	NMC grid and subset of 48 grid points used to describe similar meteorological patterns.	7
3	Location of the precipitation chemistry sites in the United States and Canada used for analysis of transport patterns.	21
4	Beale and Calinsky criteria (*F* and *C* statistics) versus the number of categories (step number), based on 850 mb wind field clusters and observed $SO_4^=$ deposition for 1983.	31
5	Reduction in variance in $SO_4^=$ wet deposition resulting from meteorological stratification.	32
6	Comparison of frequency of occurrence of the 19 meteorological categories defined in this study between 1979-1981 and 1982-1985.	35
7a-f	Monthly mean number of occurrences of meteorological categories during 1982 to 1985.	38
8a-d	Variation in amount of $SO_4^=$ deposition between categories at four locations	41
9	The ratio of the percent of $SO_4^=$ deposition to the percent of precipitation for each meteorological category.	43
10	The percentage of total $SO_4^=$ wet deposition associated with each meteorological category by site.	47
11	Cumulative explanation of total sulfate deposition using categories ranked from greatest to least deposition	49
12	T_s statistic for meteorological category 6, indicating deposition-to-precipitation ratios significantly above or below the norm at each site.	57

NUMBER PAGE

13 T_s statistic for meteorological category 7, indicating deposition-to-precipitation ratios significantly above or below the norm at each site. 58

14 T_s statistic for meteorological category 11, indicating deposition-to-precipitation ratios significantly above or below the norm at each site. 59

15 Year-by-year variation in sulfate wet deposition, nitrate deposition, sulfate deposition-to-precipitation ratio, and precipitation at Turners Falls, Massachusetts. 62

16 Year-by-year variation in sulfate wet deposition, nitrate deposition, sulfate deposition-to-precipitation ratio, and precipitation at Zanesville, Ohio. 63

17 Year-by-year variation in sulfate wet deposition, nitrate deposition, sulfate deposition-to-precipitation ratio, and precipitation at Giles County, Tennessee. 64

18 Year-by-year frequency of occurrence of events of meteorological categories 6, 7 and 11, expressed as a fraction of all events. 65

19 Comparison between annual sulfate deposition observed during 1986 and 1987 at 13 northeastern and midwestern sites with projected deposition based on 1982-1985 observations and 1986-1987 meteorology 66

20 Comparison of selection and aggregation techniques for $SO_4^=$ wet deposition in northeastern North America.using nineteen three-day episodes. 68

21a The mean annual wet sulfate deposition pattern across eastern North America for 1982-1985. (Units=mgm^{-2}). 72

21b The aggregate estimate of the mean annual wet sulfate deposition pattern across eastern North America for 1982-1985. 73

22a The mean annual wet nitrate deposition pattern across eastern North America for 1982-1985. 75

22b The aggregate estimate of the mean annual wet nitrate deposition pattern across eastern North America for 1982-1985. 76

NUMBER PAGE

23a The mean annual acidic wet deposition pattern across eastern North America for 1982-1985. 78

23b The aggregate estimate of the mean annual acidic wet deposition pattern across eastern North America for 1982-1985. 79

24a The mean summer wet sulfate deposition pattern across eastern North America for 1982-1985. 80

24b The aggregate estimate of the mean summer wet sulfate deposition pattern across eastern North America for 1982-1985. 81

24c The mean winter wet sulfate deposition pattern across eastern North America for 1982-1985. 82

24d The aggregate estimate of the mean winter wet sulfate deposition pattern across eastern North America for 1982-1985. 83

25a The mean summer wet nitrate deposition pattern across eastern North America for 1982-1985. 84

25b The aggregate estimate of the mean summer wet nitrate deposition pattern across eastern North America for 1982-1985. 85

25c The mean winter wet nitrate deposition pattern across eastern North America for 1982-1985. 86

25d The aggregate estimate of the mean winter wet nitrate deposition pattern across eastern North America for 1982-1985. 87

26a The mean summer wet acid (H^+) deposition pattern across eastern North America for 1982-1985. 89

26b The aggregate estimate of the mean summer wet acid (H^+) deposition pattern across eastern North America for 1982-1985. 90

26c The mean winter wet acid (H^+) deposition pattern across eastern North America for 1982-1985. 91

26d The aggregate estimate of the mean winter wet acid (H^+) deposition pattern across eastern North America for 1982-1985. 92

27 The spatial and temporal variation in the percent of annual wet sulfate deposition due to the categories selected 93

NUMBER PAGE

28 The year to year variability in the annual wet sulfate deposition and in the total deposition due to the categories selected at two Midwestern sites 94

29 The year to year variability in the annual wet sulfate deposition and in the total deposition due to the categories selected at two northeastern sites 95

30 Uncertainty ranges due to the aggregate estimates of wet sulfate deposition 97

31 Uncertainty ranges due to the aggregate estimates of wet nitrate deposition 98

32 Uncertainty ranges due to the aggregate estimates of wet acidity deposition 98

33 The mean probability for transport on precipitation days to Big Moose, NY, during the period 1982-1985. 101

34 The mean probability for transport on precipitation days to Gaylord, MI, during the period 1982-1985. 102

35 The mean probability for transport on precipitation days to Raleigh, NC, during the period 1982-1985 103

36 The sulfur deposition weighted probability for transport to Big Moose, NY during the period 1982-1985. 104

37 The sulfur deposition weighted probability for transport to Gaylord, MI, during the period 1982-1985. 105

38 The sulfur deposition weighted probability for transport to Raleigh, NC, during the period 1982-1985 106

39 The bias for transport associated with large $SO_4^=$ wet deposition at Big Moose, NY, during the period 1982-1985. 108

40 The bias for transport associated with large water deposition at Big Moose, NY, during the period 1982-1985. 109

41 The bias for transport associated with large $SO_4^=$ wet deposition at Gaylord, MI, during the period 1982-1985. 110

42 The bias for transport associated with large water deposition at Gaylord, MI, during the period 1982-1985. 111

NUMBER PAGE

43 The bias for transport associated with large $SO_4^=$ wet deposition at Raleigh, NC, during the period 1982-1985. 112

44 The bias for transport associated with large water deposition at Raleigh, NC, during the period 1982-1985. 113

45 The ensemble bias for transport associated with large $SO_4^=$ wet deposition at Big Moose, NY; Gaylord, MI; and Raleigh, NC, during the period 1982-1985. 114

46 Difference between climatological Q field (1982-1985) and the Q field for category 20 (unbiased set of missing days).....115

47 Difference between climatological Q field (1982-1985) and the Q field for category 1. 116

48 Difference between climatological Q field (1982-1985) and the Q field for category 5. 117

49 Difference between climatological Q field (1982-1985) and the Q field for category 6. 118

50 Difference between climatological Q field (1982-1985) and the Q field for category 7. 119

51 Difference between climatological Q field (1982-1985) and the Q field for category 8. 120

52 Difference between climatological Q field (1982-1985) and the Q field for category 9. 121

53 Difference between climatological Q field (1982-1985) and the Q field for category 10. 122

54 Difference between climatological Q field (1982-1985) and the Q field for category 11. 123

55 Percent RMS errors, ranked from smallest to largest, for the random and category-based ensembles using trajectories from all days in 30 episode sample.....127

56 Percent RMS errors, ranked from smallest to largest, for the random and category-based ensembles using trajectories from precipitating days only in 30 episode sample. 127

NUMBER PAGE

57 The Q field for Big Moose, NY derived from both precipitating and non-precipitating days within the 30 episodes....129

58 The Q field for Gaylord, MI derived from both precipitating and non-precipitating days within the 30 episodes....130

59 The Q field for Raleigh, NC derived from both precipitating and non-precipitating days within the 30 episodes....131

60 Bias in source receptor analysis resulting from use of 30-event sample instead of 4-year sample at Big Moose, NY. Bias is expressed as a percent of predicted Q-field from the 4-year analysis. Both precipitating and non-precipitating days during the 30 episodes are included in the analysis....132

61 Bias in source receptor analysis resulting from use of 30-event sample instead of 4-year sample at Gaylord, MI. Bias is expressed as a percent of predicted Q-field from the 4-year analysis. Both precipitating and non-precipitating days during the 30 episodes are included in the analysis....133

62 Bias in source receptor analysis resulting from use of 30-event sample instead of 4-year sample at Raleigh, NC. Bias is expressed as a percent of predicted Q-field from the 4-year analysis. Both precipitating and non-precipitating days during the 30 episodes are included in the analysis....134

63 Bias in source receptor analysis resulting from use of 30-event sample instead of 4-year sample at Big Moose, NY. Bias is expressed as a percent of predicted Q-field from the 4-year analysis. Only days with precipitation reported at Big Moose are included in the analysis....135

64 Bias in source receptor analysis resulting from use of 30-event sample instead of 4-year sample at Gaylord, MI. Bias is expressed as a percent of predicted Q-field from the 4-year analysis. Only days with precipitation reported at Big Moose are included in the analysis....136

NUMBER PAGE

65 Bias in source receptor analysis resulting from use of 30-event sample instead of 4-year sample at Raleigh, NC. Bias is expressed as a percent of predicted Q-field from the 4-year analysis. Only days with precipitation reported at Big Moose are included in the analysis 137

LIST OF TABLES

NUMBER		PAGE
1	Sample aggregation	12
2	Name and location of the daily (event) precipitation chemistry sites	22
3	Meteorological factors used in initial cluster analysis	29
4	Synoptic description of the nineteen 850 mb wind flow categories	33
5	Matrix of percent of total deposition by site and category	45
6	Percent of total sulfate wet deposition by meteorological category	50
7	Results of statistical regression	55
8	Initial selection of 30 days	71
9	Root-mean-square deviations between estimated and observed summer, winter and annual wet deposition at 13 eastern sites	74
10	Description of source-receptor relationships for selected meteorological categories	124

EXECUTIVE SUMMARY

This report presents methods for developing estimates for long-term (climatological) patterns of atmospheric wet deposition based on in-depth knowledge of a finite number of samples. These methods are designed to complement predictive models for physical processes in the atmosphere, which characteristically provide detailed analysis for a small number of days but are unable to represent physical processes on a multi-year time scale due to computational constraints. Predicted future effects are to be derived based on statistical methods of aggregation developed here, in combination with results obtained from physical models. The method has been applied to the specific problem of estimating future rates of wet deposition in the eastern United States in combination with the Regional Acid Deposition Model (RADM).

The method is based upon the stratification of three-day periods into categories of similar wind flow at 850 mb (roughly 1500 meters above mean sea level). The stratification has been used to identify which meteorological situations merit simulation by RADM based on their likelihood of producing sulfate deposition at multiple locations across eastern North America, their frequency of occurrence, and their seasonality. A specific ensemble of 3-day events has been recommended for future analysis by RADM, as part of ongoing efforts by the Environmental Protection Agency (EPA) to develop predictive methods for air quality. In addition to event selection, the meteorological stratification has been used as the basis of a statistical technique to derive aggregate estimates for long-term average wet deposition. The aggregation technique has been simulated using four years of precipitation chemistry data to demonstrate that uncertainties in estimates of seasonal and annual sulfur deposition using the aggregation technique is significantly less than those obtained from random (non-stratified) sampling of the data.

The following specific tasks have been completed as part of this project:

(1) An extensive data base with daily precipitation and wet deposition of sulfate, nitrate and total H^+ was developed. The data base covered the years 1982-1985 and included 23 sites in the northeastern, southern and midwestern U.S. and southern Canada. Meteorological information to be used in subsequent analysis was also collected.

(2) Techniques of cluster analysis were used to stratify 3-day events over the 4-year period into categories based on the meteorological data described above. Four independent stratification schemes were investigated: stratification by 850 mb wind field, stratification by 850 mb geopotential and mean surface pressure, stratification by 850 mb temperature advection and 500 mb vorticity, and stratification by 500 mb vorticity advection and 850 mb relative humidity. These four stratification schemes were evaluated to find the combination of meteorological parameters which best explained variations in sulfur wet deposition.

(3) A set of 19 meteorological categories was compiled based on similarity in wind flow at 850 mb. These 19 categories were each subdivided into "wet" and "dry" cases, making 38 categories. These 38 categories were used as the basis for selection of individual days and derivation of aggregated estimates for annual deposition.

(4) A statistical correlation has been developed between observed sulfate and nitrate wet deposition during 1982 through 1987 and wind flow category. Results show that wet deposition rates over eastern North America show significant differences for events with different 850 mb circulation.

(5) Accuracy and validity of the 38-category stratification was evaluated based on the ability to predict annual sulfate deposition at eastern and midwestern sites from a finite sample of 3-day events. We compared estimates for annual deposition derived from a random sample of 3-day events with estimates from a cluster-based sample of events. The standard deviation between estimated and actual deposition was lower by 25% with cluster-based selection.

(6) A preliminary selection of 30 individual 3-day events for in-depth study with RADM was made. The selected events included representatives of a wide variety of circulation patterns, including meteorological categories that account for the bulk of wet deposition at sites throughout the eastern U.S. A selection of relatively rare winter circulation patterns and events without rainfall for evaluation of dry deposition are also included. Aggregate estimates for sulfate and nitrate wet deposition have been derived based on the 30-event sample. Deviations between the aggregate estimate and observed wet deposition during 1982-1985 are of the same magnitude as the natural variation in wet deposition from one year to the next.

(7) A simplified model for identifying emitted sources of wet deposition has been applied to the selected 30-event sample and also to the entire 1982-1985 period for selected sites in eastern North America. Differences between predicted source-receptor relationships based on the 30-event sample and based on the entire 4-year period are assessed.

1. INTRODUCTION

1.1. GOALS AND PURPOSES

The development of policies to address problems arising from acid deposition requires a thorough understanding of processes that affect acid deposition. To this end the United States Environmental Protection Agency (EPA) has supported investigations into the physics, chemistry and meteorology of acid deposition. These efforts have culminated in the development of the Regional Acid Deposition Model (RADM) (Chang et al., 1987), which simulates the processes involved in the formation of acid deposition and other pollutants.

In order to complete the evaluation of acid deposition processes it is necessary to establish a relationship between individual deposition events and the long-term climatology of acid deposition. The relationship between individual events and climatology is difficult because deposition varies greatly from one event to the next in terms of both the amount of deposition and the relation between deposition and emission sources. Establishment of long-term deposition patterns and source-receptor relationships requires analysis over an extended time period, preferably including several years to account for meteorological variability. Such a lengthy analysis is beyond the capacity of the resources available to the National Acid Precipitation Assessment Program.

The goal of this study has been to provide methods for representing aggregate long-term patterns of acid deposition from a finite number of samples. These methods involve both the selection of individual deposition events which are representative of recurring climatic patterns and the calculation of climatic averages based on a finite sample. The aggregation methods have been applied to the specific problem of representing the climatology of acid deposition based on in-depth analysis by RADM for a finite sample of events. An array of 30 three-day events has been identified which includes the major climatic patterns that contribute to acid deposition over eastern North America. RADM is currently being used to analyze physical processes during these 30 events. Assessment of the impact of future changes in precursor emissions will be performed by (1) using RADM to predict impacts for the thirty sample events, and (2) estimating long-term impacts by aggregating from the 30 sample events, based on the techniques described in this report. While designed specifically in support of RADM the methods described here may have broad applicability to problems that involve the characterization of long-term climatic impacts of human activities.

Identification of representative deposition events and methods of aggregation are based on

meteorological and statistical analyses of deposition events that occurred over a 4-year period (1982-1985). Events during this period were divided into categories with similar three-day patterns of 850 mb wind flow across eastern North America. The three-day time period and 850 mb wind fields are broadly representative of the evolution of distinctive storm patterns that are likely to affect atmospheric transport and deposition rates. Events have been selected for analysis by RADM from among the meteorological strata based on their likelihood of producing sulfate ($SO_4^=$) wet deposition at multiple locations across eastern North America, their frequency of occurrence, and their seasonality.

The method developed here represents a significant improvement over the alternative of selecting events for RADM analysis purely at random. Analysis of observed wet deposition during the 1982-1985 time period shows that deposition rates are statistically correlated with meteorological category with greater than 95% confidence at most sites in eastern North America. The aggregation technique has been used to obtain estimates for annual deposition at 21 sites in eastern North America based solely on observed deposition during the selected 30-day ensemble. The resulting estimates differ from the observed 4-year average wet deposition by amounts comparable to normal year-to-year variations. Aggregated estimates based on meteorological strata are also significantly more accurate than estimates from randomly selected events.

The aggregation project has served two purposes:

1. to provide the RADM project with a list of simulation periods which represent the range of storm patterns present over eastern North America. The selection of storm types was based on their likelihood of producing $SO_4^=$ wet deposition at multiple locations across eastern North America, their frequency of occurrence, and their seasonality; and

2. to provide the RADM project with scaling factors for use in weighing episodic simulation results to seasonal and annual deposition.

1.2. HISTORY

The use of synoptic climatological methods (meteorological stratification) to identify homogeneous weather types is a popular tool for use in studying climate-environment relationships. Kalkstein and Corrigan (1986) presented a methodology to characterize air masses at a given locale using principal component analysis to reduce the dimensionality of surface weather variables followed by cluster analysis on the most important components. The means of the original variables and other parameters were determined for each category and a physical explanation was attached to the results. Kalkstein, *et al.* (1987) refined the method and demonstrated it for two other sites. Samson and Moody (1986, see also Moody and Samson,

1989) used cluster analysis to stratify deposition events at a single location based upon back-trajectories. The concentrations of $SO_4^=$, NO_3^-, NH_3^+ and H^+ in precipitation were found to be statistically different between strata but there was also a considerable amount of within strata variation and overlap between strata. Moody and Galloway (1988) studied the influence of atmospheric flow patterns (isobaric back-trajectories) on the precipitation chemistry at Bermuda. They identified the important wind flow categories for both warm and cold seasons and concluded that transport was an important but not sole factor influencing the composition of precipitation.

Initially this project attempted to cluster patterns of precipitation across eastern North America. The stochastic nature of daily precipitation patterns lead to the production of categories which, in essence, represented the days when a particular station dominated the precipitation of the region. This course was abandoned in favor of a categorization scheme based on wind flow patterns.

Fernau (1988) categorized three-day periods of the vectors of trajectories at precipitation chemistry locations in the United States and Canada. These categories were shown to resemble meteorological patterns common to eastern North America. Eighteen categories of three-day wind flow patterns were found using cluster analysis. These categories represented periods whose mean three-day atmospheric transport patterns were statistically different from one another. Fernau (1988) also showed that the behavior of $SO_4^=$ wet deposition varied between these categories and that the differences held statistical significance. Nonetheless, there was concern that the results may have been influenced by the lack of rawinsonde observations over the Atlantic Ocean. It was therefore decided that the analysis should switch to use of the National Meteorological Center (NMC) global meteorological data base which included analyzed meteorological information at selected pressure surfaces over all of the Northern Hemisphere.

1.3. CONCEPTUAL APPROACH

The aggregation technique is based on the hypothesis that there are recurring weather patterns which can be characterized and described in terms of observable meteorological parameters (wind fields, precipitation, etc.). It is further hypothesized that distinct weather patterns will be associated with characteristic patterns of wet deposition, both in terms of spatial extent and deposition amounts. Given those assumptions, long-term wet deposition processes may be analyzed based on a finite number of individual deposition events, each of which is "representative" of a major meteorological category. The goal of the aggregation project has been to identify the degree to which weather patterns may be separated into identifiable categories and to assess how this information would improve our ability to extrapolate case study results to longer-term deposition estimates.

The initial stratification of events into meteorological categories is used both in the selection of individual events for in-depth analysis with RADM and in the calculation of aggregated estimates for total wet deposition from 30-event samples. Event selection has been designed to include representatives from all major meteorological categories and to insure that the selected ensemble includes events with significant wet deposition at sites throughout eastern North America. Estimates for long-term deposition are derived from known deposition rates (either from observations or from RADM analyses) for the 30-event sample. The aggregation concept, illustrated in Figure 1, represents long-term deposition as the sum of deposition from sample events weighted by the frequency of occurrence of each meteorological category. The aggregation technique has subsequently been modified to make use of statistical correlations between wet deposition, category and other meteorological parameters (precipitation, season, etc.) in deriving estimates for long-term deposition.

Testing the aggregation technique poses a special problem because the most important issue, response of the method to changes in precursor emission rates, cannot be tested empirically. A variety of techniques have been used to explore aggregation accuracy. These include the establishment of statistical correlations between observed wet deposition, wind flow pattern and other meteorological variables and application of the aggregation technique to arrays of randomly selected events. Discrepancies between aggregate estimates and observed deposition are compared to the natural uncertainty arising from year-to-year variation in wet deposition. Lastly, an abbreviated model for source-receptor relationships is used to identify similarities and differences between randomly selected 30-day ensembles and long-term averages. These combined tests should establish both the level of accuracy and limitations of the aggregation technique.

The presentation is divided into a discussion of methods (Section 2) and presentation of results (Section 3). The discussion of methods includes a description of the meteorological stratification technique, procedures for deriving aggregated estimates based on finite samples, selection of sample events based on the meteorological stratification, and methods used to test the aggregation procedure. A description of the simplified model for source-receptor relationships is also included. Results of the analysis are presented in Section 3. These include meteorological descriptions of individual wind flow categories, results of statistical correlations between wind flow and observed wet deposition, selection and identification of thirty 3-day events for RADM analysis, and aggregated estimates for wet deposition and source receptor relationships based on the chosen sample.

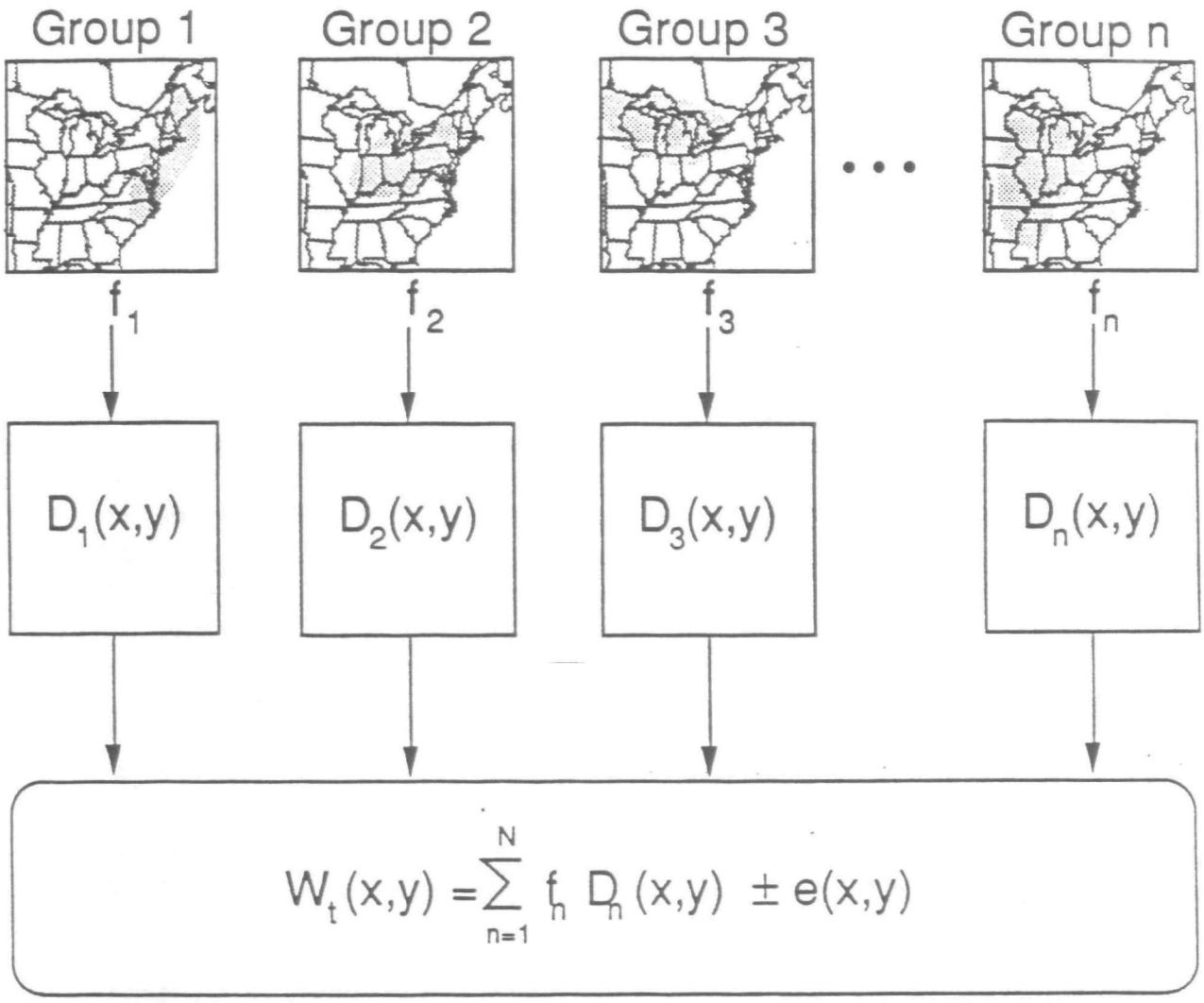

Figure 1. Illustration of the aggregation concept. Each meteorological category occurs with some mean frequency, f_n, and has associated with it a mean deposition pattern $D_n(x,y)$. These are aggregated through a weighting scheme (though not necessarily the simple frequency weighting shown) to achieve an estimate of the spatial pattern of deposition, $W_t(x,y)$ with an uncertainty $e(x,y)$ which includes variability in frequency and deposition patterns from year-to-year. The goal is to estimate $W_t(x,y)$ accurately and keep $e(x,y)$ less than the observed magnitude of interannual variation in deposition.

2. METHODS

2.1. AGGREGATION APPROACH

2.1.1. Meteorological Stratification

The method for selection of representative 3-day deposition events is based on a stratification scheme that classifies all events into categories based on meteorology. The purpose of the meteorological stratification is to systematically identify the different types of storm patterns that contribute to acid deposition in the eastern United States. Category-based selection will then insure that all major storm types are included in the ensemble of representative events. Stratification schemes were attempted based on a variety of meteorological parameters, including sea level pressure, temperature, 850 millibar geopotential height, vorticity advection and wind fields.

To portray the "life-cycle" of a typical eastern North American "storm" the duration of RADM simulations has generally been on the order of three days (not counting initialization days). To allow compatibility with RADM the categories have been based on three-day periods. This necessitated re-organizing the meteorological data into running three-day periods (record one = days 1, 2, 3; record two = days 2, 3, 4; etc.) prior to stratification.

For purposes of categorization each three-day event is evaluated based on the values assumed by 2 independent meteorological parameters over the three-day period on a 48-point horizontal grid covering eastern North America. Each three-day event is characterized by an array of 288 parameters, which consist of the values of the 2 independent parameters on 3 successive days at 48 grid points. Location of grid points is shown in Figure 2. The 288 parameters represent the maximum number of parameters that could be included in the meteorological stratification, given computational constraints. The choice of 48 grid points and two independent parameters were dictated by this constraint.

Classifying all of the running three-day periods into similar meteorological categories required computer assistance. The statistical method of cluster analysis was selected for this purpose. Ideally the data from the entire time period should have been clustered together, however, due to the computer memory constraints of the statistical software used this was not possible. To circumvent this limitation, consecutive periods (record 1 = days 1,2,3; record 2 = days 4,5,6; etc.) from independent years were selected. It was anticipated that this would

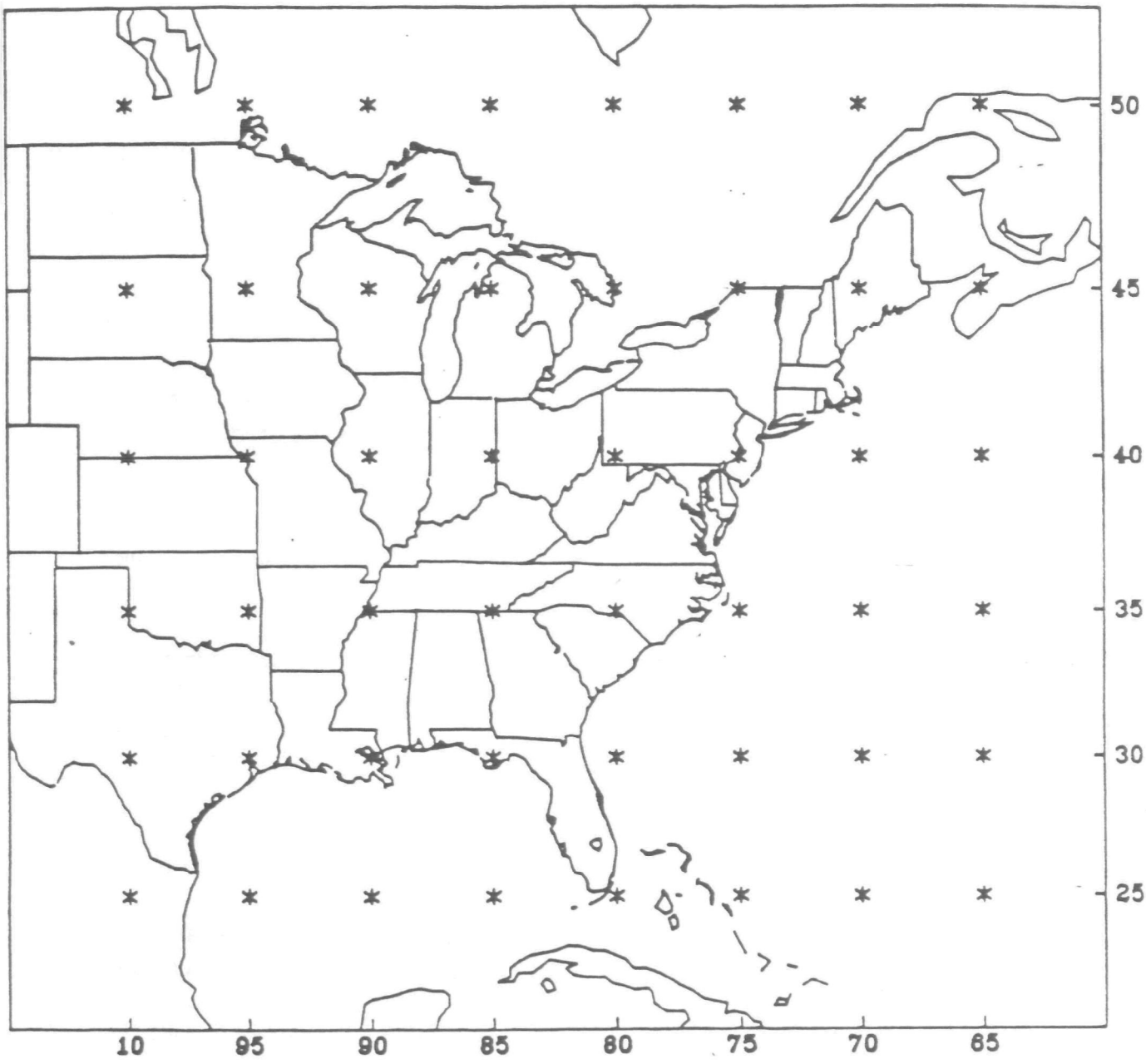

Figure 2. NMC grid and subset of 48 grid points used to describe similar meteorological patterns.

minimize the effect of missing data and capture a broader cross-section of situations. Additionally, the limitation on computer memory allowed only the use of three years of data. Due to this limitation the cluster analysis was used to generate meteorological categories based on the years 1979, 1981 and 1983 only.

Ward's method of cluster analysis (Ward, 1963) was selected to stratify the reduced set of cases. The goal of Ward's method, as with other cluster analysis techniques, is to divide a data set into categories consisting of similar cases that are as distinct from the other categories as possible. Evaluation of similarity between events is based on the euclidean distance between events for a specified array of parameters, defined as

$$x_{AB} = \sqrt{\frac{1}{n}\sum_{j=1}^{n} [P_{Aj} - P_{Bj}]^2} \qquad (1)$$

where x_{AB} is the euclidean distance between points A and B and P_{Aj} and P_{Bj}. represent the value of the jth parameter for events A and B respectively. Euclidean distances are used to compare both individual events and category means in Ward's method.

Identification of individual categories follows a hierarchical sequence beginning with a case in which each individual event is regarded as a separate category. Successive categorization schemes are then generated, with the total number of categories reduced by one at each stage. Category selection is performed in a manner to minimize the *cluster variance* , or within-group sum of squares (E). The cluster variance is the sum of squared Euclidean distances from each data point to the centroid (mean) for its assigned category, with distance defined in Equation (1). Cluster variance provides a measure of the degree of similarity within each category in terms of the selected meteorological parameters. The minimal-variance criterion insures that events within the same category are most similar to each other.

2.1.2. Selection of Stratification Parameters

Stratification based on Ward's method generates optimal categorization schemes for the specified base of meteorological parameters and for the specified number of categories. Completion of the stratification process requires selection of the appropriate number of parameters and number of categories. A large number of individual categories permits finer distinctions between meteorological events, but a large number of categories becomes unwieldy and lacks statistical robustness.

As discussed by Anderberg (1973, p. 194 and 212) evaluation of clustering may be based on its effectiveness in distinguishing an external variable, rather than the parameters that formed the basis of the initial stratification. In this instance, generation of meteorological strata is based on the meteorological parameters discussed in the preceding section. However the evaluation of the proper number of categories is based on the ability of the strata to distinguish between events with high and low $SO_4^=$ wet deposition.

Observed $SO_4^=$ deposition is available from 21 sites (See Section 2.2 below). Deposition-based differences between events are established by determining Euclidean distances (Equation 1 above) with $SO_4^=$ deposition at the individual sites as the independent parameter. Cluster variance, defined above, may also be calculated based on differences in $SO_4^=$ deposition and represents similarity (in terms of $SO_4^=$ deposition) of events within the same category. Note that the cluster variance based on $SO_4^=$ deposition is different from the variance based on meteorological parameters which are used to define the meteorological categories.

The separation of categories in terms of $SO_4^=$ deposition was determined by comparing the total within-groups error sum of squares (E). If a category of n_1 units is merged with a category of n_2 units, the within-group sum of squares for the merged categories equals the sum of the within-group sum of squares of the two categories merged plus $n_1 n_2/(n_1 + n_2)$ times the square of the Euclidean distance between the means of the two categories. A merger thus increases the within-groups sum of squares by a quantity proportional to the (distance)^2 between the merged categories. So if E_{g+1} is the total within-groups error sum of squares when there are g+1 categories and E_g is the same quantity when two categories are merged,

$$E_g - E_{g+1} = \frac{n_a n_b}{n_a + n_b} \left(\overline{X}_a - \overline{X}_b\right) \left(\overline{X}_a - \overline{X}_b\right) \qquad (2)$$

where n_a, n_b, are sizes of the categories and $\overline{X}_a$ and $\overline{X}_b$ are the column vectors of their means.

Initially, when each of N data records is a separate category there is no within-group error sum of squares; hence $E_N = 0$. When multivariate analysis of variance is carried out for g categories the total sum of squares of the within-groups matrix is E_g and the sum of squares of the between-groups matrix B_g (used below) is defined as

$$B_g = E_g - E_1 \qquad (3)$$

The relative advantage gained by increasing the number of categories may be evaluated based on the reduction in within-group sum of squares (E_g) with increasing categorization. Two other measures of the marginal effectiveness of increasing numbers of categories are Beale's criterion (Beale, 1969), computed at each step as:

$$F = \frac{(E_{g-1} - E_g)}{E_g/(N-g)}, \quad g = 2,3, \cdots, N \qquad (4)$$

and the criterion of Calinsky and Harabasz (1974), computed as

$$C = \frac{B_g/(g-1)}{E_g/(N-g)}, \quad g = 2,3, \cdots, N-1 \qquad (5)$$

The Beale (F) and Calinsky (C) criteria both provide measures for the decrease in within-

cluster variance and the increase in variance between clusters as the number of steps increases. If F is large, g categories are better than g-1. The "best" number of categories was obtained by plotting F against g and choosing the value of g corresponding to large F. Similarly, the value of g which maximized C was the best value according to the C criterion. A monotonically decreasing C indicated a hierarchical structure. However, C, rising to a maximum at g, suggests the presence of g categories.

2.1.3. Categorization for Other Years

As described above, meteorological categorization is developed based on data from three individual years, 1979, 1981 and 1983. Once the categorization is established it is necessary to identify appropriate categories for running three-day periods for other years. To classify a particular case into a given category, the 288 meteorological parameters that define each category are compared to parameter values for the individual 3-day event. This was done by computing the Euclidean distance (Equation 1) between the event and the category mean. The events are assigned to the category producing the smallest Euclidean distance.

2.1.4. Aggregation Procedures

The goal of the aggregation procedure is to estimate annual deposition of sulfate and other species based on a finite number of episodes. Ideally, an aggregation procedure would be derived based on observations that correlate changed deposition during individual events with changes in long-term deposition patterns. Data of this sort is unfortunately not available from the historical record. However a reasonable approximation to the desired situation may be obtained by developing procedures for estimated annual deposition based on finite samples of randomly selected events. We postulate that future changes in deposition during an individual event may be correlated with changes in long-term deposition in the same way that observed deposition for a random ensemble may be correlated with observed long-term deposition.

The aggregation approach makes use of the varying frequency of occurrence and expected $SO_4^{=}$ and NO_3^{-} deposition within each category. As will be demonstrated below (Sections 2.3.2 and 3.1.5) selection of days by category provided a more accurate estimate of annual deposition than is provided by purely random selection.

An initial estimate for annual deposition may be derived from an array of samples by projecting the average rate of deposition over a 365-day period. When an ensemble of days is selected based on subjective criteria (such as from extreme events), projection over a 365-day period is more likely to result in a biased sample, since the selected categories ensure that deposition on the sample days will differ from average deposition. The sample deposition must be adjusted by scaling factors in order to arrive at an unbiased estimate.

In addition to the scaling factor, a weighting factor is applied in the summation of depo-

sition from the individual days. The weighting factor (w_i) reflects the frequency of occurrence of categories, so that days which represent frequently occurring categories are weighted more heavily than days which represent unusual meteorology. The weighting factors are equal to the frequency of occurrence, f_i, of each category divided by the number of days from the category, n_i, included in the representative sample of days:

$$w_i = \frac{f_i}{n_i} \tag{6}$$

The aggregated estimate for annual deposition has the following form:

$$DEPOSITION = \frac{D_{annual}}{\sum_1^N w_i \hat{D}_i} \sum_1^N w_i D_i \tag{7}$$

where D_i is the observed deposition during the ith event of the sample to be used in the aggregation; w_i is a weighting factor that reflects the relative frequency of occurrence of the meteorological category associated with the ith event; D_{annual} is the average annual deposition over the period 1982-1985 at the site; and $\hat{D}_i$ represents a statistical estimate for deposition during the ith event, based on available information prior to selection of the individual event.

The statistical estimate for deposition ($\hat{D}_i$) varies depending on the nature of the sample to be used in the aggregation and on the specific purpose of the aggregation. When sample events are selected at random, $\hat{D}_i$ is equal to the average deposition per event, and the ratio of D_{annual} to $\sum_1^N w_i \hat{D}_i$ simply projects the sample deposition over a 365-day period. When sample events are selected based on meteorological categories, $\hat{D}_i$ represents the average deposition for events within the category associated with the ith event. The accuracy of the aggregate estimate can further be improved by using statistical correlations with other factors in estimating $\hat{D}_i$. For example, it will be shown below that $SO_4^=$ and NO_3^- wet deposition for individual events can be statistically correlated with precipitation, and that an estimate for deposition may be developed by linear regression:

$$\hat{D}_i = \beta_{cat(i)} P_i \tag{8}$$

where $\beta_{cat(i)}$ represents the least-squares estimate (i.e. average deposition-to-precipitation ratio) over all events within the meteorological category containing event i, and P_i is the precipitation amount for the event.

TABLE 1. A SAMPLE AGGREGATION OF ANNUAL $SO_4^=$ WET DEPOSITION CALCULATED FOR BIG MOOSE, N.Y., BASED ON A 30-EVENT SAMPLE. THE AGGREGATION PROCEDURE FOLLOWS EQUATION (7) WITH $\hat{D}_i$ EQUAL TO THE AVERAGE DEPOSITION ASSOCIATED WITH THE METEOROLOGICAL CATEGORY. CATEGORIES ARE DESCRIBED IN SECTION 3.1.

EVENT	CATEGORY	WEIGHTING FACTOR (w_i)	DEPOSITION FOR CATEGORY ($\hat{D}_i$)	DEPOSITION FOR EVENT (D_i)
4/16/82	1W	0.0397	55.5	174.9
11/3/85	3W	0.0380	15.2	0.0
5/30/83	5W	0.0463	49.0	82.3
3/18/84	5W	0.0463	49.0	0.9
7/13/85	6W	0.0419	35.8	7.9
9/10/83	6W	0.0419	35.8	44.8
10/12/85	6W	0.0419	35.8	68.8
11/2/83	7W	0.0397	56.1	53.8
8/22/84	7W	0.0397	56.1	108.4
6/14/84	7W	0.0397	56.1	40.9
4/3/85	8W	0.0545	33.0	0.0
9/10/84	9W	0.0331	35.5	65.0
9/15/83	9W	0.0331	35.5	0.0
9/25/82	9W	0.0331	35.5	8.0
8/5/83	9W	0.0331	35.5	0.0
11/17/85	10W	0.0397	48.6	19.2
9/27/85	11W	0.0391	42.5	18.1
7/16/84	11W	0.0391	42.5	35.8
12/16/82	11W	0.0391	42.5	27.4
4/30/82	7D	0.0231	1.0	0.0
9/14/85	8D	0.0231	2.6	0.6
7/23/85	8D	0.0231	2.6	9.0
12/24/84	10D	0.0314	8.1	6.5
1/2/84	18D	0.0397	3.8	4.2
11/6/83	19D	0.0397	1.4	2.2
2/2/82	2W	0.0149	8.4	10.2
12/10/83	4W	0.0066	18.1	5.3
11/5/85	12W	0.0116	19.9	6.9
3/30/85	14W	0.0182	10.1	0.0
11/14/83	17W	0.0099	17.6	0.0

$\sum_1^N . w_i \hat{D}_i =$	33.6
$\sum_1^N . w_i D_i . =$	31.4
$D_{annual} =$	3107 mgm^{-2}
estimated deposition =	2910 mgm^{-2}

The procedure for deriving estimates for annual deposition may also be modified to derive an estimate for seasonal deposition (i.e. summer half-year, winter half-year, etc.). Seasonal estimates may be derived from a given ensemble of events by application of equations 6 and 7 along with the following changes:

(1) Average annual deposition for 1982-1985 (D_{annual}) is replaced by the average deposition for the season in question (D_{summer}, D_{winter}).

(2) The weighting factor (w_i) is set equal to zero for all events outside the specified season, so that summer deposition is estimated based on summer events only, etc.

(3) The estimated deposition ($\hat{D}_i$) is derived based the 1982-1985 average for events from the specified season, rather than from all events.

An example of the aggregation procedure is shown in Table 1. Aggregated annual deposition is calculated for Big Moose, N.Y., based on a 30-event sample. The aggregation procedure follows equation (7) with $\hat{D}_l$ equal to the average deposition for events associated with each category[1]. Weighted sums are $\sum_1^N . w_l \hat{D}_l$ and $\sum_1^N . w_l D_l$.

2.1.5. Selection Process

Selection of individual events for detailed analysis by the RADM simulation meets two broad criteria. First, the selection process must provide an ensemble of events that are broadly representative of the range of meteorological conditions that contribute to wet and dry deposition in eastern North America. Note in particular that the ensemble must include representative deposition events at sites throughout the region, rather than at a few sites only. Second, the selection process is based on rigidly defined objective criteria, rather than on subjective judgement.

The selection process involved generation of groups of individual events from the 1982-1985 period, each of which reflected desired characteristics for the final event ensemble. The grouping of events in the selection process was based partly on the meteorological categories (Section 2.1.1) and partly on criteria discussed below. Once the groupings were determined, a series of event ensembles were chosen as candidates for final selection. The candidate ensembles were each composed of a pre-determined number of events from each category, with the indi-

---

[1]The reader may note that the estimated deposition reported in Table 1 differs from the estimate for Big Moose shown in Figure 21b below. The final estimates shown in Figures 21-25 make use of observed correlations between deposition and precipitation (Equation 8) to calculate $\hat{D}_i$. The simpler calculation illustrated in Table 1 ignores precipitation and sets $\hat{D}_i$ equal to the average deposition for the meteorological category.

vidual events selected randomly from within each group. These candidate ensembles were then put through a two-part evaluation procedure to establish the final selection. This evaluation was based on calculation of aggregated estimates for annual $SO_4^=$ deposition and total annual precipitation.

The grouping of events for selection was based primarily on meteorological categories generated by the wind-based cluster analysis described above. The meteorological categories identified by the cluster analysis were assumed to represent characteristic atmospheric circulation patterns over eastern North America; and selection of events from these categories assures that an appropriate range of circulation patterns are represented in the final ensemble. In addition, the initial cluster-based categories were further divided into subcategories that reflect desired characteristics for the ensemble. Since our primary concern is to represent wet deposition processes, it was decided to select the majority of events from groupings that include substantial wet deposition. To this end the initial categories were divided into "wet" and "dry" subcategories based on $SO_4^=$ wet deposition received at 13 eastern sites (sites are described below). The "wet" subcategories consist of events with greater than $SO_4^=$ wet deposition; the "dry" subcategories consist of events with less than median $SO_4^=$ wet deposition.

Candidate events were selected primarily from "wet" subcategories, although a number of extreme "dry" events (with little wet deposition or precipitation at the eastern sites) were prescribed to permit evaluation of dry deposition processes. The ensembles of candidate events (candidate ensembles) generated based on these criteria are presumed to represent the desired range of atmospheric circulation patterns as represented by the cluster analysis. However the candidate ensembles do not necessarily represent typical patterns of wet deposition or precipitation, as neither deposition nor precipitation have been accounted for by the meteorological categories. In particular, candidate ensembles may include abnormally high precipitation and deposition at certain sites and abnormally low deposition at others.

Evaluation of deposition and precipitation in the candidate ensembles is accomplished by aggregating estimates for annual and seasonal wet deposition and precipitation from candidate ensembles. The aggregation procedure essentially represents a projection of annual deposition based on (a) long-term average deposition (or average deposition-to-precipitation ratios) for the meteorological categories from which events were selected; and (b) deposition received during the individual events of the candidate ensemble. When deposition and precipitation for candidate events are broadly representative of average conditions for the associated meteorological category, the aggregation procedure yields a reasonably accurate estimate for annual deposition. When the candidate ensemble includes extreme or unrepresentative events, the aggregation procedure yields large errors.

The candidate ensembles are evaluated based on three separate aggregation procedures. These are:

(a) Aggregated wet deposition, calculated based on the difference between ensemble wet deposition and average wet deposition within each meteorological subcategory;

(b) Aggregated wet deposition, calculated based on the difference between ensemble and average wet deposition-to-precipitation ratios; and

(c) Aggregated annual precipitation, based on the difference between ensemble precipitation and average precipitation within each subcategory

The three aggregation evaluations tested the extent to which the candidate ensembles are characterized by: (a) wet deposition rates, (b) wet deposition-to-precipitation ratios, and (c) precipitation rates that represent average values for the chosen meteorological subcategories.

Accuracy of the aggregated estimates for each candidate ensemble is evaluated based on the root-mean-square difference (*RMSD*) between estimated and observed deposition over 13 eastern sites, calculated by

$$RMSD = \sqrt{\frac{1}{13}\sum_{j=1}^{13} [\hat{D}_j - D_j]^2} \qquad (9)$$

where $\hat{D}_j$ is the aggregated estimate for annual deposition at the jth site from Equation (7) and D_j is the observed annual deposition (1982-1985). In the final selection process 20 candidate ensembles were generated and the candidate with the lowest *RMSD* for in the three aggregation tests was selected for use by RADM.

2.1.6. Source/Receptor Relationships

2.1.6.1. Trajectory Calculations—

The transport of air to measurement locations was estimated using the NOAA ARL-ATAD trajectory model (Heffter, 1980). This model calculates the mean upwind track of the air within the "mixed-layer" of the atmosphere (a layer of variable height extending from the surface to roughly 1500 m above the surface in the summer and 800 m above the surface in the winter). Rawinsonde measurements of wind, temperature and humidity in the vertical were used to calculate the trajectories. The upper air observing network recording these data over North America has a spatial resolution of about 500 km and a temporal resolution of 12 hours with measurements taken at 00Z and 12Z (Z=GMT). The trajectory model interpolates the upper data in time and space ($1/r^2$), utilizing all information within 400 km of the receptor or previous trajectory endpoint, to determine the backward motion of the air. The model outputs a new position (latitude and longitude) for the air parcel after each three-hour period out to 72 hours (24 three-hour segments). Four trajectories, arriving at the receptor at 00Z, 06Z, 12Z and 18Z, are calculated for each day.

Determining the mean wind velocity along each trajectory segment required a value for the height of the mixed-layer at that location and time. This value was estimated for 00Z and 12Z by scanning the vertical temperature profile for the height of the first non-surface based inversion. When no such inversion was found the top of the layer was set at 3000 meters above the elevation of the nearest rawinsonde station. The 00Z and 12Z estimates are linearly interpolated in time to yield a mixing height for the trajectory segment in question. The wind velocity measurements taken below this height were then used to calculate the mean motion of the mixed-layer over the next three-hour period. This procedure is repeated up to 24 times (72 hours back in time) or until there is no data within 400 Km. As with all methods for calculating trajectories those employed here contain uncertainties which arise due to the fact that the data are limited (cf. Kahl and Samson, 1988) and because it is not possible to model in detail all of the complex motions within the atmosphere. ARL-ATAD trajectories were compared to data from the Cross-Appalachian Tracer Experiment (CAPTEX). The results showed lateral displacement uncertainties on the order of 100 to 200 Km at 24 h upwind and 100 to 400 Km at 72 h upwind (Kahl and Samson, 1986; Draxler, 1987). Relative to southwest trajectories arriving at Big Moose, NY these errors amount to an an area about the size of the state of Ohio. These uncertainties are not significantly different than those resulting from other methods of calculating trajectories. Given the availability of the mixed-layer trajectories, they were selected for the assessment of source-receptor relationships within the context of this study. In using them it was assumed that they represent the most probable path of any air parcel advected with the mean motion of the mixed-layer.

2.1.6.2. Quantitative Transport Analysis—

The transport potential for a given sampling time includes the mean transport computed using the trajectory model plus the horizontal spread imposed by atmospheric dispersion and uncertainty in transport estimates (Samson, 1980). The probability of a reactive, depositing tracer arriving at a point x at a time t, $A_r(x,t)$, can be expressed as

$$A_r(x,t) = \int_{t-\tau}^{t} \int_{-\infty}^{+\infty} \int_{-\infty}^{+\infty} T(x,t|x',t')\, dx'\, dt' \qquad (10)$$

where $T(x,t|x',t')$, the potential mass transfer function in two dimensions, is defined by

$$T(x,t|x',t') = Q(x,t|x',t')\, R(t|t')\, D(x',t')\, \Lambda(x',t') \qquad (11)$$

and $Q(x,t|x',t')$ is the transition probability density function of an air parcel located at x' at time t' arriving at a receptor x at time t, $R(t|t')$ is the probability of the tracer not being reacted to another species from time t' to time t, $D(x',t')$ is the probability that the tracer was not dry deposited at (x',t') and $\Lambda(x',t')$ is the probability that the tracer was not wet deposited at (x',t'). The integration is conducted over a period τ which was prescribed in this study as 72 hours (or less if the trajectory calculation terminated prematurely due to missing input data).

The transition probability density function, $Q(\boldsymbol{x},t|\boldsymbol{x}',t')$, is most important in understanding source-receptor relationships since it describes the motion of the air transporting the pollutants. If a particular source is located at $\boldsymbol{x}'$ at time t' then the probability that it will impact upon the receptor at $\boldsymbol{x}$ at time t, is given by ,$Q(\boldsymbol{x},t|\boldsymbol{x}',t')$. The last three probability functions on the right side of (7) are not well defined for soluble elements. In this work they are assumed to equal *one* so that the effects of dry and wet deposition and chemical reactions are neglected. The main drawback to these simplifications is that they eliminate the possibility of determining the relative importance of local versus distant sources.

The transition probability density function can be approximated from the upwind trajectories. The axis of the computed trajectory is assumed to represent the highest probability at any time upwind for contributing to the trace element composition at the monitor. The spatial distribution of the transition probability function away from the axis of the trajectory depends upon the degree of vertical mixing, coupled with the magnitude of the wind velocity shear. As a first approximation, it has been assumed that the "puff" of transition probability is normally distributed about the trajectory with a standard deviation which increases linearly with time upwind (Samson, 1980; Draxler, 1982). Thus $Q(\boldsymbol{x},t|\boldsymbol{x}',t')$ is assumed to be expressed as:

$$Q(x,t|x',t') = \frac{1}{2\pi\sigma_x\sigma_y} exp\left[-\left(\frac{x''^2}{2\sigma_x^2} - \frac{y''^2}{2\sigma_y^2}\right)\right] \qquad (12)$$

where $x'' = X - x'(t')$ and $y'' = Y - y'(t')$ with (X,Y) being the coordinates of the grid and $x'(t')$ and $y'(t')$ being the coordinates of the centerline of the trajectory. If x'' or y'' is greater than $3\sigma_x$ or $3\sigma_y$ which are defined below, then segment i is not counted in grid box (X,Y). It is assumed that σ_x and σ_y can be approximated by

$$\sigma_x(t') = \sigma_y(t') = a\ t' \qquad (13)$$

with a dispersion speed, a, equal to 5.4 km hr^{-1} (Samson, 1980). To determine the overall probability field (Q-field), $Q(\boldsymbol{x},t|\boldsymbol{x}',t')$ is integrated over time and space as in (10). This field shows where over time period, τ, the air was most and least likely to have originated; i.e. the probability of the air over any point moving over the receptor during the time period, τ. In practice this is carried out by summing the values of $Q(\boldsymbol{x},t|\boldsymbol{x}',t')$ in each grid box over all trajectory segments and dividing by the total number of segments.

Various weighting schemes can be applied in the determination of the Q-field to derive an "implied" transport bias (Keeler and Samson, 1989). For example, trajectories associated with large amounts of pollutant deposition or precipitation can be given more weight so that the resulting probability fields are skewed towards those regions more often associated with these types of events. The weighted Q-field, Q_w, is determined by

$$Q_w = \sum_{i=1}^{nseg} \frac{w_i}{2\pi\sigma_x\sigma_y} exp\left[-\left(\frac{x''^2}{2\sigma_x^2} - \frac{y''^2}{2\sigma_y^2}\right)\right] \quad (14)$$

where x'', y'', σ_x and σ_y are defined as in (12) and (13). The total number of three-hour trajectory endpoints (segments), *nseg*, depends upon the number of trajectories considered. Each one can contribute up to 24 segments (72-hour back-trajectories) depending on the availability of meteorological information. The weighting factor applied is given by,

$$w_{i'} = \frac{D_j}{D_{total}} \cdot \frac{nseg}{mseg} \quad (15)$$

D_j is the value of the factor used in the weighting associated with trajectory, *j*, (eg. wet $SO_4^=$ deposition) and D_{total} is the total value of that factor over all trajectories. The weighting factor is also scaled by *nseg*, the total number of non-missing three-hour segments, and by *mseg*, the number of non-missing segments associated with trajectory *j*. Trajectories arriving at the receptor that are associated with large weights (i.e.. during high deposition events) are thus counted more heavily than those associated with smaller weights. For an individual receptor the Q_w field produced when weighted by $SO_4^=$ wet deposition indicates the probable pathway associated with high and low deposition amounts.

2.1.6.3. The Potential Source Contribution Function —

The potential source contribution function (PSCF) is described by Zeng *et al.* (*1989*). It basically consists of a ratio between weighted and non-weighted Q-fields. The main differences between the approach of Zeng *et al.* (*1989*) and the approach followed here are that in this study uncertainties in the trajectories, which are accounted for by Gaussian "puff-like" spreading (equation 12), are assumed to exist. Zeng *et al.* simply counted the number of trajectory endpoints in each grid box when generating the probability fields. In addition, all trajectories are included and weighted by deposition in this study, while their weighted transition probabilities were determined by only including trajectories associated with events exceeding a preset concentration (equivalent to the average concentration at the site in question). The *PSCF* as employed in this study is determined by:

$$PSCF = \frac{Q(x,t|x',t')_{weighted}}{Q(x,t|x',t')_{non\text{-}weighted}} \quad (16)$$

Values greater than one imply an enhanced probability of the air residing over that region prior to high wet $SO_4^=$ deposition events.

2.2. DESCRIPTION OF DATA BASE

2.2.1. Meteorological Data

Meteorological data were obtained from the National Meteorological Center (NMC) global analyses, available at the National Center for Atmospheric Research (NCAR). This data set was selected because it includes information over the oceans. An alternative data set based on rawinsonde observations was used in a preliminary study (Fernau, 1988), but was rejected for this effort because it failed to represent circulation over the western Atlantic Ocean, crucial for the development of storms affecting eastern North America. In addition, the NMC data offered better spatial resolution over the entire region of interest. The NMC data also included information from a larger variety of sources and had been subject to more extensive quality control procedures to insure accuracy and consistency (Trenberth and Olson, 1988).

Synoptic and asynoptic meteorological data were collected via NMC's Global Data Assimilation System (GDAS) twice daily from numerous sources. Included among these were: surface observations, rawinsondes, aircraft, ships, satellites and buoys. In compiling the final analysis NMC permitted a data collection cut-off time of up to ten hours beyond the actual analysis time. The irregularly spaced data (time and space) were interpolated to a regular 2.5° grid across the entire globe for both 00Z and 12Z. To calculate the data values at the grid points an optimal interpolation scheme was used and the first guess fields for the interpolation were generated from six or occasionally twelve hour global model predictions.

The Global Data Assimilation System at NMC, has been evolving since September 1978. Changes were largely implemented to improve the accuracy, coverage and/or detail of the analysis. Other modifications were necessary to resolve operational difficulties as they occurred or were discovered. The details of the changes that occurred, and their effect on the analysis, are discussed in Trenberth and Olsen (1988). During the 1978-1987 period the majority of the changes had no effect on the information used in this study. However, from March 1984 to March 1986 there were difficulties that resulted in up to a 5 m-sec^{-1} error in the 850 mb level winds. This problem was attributed to small scale noise in the 1000 mb temperature field and it is believed that the resulting errors were not systematic.

NCAR houses NMC data from July 1976 to nearly the present for temperature, relative humidity, geopotential height, zonal and meridional wind components and pressure at up to 14 different levels. During this period, however, NMC failed to archive portions of the data and thus there are periods of missing information in the data set. The amount and type of missing data were also summarized by Trenberth and Olsen (1988). In the years 1978-1986 an average of 7.8% of the data were missing. The minimum amount lost was 2.5% in 1986 and the maximum was 13.6% in both 1982 and 1984.

For this study we obtained the information from NCAR for the years 1979-1985. The 14-layer, 2.5° global data were reduced to 5° and 5 layers for 00Z covering eastern North America. The choice of 5° intervals is discussed in Section 2.1.1. The extent of the horizontal grid is shown Figure 2. The 00Z data were then arranged into overlapping three-day records in order to correspond to the three day duration of RADM simulation periods. The first record of the year contained information from days 1, 2 and 3; the second record contained days 2, 3, and 4 etc.. This process increased the amount of missing cases since a three-day record was not considered complete unless all three days were available. One isolated missing day from the NMC data would become three missing cases because it would be included in three separate cases.

2.2.2. Precipitation Chemistry Data

Precipitation chemistry data were obtained from event precipitation chemistry monitoring locations. The data in the United States were obtained from the Utility Acid Precipitation Study Program (UAPSP) which provided a six-year (1982-1987), 19-site precipitation chemistry data set covering the eastern United States (Mueller and Allan, 1987). The UAPSP data were augmented by precipitation chemistry measurements from two Canadian sites. Figure 3 shows the location of sampling stations chosen for this study. Table 2 lists the number and location of the sites. Since the focus of this study is on eastern sites with high deposition the precision of the aggregation technique is tested for sites located in the northeast and midwest, including the southern border and Ontario sites but excluding sites from the deep south and Great Plains. The sites commonly included in northeast/midwest analyses are identified in Figure 3 and Table 2.

The UAPSP data provided extensive information including: the start day and hour of the first precipitation event, the end day and hour of the last precipitation event (occasionally the timing of multiple events were specified), the precipitation amount, the pH, and a thorough chemical analysis that included the determination of the major ionic species in solution. The only meteorological information included in the data set were in the form of sample codes which distinguished events as either (1) snow and ice events, (2) mixed (liquid and solid sample) events or hail events, (3) rain (uncoded events), and (4) events with thunder.

All chemistry records were examined for incorrect data. Some errors in the dates and times of precipitation begin/end and sample removal date/time had to be corrected or set to missing. Midpoint times and durations were calculated from the precipitation begin/end information. Some chemical measurements were discarded, including phosphate, total acidity, aluminum, sulfite, nitrite and total organic carbon. Hydronium ion concentration was calculated using the lab pH or, if missing, the field pH according to the formula

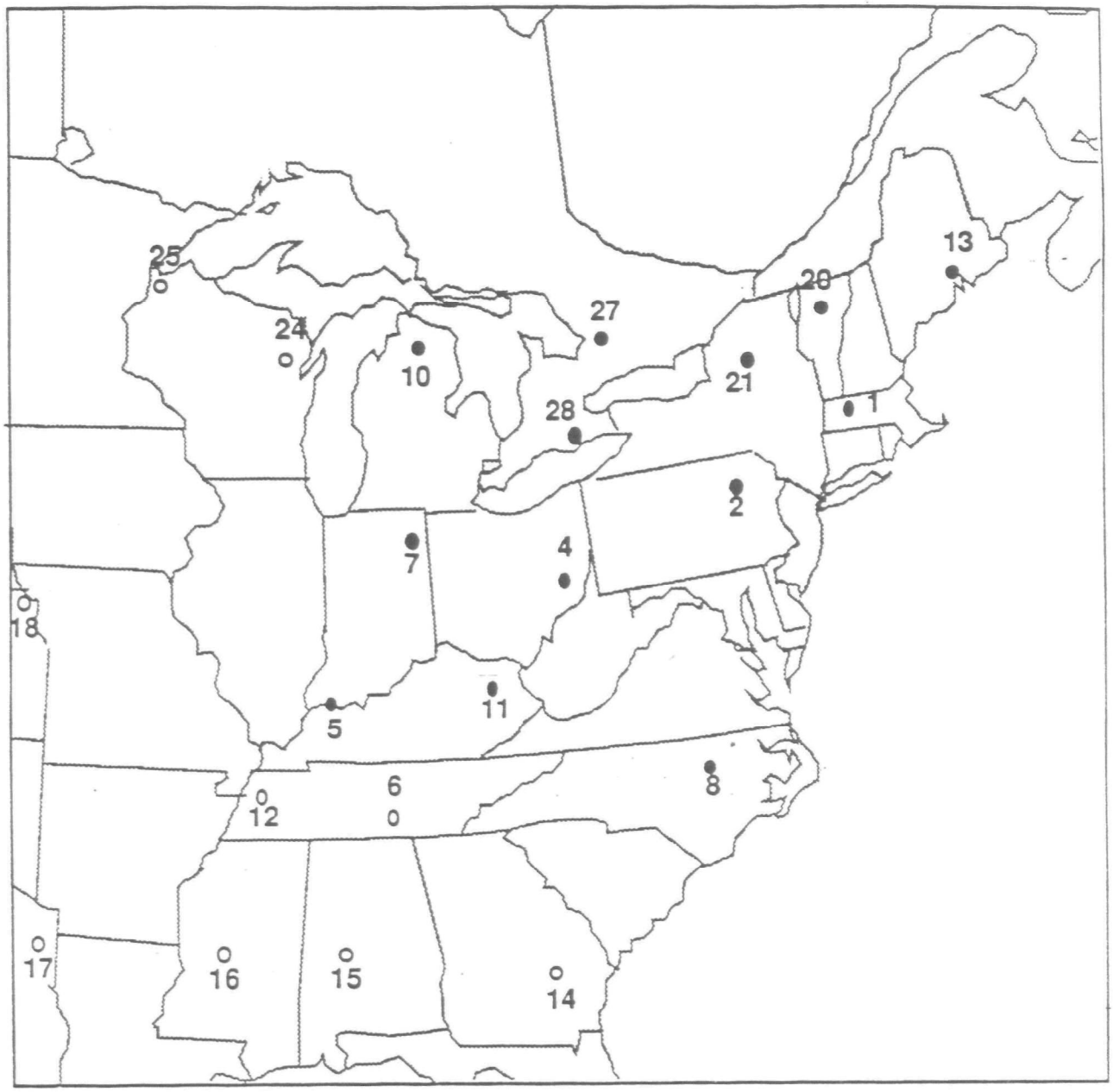

Figure 3. Location of the precipitation chemistry sites in the United States and Canada used for analysis of transport patterns. These sites represent locations of daily precipitation monitoring locations. Sites indicated by solid circles were used to test precision of aggregation technique.

TABLE 2. NAME AND LOCATION OF DAILY (EVENT) PRECIPITATION CHEMISTRY SITES. INCLUDES SELECTED SITES FROM THE UTILITY ACID PRECIPITATION STUDY PROGRAM (UAPSP) AND FROM TWO CANADIAN NETWORKS. ASTERISKS (*) DENOTE NORTHEASTERN AND MIDWESTERN SITES USED TO TEST THE PRECISION OF THE AGGREGATION TECHNIQUE.

SITE	LOCATION	LATITUDE	LONGITUDE
	UAPSP		
*1	Turners Falls, Massachusetts (> 8/80)	42°59'	72°55'
*2	Tunkhannock, Pennsylvania	41°35'	76°00'
*4	Zanesville, Ohio	39°59'	82°01'
*5	Rockport, Indiana	37°53'	87°08'
*6	Giles County, Tennessee	35°17'	86°54'
*7	Fort Wayne, Indiana	41°03'	85°19'
*8	Raleigh, North Carolina	35°44'	78°41'
*10	Gaylord, Michigan	44°57'	84°39'
*11	Clearfield, Kentucky	38°08'	83°27'
12	Alamo, Tennessee	35°48'	89°08'
*13	Winterport, Maine	44°37'	68°59'
14	Uvalda, Georgia	32°03'	82°29'
15	Selma, Alabama	32°28'	87°05'
16	Clinton, Mississippi	32°21'	90°17'
17	Marshall, Texas	32°40'	94°25'
18	Lancaster, Kansas	39°34'	95°18'
19	Brookings, South Dakota	44°20'	96°50'
*20	Underhill, Vermont	44°32'	72°52'
*21	Big Moose, New York	43°49'	74°54'
24	Shawano, Wisconsin	44°42'	88°37'
25	Round Lake, Wisconsin	46°13'	91°56'
	CANADIAN		
*27	Dorset, Ontario	45°13'	78°56'
*28	Longwoods, Ontario	42°49'	81°24'

$$H^+ (\mu moles\ l^{-1}) = 10^{6-pH}. \quad (17)$$

Quality flags were also included in the data set. They were processed after the method of Endlich et al. (1986) and the major steps in this process are described as below. All measurements were set to missing if the sampler was inoperative, water was in the dry bucket, or agricultural activity, dust or smoke were reported in the vicinity of the sampler. If lab and field pH differed by more than 0.7 below pH 5 or 1.0 above pH 5 both measurements were set to missing. Events with sample precipitation volume differing from gauge precipitation volume by more than 30% (a measure of collection efficiency) were flagged. Ion balance was checked using the following formula:

$$\frac{|\text{Total Anion} - \text{Total Cation}|}{(\text{Total Anion} + \text{Total Cation})/2} \geq 0.6 \quad (18)$$

Events failing (value ≥ 0.6) were coded as missing. Anions and cations used in the test were nitrate, sulfate, chloride, hydronium ion, ammonium, sodium, potassium, calcium and magnesium. Measurements below detection level were flagged and negative values were set to zero. After application of the percent test, as described below, multiple events on the same day were totalled and events captured by co-located samplers were combined using arithmetic averages of the measurements. If one of the two co-located samples was considered to be of better quality either overall or for a given analyte then only the less suspect record or measurement was kept.

In an attempt to detect outliers, selected data were subjected to the "percent test" (Endlich, et al., 1986). The test was only applied to events which were suspect due to leakage, contamination, pH disagreement, ion balance failure or collection efficiency failure. In performing the percent test the data for all sites are grouped together by analyte. For each analyte the 90th, 95th, 99th and 99.9^{th} percentile are found using the pooled data. Then the analyte values at each site are compared to these global percentiles. For a given precipitation event, if one analyte exceeds its 99.9^{th} percentile, two analytes exceed their 99th percentiles, three analytes exceed their 95th percentiles, or four analytes exceed their 90th percentiles the event is considered to have failed the percent test and is flagged as such. Flagged events were eventually treated as missing.

The UAPSP data only cover the United States, however, southern Ontario also experiences large annual $SO_4^=$ wet deposition (Finkelstein and Seilkop, 1986). Thus, for completeness, two Canadian sites were added to the data base (Figure 3, Table 2). The sites are from the Acid Precipitation in Ontario Study (APIOS) network and are also daily/event samples. These data were subjected to the same procedures utilized for the UAPSP data, allowing for minor differences in content, and were placed in the same data format as the UAPSP measurements.

2.3. TESTING

Testing of the aggregation and selection process was accomplished by a variety of procedures which investigate the accuracy of successive stages of the analysis. The following steps were included:

(1) The procedure for selecting sample events and generating aggregated estimates for annual deposition was tested by comparing estimates for annual deposition derived from meteorologically stratified samples both against observed deposition patterns and against estimated deposition from samples selected at random. The discrepancy between observations and aggregated estimates will also be compared to the natural year-to-year variability in observed wet deposition rates.

(2) The statistical significance of the observed relations between deposition and meteorological categories will be tested using the techniques of statistical regression. The regression model also allows testing relationships between deposition and other meteorological variables (i.e. precipitation) that are used in the aggregation process.

(3) A simplified model identifying source-receptor relationships for observed wet deposition was developed and applied based on (a) the final ensemble of events selected for future in-depth analysis, and (b) all events over the 1982-1985 period. A comparison between the two estimates illustrates both the accuracy and the potential limitations involved in predicting source-receptor relationships from a finite sample.

2.3.1. Aggregation Versus Random Selection

Techniques for deriving aggregated estimates for annual deposition based on a finite sample of events have been described above (Section 2.1.3) . These aggregation techniques may be applied to ensembles generated entirely at random or to ensembles generated based on meteorological stratification. In addition, the aggregation procedure itself can include knowledge gained from meteorological strata, or the procedure can be constrained to specifically exclude such knowledge. Referring to Equation (7), the prior estimate for deposition per event ($\hat{D}_i$) can be derived either with or without knowledge of the meteorological stratum associated with each event. The prior estimate can also make use of other information (e.g. time of year, precipitation) during each event.

A preliminary estimate of the usefulness of meteorological stratification in selection of events can be obtained by comparing aggregated estimates for random ensembles derived with

and without knowledge of meteorological strata. The accuracy of the aggregated estimates is estimated by the root-mean-square difference over 13 eastern sites (RMSD, Equation 9). The advantage gained by the use of strata, both in the selection of individual events and in the aggregation estimate, will be demonstrated by an improvement in the aggregated estimates derived with knowledge of meteorological strata.

In an associated test, the RMSD for aggregate estimates is compared to the natural year-to-year variability in observed wet deposition. Year-to-year variability provides a measure of inherent uncertainty in estimates for annual deposition. If the RMSD for the aggregate estimate is no larger than the RMSD between annual and multi-year average wet deposition, then the aggregated estimate may be judged equivalent to an estimate derived from data for a complete year.

2.3.2. Statistical Regression

The significance of differences in the observed pattern of wet deposition for events from different meteorological strata have been tested by means of multivariate linear and logarithmic statistical regression models. The specific advantage of regression models (e.g. Johnson and Wichern, 1982) is that it permits a persistent correlation between variables to be distinguished from a correlation that may be due to random chance. Regression analysis is a necessary step in demonstrating that the relation between deposition and meteorological strata which form the basis of the aggregation procedure and selection process is based on long-term trends in deposition rather than on arbitrary correlations.

Because wet deposition must depend on precipitation, a common starting point is to assume a relationship between deposition and precipitation amounts. Wet deposition and precipitation have previously been correlated through both linear (Wilson et al., 1982; Buishand et al., 1988; Berge, 1988; Hooper and Peter, 1988) and log-linear (Stein and Niu , 1988) regression models. A linear regression model for wet deposition with precipitation that also includes variation by meteorological category has the following form:

$$\hat{D}_i = \beta_{cat(i)} P_i \qquad (19)$$

where $\hat{D}_i$ is the estimated deposition for event i, $\beta_{cat(i)}$ represents the least square estimate (i.e. average deposition-to-precipitation ratio) over all events within the meteorological category containing event i, and P_i is the precipitation amount for the event. The regression parameters have been determined independently at each site for which observed wet deposition and precipitation are available.

The importance of meteorological category in explaining deposition can be verified by demonstrating that the deposition-to-precipitation ratio ($\beta_{cat(i)}$) varies significantly for events from different meteorological categories. Variation in $\beta_{cat(i)}$ can be evaluated with the

following test statistic (heterogeneity of slopes, in Freund et al., 1986):

$$F_s = \frac{\sum_{i=1}^{n} [(D_i - \beta_o P_i)^2 - (D_i - \beta_{cat(i)} P_i)^2]/(N-1)}{\sum_{i=1}^{n} (D_i - \beta_{cat(i)} P_i)^2/(n'-1)} \qquad (20)$$

where D_i and P_i represent deposition and precipitation during the ith three-day event at an individual site, β_o represents the overall deposition to precipitation ratio for the site, N is the number of categories and n' is the number of events with non-zero deposition and precipitation. Note that events with zero precipitation (and therefore zero wet deposition) are excluded from the analysis to avoid introducing bias. The test statistic F_s has an F-distribution with $(N,n'-1)$ degrees of freedom. When this statistic assumes a value greater than a pre-determined critical level (1.66 for most cases examined here), the null hypothesis that that observed variations in wet deposition by meteorological category (i.e. variations in $\beta_{cat(i)}$) are due to chance may be rejected with 95% confidence.

Further insight into the the variation of deposition among meteorological categories may be gained by comparing slopes ($\beta_{cat(i)}$) for individual meteorological categories with the average slope (β_o) for all wet deposition events at a site. The difference between $\beta_{cat(i)}$ and β_o for an individual category are tested by the following statistic

$$T_s = \frac{\beta_{cat(i)} - \beta_o}{\sum_{i=1}^{n^*} (D_i - \beta_{cat(i)} P_i)^2/(n^*-2) \sum_{i=1}^{n^*} (P_i - P_{avg})^2} \qquad (21)$$

where n* is the number of events with nonzero deposition and precipitation contained within category cat(i) and P_{avg} is the average precipitation among those events. T_s has a t-distribution with n*-2 degrees of freedom and indicates when the deposition rate for a particular category is significantly above or below the average deposition rate for the site. When T_s assumes a value greater than some critical level (1.66 for data examined here), then it may be concluded with 95% confidence that deposition-to-precipitation ratios for the specified category exceed the average deposition-to-precipitation ratio. Likewise, when T_s is less than -1.66 it may be concluded with 95% confidence that deposition-to-precipitation ratios associated with the category are below average.

Lastly, the overall success of the statistical models in explaining observed variation in deposition are evaluated by the coefficient of determination (R^2):

$$R^2 = \frac{\sum (D_i - \hat{D}_i)^2}{\sum (D_i - D_{average})^2} \qquad (22)$$

where $D_{average}$ is average deposition per event at the site. The coefficient of determination represents the fraction of observed variation in deposition that is explained by the regression estimate ($\hat{D}_i$)

The techniques that have been demonstrated here in a linear regression model may also be used in a logarithmic model with the form

$$\log \hat{D}_i = \gamma + \beta \log P_i \tag{23}$$

or in a linear model that relates wet deposition to the precipitation quantity raised to a power other than one:

$$\hat{D}_i = \beta_{cat(i)} \; P_i^{\gamma} \tag{24}$$

The advantages and disadvantages of these models for use in estimating wet deposition will be explored below.

2.3.3. Source-Receptor Relationships

Variation between categories is important because if they tend to favor different source-receptor relationships a sample of episodes from a number of categories should contain a better overall mix of wind flow patterns. This would insure that the resulting aggregate estimates of wet deposition are not biased towards a small number of potential source regions.

The wet differential probabilities, ΔQ_{wet}, were generated as:

$$\Delta Q_{wet} = Q_{ij}^{c} - \bar{Q}_{ij} \tag{25}$$

to demonstrate that some of the categories exhibited bias towards transport from various regions in eastern North America. The wet differential probability is the difference between the probability, Q_{ij}^{c}, for contribution from grid cell *i,j* due to the transport associated with category c on days with precipitation, and the mean probability, $\bar{Q}_{ij}$, for contribution from from cell *i,j* for all days with precipitation.

The source-receptor relationships estimated using a small number of episodes (19-30) were evaluated by comparing Q-fields. RMS errors (*RMSE*) between the actual Q-field and its estimates were calculated according to:

$$RMSE = \sqrt{\frac{1}{S \times N} \sum_{j=1}^{3} \sum_{i=1}^{N} [\, Q_{ij}^{E} - \bar{Q}_{ij}]^2} \tag{26}$$

where Q_{ij}^{E} is the 19 or 30 day aggregate estimate of transition probability and $\bar{Q}_{ij}$ is the climatological transition probability value in grid cell i for site j. S is the number of sites considered and N corresponds to the number of grid cells over which the differences are calculated. To convert to percents the RMS error is divided by the mean transition probability over $N \times S$ grid points.

3. RESULTS

3.1. METEOROLOGICAL CATEGORIES

3.1.1. Choice of Stratification Parameters

Attempts at the stratification of the three-day periods into meteorological categories were made using the four different combinations of meteorological data listed in Table 3. These factors were thought to be most likely related to precipitation and/or $SO_4^=$ deposition based on dynamical considerations. These variables were extracted or derived from the NMC data set. These included those related to wind patterns: 850 mb wind velocity; 850 mb geopotential height; sea level pressure; and those related to vertical motion and/or precipitation potential: 1000 mb relative humidity; 850 mb temperature advection, 850 mb vorticity advection and 500 mb vorticity advection. The four combinations were generated at each grid point for 1983.

TABLE 3. METEOROLOGICAL FACTORS USED IN INITIAL CLUSTER ANALYSIS

1. Sea level pressure and 850 mb geopotential height (TR),
2. 850 mb *u* and *v* components (UV),
3. 850 mb temperature and 500 mb vorticity advection (AD), and
4. 1000 mb relative humidity and 850 mb vorticity advection (RV)

The AD and RV factors were not as well suited to the goals of this study because, while they consider vertical motions and/or moisture, they do not include representation of transport patterns directly. The categories resulting from the clustering of RV and AD factors were also quite imbalanced in size with a couple large categories and many small "outlier" categories.

The TR and UV factors are similar in physical meaning in that both are related to wind flow. The UV factors are based solely on three-day progressions of 850 mb wind velocity (i.e. one level at approximately 1500 meters above MSL). The TR factors also account for wind velocities and, in addition, consider the strength and development of cyclones. Consequently statistical analysis of the UV and TR categories yielded similar results. It was found that the UV components were more sensitive to changes in the number of categories than the TR factors. This provides a better means of determining the optimum number of categories. Therefore the

UV components were selected as the parameters of choice for this project.

Due to the computer memory constraints of the statistical software used in this project it was not possible to place all the cases during 1979-1985 into a single cluster analysis. Only one year's worth of running cases (365 cases) at 48 grid points could be clustered at one time. Therefore, in order to minimize the effect of missing *u-v* data and to capture a broader cross-section of cases, consecutive three-day periods (record 1 = days 1,2,3; record 2 = days 4,5,6; etc.) for 1979, 1981 and 1983 were pooled for cluster analysis.

Selection of the number of meteorological categories was based on the ability of the categorization to separate events with observable differences in $SO_4^=$ wet deposition. The value of increases in step number (i.e. increasing number of categories) was evaluated by calculating the Beale (*F*) and Calinsky (*C*) criteria for within-group variance of $SO_4^=$ deposition (defined in Section 2.1.2). High values of *F* and *C* indicate that significant improvements in the ability to stratify $SO_4^=$ deposition occur as a result of increased step number. Results are shown in Figure 4. As expected, the highest values of *F* and *C* occur when the step number is low, with diminishing returns as the number of categories is increased. Figure 5 shows total within-group variance of $SO_4^=$ deposition (defined in Sections 2.1.1 and 2.1.2) as a function of number of categories. Within-group variance decreases as the step number is increased, reflecting improved ability to stratify $SO_4^=$ deposition with increasing number of categories. The pattern of diminishing returns with increasing step number is also apparent in Figure 5.

Choice of the proper number of categories necessitates a trade-off between the desire for precision in distinguishing between different meteorological patterns (facilitated by a large number of categories) and the need for robustness in statistical estimates and ease of computation (facilitated by a small number of categories). Appropriate number of categories can be identified in Figures 4 and 5 by identifying step numbers that show relative peaks in *F* and *C* and significant reductions in cluster variance. Critical points (identified by changes in slope) appear to occur at steps 8, 14 and 19. Based on this guidance we initially proposed a choice of 19 categories.

3.1.2. Description of Categories

As described above (Section 3.1.1) it was decided to base the meteorological stratification on the 850 mb wind fields (U and V components of wind vectors as the two independent meteorological parameters) and to base the stratification on 19 independent categories. This section presents a description of the categories in terms of meteorology and in terms of deposition (Section 3.1.2.1). We also describe the choice to divide each category into subcategories representing "wet" and "dry" events, i.e. events with greater than average or less than average total sulfate wet deposition at the 13 eastern sites (Section 3.1.2.2). The 38 subcategories, representing "wet" and "dry" halves of the original 19 categories determined by wind field, were used as the basis for event selection and aggregation.

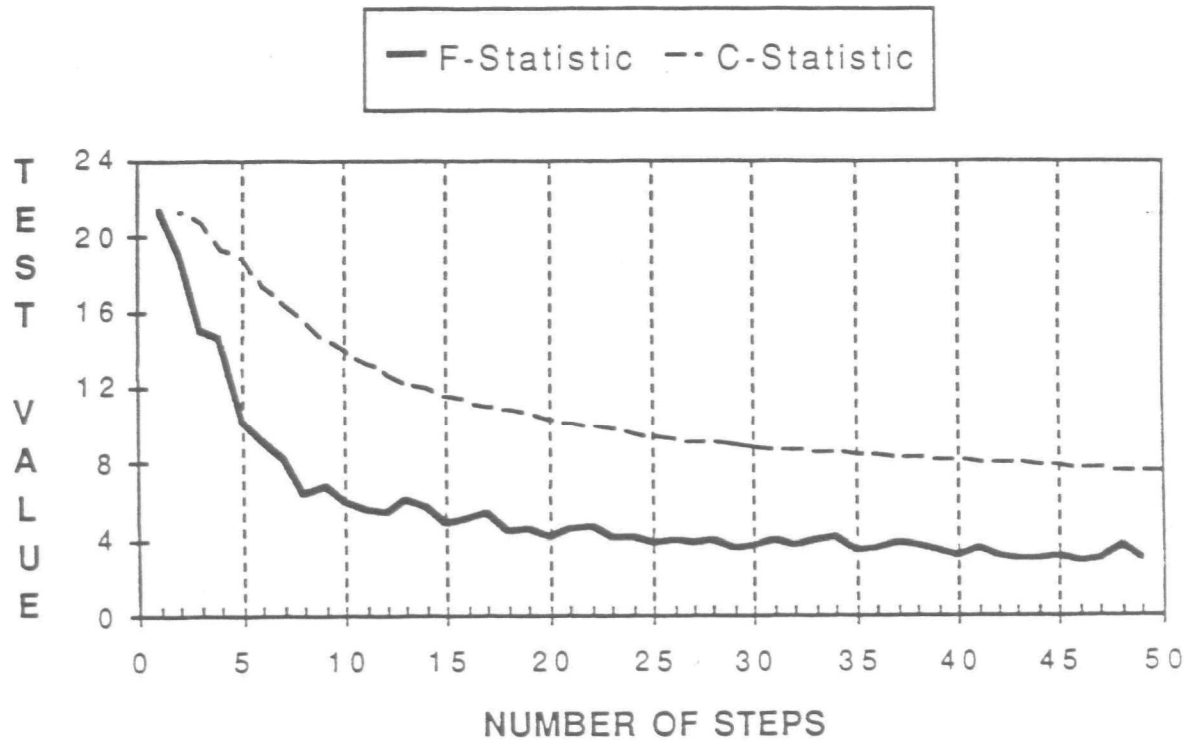

Figure 4. Beale and Calinsky criteria (*F* and *C* statistics) versus the number of categories (step number), based on 850 mb wind field clusters and observed $SO_4^=$ deposition for 1983. High values for *F* and *C* indicate significant reductions of within-group variance of $SO_4^=$ wet deposition with increasing step number.

The mean 850 mb wind flow patterns on each of the three days were plotted to ensure that the 19 categories made sense meteorologically (i.e. all major storm patterns were represented). The plots depicting the flow patterns for the 19 categories are included as an Appendix. Each category demonstrates some unique mixes of cyclonic and anticyclonic circulations. Table 4 is a summary of the major features associated with each of the 19 categories.

3.1.2.1. Wind Flow Patterns—

The 19 meteorological categories represent clusters of 3-day events and can be characterized by the evolution of the meteorology from day #1 to day #3, averaged for all events contained within the category. The mean 850 mb wind flow patterns on each of the three days have been plotted and examined to ensure that the 19 categories made sense meteorologically (i.e. all major storm patterns were represented). The plots depicting the flow patterns for the 19 categories are included as an Appendix. Each category demonstrates some unique mixes of

cyclonic and anticyclonic circulations. Table 4 is a summary of the major features associated with each of the 19 categories.

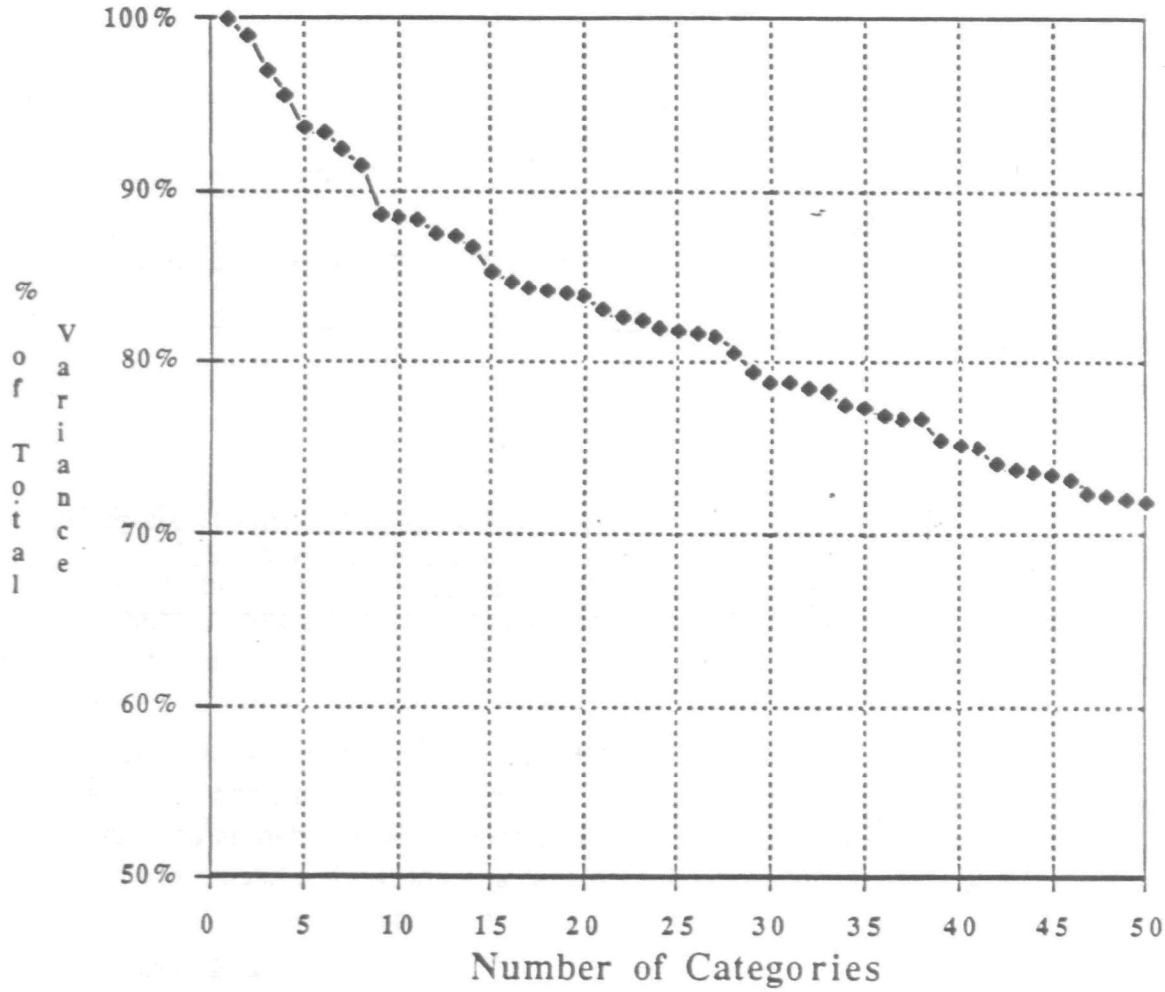

Figure 5 Cluster variance (within-group sum of squares) for $SO_4^=$ wet deposition versus number of meteorological categories included in the stratification, based on 850 mb wind field clusters and observed $SO_4^=$ deposition for 1983.

TABLE 4. SYNOPTIC DESCRIPTION OF THE NINETEEN 850 MB WIND FLOW CATEGORIES. *N* CORRESPONDS TO THE NUMBER OF OCCURRENCES; 3YR - 1979, 1981 AND 1983 (CONSECUTIVE 3-DAY PERIODS); 7YR - 1979-1985 (RUNNING 3-DAY PERIODS); AND 4YR - 1982-1985 (RUNNING)

Category	*N* (3yr)	*N* (7yr)	*N* (4yr)	Description
1	13	76	41	Trof from James Bay to KS with a mdt SW flow to E. Hi well off FL coast. Trof rotates and moves slowly Ewd to Wrn Que thru TN with W to NW fLow behind and W-SW ahead. Hi moves Ewd.
2	12	56	38	Sharp rdg from Lk Sup SEwd. Mdt Sly winds between the rdg and a wk trof in the Dakotas. Trof strengthens and moves across MI ending up N to S thru OH. Good cyclonic circulation around the trof.
3	6	49	28	Well developed Lo moves from IA to Lk Ont. Strong, closed cyclonic circulation around the Lo.
4	8	42	21	Stationary front W to E thru Lk Erie. Sly winds S of front and wavy Wly flow to the N.
5	25	135	72	Wk Lo over Nrn MN with front curling S and W into TX. Lo strengthens and moves E to Ont-Que boarder with front thru E TN. W-SW winds ahead of system and mdt NWly winds behind.
6	29	249	157	Stg Hi over NC drifts very slowly E as a wk trof moves SEwd into Lk Sup. Mdt SW flow over the MS valley spreads Ewd to Atlantic coast during the period.
7	32	201	112	Continental Hi over SErn US weakens as Nly winds spread Swd over the Grt Lks and New England. A rdg re-develops from the Hi across Lk Mi as Nly winds move E.
8	18	159	92	A cold front along the NE Atlantic coast moves slowly offshore. An extensive area of Hi pressure moves over the Ern US and a mdt Sly flow develops W of the MS river.
9	33	263	139	Bermuda Hi remains nearly stationary over TN/GA. A very wk trof moves quickly across the Grt Lks. A lgt anticyclonic circulation covers the Ern US throughout the period.
10	8	108	76	Trof thru Lk Sup and SErn KS moves E and rapidly weakens. Mdt to stg Wly winds persist W of the MS river and S of the Grt Lks.

ABBREVIATIONS KEY

trof - trough of low pressure	N, S, E, W - north, south, east, west
rdg - ridge of high pressure	NE, SW, SE - northeast, southwest, southeast etc.
Lo - low pressure system	Nly - northerly (same format with other directions)
Hi - high pressure system	Nrn - northern (same format with other directions)
stg - strong	Nwd - northward (same format with other directions)
mdt - moderate	
wk - weak	All standard State abbreviations are applicable
thru - through	
Lk - lake	
Grt Lks - Great Lakes	

TABLE 4 (CONTINUED) *(N* CORRESPONDS TO THE NUMBER OF OCCURRENCES; 3YR - 1979, 1981 AND 1983 (CONSECUTIVE 3-DAY PERIODS); 7YR - 1979-1985 (RUNNING 3-DAY PERIODS); AND 4YR - 1982-1985 (RUNNING))

Category	*N* (3yr)	*N* (7yr)	*N* (4yr)	Description
11	27	223	124	A cold front N-S thru OH weakens and moves just off E coast. Stg NW winds behind front also weaken and shift to the W as a Hi develops over TX.
12	15	90	48	Well developed Lo NE of Georgian Bay with a trof extending Swd moves just E of ME. NW winds cover entire Ern US behind system
13	8	50	16	Nw flow to the W of the Grt Lks moves across Ern US and strengthens over the Atlantic. A Hi develops over TX and builds across OH valley.
14	5	27	19	A sharp rdg from Lk Sup thru GA with stg NW winds to E and stg S winds to the W moves offshore. A Lo with a stg cyclonic circulation moves over NE IA from CO.
15	5	34	16	Stg Lo over New Brunswick drifts E. A weak Hi over the Gulf is replaced by a weak Lo over GA. Entire Ern US ends up in a weak cyclonic flow around the Lo.
16	6	23	14	A well developed Lo over Georgian Bay moves quickly NE and another stg Lo moves into MO. Stg S flow develops ahead of second Lo and W of a wk rdg separating the two Lows.
17	13	68	37	Strengthening trof over MN moves to Wrn MI and extends Swd to LA. SW flow increases E of trof as does the NW flow W of the trof.
18	13	96	30	A Hi over the Gulf which extends to IA weakens allowing consistent NW winds to cover most of the Ern US.
19	10	78	48	Well developed coastal Lo near DE moves NE as a rdg along MS river moves over Ern states. Mdt Sly flow W of rdg and ahead of wk trof NE-SW thru MN.
		2027	1172	
	266	289	252	
			8324	

ABBREVIATIONS KEY

trof - trough of low pressure	N, S, E, W - north, south, east, west
rdg - ridge of high pressure	NE, SW, SE - northeast, southwest, southeast etc.
Lo - low pressure system	Nly - northerly (same format with other directions)
Hi - high pressure system	Nrn - northern (same format with other directions)
stg - strong	Nwd - northward (same format with other directions)
mdt - moderate	
wk - weak	All standard State abbreviations are applicable
thru - through	
Lk - lake	
Grt Lks - Great Lakes	

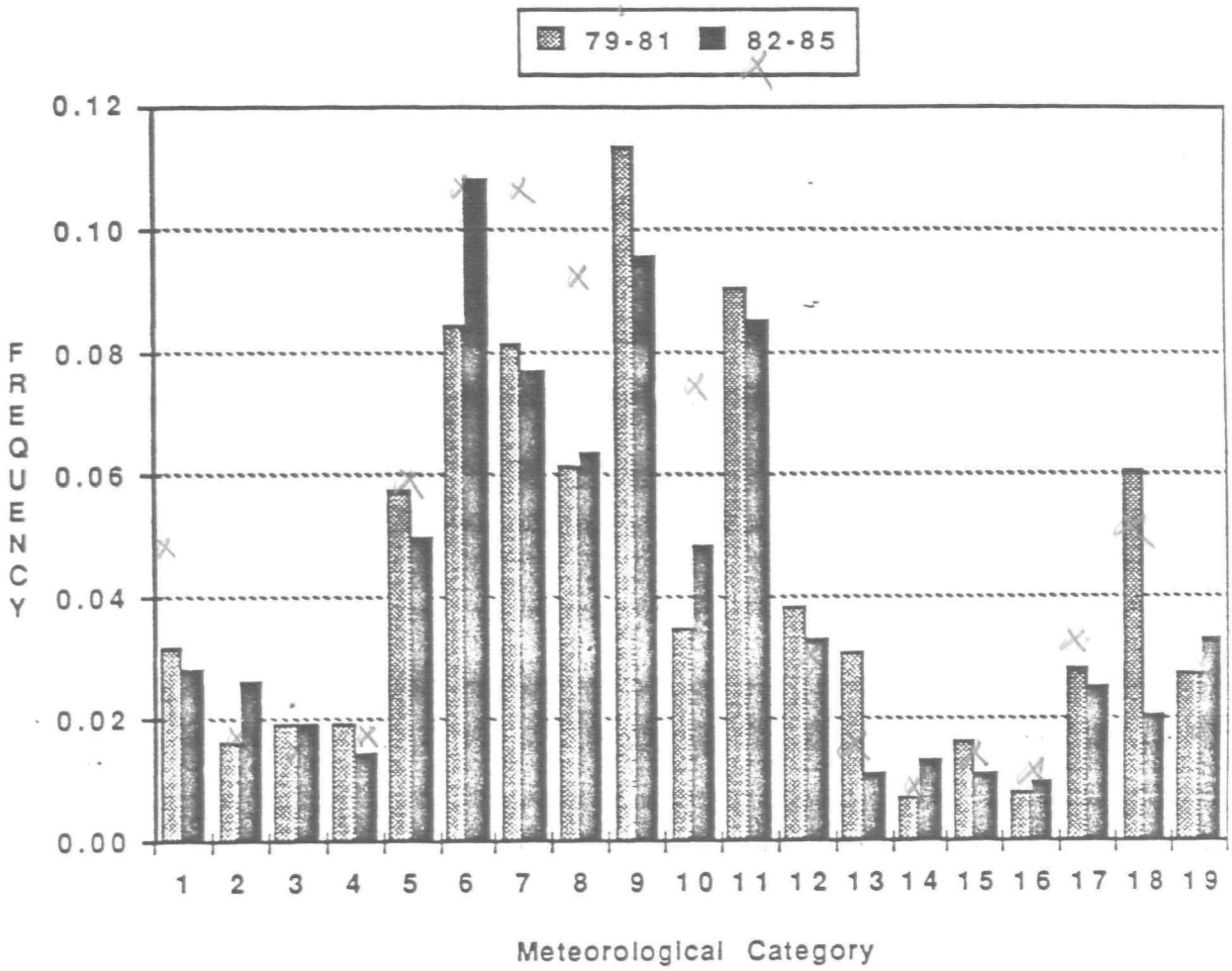

Figure 6. Comparison of frequency of occurrence of the 19 meteorological categories defined in this study between 1979-1981 and 1982-1985.

During the seven year period there were marked differences in the overall frequency and seasonal frequency of each category. Some types of events were rare while others occurred quite often. The number of occurrences of each category over seven years are listed in Table 4. Categories 6, 7, 8, 9 and 11 were the most frequent and categories 4, 13, 14, 15, and 16 were relatively infrequent during 1979-1985. The change in category frequency between the 1979-81 period and the 1982-85 is shown in Figure 6. The overall importance of each category did not change significantly.

Initially it was thought that it may be necessary to impose seasonal requirements on category selection due to the seasonal variations known to exist for $SO_4^=$ deposition. This would ensure that storms at all times of the year were represented. Figures 7a-g, however, demonstrate that seasonality is already inherent in the categories. For example, categories 1, 2 and 3 were basically cold season events. Figure 7b shows that category 4 occurred in all seasons with a tendency towards Fall. Categories 5 and 6 also occurred year round, but they are more dominant in the Spring and Fall. Categories 7, 8, and 9 (Figure 7c) were predominantly warm season situations while 10 and 12 (Figure 7d) were cold season type events. Category 11 occurred fairly often in all months but were most frequent between December and June. Cases in categories 13-16 were all most frequent during the cold season as were the cases in categories 17, 18 and 19. However, cases in 17 and 18 seemed to occur more in winter and category 19 cases in spring. Missing events, which resulted whenever the 850 mb data for any of the three days were missing were recorded in every month, however, there were more in August and less in May and June. On average there were approximately 5 events missing per month during the four-year period.

3.1.2.2. Deposition Patterns—

While the underlying reason for using the wind flow to stratify deposition episodes was to insure representation of all major air flow patterns, it was hoped that the meteorological stratification would also produce distinct $SO_4^=$ deposition patterns associated with each category. It was found that this was partially true. The stratification separated relatively "wet" periods from relatively dry periods and thus separated those periods of enhanced pollutant deposition as well.

The ability to explain the variability in wet deposition by meteorological stratification was tested in a number of ways. First, the spatial patterns of the 85th percentiles of $SO_4^=$ wet deposition associated with each category, were studied. All available data (up to 7 years) from each separate location that satisfied the quality assurance measures discussed earlier were used to calculate the percentiles. The spatial patterns changed between categories but the differences were not always great. For certain categories, the magnitudes and locations of the relative maxima and minima were significantly different compared to the other categories and some categories appeared to be rather unique at certain sites and not at others.

The 85th percentiles of $SO_4^=$ deposition for each meteorological category were compared at four locations in Figures 8 a-d. Deposition appears to vary between categories and at each of the sites explored there were different categories or groups of categories that resulted in high 85th percentile depositions. This suggests that the 850 mb flow patterns that were important for $SO_4^=$ wet deposition at some sites were not necessarily important for other sites. Nonetheless, there appeared to be some consistency in rank of categories between sites. Category 5 consistently produced relatively large amounts of $SO_4^=$ wet deposition at all four sites while categories 12 and 13 produced small amounts.

The utility of stratification in estimating long term averages relied on the assumption that the variance within the strata were less than the overall variance. Figure 5 above showed that there was less variance within each meteorological strata as compared to the variance over all the data. The average variance within the 19 categories was approximately 85% of the total variance. Thus, the 850 mb wind categories did reduce the variance of the aggregate estimates. Statistical significance of the relation between wet deposition and meteorological category will be discussed in detail in Section 3.1.3 below. Although there were statistically significant differences in wet deposition among categories, it is obvious that factors other than wind flow (i.e. precipitation amount and location) explains most of the variance in wet deposition.

One factor that influenced the relative importance of a category was its frequency of occurrence. As a first guess, one would expect that the most commonly occurring categories would be relatively important. However, this was not always be the case. High pressure systems occurred fairly frequently but they generally produced significantly less precipitation. Therefore, in order to better identify which categories were the most important, the total amount of $SO_4^=$ deposition associated with each category during 1982-1985 was compared. Percent of total deposition due to each category were calculated for every site. There were a group of categories that consistently contributed a large percentage of the deposition at each one. Storms associated with categories 11, 9, 6, 5 and 7 appear to be the most important for the wet deposition of $SO_4^=$. Some categories were important because they were frequently associated with precipitation. Others were important because the average deposition per event was large. In Figure 9 the ratio of the percent of $SO_4^=$ deposition to the percent of precipitation has been graphed for each category. In general, one can assume that changes in precipitation should result in proportional changes in deposition. Therefore, ratios above one in Figure 9 indicate relatively "dirty" categories. While categories 5, 6, 7, and 9 had ratios greater than one (as did category 8, which was also fairly important), category 11, was not among the "dirty". Its importance was apparently more related to the fact that it frequently resulted in precipitation at most of the sites. In fact, the category 11 storms were responsible for the largest percentage of precipitation at many sites in eastern North America.

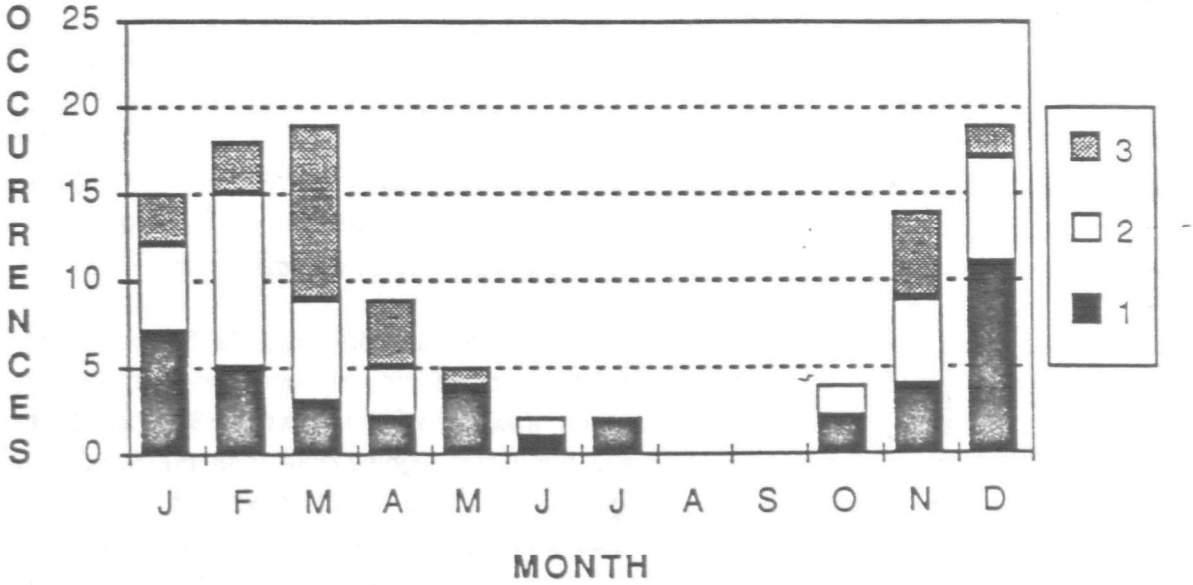

Figure 7a Monthly mean number of occurrences of meteorological categories 1, 2, and 3 during 1982 to 1985 (Note scale is 0-25).

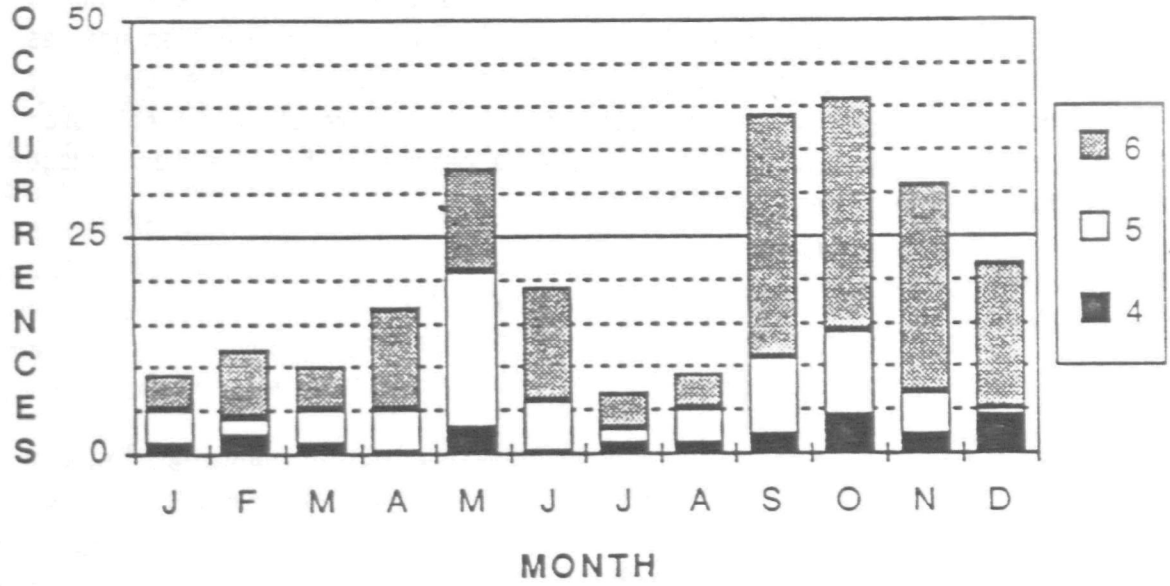

Figure 7b Monthly mean number of occurrences of meteorological categories 4, 5, and 6 during 1982 to 1985 (Note scale is 0-50).

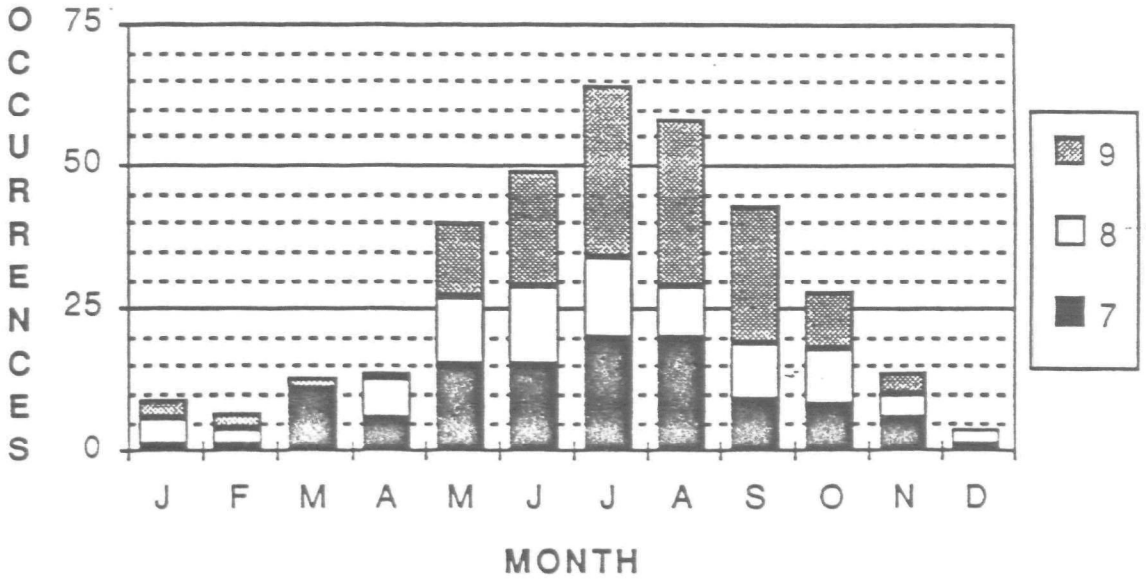

Figure 7c Monthly mean number of occurrences of meteorological categories 7, 8, and 9 during 1982 to 1985 (Note scale is 0-75).

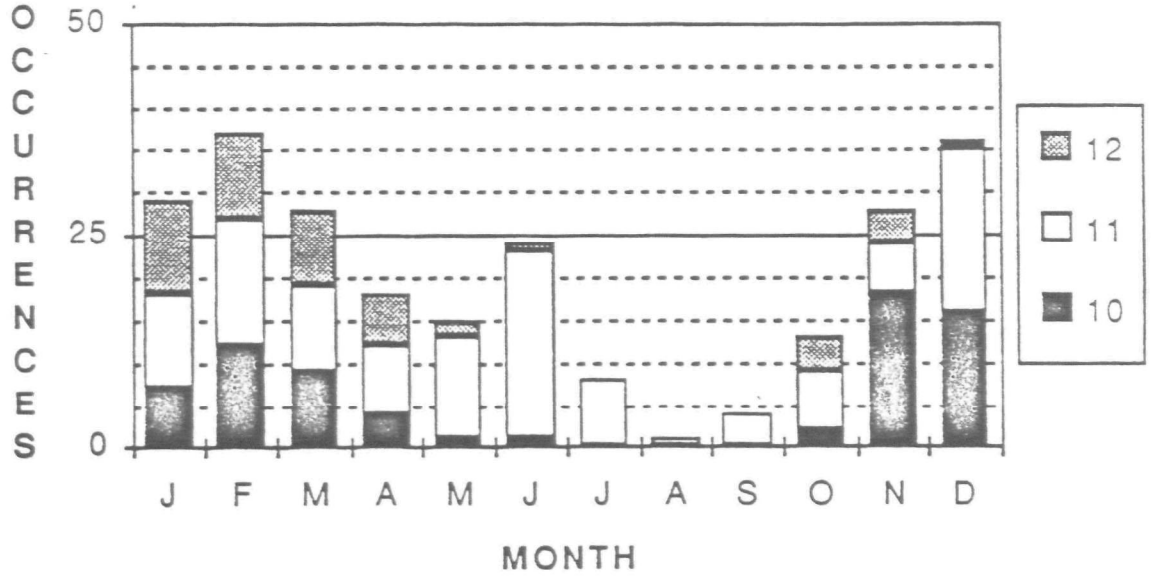

Figure 7d Monthly mean number of occurrences of meteorological categories 10, 11, and 12 during 1982 to 1985 (Note scale is 0-50).

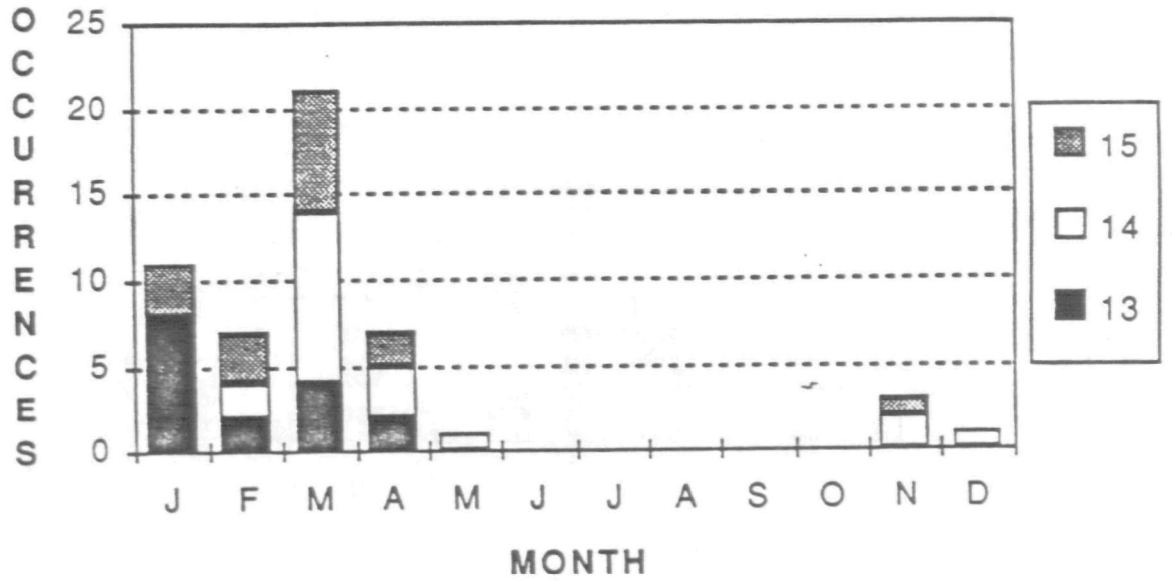

Figure 7e Monthly mean number of occurrences of meteorological categories 13, 14, and 15 during 1982 to 1985 (Note scale is 0-25).

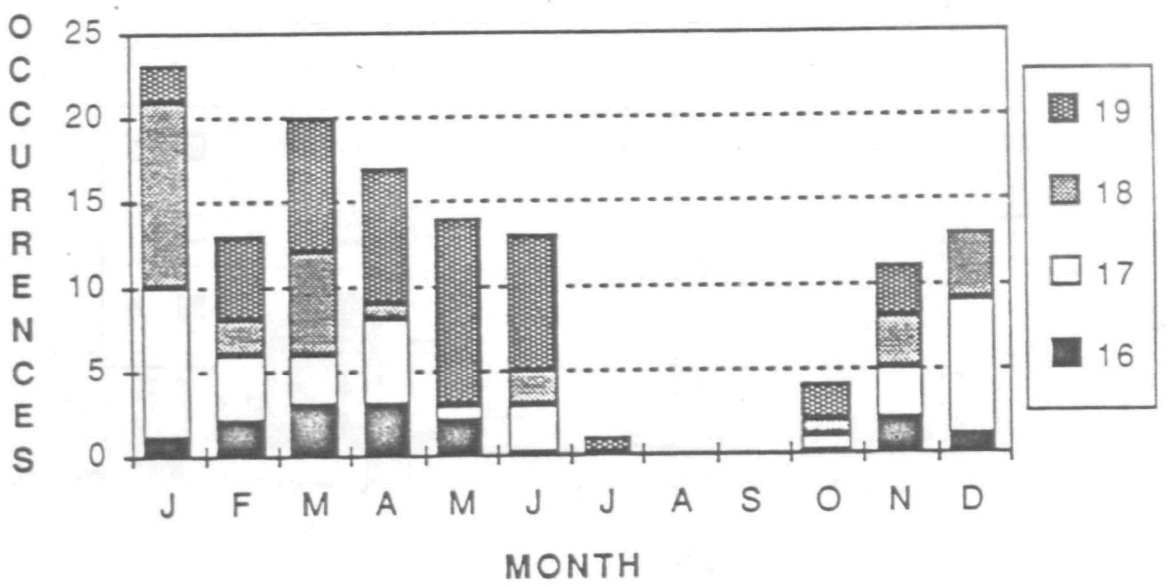

Figure 7f Monthly mean number of occurrences of meteorological categories 16, 17, 18, and 19 during 1982 to 1985 (Note scale is 0-25).

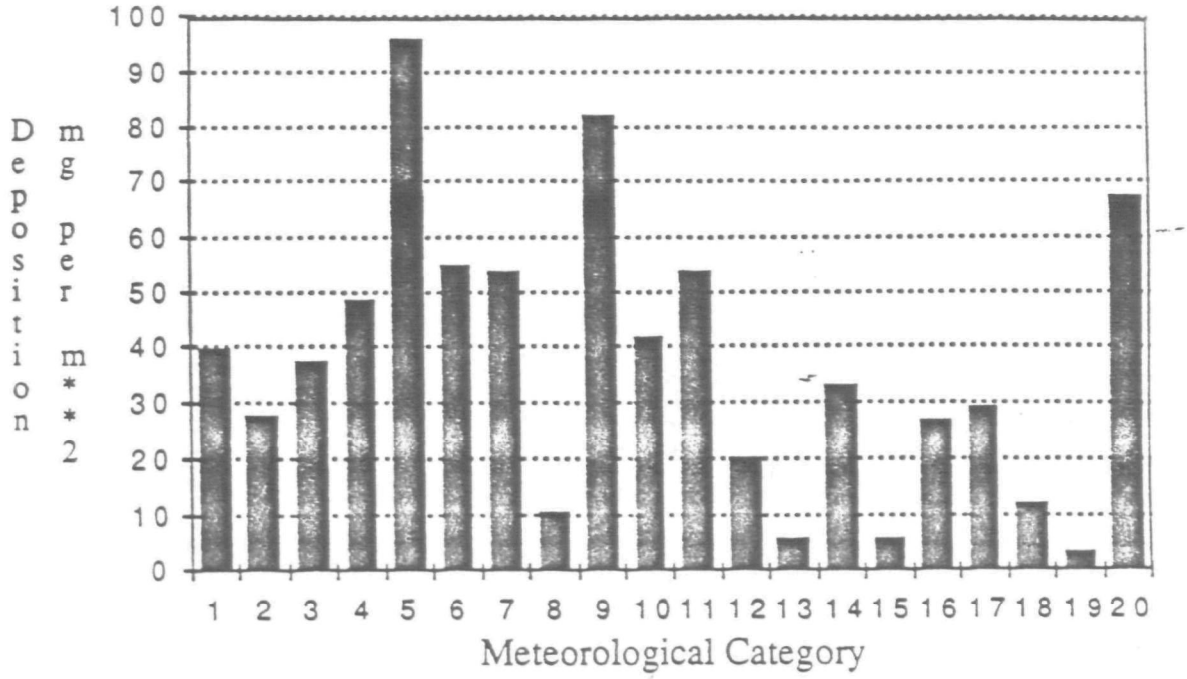

Figure 8a. Variation in amount of $SO_4^{=}$ deposition between categories at Big Moose, New York.

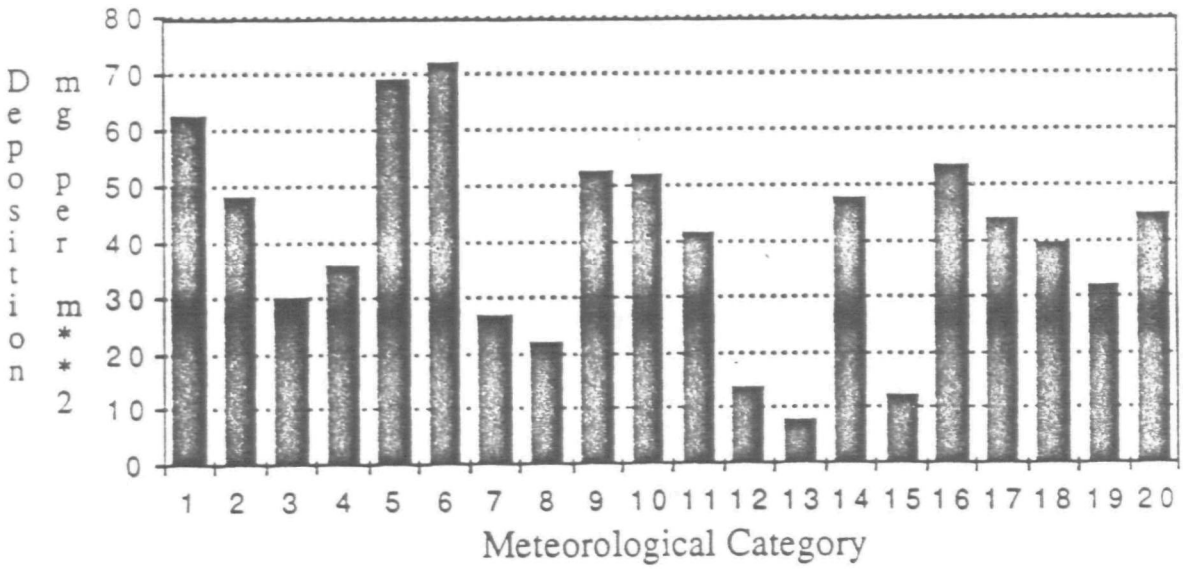

Figure 8b. Variation in amount of $SO_4^{=}$ deposition between categories at Dorset, Ontario

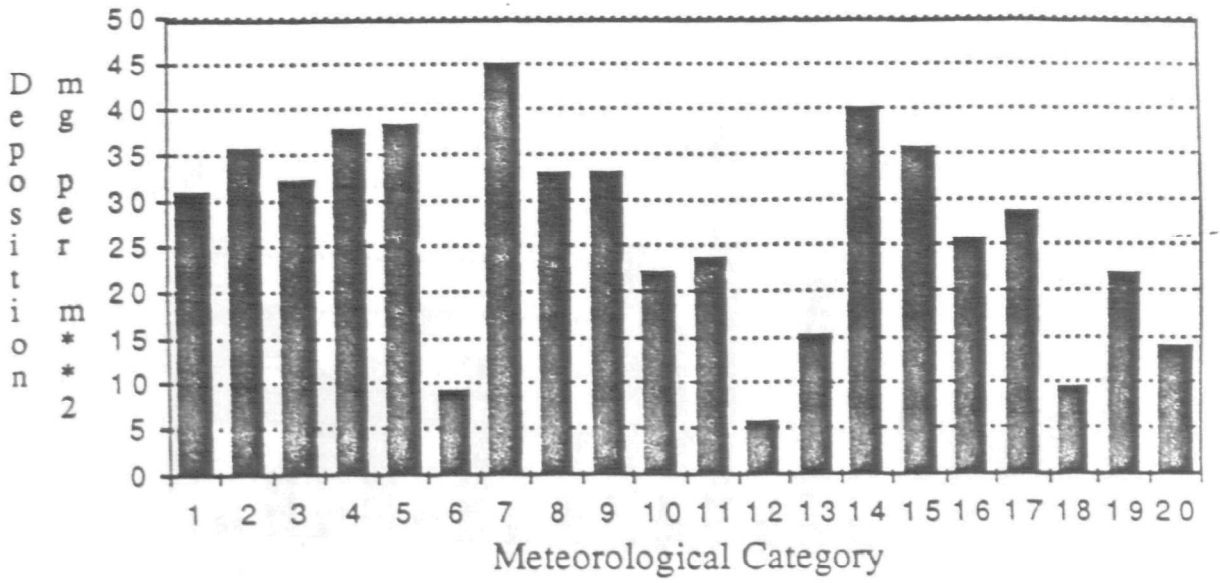

Figure 8c Variation in amount of $SO_4^{=}$ deposition between categories at Raleigh, North Carolina.

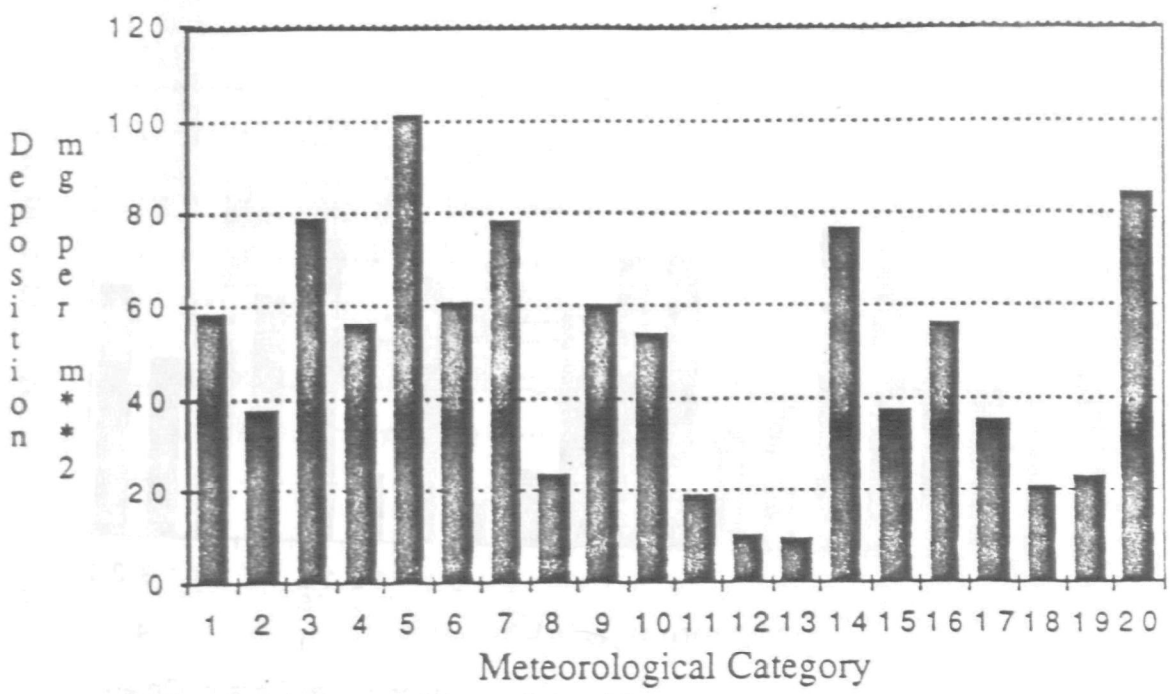

Figure 8d. Variation in amount of $SO_4^{=}$ deposition between categories at Zanesville, Ohio.

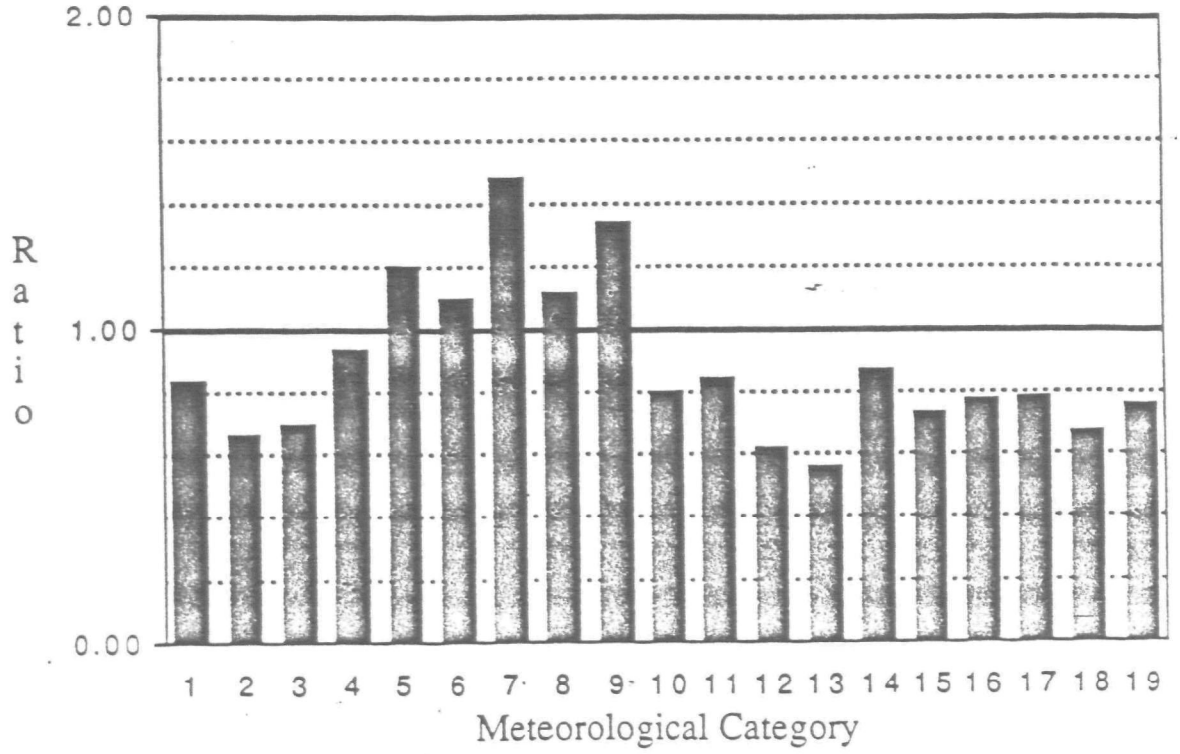

Figure 9. The ratio of the percent of $SO_4^=$ deposition to the percent of precipitation for each meteorological category. Values greater than one imply more deposition than expected due to variations in precipitation amount.

To gain a better understanding of the actual weather associated with each category the sea level analysis from the NOAA Weekly Summaries were examined. It was hoped that definite similarities would appear between the cases within categories and that we would then be able to select a set of "most representative" cases for each category. These cases would then be used in the aggregation. Unfortunately, there was still too much variability within categories and it was next to impossible to identify typical cases. This was because there were many meteorological and deposition related parameters still varying within each category.

For the purpose of event selection, it is desirable to establish a pool of events with above average $SO_4^=$ wet deposition in eastern North America. The ultimate goal of the categorization process is to represent meteorological events that contribute significantly to deposition in eastern North America, using a minimal number of sample events. This aim would be thwarted by a selection process that includes large numbers of events with minimal total wet deposition.

In order to improve the selection process the original 19 wind flow categories were divided into "wet" and "dry" subcategories. The split into "wet" and "dry" halves was based on actual $SO_4^=$ wet deposition received at the 13 northeastern sites during the years 1982-1985, with the "wet" subcategories consisting of events with total $SO_4^=$ wet deposition above the median. This resulted in 38 new categories consisting of the "wet" and "dry" halves of the original 19 wind flow categories.

An examination of 850 mb wind flow for the 38 subcategories revealed little difference between equivalent "wet" and "dry" halves. The major difference between wet and dry subcategories concerns total precipitation, which is related to meteorological parameters (e.g. absolute and relative humidity, atmospheric stability indices) other than 850 mb wind flow. The split into wet and dry subcategories based on $SO_4^=$ wet deposition corresponded closely to a split based on total precipitation. We have used the 38 wet and dry subcategories as the basis for event selection and aggregation, while analyses for statistical significance (Section 3.1.3 below) were based on the 19 wind flow categories with precipitation as an independent parameter.

The percent of total deposition due to each of the 38 subcategories were calculated as for the original 19 categories. Table 5 is a matrix of percent of total deposition by site and category ('CT'). The same information is portrayed graphically in Figure 10. The "wet" subcategories are numbered 21-40 with 21 corresponding to 1, 22 to 2, 23 to 3 etc. The categories that consistently accounted for a relatively large percentage of the deposition at all of the sites were 25, 26, 27, 29, and 31. These were all from the "wet" subset and corresponded to the important categories selected earlier from the undivided set of 19. These categories alone accounted for 30 to 60% of the 1982-1985 $SO_4^=$ and NO_3^- wet deposition at the sites for which data was available.

A crucial step in the development of the aggregation scheme was the selection of an array of categories from which to select events. It was decided that the categories selected should account for close to 75% of the total SO_4^{2-} wet deposition. A significant number of events would be selected from the major categories (25,26,27,29 and 31). However selection from additional categories were necessary to bring the SO_4^{2-} wet deposition for included categories up to 75% of total deposition at most sites. The relative importance of the remaining categories varied significantly from one site to the next, as some wind flow patterns contributed significant wet deposition at some sites but little deposition at others.

TABLE 5: MATRIX OF PERCENT OF TOTAL DEPOSITION BY SITE AND CATEGORY

	SITE NUMBER									
CT	1	2	4	5	7	8	10	11	12	13
1	1.3	0.3	0.4	0.33	0.45	1.34	0.15	.88	1.86	1.17
2	0.6	0.2	0.8	1.71	0.66	2.83	1	0.9	1.72	0.35
3	0.5	0.1	0.2	0.01	0.06	0.31	0.24	0.25	0.35	0.02
4	0.3	0.2	0.2	0.87	0.07	0.92	0.2	0.37	0.97	0.17
5	0.4	0.7	0.5	0.61	0.57	1.08	1.9	0.85	1.11	0.38
6	1.2	1.1	1.4	2.86	2.8	0.75	6.33	1.3	8.1	1.56
7	0.9	0.9	1.4	1.78	1.56	1.2	1.52	1.81	0.15	2
8	2.1	1.6	1	0.7	1.06	6.26	0.61	1.93	1.23	4.09
9	2.5	2.4	1.4	2.1	0.78	3.69	2.99	1.07	7.66	1.38
10	1	0.2	0.8	1.69	1.34	2.44	0.75	1.89	3.73	1.78
11	2.4	1	0.8	0.67	0.61	3.59	1.6	2.04	1.59	3.04
12	1.8	0.7	0.6	0.22	0.52	0.93	0.28	1.31	0	3.39
13	0.1	0	0.3	0.34	0.21	0.77	0.11	0.34	0.75	0.09
14	0.3	0.2	0.1	0.39	0.2	0.58	0.15	0.17	0.51	0
15	0.1	0.2	0.4	0.65	0.27	0.99	0.06	0.91	0.6	0
16	0.3	0	0.2	0.62	0.12	0.15	0.05	0.1	2.28	0.64
17	0.5	0.1	0.4	0.8	0.68	0.81	0.58	0.92	0.87	0.64
18	0.2	0.1	0.2	0.28	0.45	0.29	0.39	0.42	0.41	0.46
19	1.5	0.3	0.5	1.58	0.38	2.31	1.29	0.53	0.84	3.12
21	4	4.1	4.2	5.26	6.79	2.16	3.5	2.4	6.31	4.7
22	1.1	0.7	1.1	2.14	0.77	1.9	1.67	0.32	1.75	0.53
23	4	3.3	4.3	3.33	3.28	5.94	4.01	3.75	4.66	2.93
24	0.8	1.3	2.6	1.28	1.51	1.93	0.89	1.05	0.99	0.6
25	8.9	9.4	11	10.7	8.61	8.15	14	9.37	8.73	10.9
26	8.4	7.3	15	12.5	15.3	1.39	17.6	6.06	8.15	10.6
27	8.9	20	13	11.5	15.4	9.75	8.87	11.8	2.8	6.41
28	6.3	7.8	6.5	3.02	3.03	4.83	1.94	6.91	0.97	3.26
29	14	14	13	9.78	12	9.42	11.7	16.8	12	8.22
30	2.1	2.4	3.3	4.9	3.63	0.59	3.02	3.19	2.36	1.84
31	14	11	8.6	6.25	7.65	12.9	7.21	11.9	7.87	16
32	3.7	3.7	1.3	0.81	1.01	2.66	0.65	2.06	1.19	3.79
33	0	0	0.2	0.27	0	0	0	0.23	0	0
34	1.3	1.2	2.4	5.37	3.23	1.91	2.06	1.46	3.12	0.51
35	0.9	0.4	0.1	0.75	0.57	0.41	0	0.5	0.67	1.03
36	1.3	1.1	0.4	1.23	1.24	0.11	0.66	0.9	1.66	1.98
37	1.2	1.1	1.3	1.52	2.22	2.14	1.4	1.74	1.79	1.49
38	0	0.4	0.4	0.07	0.58	1.1	0	0.84	0	0.15
39	1.2	0	0.7	1.18	0.48	1.42	0.59	0.71	0.25	0.8
Tot	100	100	100	100	100	100	100	100	100	100

TABLE 5 (CONTINUED)

	SITE NUMBER									
CT	14	15	16	17	18	19	20	21	27	28
1	1.76	2.47	4.64	2.05	0.4	0.3	0.3	1.1	0.3	0.5
2	2.99	3.94	2.73	1.58	1.16	1.1	0.5	0.5	0.9	1.1
3	1.24	0.18	0.98	0.46	0.01	0	0.1	0.1	0	0.1
4	0.45	0.91	2.08	2.24	1.05	1.8	0.2	0.4	0.4	0.8
5	2.69	1.79	1.48	1.5	0.76	1	0.2	0.4	1.3	1.3
6	3.45	3.93	3.66	9.01	7.8	9.7	1.7	1.7	3.7	2.9
7	3.66	2.07	7.05	1.78	2.91	2.4	1.6	1.1	1.2	1.1
8	11.4	4.93	3.67	4.25	6.18	8.4	1.7	1.1	1.4	0.6
9	8.68	8.5	5.68	3.71	5.06	8.1	0.7	1.7	2.1	1.5
10	1.32	3.03	3.82	4.09	1.34	0.5	0.9	2	1.4	1.4
11	3.89	5.84	4.31	2.22	0.33	0.4	1.6	1.6	1.4	1.0
12	1.32	0.71	0.96	0.21	0.07	0.0	1.6	1.1	0.8	0.2
13	2.86	1.61	1.4	1.21	0.74	0.1	0.2	0.1	0.3	0.5
14	0.73	0.95	0.09	0.62	1.26	0.0	0.0	0.0	0.3	0.1
15	3.18	1.58	1.95	1.6	0.69	0.1	0.4	0.2	0.2	0.2
16	0.29	0.81	1.51	1.23	1.38	0.3	0.5	0.4	0.1	0.4
17	1.9	1.63	1.28	1.86	0.61	0.5	0.5	0.5	0.3	0.5
18	0.19	0.69	0.98	1.01	0.25	0	0.3	0.3	0.9	0.7
19	4.15	1.13	3.01	3.4	5.65	4.1	2.0	0.7	0.1	0.1
21	3.3	3.62	3.07	3.18	1.93	0.8	3.9	5.8	5.8	5.1
22	1.12	1.75	1.59	2.2	0.48	0	0.5	0.5	1.3	1.3
23	4.17	4.75	2.69	1.55	1.66	0.8	1.2	1.4	2.5	2.0
24	0.7	2.23	2.7	2.77	1.67	0.1	1.0	3.2	1.5	2.9
25	1.89	6.66	5.73	5.42	6.65	6.0	8.0	11	13	13
26	1.66	3	3.96	8.92	8.82	18	13	11	17	10
27	11.9	4.27	7.54	8.75	13.4	12	15	15	5.8	12
28	2.55	2.12	2.24	2.36	3.36	2.2	5.8	4.6	1.9	2.3
29	4.41	7.03	5.42	6.17	12.9	15	11	13	13	17
30	0.58	1.42	1.32	2.87	1.56	0.8	4.0	3.4	4.8	3.9
31	7.44	9.35	6.56	6.1	2.42	1.5	15	12	13	8.7
32	0.83	0.48	0.84	0.54	0.46	0.3	2.6	1.3	0.5	1.2
33	0	0.17	0	0	0.08	0	0.1	0	0	0
34	1.43	1.86	2.21	2.54	2.41	1.6	0.5	0.7	0.4	2.2
35	0.26	0.8	0.41	0.72	0.64	0	0.1	0.1	0.1	0
36	0.27	1.49	1.1	1.16	0.78	0.4	0.9	1.3	0.4	0.3
37	0.73	2.11	1.11	0.42	0.7	0.2	1.2	0.8	1.7	3
38	0	0.03	0.08	0.16	0.92	0.2	0.1	0.3	0	0.1
39	0.56	0.15	0.12	0.18	1.47	1.8	1.1	0.3	0.3	0.2
Tot	100	100	100	100	100	100	100	100	100	100

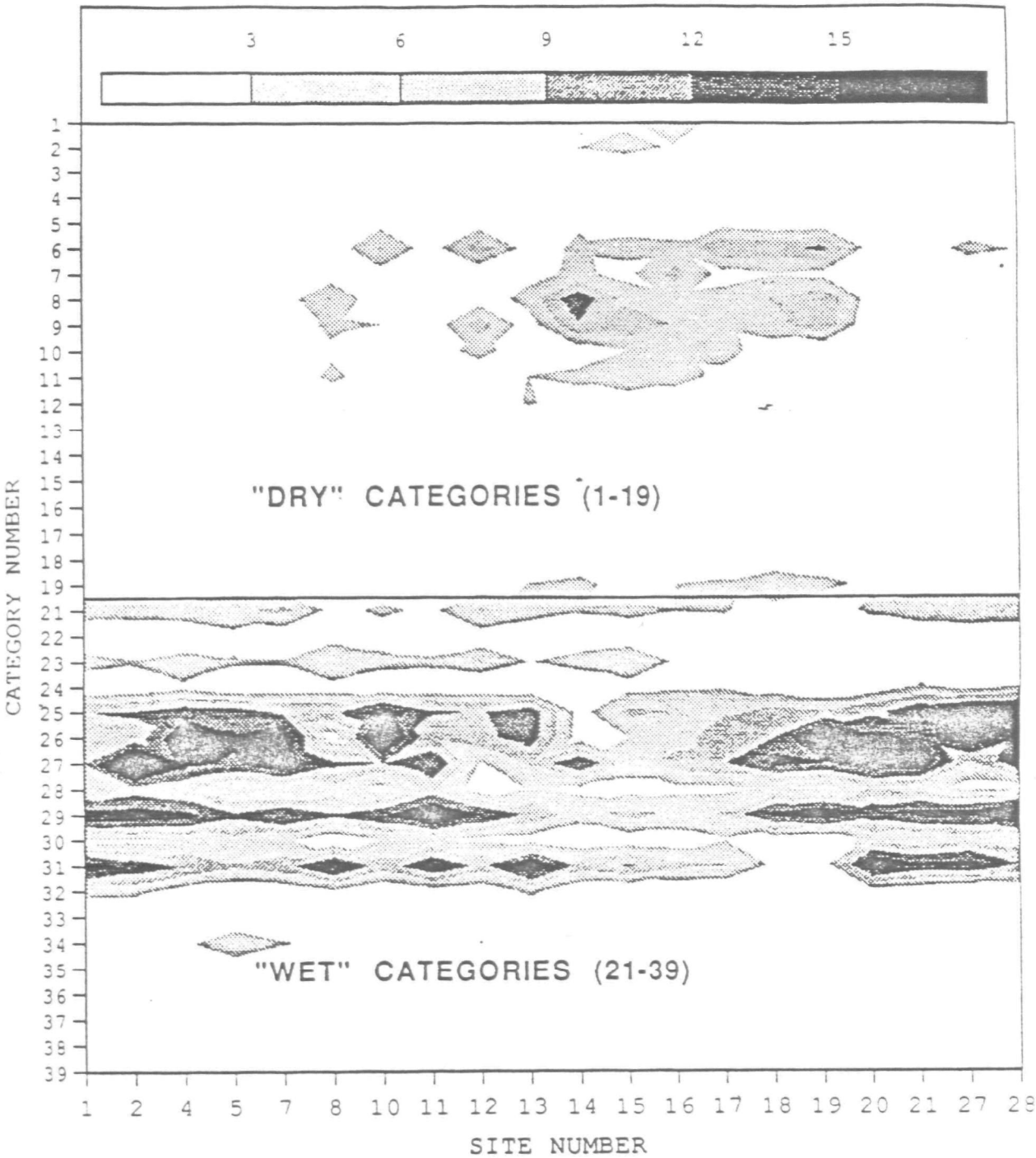

Figure 10. The percentage of total $SO_4^=$ wet deposition associated with each meteorological category by site.

A total of 9 to 15 categories (from the 38) were needed to explain 75% of the wet $SO_4^=$ deposition at each site during 1982-1985. Rather than try to produce an aggregate estimate which would be best for the entire domain shown in Figure 1 (which would require up to 15 categories) it was decided to focus on a smaller northeastern region encompassing 13 sites. (The eastern sites have been identified in Figure 1 and Table 2). With the domain restricted to the eastern sites a total of 9 categories were needed to approach the 75% goal. These 9 categories represent a minority of the 850 mb wind flow patterns, it is likely that a modest number of sample events will represent the meteorological processes that affect $SO_4^=$ wet deposition across eastern North America. The identified categories also make sense in terms of the physical processes (i.e. storm tracks) represented.

Table 6 shows that the 9 categories with greatest $SO_4^=$ deposition (21, 23, 25, 26, 27, 28, 29, 30 and 31) accounted for about 72% of the total $SO_4^=$ deposition within the 13 site region. The curve in Figure 10 indicates the total amount of deposition accounted for as the number of categories selected increased. To explain more and more of the deposition one needed more categories at an increasing rate. The cost-to-benefit ratio changed drastically with more stringent requirements. As a first approximation the nine categories mentioned above were selected to be represented in the aggregation scheme.

While the 9 major categories account for the bulk of $SO_4^=$ wet deposition, concern has arisen that some important physical processes may be excluded by the 9-category selection criterion. Many of the important categories occurred primarily in the warm season. Cold-weather processes (which may be highly nonlinear in terms of source-receptor relationships) might be neglected by a selection process limited to the major categories. In addition, it was decided to include a number of 3-day events on which very little precipitation fell in the final ensemble. Inclusion of "dry" events enable the final analysis to include dry deposition processes.

It was decided that due to external constraints (RADM modeling budget) no more than 30 cases could be included in the final ensemble. It was also decided that from the nine important categories up to 20 cases would be selected to reproduce the annual $SO_4^=$ deposition pattern and that the other ten cases would be selected to account for other, less prevalent conditions (winter precipitation, unusual meteorology and dry deposition). The final mix of episodes included (1) an array of episodes chosen from categories that account for the bulk of the annual $SO_4^=$ wet deposition, and (2) an array of episodes chosen to represent potentially neglected processes: cold season events and events with little rainfall that may contribute significant dry deposition.

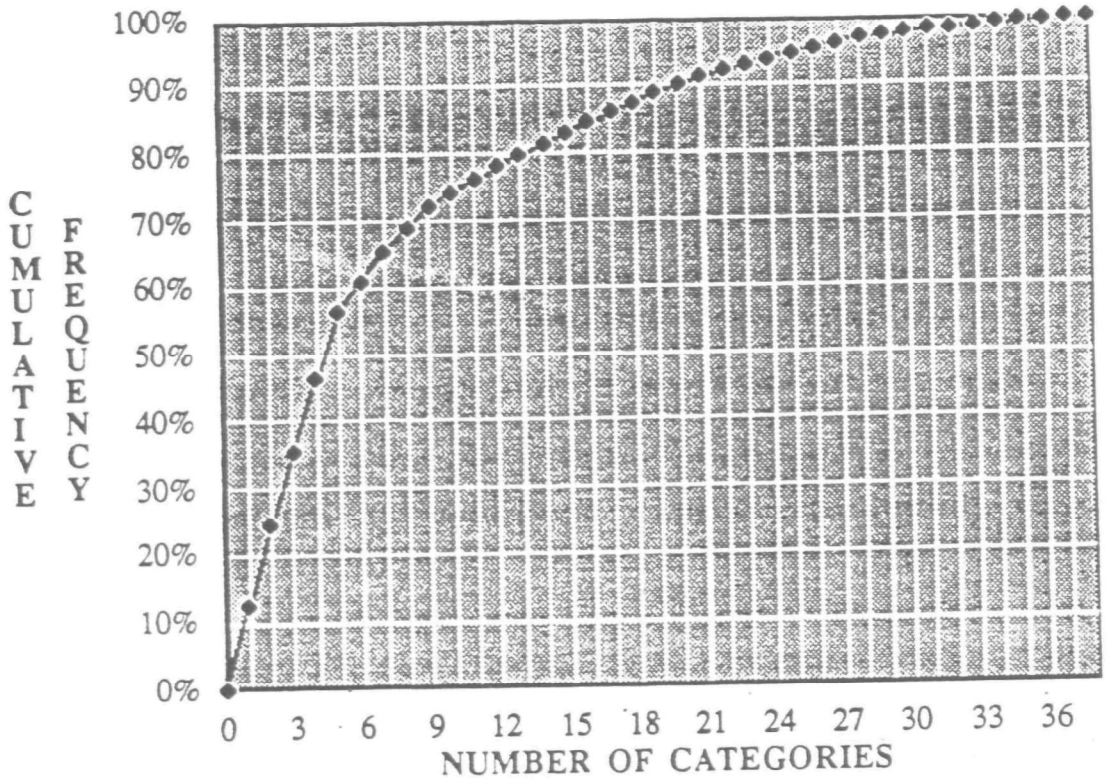

Figure 11. Cumulative explanation of total $SO_4^=$ deposition using categories ranked from greatest to least deposition.

To determine how the cases should be partitioned among the 9 important categories the percent of total wet $SO_4^=$ deposition figures shown in Table 6 were considered. Relative to their percent contribution, a proportionate number of samples were selected from each of the categories. The frequency of occurrence was also taken into consideration. Constrained to whole numbers, the following breakdown of category sampling was subjectively determined: four cases were to be selected from category 29, three from 27, 26 and 31, two from 25 and one from 21, 23, 28 and 30. Initial tests of the aggregation procedure were then based upon 19 cases selected at random but according to the predetermined sampling criteria.

TABLE 6. PERCENT OF TOTAL SULFATE WET DEPOSITION BY METEOROLOGICAL CATEGORY

Category	Total Dep.	% of Tot.
1	1,927	0.72
2	2,459	0.92
3	474	0.18
4	1,042	0.39
5	2,112	0.79
6	5,638	2.11
7	3,683	1.38
8	4,189	1.57
9	4,570	1.71
10	3,857	1.44
11	4,474	1.67
12	2,854	1.07
13	796	0.3
14	517	0.19
15	970	0.36
16	789	0.3
17	1,582	0.59
18	1,060	0.4
19	2,459	0.92
21	11,953	4.47
22	3,347	1.25
23	8,683	3.25
24	4,381	1.64
25	27,497	10.29
26	28,978	10.84
27	32,625	12.21
28	11,725	4.39
29	33,151	12.4
30	9,108	3.41
31	29,049	10.87
32	5,134	1.92
33	254	0.09
34	5,252	1.96
35	1,046	0.39
36	2,467	0.92
37	4,212	1.58
38	917	0.34
39	2,072	0.78

Eleven additional cases were selected to represent winter situations, which were hypothesized to have a higher proportion of non-linear effects, and dry deposition events. The basic criteria for sampling these days were as follows: five relatively wet winter cases and six dry cases (the sum of the 13 site $SO_4^=$ deposition was less than 50 mgm^{-2}) from previously unsampled categories. Given the number of categories from which these cases could be selected it was impossible to sample proportionately, therefore, other criteria were developed. The winter cases were selected from the "wet" (21-39) categories that displayed a relatively high frequency in winter. This reduced the number of possible categories to 22, 24, 32, 34 and 37. From this set the five cases were selected randomly, one from each. For the dry situation the first step in determining the set of categories from which to sample was to consider only the "dry" half (categories 1-19) . The second step was to isolate the more frequently occurring categories which also had a low mean deposition. Categories 6, 7, 8, 9, 11, and 19 met these requirements. From this subset, six cases, each with a total 13-site wet $SO_4^=$ deposition of less than 50 mgm^{-2} were randomly selected, one from each category.

3.1.3. Statistical correlations between category and observed deposition

As described above, wet deposition amounts received at various sites show considerable variation for events among different categories. In this section results of statistical tests of the correlation between deposition, precipitation and meteorological category will be presented.

3.1.3.1. Three alternative statistical approaches—

The statistical analysis will be based on the techniques of regression discussed above which use correlations between wet deposition and (a) observed precipitation, (b) time of year, and (c) meteorological category. Of the various factors which may be correlated with deposition precipitation is apparently the most important, and results of regression analyses may depend critically on the treatment of the relationship between deposition and precipitation. Three alternative correlations between wet deposition and precipitation were investigated. These were:

- Linear correlation between wet deposition and precipitation (Equation 19);
- Logarithmic correlation between wet deposition and precipitation (Equation 23); and
- A hybrid model correlating deposition with precipitation raised to an exponential power (Equation 24).

Each of the three approaches has advantages. A straight linear regression has the advantage of simplicity; and the regression parameters ($\beta_{cat(i)}$ in Equation 19) simply correspond to the summed deposition-to-precipitation ratio observed during events associated with each meteorological category. The logarithmic model, by contrast, has the advantage of accounting for

the observed tendency for $SO_4^=$ and NO_3^- concentrations to decrease during high-precipitation events (Stein and Niu, 1988). This tendency is especially important at coastal sites. However the logarithmic model has two serious disadvantages. First, evaluations of the accuracy of the logarithmic regression are based on the estimate for log D_i rather than for D_i itself. Consequently the logarithmic regression gives undue weight to events with very small amounts of deposition, which have negligible impact on total wet deposition received at a site. On low-deposition days, the recorded discrepancy between observed deposition and deposition estimated from a linear regression model ($D_i - \hat{D}_i$) will be small, but the discrepancy recorded with a logarithmic model ($\log D_i - \log \hat{D}_i$) can be very large. For this reason we evaluated the accuracy of logarithmic models based on the linear coefficient of variation (i.e. ability to predict D_i , Equation 22) rather than based on its ability to predict log D_i .

A second disadvantage of the logarithmic model is that it requires twice as many regression variables as does a simple linear regression. Referring to Equation 23, if both regression variables (β and γ) are allowed to be category-dependent, then the regression will contain 40 independent variables. Accounting for other factors (i.e. time of year) increases the number of independent variables still further. It becomes increasingly difficult to demonstrate statistical significance when a model contains such a large number of independent variables.

The combined model represents an attempt to preserve the advantages of linear as opposed to logarithmic models while at the same time allowing for the tendency for $SO_4^=$ and NO_3^- concentrations to decrease during events with heavier precipitation. The combined model is based on a linear regression of wet deposition with P_i^{γ} as the independent variable. The exponent γ is derived from logarithmic regression (Equation 23). The exponent is allowed to vary for different sites and for different species (i.e. $SO_4^=$ and NO_3^-) but is not allowed to vary with time of year or meteorological category. Category-based variations in deposition are represented by allowing the linear regression parameter ($\beta_{cat(i)}$ in Equation 24) to vary with category.

3.1.3.2. Time-of-Year Term —

Wet deposition rates for both $SO_4^=$ and NO_3^- both show strong seasonal dependence, with $SO_4^=$ wet deposition rates typically much larger in summer than in winter and NO_3^- showing the opposite trend. It has been suggested by Stein (1989) that the observed correlation between wet deposition and meteorological category might result from the seasonal nature of wet deposition rather than from intrinsic differences in circulation pattern among the categories. In order to avoid this error we have introduced time of year as an additional independent parameter in the regression analysis. Inclusion of the time-of-year term serves two purposes: (a) it improves the overall performance of the regression model by including season-based variations in wet deposition within the model; and (b) it insures that correlations between observed wet deposition and meteorological category are not just a reflection of seasonal variations.

Season-based variability is represented in the combined regression model by adding a

time-of-year term Y_i with a value based on the day of the year:

$$Y_i = \sin [2\pi(N_D-81)/365] \tag{26}$$

where N_D is the Julian day, ranging from 1 (January 1) to 365 (December 31). The time-of-year term is incorporated in the linear and log-linear regression models by replacing the regression equation (24) with the following:

$$\hat{D}_i = \beta_o (1+\delta Y_i) P_i^{\gamma} \tag{27}$$

where δ is a regression parameter which is regarded as independent of meteorological category. The combined regression model (27) was developed in stages, with β_o (without category-dependence) and δ initially determined from a linear regression independent of meteorological category. After δ was determined, a second linear regression was performed to identify the category specific parameters $\beta_{cat(i)}$. The second linear regression used the following equation

$$\hat{D}_i = \beta_{cat(i)} (1+\delta Y_i) P_i^{\gamma} \tag{28}$$

with the category-specific $\beta_{cat(i)}$ parameters determined by regression of D_i against the linear variable $(1+\delta Y_i)P_i^{\gamma}$ (with γ and δ fixed). This indirect method was chosen to minimize the number of independent regression parameters and to insure that the the parameters represent physically meaningful quantities. In the completed model (Equation 28) there were 22 independent variables, including 20 category-specific $\beta_{cat(i)}$ parameters plus γ and δ.

3.1.3.3. Results —

The linear, logarithmic and combined models were evaluated as predictors of $SO_4^=$ and NO_3^- wet deposition based on linear coefficient of determination (R^2) (Equation 22). Note that R^2 associated with the logarithmic model is the linear R^2 and tests model ability to predict deposition, rather than log *D*. Results (Table 7) show that the logarithmic model achieves significantly higher R^2 values than the linear model for some sites, especially coastal sites (e.g. Turners Falls, MA) where the correlation between deposition and precipitation was weak. However the linear model achieves higher R^2 than the logarithmic model at other locations (e.g. Longwoods, ON).

The combined model appears to represent a significant improvement over both the linear and logarithmic models. The R^2 coefficients were higher for the combined model than for the logarithmic model at all sites, despite the fact that the combined model had fewer independent parameters (21 as opposed to 40 in the logarithmic model). The combined model also had higher R^2 than the linear model at most sites. However there were some sites where the linear model achieved an R^2 equal to or greater than the combined model.

Incorporating the time-of-year parameter in the combined model resulted in a significant improvement at many sites, with reductions in the residual uncertainty ($1-R^2$) of up to 25%.

At other sites incorporation of the time-of-year term had negligible effect. The time-of-year term had greatest impact at locations with severe winters (e.g. Underhill, VT) and at coastal sites, and little impact at southern or western sites.

Incorporation of category-dependent β parameters (as opposed to a single β_0 independent of meteorological category) caused an improvement in R^2 in all models. Inclusion of category dependence caused an improvement even when the seasonal dependence of wet deposition had already been included in the regression. Residual uncertainty was reduced by ~10% when category-dependent β's were included (e.g. R^2 increases from 0.55 to 0.59 at Tunkhannock, PA).

Statistical significance of category-dependent parameters $\beta_{cat(l)}$ was evaluated by the heterogeneity-of-slopes statistic F_s (Equation 20). As described earlier the null hypothesis that meteorological category had no impact on deposition ($\beta_1 = \beta_2 = ... = \beta_l$ for all categories) was rejected with 95% confidence whenever F_s assumed a value of 1.66 or greater.

Also shown in Table 7A, the F_s statistic demonstrated that category-based variations in $SO_4^=$ wet deposition were significant at the 95% confidence interval or higher at all sites included in this study. For NO_3^- (Table 7B) wet deposition category-based variations were significant at 18 of the 20 sites. The remaining two sites, Selma, AL and Brookings, SD, were both at the geographic edge of the region represented by the meteorological categorization scheme.

Coefficients of determination (R^2) in the combined model were greater than 0.5 at most sites, indicating that the regression was able to account for 50% or more of the variation in observed wet deposition. The R^2 coefficient was significantly lower at coastal sites (Turners Falls, MA and Winterport, ME) and at sites that may be influenced by a nearby emission source (i.e. Fort Wayne, IN., downwind of Chicago). At these sites significant variations in wet deposition rates could have been caused by small changes in local wind direction.

TABLE 7A. LINEAR R^2 COEFFICIENTS ARE SHOWN FOR THE LINEAR REGRESSION MODEL FOR $SO_4^=$ WET DEPOSITION (USING EQUATION 19), LOGARITHMIC MODEL (EQUATION 23), COMBINED MODEL (EQUATION 24) AND COMBINED MODEL WITH TIME-OF-YEAR TERM INCLUDED (EQUATION 29). ALL MODELS HAVE β PARAMETERS VARYING WITH METEOROLOGICAL CATEGORY. THE HETEROGENEITY-OF-SLOPES STATISTIC F_S (EQUATION 20) IS SHOWN FOR THE COMBINED MODEL (TIME OF YEAR TERM INCLUDED).

	R^2 (Sulfate Wet Deposition)				
SITE	LINEAR	LOG	COMBINED	COMBINED + TIME-OF-YEAR	F_S
Turners Falls, MA	.144	.236	.273	.373	2.33
Tunkhannock, PA	.357	.438	.448	.591	3.29
Zanesville, OH	.731	.682	.730	.790	7.62
Rockport, IN	.631	.599	.641	.719	4.96
Giles County, TN	.575	.574	.590	.653	1.91
Fort Wayne, IN	.305	.313	.373	.433	1.78
Raleigh, NC	.656	.619	.658	.683	2.95
Gaylord, MI	.609	.547	.605	.662	5.08
Alamo, TN	.406	.373	.463	.542	3.32
Winterport, ME	.347	.384	.422	.481	5.79
Uvalda, GE	.266	.214	.276	.355	1.97
Selma, AL	.379	.430	.467	.510	4.42
Clinton, MS	.365	.403	.432	.471	2.77
Marshall, TX	.591	.651	.666	.682	1.81
Lancaster, KN	.727	.707	.731	.735	3.80
Brookings, SD	.726	.731	.744	.745	1.81
Underhill ,VT	.436	.396	.455	.603	8.18
Big Moose, NY	.418	.358	.428	.617	5.63
Dorset, ON	.576	.516	.573	.639	3.79
Longwoods, ON	.780	.678	.746	.822	4.16

TABLE 7B. LINEAR R^2 COEFFICIENTS ARE SHOWN FOR THE LINEAR REGRESSION MODEL FOR NO_3^- WET DEPOSITION (USING EQUATION 19), LOGARITHMIC MODEL (EQUATION 23), COMBINED MODEL (EQUATION 24) AND COMBINED MODEL WITH TIME-OF-YEAR TERM INCLUDED (EQUATION 29). ALL MODELS HAVE β PARAMETERS VARYING WITH METEOROLOGICAL CATEGORY. THE HETEROGENEITY-OF-SLOPES STATISTIC F_S (EQUATION 20) IS SHOWN FOR THE COMBINED MODEL (TIME OF YEAR TERM INCLUDED).

	R^2 (Nitrate Wet Deposition)				
SITE	LINEAR	LOG	COMBINED	COMBINED + TIME-OF-YEAR	F_S
Turners Falls, MA	.064	.184	.223	.284	1.60
Tunkhannock, PA	.282	.479	.490	.547	2.37
Zanesville, OH	.623	.613	.667	.695	5.36
Rockport, IN	.498	.516	.552	.644	4.89
Giles County, TN	.480	.555	.577	.589	2.34
Fort Wayne, IN	.283	.349	.404	.488	1.92
Raleigh, NC	.496	.496	.532	.532	2.32
Gaylord, MI	.591	.535	.599	.631	4.26
Alamo, TN	.340	.462	.524	.612	2.93
Winterport, ME	.024	.170	.226	.286	6.62
Uvalda, GE	.360	.336	.389	.504	1.98
Selma, AL	.366	.478	.507	.647	1.04
Clinton, MS	.444	.507	.538	.667	1.74
Marshall, TX	.524	.577	.597	.682	3.68
Lancaster, KN	.752	.737	.755	.780	3.05
Brookings, SD	.709	.716	.740	.751	1.30
Underhill ,VT	.401	.439	.472	.498	7.05
Big Moose, NY	.329	.384	.425	.433	5.24
Dorset, ON	.426	.419	.458	.464	1.96
Longwoods, ON	.666	.568	.629	.670	6.99

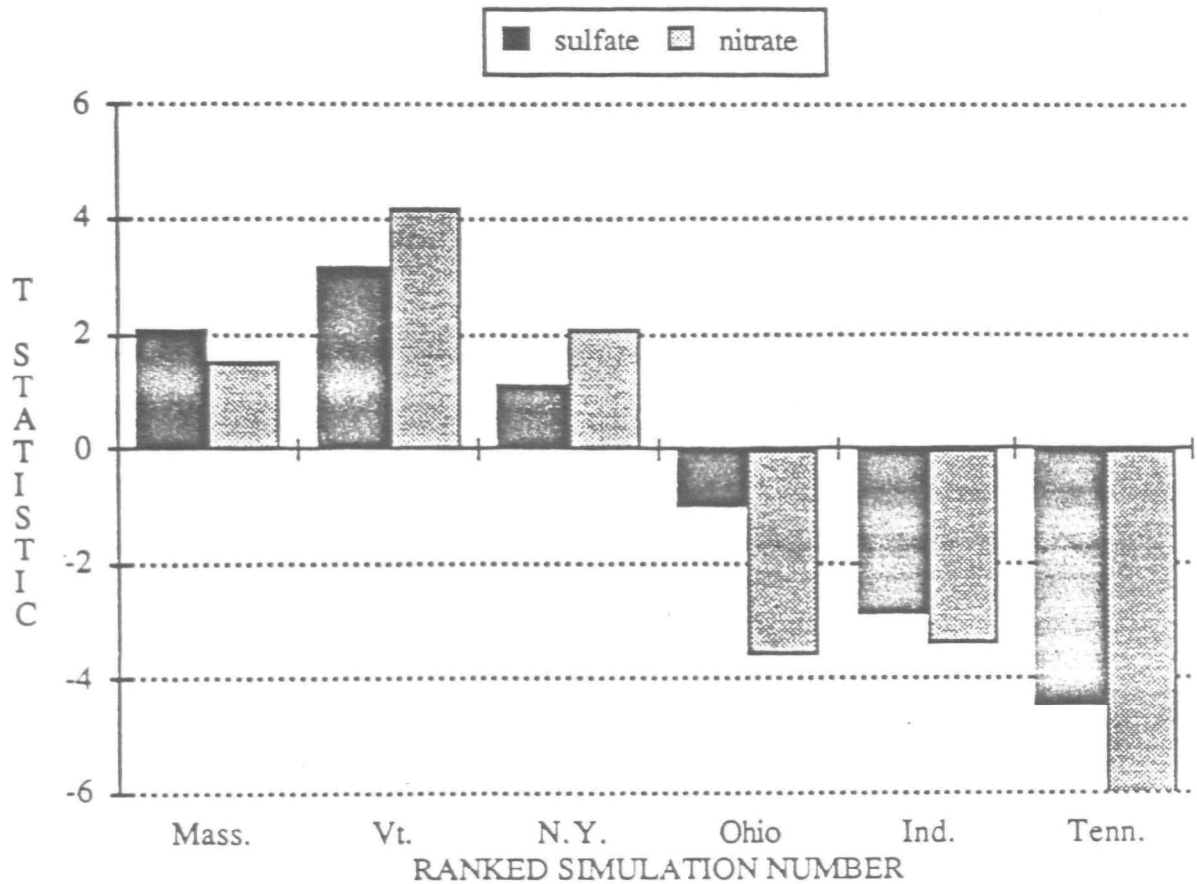

Figure 12. T_s statistic for meteorological category 6, indicating deposition-to-precipitation ratios significantly above or below the norm at each site. Values of greater than 1.66 or less than -1.66 are statistically significant at the 95% confidence level.

Although much of the remaining variations in $SO_4^=$ and NO_3^- wet deposition may be due to random fluctuations, there was evidence that at least some of the remaining variations may be related to meteorological factors other than the ones represented here. Evidence of further meteorological influence was based on the high correlation (correlation coefficients >0.8) between residual errors in $SO_4^=$ wet deposition at a given site and residual errors in NO_3^- at a given site. In other words, when the amount of $SO_4^=$ wet deposition observed during a specific event exceeded the amount predicted from the statistical correlation, there was a high probability that the amount of NO_3^- also exceeded the predicted value. Residual errors in $SO_4^=$ wet deposition at each site were also positively correlated with residual errors at neighboring sites (especially in the Northeast), though there was little correlation with errors at distant sites. These two results suggest that the residual errors were associated with aspects of atmospheric circulation that were not adequately represented in the categorization.

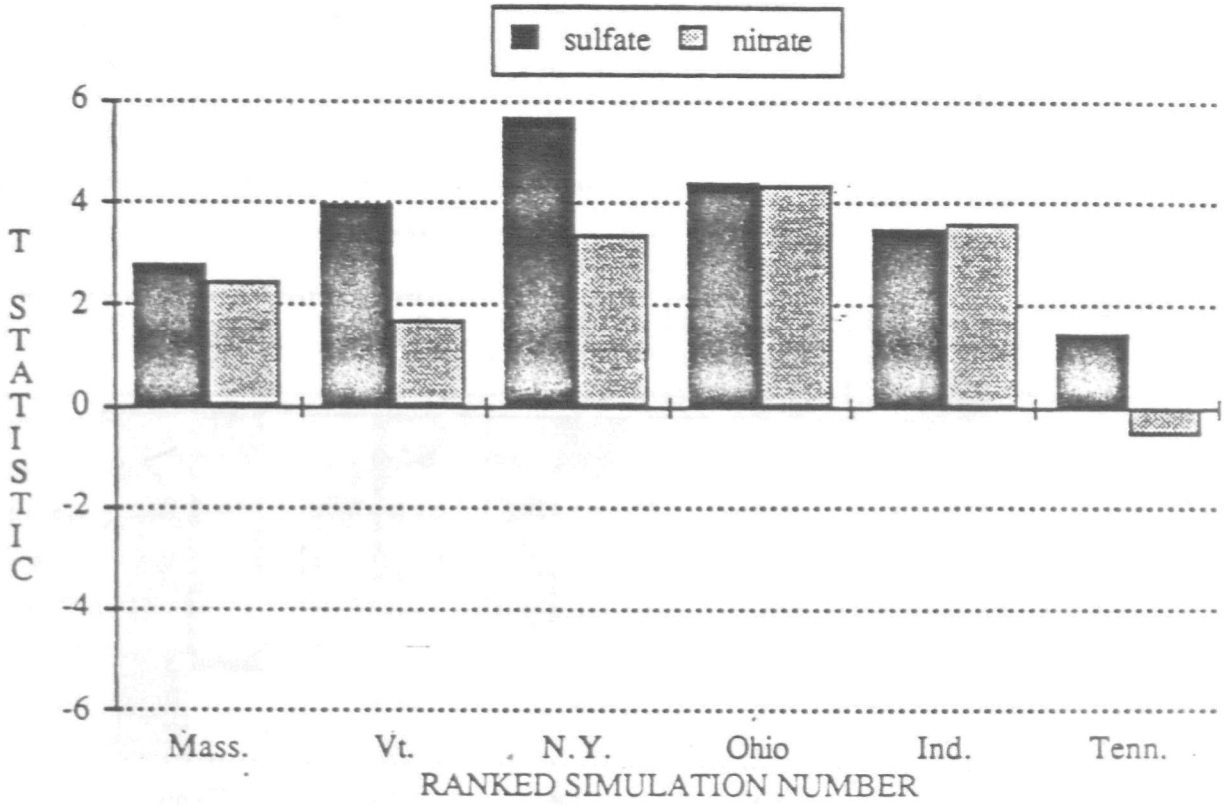

Figure 13. T_s statistic for meteorological category 7, indicating deposition-to-precipitation ratios significantly above or below the norm at each site. Values of greater than 1.66 or less than -1.66 are statistically significant at the 95% confidence level.

Additional insights regarding deposition rates for various categories was obtained by comparing the statistical significance of deposition associated with individual meteorological categories with the norm at individual sites. As described earlier, the statistic T_s (Equation 21) indicated when deposition associated with individual categories was significantly greater or less than the norm. Some values for the T_s statistic are shown in Figures 12 through 14, based on the initial linear model (Equation 19).

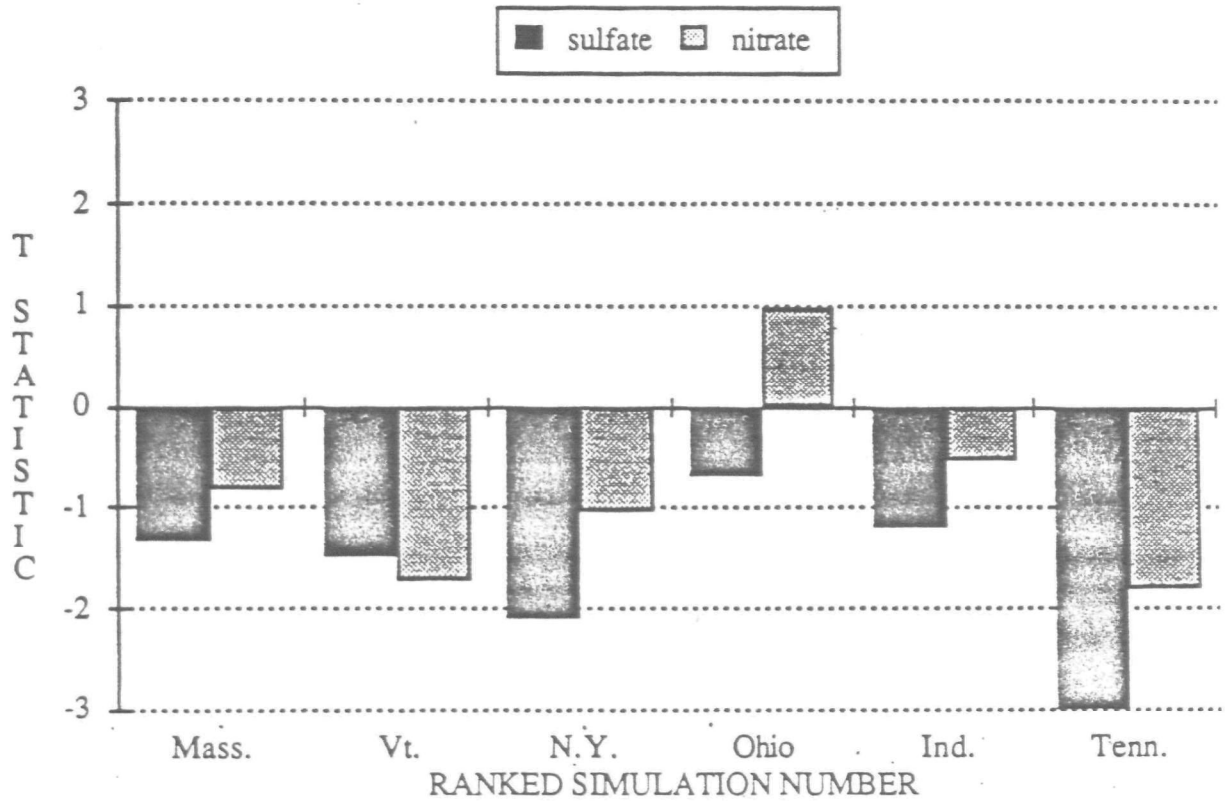

Figure 14. T_s statistic for meteorological category 11, indicating deposition-to-precipitation ratios significantly above or below the norm at each site. Values of greater than 1.66 or less than -1.66 are statistically significant at the 95% confidence level.

Results showed that some categories (most notably the stagnant "waffling high", category 7) had significantly greater than average deposition at sites across the eastern and midwestern U.S., while categories marked by more vigorous circulation (e.g. category 11) have deposition below average. An interesting result was obtained for category 6, where deposition was significantly greater than average at northeastern sites and significantly below average at sites in the Ohio valley. Category 6 was characterized by a cold front in the eastern U.S. with a weak southwesterly flow ahead of the front and more vigorous winds behind it.

Figures 12 through 14 also illustrate the similarity in patterns of wet deposition of $SO_4^=$ and of NO_3^-. Greater than average wet deposition of NO_3^- was consistently associated with above

average wet deposition of $SO_4^=$, despite the fact that $SO_4^=$ and NO_3^- show different seasonal variations.

3.1.4. Interannual Variability

The use of either analytical or statistical techniques to predict future wet deposition rates raises questions concerning year-to-year variations in both deposition and meteorology that might affect the accuracy of predictions. Wet deposition can vary from year to year due to meteorological fluctuations, including changes in precipitation and changes in atmospheric circulation patterns; and some of this variance may be the result of long-term climatic changes. Although the meteorological categorization and aggregation methods presented here have been based on observations made during the period from 1982 to 1985, we believe the same techniques may be applied to future years.

This section will present a summary of interannual variations in $SO_4^=$ and NO_3^- wet deposition observed during the period 1982-1987, and to possible correlation with meteorology. The extent of interannual variations will be used to establish the level of uncertainty in aggregated estimates for annual deposition. This uncertainty may be reduced somewhat if year-to-year variations are correlated with observable (and possibly predictable) changes in meteorology. Special attention will be given to results from the years 1986 and 1987, which were not included in the development of the meteorological categorization and aggregation techniques.

Figures 15 through 17 show annual fluctuations in wet $SO_4^=$ wet deposition, precipitation and $SO_4^=$ wet deposition-to-precipitation ratios at three sites: Turners Falls, MA, Zanesville, OH and Giles County, TN; respectively. Two features of these fluctuations are worth comment. First, the year-by-year pattern shows significant differences among the three sites. Annual fluctuations in both wet deposition and precipitation are much greater at the Massachusetts site than in the two inland locations, possibly reflecting the importance of local meteorology at a location closer to the ocean. Year-to-year fluctuations in wet deposition average ~25% at the Massachusetts site, while at the Ohio site an annual variation of ~12% was more common. These differences are significant at a 95% confidence level. Second, the year 1987 stands out as a year of unusually low $SO_4^=$ wet deposition, although this may be partly due to errors in the data.[2] At the Massachusetts and Tennessee sites observed $SO_4^=$ wet deposition rates are 30%-40% lower during 1987 than for the 1982-1985 period. Precipitation at these sites during 1987 is only slightly below normal, and the observed deposition-to-precipitation ratios are much lower than in the preceding years. This pattern of lower $SO_4^=$ wet deposition during 1987 was repeated at most other sites included in this study, with $SO_4^=$ wet deposition in 1987 aver-

---

[2]The sulfate wet deposition data for the second half of 1987 has recently been identified as in error due to problems in data analysis.

aging 24% lower than the 1982-1985 rates.

Nitrate deposition during 1987 is much closer to the 1982-1985 norm, although reduced NO_3^- was observed at the Massachusetts and Tennessee sites. At the Ohio site observed $SO_4^=$ wet deposition during 1987 close to the 1982-1985 average, and NO_3^- wet deposition is actually higher than average. The $SO_4^=$ wet deposition-to-precipitation ratio is also above average at the Ohio site. Statistical correlations (described below and in Section 3.1.3) show that nitrate deposition during 1987 was significantly below the 1982-1985 average at 5 of the 11 sites in the northeastern and midwestern United States,[3] and significantly above the 1982-1985 average at just one site.

The extent of year-to-year variations can be estimated by calculating the root-mean-square difference (RMSD) between wet deposition during individual years at each site and the 6-year average deposition at the site, i.e.

$$RMSD = \sqrt{\frac{1}{78}\sum_{i=1}^{6}\sum_{j=1}^{13}[D_{ji} - D_{j0}]^2} \qquad (29)$$

where D_{ji} is the observed deposition at site j for the ith year and D_{j0} is the observed 1982-1985 average deposition at site j. This interannual RMSD is equivalent to the RMSD used to evaluate aggregate estimates (Equation 9) and will be used both as a measure of inherent uncertainty and as a standard for evaluating aggregate estimates. The interannual RMSD for sulfate wet deposition at the 13 northeastern sites, expressed as a percentage of average annual deposition, is 0.13. For nitrate the interannual RMSD is 0.14.

Reasons for the observed year-to-year variations in wet deposition are not immediately apparent. There is some evidence that year-to-year variations may be due to local meteorological fluctuations, since there is a strong correlation between variations in sulfate deposition and variations in nitrate at each site. The tendency for sulfate and nitrate to exhibit similar variations is apparent in Figures 15-17. There is little correlation between sulfate and nitrate deposition at different locations, as would be expected if year-to-year variations were due to changed emission rates. However there is also little correlation between observed annual deposition and meteorological parameters (i.e. precipitation) or circulation patterns. Although there is some correlation between wet deposition to precipitation, the ratio of annual sulfate wet deposition to annual precipitation, also shown in Figures 15-17, varies significantly from one year to the next.

---

[3] Figure 2 identifies 13 northeastern and midwestern sites. The multi-site analysis in this section is based on 11 sites rather than 13, since data for 1986 and 1987 were missing for the two Canadian sites.

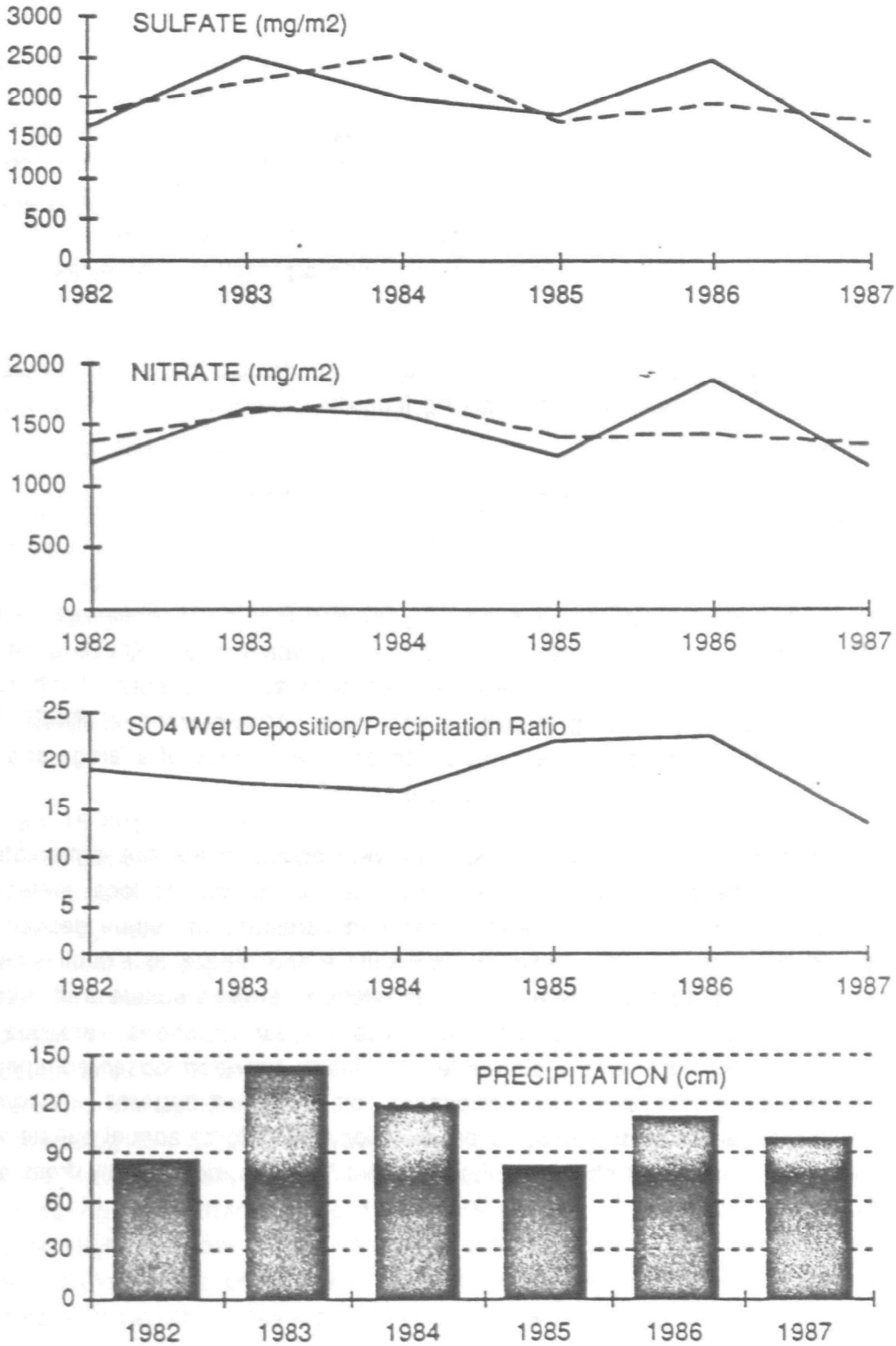

Figure 15. Year-by-year variation in $SO_4^=$ wet deposition, NO_3^- wet deposition, $SO_4^=$ wet deposition-to-precipitation ratio, and precipitation at Turners Falls, Massachusetts. Dashed lines represent predicted annual deposition based on meteorology and 1982-1985 statistical correlation.

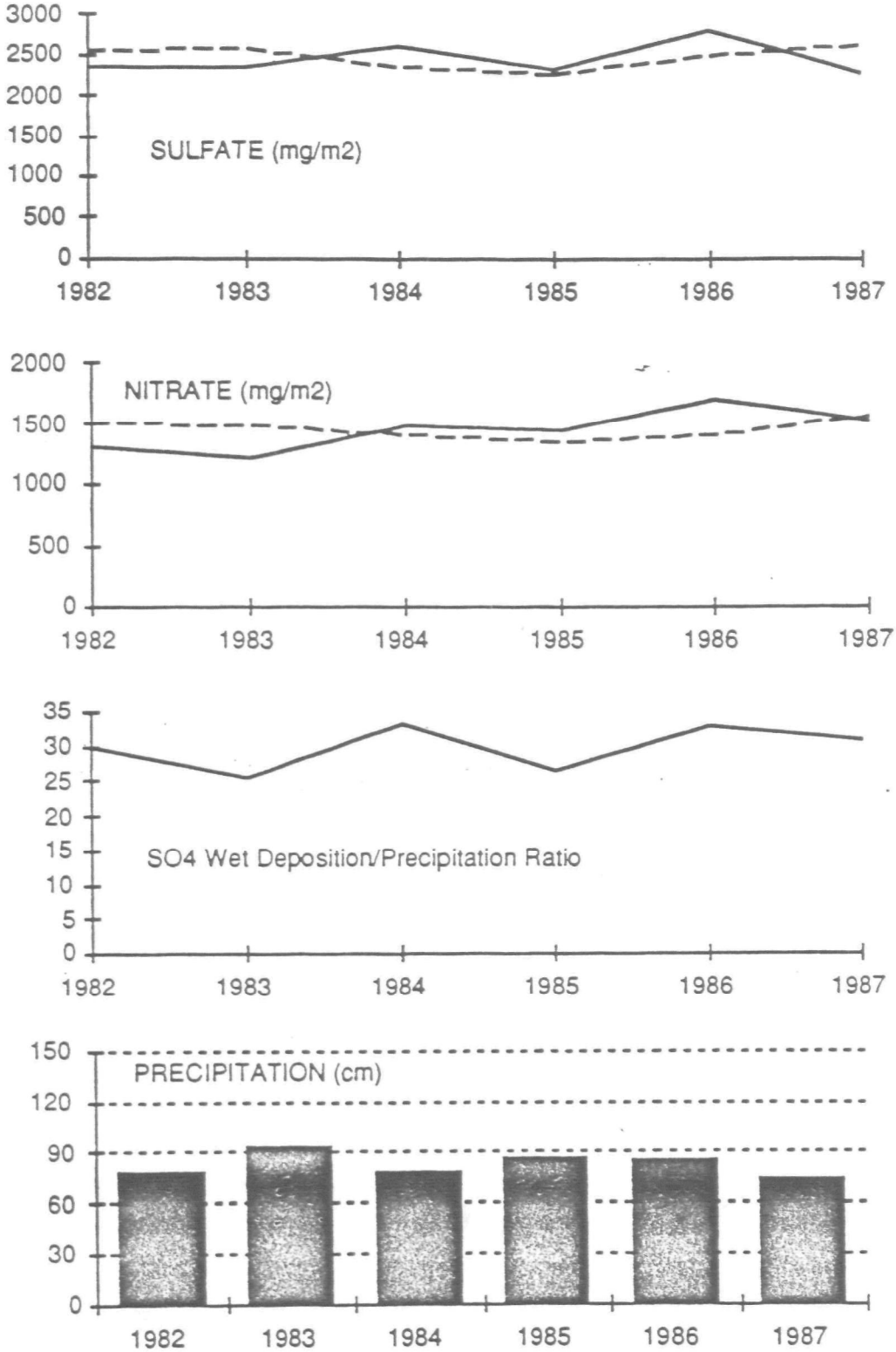

Figure 16. Year-by-year variation in $SO_4^=$ wet deposition, NO_3^- wet deposition, $SO_4^=$ wet deposition-to-precipitation ratio, and precipitation at Zanesville, Ohio. Dashed lines represent predicted annual deposition based on meteorology and 1982-1985 statistical correlation.

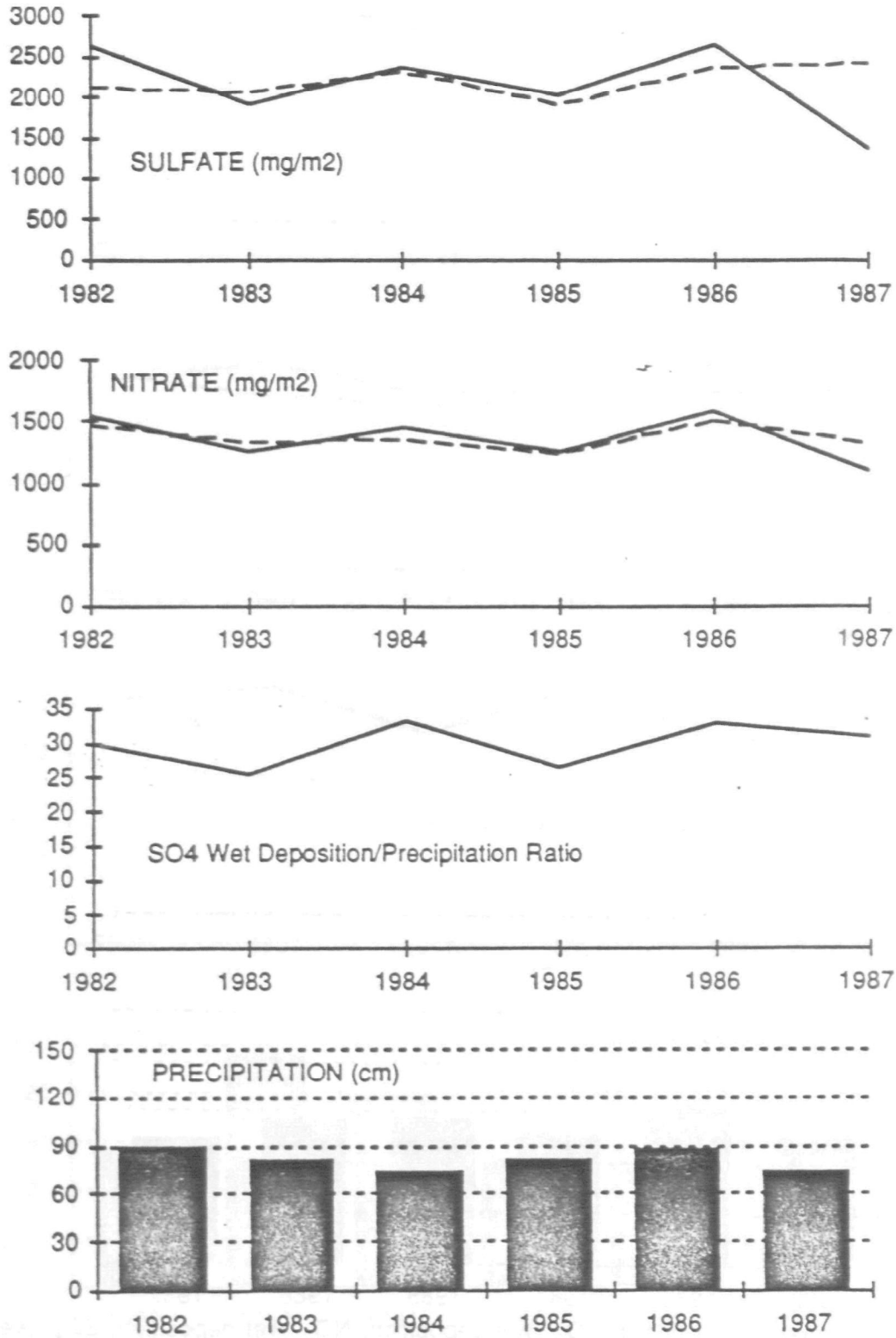

Figure 17. Year-by-year variation in $SO_4^=$ wet deposition, NO_3^- wet deposition, $SO_4^=$ wet deposition-to-precipitation ratio, and precipitation at Giles County, Tennessee. Dashed lines represent predicted annual deposition based on meteorology and 1982-1985 statistical correlation.

Year-to-year changes in atmospheric circulation can be represented by the frequency of occurrence of events corresponding to specific meteorological categories. Changes in frequency of occurrence have been plotted in Figure 18 for three of the most frequently occurring categories ("weak trof-southerly flow", category 6; "waffling high", category 7; and "northeast cold front", category 11). Variations in category frequency are approximately the same order of magnitude as year-to-year variations in precipitation or wet deposition (~10%). Since these categories can be associated with high or low wet deposition (see Figures 7 and 12-14), it is possible that these variations may explain some of the interannual variability.

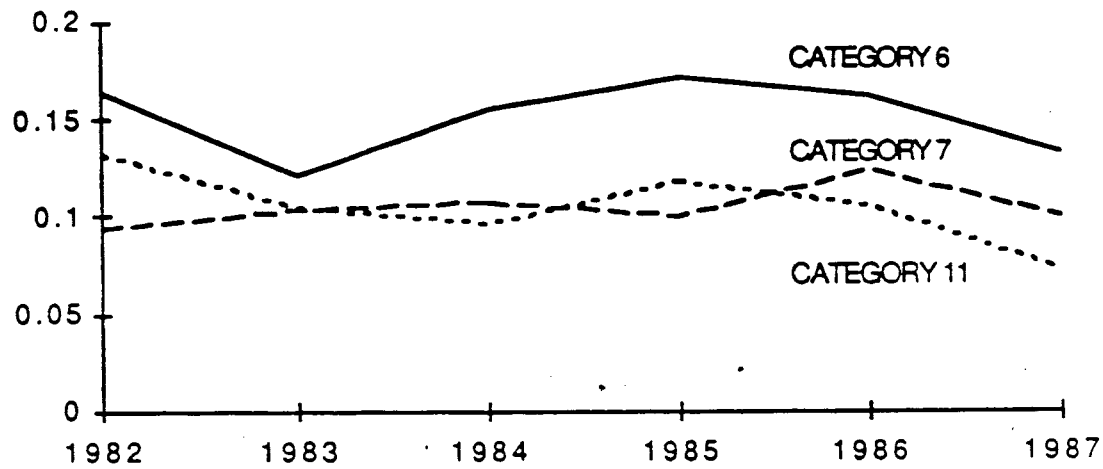

Figure 18. Year-by-year frequency of occurrence of events of meteorological categories 6, 7 and 11, expressed as a fraction of all events.

The impact of precipitation and meteorology on wet deposition for specific years can be estimated by applying the statistical model for event-specific correlations (Section 3.1.3) to the observed annual meteorological patterns. In the model deposition per event is correlated with precipitation during the event, meteorological category and time of year, derived from observations during 1982-1985. An estimate for deposition for a specific year can be obtained by applying the statistical correlation (Equation 28) to the meteorological record (day-to-day precipitation, time of year and meteorological category) for the year. The resulting estimate provides an indication for the extent of year-to-year variations that may be induced by meteorology. The annual estimate also provides a test of the ability to predict deposition for future years.

Projected deposition values from this statistical correlation are also shown for 1982 through 1987 at the Massachusetts, Ohio and Tennessee sites in Figures 15 through 17 (dashed

lines). Results of the statistical model project year-to-year variations in wet deposition that are nearly as large as the observed fluctuations, suggesting that changes in meteorology may be a plausible explanation for the observed changes. However the predicted deposition values do not always correspond with the observed annual fluctuations. For 1987 the statistical model predicts lower than average deposition at the Massachusetts site but not for Tennessee. Tests for statistical significance at the 95% confidence level (T_S, Equation 21) indicate that sulfate deposition during 1987 was significantly lower than in previous years, even accounting for changes in precipitation and meteorological category, at 13 of the 18 sites for which 1987 data is currently available. Nitrate deposition is significantly lower at 6 of the 18 sites and significantly higher at one site. There is room for considerable improvement in models to predict changes in future deposition associated with meteorology.

Figure 19 shows a comparison between observed $SO_4^=$ wet deposition during 1986 and 1987 and statistically projected deposition (based on 1982-1985 observations) for all sites included in this study. Results show that observed deposition tends to be lower than projected values, largely due to the anomalous year 1987. Projected deposition falls within 20% of the observed values at most locations. Tests for statistical significance show that the use of meteorological categories in the statistical projections result in an improved ability to predict variations in deposition that is significant at 95% confidence.

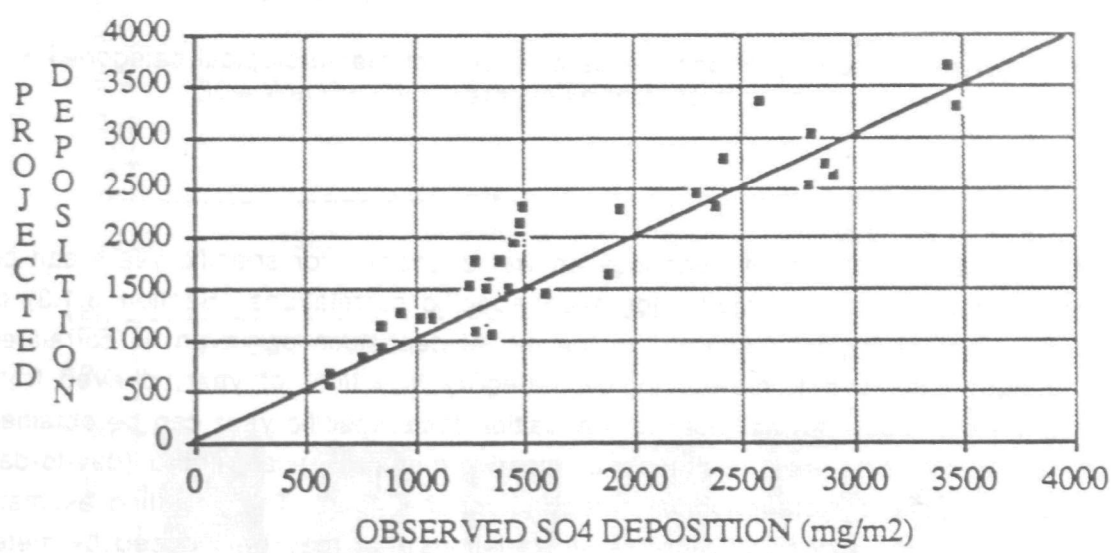

Figure 19. Comparison between annual $SO_4^=$ wet deposition observed during 1986 and 1987 at 13 northeastern and midwestern sites with projected deposition based on 1982-1985 observations and 1986-1987 meteorology.

3.1.5. Evaluation of the category-based aggregation method

Evaluation of the aggregation technique focused on comparing nineteen-day aggregate estimates generated using five different event selection and weighting techniques. Using each technique one-hundred independent ensembles, each containing nineteen three-day periods, were selected randomly from 1982-1985 observations. In the first scenario events were taken from the entire pool of observations and no additional knowledge was used in estimating annual depositions. In each of the other cases more information was employed. For the second and third scenarios events were again selected with no guidance, but aggregation was performed with prior knowledge of the amount of precipitation that fell at each site during each event (second scenario), and with prior knowledge of both precipitation and the season of each event (third scenario). In the fourth case events were selected (randomly) with a prescribed distribution among the seasons, and aggregated using the precipitation and seasonal information. For the fifth case the events were selected (randomly) from prescribed categories and annual depositions were estimated with the aid of category-based scaling (as outlined above). Aggregation was based on equations (7) and (8) with the prior estimate for deposition ($\hat{D}_i$) reflecting the extent of prior knowledge available for each case.

The results of the various scenarios are compared in Figure 20. Evaluation was based on the root mean-square difference (RMSD, Equation 9) between estimated mean annual deposition and actual annual deposition for the 13 sites in the northeast and midwest. The RMSD was calculated for each ensemble. Figure 20 shows that the deviations between estimated and observed deposition are smallest for the ensembles chosen by meteorological category and that the inclusion of more and more information sequentially improved upon the ensembles selected at random. Table 8 clarifies the meanings of the labels shown in the legend of Figure 20. For the category-based selection the average deviation is 18% of the observed deposition (2380 mg m^{-2} over the 13 sites), while the smallest deviation for a 19-day ensemble is 11%. Note that the 11% deviation is lower than the RMSD for year-to-year variations in wet deposition (Equation 27). Deviation for ensembles selected at random are significantly higher than for ensembles selected by category. Use of observed precipitation in deriving aggregate estimates results in greatly improved accuracy. Aggregation based on random selection, even accounting for precipitation and season, results in an average deviation of 22% (2850 mg m^{-2} over the 13 sites). Category-based selection reduces this deviation by approximately 25%.

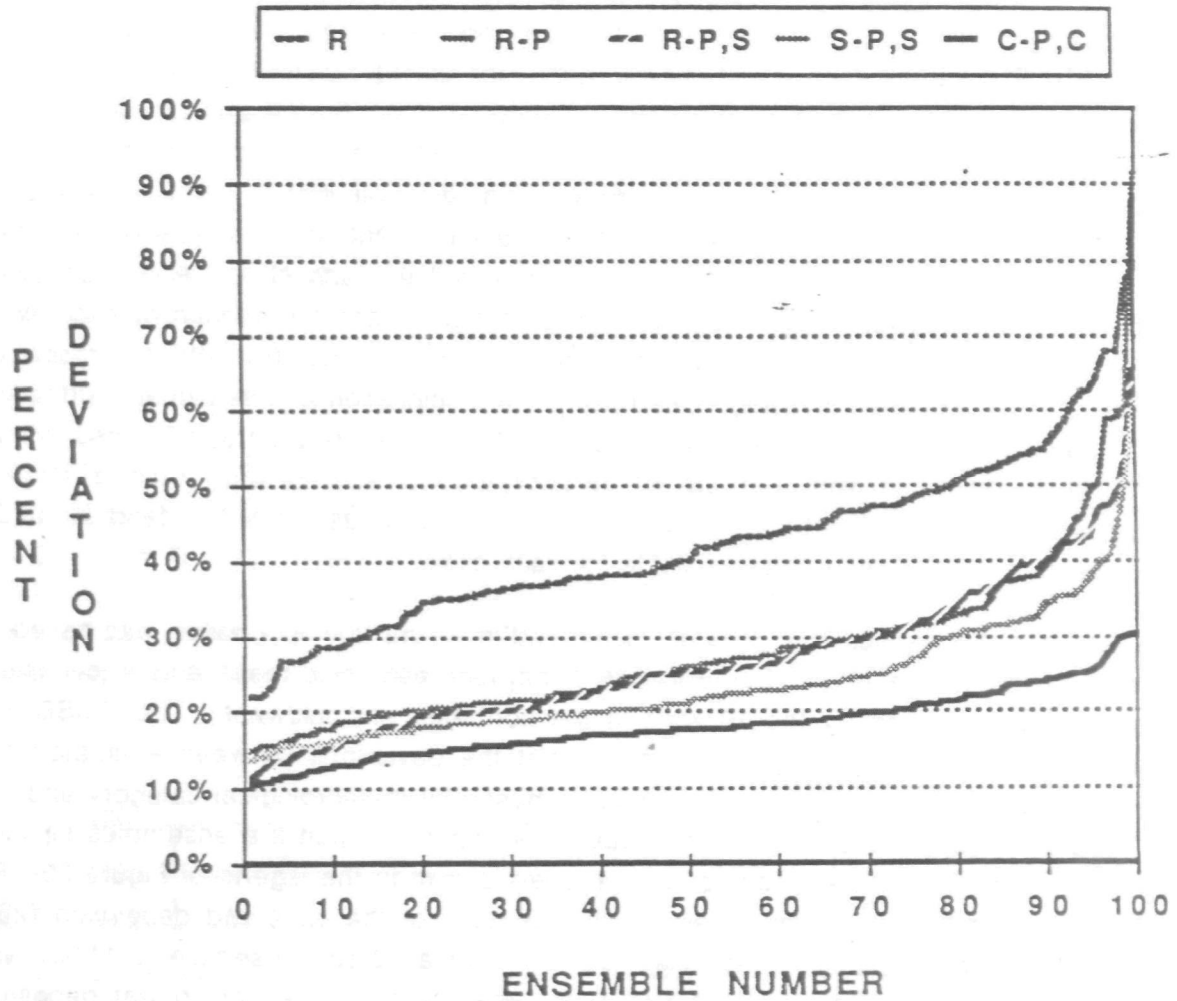

Figure 20 Comparison of selection and aggregation techniques for $SO_4^=$ wet deposition in northeastern North America.using nineteen three-day episodes. The selection techniques include ensembles of events selected purely at random (R), selected with prescribed seasonal distribution (S) and selection with prescribed distribution among meteorological categories (C). Aggregation techniques are based on no prior knowledge of meteorology (R); prior knowledge of precipitation for each event (-P); prior knowledge of both event precipitation and season (-P,S); and prior knowledge of event precipitation and meteorological category (-P,C).

3.2. SELECTION OF CASES

A total of 30 three-day events have been chosen for initial use in the analysis of annual deposition. Selection was based on methods outlined in Section 2.1.5 with selection from meteorological categories described in Section 3.1.2. Events were selected from prescribed meteorological categories (including the split into 'wet' and 'dry' subcategories), with the categories chosen (1) to represent meteorological processes that account for the majority of total wet deposition in eastern North America, and (2) to include important meteorological patterns (i.e. cold-season events and events with little precipitation for evaluation of dry deposition) that might be overlooked in the first criteria. Selection of categories was based on the following specifications:

(a) 19 3-day events were selected from the 9 'wet' categories which accounted for the greatest deposition on an annual basis. We estimate that these 9 categories account for about 75% of total annual $SO_4^=$ wet deposition at all northeastern and midwestern sites (see Section 3.1.2).

(b) 6 additional 3-day events were selected to represent dry deposition processes. These days were selected according to the criteria that the sum of 3-day $SO_4^=$ wet deposition for the 13 northeastern and midwestern sites total less than 50 mgm^{-2}.

(c) 5 additional 3-day events were selected from among winter days (November-March). These days were selected from categories that were not included in the original 19 and which may offer unusual conditions.

Choice of the individual events was designed to meet two additional criteria: random selection to avoid the introduction of bias, and accurate representation of deposition at the 13 northeastern and midwestern sites. Evaluation of the accuracy of individual ensembles was based on the aggregated estimates for annual deposition at each site derived from observed deposition on the sample days. Selection was made according to the following procedure:

(1) The distribution of sample 3-day events among the 38 categories was prescribed based on deposition attributable to each category and frequency of occurrence (see Section 3.1.2).

(2) Once the distribution among categories was selected, ensembles of specific 3-day events were generated. Each ensemble consists of a series of 3-day events with the pre-determined distribution among the 38 categories. The individual 3-day events representing each category were selected at random.

(3) For each ensemble of specific events, estimated annual deposition was determined for the 13 northeastern and midwestern sites, based on observed deposition during the ensemble events and the category-based scaling factors. The standard deviation between estimated and actual annual deposition for the 13 sites was determined for the ensemble.

(4) Ensembles were ranked based on standard deviation, and the best ensemble (with the lowest standard deviation among 20 randomly generated ensembles) was selected as the representative ensemble.

The selection was performed in two stages. Initially, the ensemble of 19 3-day events representing categories with the highest deposition was selected. The additional 11 events representing dry and winter deposition were selected after the initial ensemble had been selected. In the selection of the additional 11 events, estimated annual deposition was based on an ensemble of 30 events, with the prior 19 added to the randomly selected 11 events. The 11 additional events were chosen to provide the most accurate 30-event ensemble. The selected 3-day periods are shown in Table 8.

3.3. COMPARISON OF AGGREGATE ESTIMATE WITH LONG-TERM DEPOSITION

This section explores the accuracy of aggregate estimates derived based on the selected 30-event ensemble (Table 8). Aggregate estimates have been derived for sulfate and nitrate wet deposition and for total acidity, including estimates for annual and seasonal totals. The estimates are based on the observed wet deposition for the selected events, and on observed correlations between wet deposition, precipitation and meteorological category for the 1982-1985 period (Equations 7 and 8). Aggregate estimates are compared with observed wet deposition during 1982-1985.

3.3.1. Annual Wet Deposition

The following section examines the ability of the aggregation technique to reproduce annual deposition patterns for $SO_4^=$, NO_3^- and H^+ wet deposition. The observed deposition values for the 30 episodes recommended for RADM simulation were used to estimate deposition using the proposed aggregation technique. From these results, plots of deposition across eastern North America were drawn. Estimates of annual and seasonal $SO_4^=$, NO_3^- and H^+ depositions were determined for all 22 sites. The spatial patterns were analyzed for agreement with the actual mean deposition patterns for 1982-1985.

TABLE 8. DATES OF THREE-DAY EPISODES (MIDDLE DAY) SELECTED FOR AGGREGATION. CATEGORY NUMBERS CORRESPOND TO DESCRIPTIONS GIVEN IN TABLE 4, WITH 'W' AND 'D' REFERRING TO THE SPLIT INTO "WET" AND "DRY" SUBCATEGORIES BASED ON SULFATE DEPOSITION (SECTION 3.1.2)

Date	Category	Date	Category
(Original 19 Periods)			
April 15-17, 1982	1W	May 2-4, 1985	8W
November 2-4, 1985	3W	September 9-11, 1984	9W
May 29-31, 1983	5W	September 14-16, 1983	9W
March 17-19, 1984	5W	September 25-27, 1982	9W
July 12-14, 1985	6W	August 4-6, 1983	9W
September 9-11, 1983	6W	November 16-18, 1985	10W
October 11-13, 1985	6W	September 26-28, 1985	11W
November 1-3, 1983	7W	July 16-18, 1984	11W
August 21-23, 1984	7W	December 15-17, 1982	11W
June 12-14, 1984	7W		
(6 dry periods)			
April 28-30, 1985	19D	December 16-18, 1985	11D
June 10-12, 1983	8D	May 14-16, 1982	7D
July 17-19, 1985	9D	November 6-8, 1982	6D
(5 winter periods)			
February 1-3, 1982	2W	February 9-11, 1985	14W
December 9-11, 1983	4W	November 13-15, 1983	17W
November 4-6, 1985	12W		

3.3.1.1. Sulfate Wet Deposition—

Figures 21a and b show the observed annual $SO_4^=$ deposition over the four-year period (1982-1985) and the estimated annual deposition based on the 30-day ensemble. In general, the estimated depositions and spatial patterns agreed well with observed values within the thirteen site domain. The annual and seasonal results are summarized Table 9. The mean RMS errors shown were determined across all sites and are expressed as a percent of the average deposition across all of these sites. Annual aggregate estimates were within 18% of the actual deposition at the thirteen northeastern sites and within 10% at eight of those sites. The mean RMS error as a percent of the average 22 site $SO_4^=$ wet deposition was 13%.

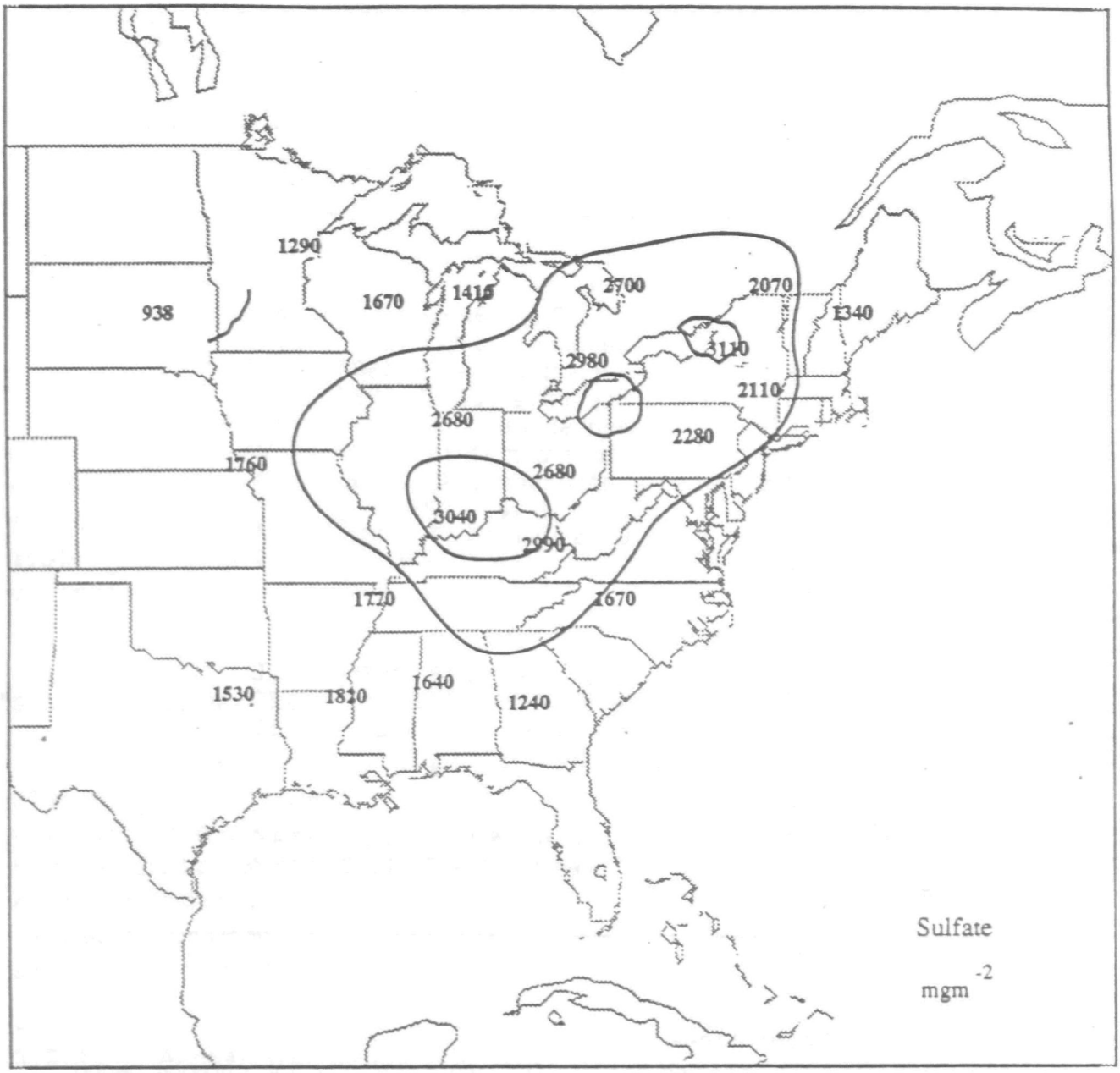

Figure 21a The mean annual $SO_4^=$ wet deposition pattern across eastern North America during 1982-1985. (Units=mgm^{-2}). Contours correspond to 1000, 2000 and 3000 mgm^{-2}.

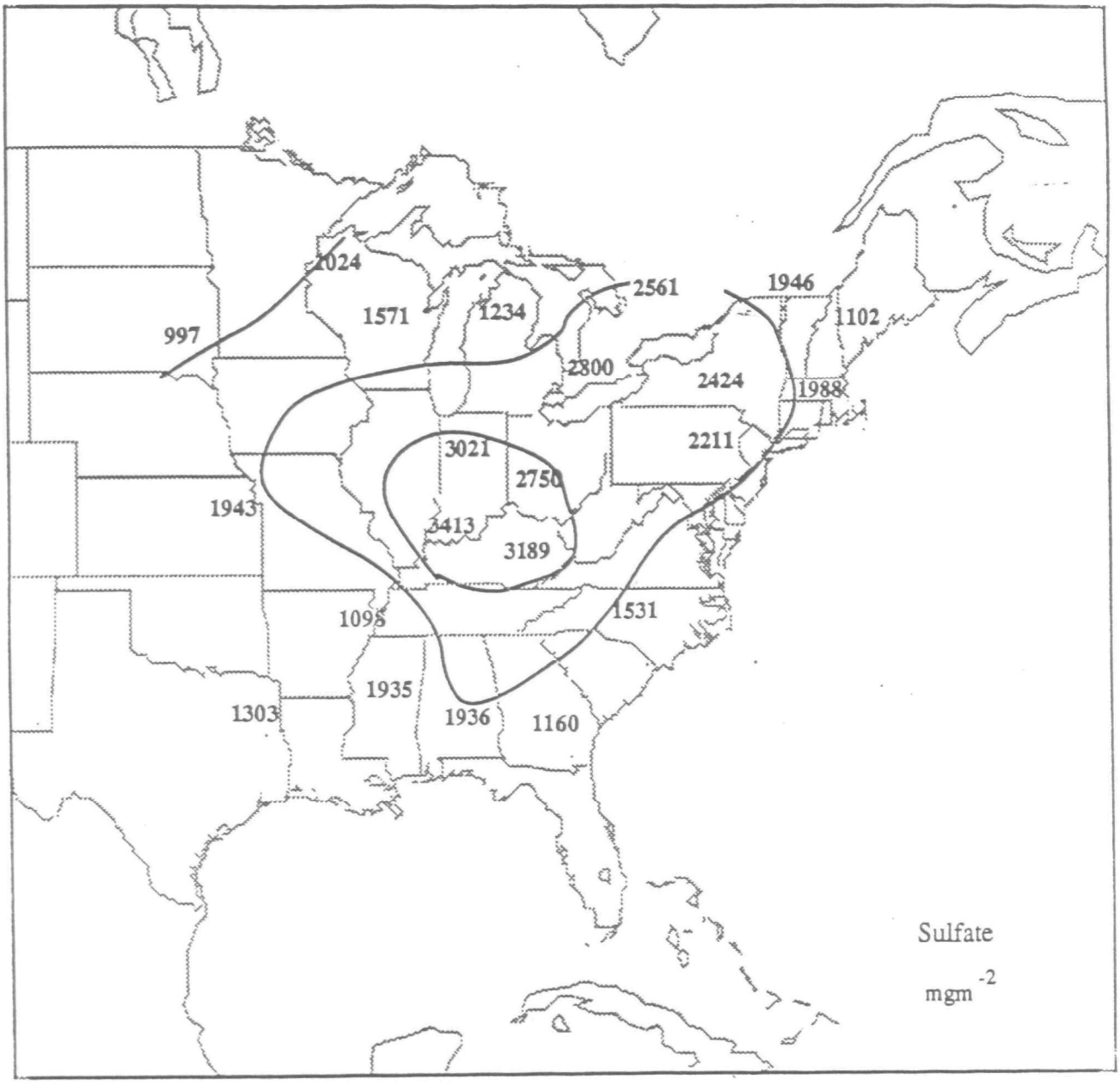

Figure 21b The aggregate estimate of the mean annual $SO_4^=$ wet deposition pattern across eastern North America for 1982-1985. (Units=mgm^{-2}). Contours correspond to 1000, 2000 and 3000 mgm^{-2}.

TABLE 9. ROOT-MEAN-SQUARE DEVIATIONS BETWEEN ESTIMATED AND OBSERVED SUMMER, WINTER AND ANNUAL WET DEPOSITION AT 13 EASTERN SITES. DEVIATIONS ARE EXPRESSED AS A PERCENTAGE OF OBSERVED DEPOSITION

Species	Annual	Summer	Winter
Sulfate	13 %	20 %	20 %
Nitrate	20 %	27 %	35 %
Hydrogen	17 %	24 %	21 %

It can be seen that throughout eastern North America there was no clear tendency for under or over estimation of $SO_4^=$ deposition. However there was a tendency to overpredict or underpredict deposition in certain regions. Overprediction occurred at sites in the southern Midwest (Kentucky, Ohio, Indiana). Underprediction tended to occur at northerly sites (Wisconsin, Michigan, Ontario, New York, Vermont, Maine and Massachusetts). Underestimation also occurred North Carolina, Tennessee and Georgia, while predictions at the Mississippi and Alabama sites tended to be high. Summer and winter depositions showed similar tendencies towards over- and underprediction in specific geographic regions. This apparent regional consistency in over- and underestimation was not considered unrealistic. On the regional scale the spatial variation in precipitation amounts due to a typical weather system varies significantly. Since only a small number of episodes are used in the aggregation, the spatial variation associated with them is carried over to the long-term pattern.

3.3.1.2. Nitrate Wet Deposition—

On an annual basis the actual and estimated plots of NO_3^- wet deposition are shown in Figures 22a and b. The mean RMS error as a percent of the average 22 site annual deposition was 20%. The RMS error is greater for nitrate wet deposition than for sulfate, possibly reflecting the greater importance of local meteorology in controlling the rate of nitrate deposition. Also in contrast to sulfate, the RMS error for nitrate was significantly larger than the year-to-year RMS deviation (13%, from Section 3.1.4)

Qualitatively the spatial variations of sulfate and nitrate wet deposition were quite similar. The area of greatest deposition extended from the Midwest to the Northeast. While depositions were least in the northwest and south. As with $SO_4^=$, whether or not the NO_3^- wet deposition at a given location was over and underestimated depended its geographical location. In the lower Midwest the estimates were somewhat overpredicted in northern Indiana and Ohio. Similar to $SO_4^=$, the deposition estimates were generally low from southern Ontario and northern Pennsylvania to the Northeast coast. The largest deviation was at the Tunkhannock, PA receptor. As with $SO_4^=$, overall the was no bias towards under- or overprediction. The slight changes in regional biases between NO_3^- and $SO_4^=$ wet deposition were likely due to the differences in the emission patterns and in the differences in their chemistry and rain-out characteristics.

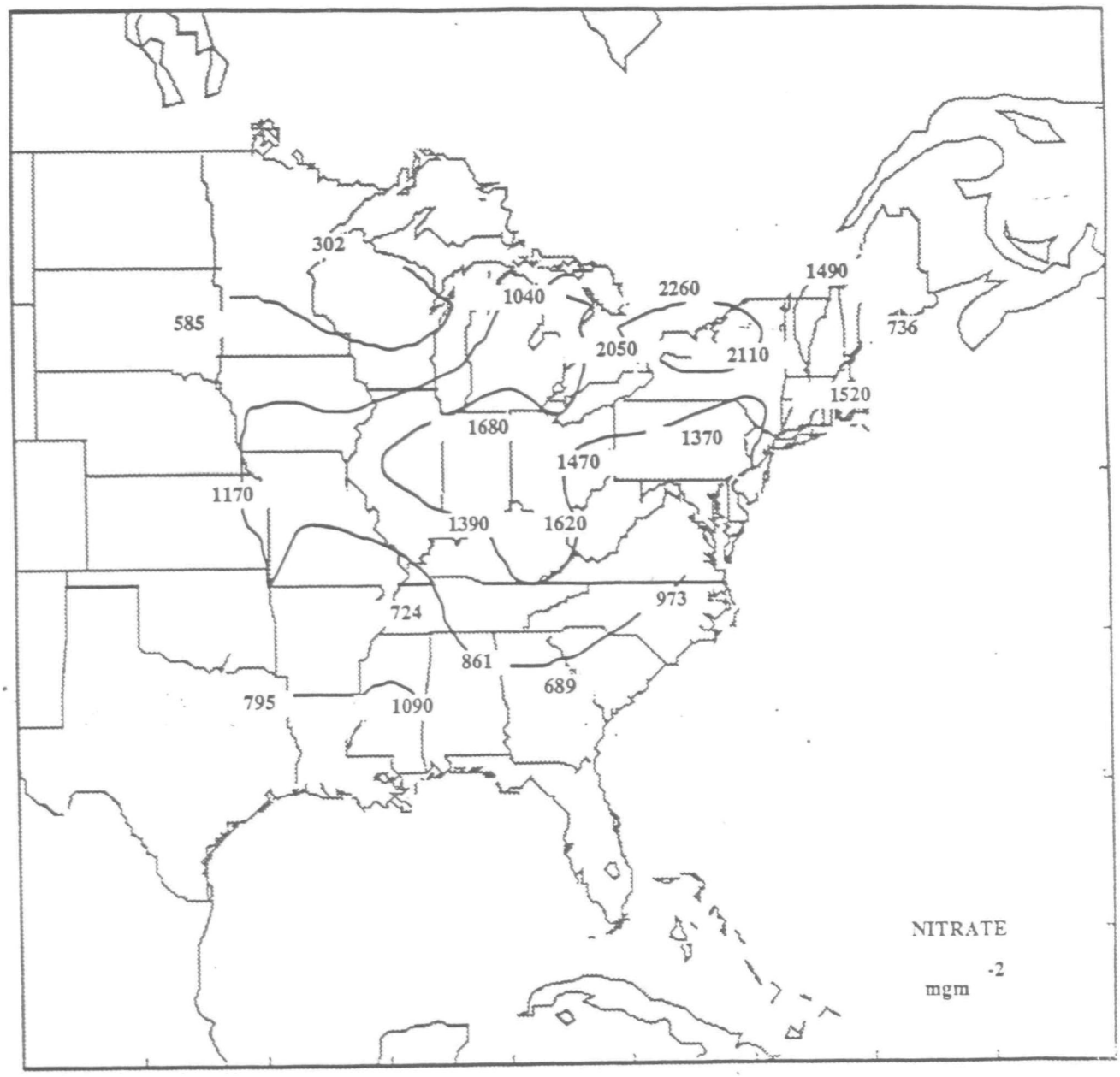

Figure 22a The mean annual NO_3^- wet deposition pattern across eastern North America during 1982-1985. (Units=mgm^{-2}). Contours correspond to 500, 1000, 1500 and 2000 mgm^{-2}.

Figure 22b The aggregate estimate of the mean annual NO_3^- wet deposition pattern across eastern North America for 1982-1985. (Units=mgm^{-2}). Contours correspond to 500, 1000, 1500 and 2000 mgm^{-2}.

3.3.1.3. Acidity Wet Deposition—

As expected the pattern of annual H^+ deposition reflected the behavior of NO_3^- and $SO_4^=$ deposition with maximum values from the lower Midwest across the eastern Great Lakes to the Northeast United States (Figures 23a and b). The mean RMS error of 17% is between those of NO_3^- and $SO_4^=$. The pattern of significant underestimation in the Northeast, in particular in northeastern Pennsylvania and upstate New York, was again apparent. Some of the episodes selected for aggregation were either associated with small amounts or precipitation or low pollutant concentrations (or both). It is likely that only one or two of the episodes were biasing the results. With only 30 events, of which only 21 had precipitation at Big Moose for example, the characteristics of each one will significantly influence the deposition approximations. It would be extremely difficult to identify an ensemble of 30 events that did not result in some bias somewhere in eastern North America.

3.3.2. Seasonal Wet Deposition

3.3.2.1. Sulfate Wet Deposition—

Figures 24 a-d show estimated and observed $SO_4^=$ deposition for the summer and winter halves of the year. The mean seasonal results were also summarized in Table 9. The errors resulting from the estimation of wet deposition using the aggregation method were less than 20% for eleven of the sites during summer and nine in winter.

3.3.2.2. Nitrate Wet Deposition—

The actual and aggregate patterns for wet NO_3^- deposition in the summer and winter are included in Figures 25 a-d. In the summer the highest values were reported in Ontario. Using the aggregation routine, the episodes selected predicted large wet deposition values to occur in that area. The deposition values were somewhat over-predicted in the Midwest excluding Rockport, IN and were again under-predicted in the Northeast. At the New York, Pennsylvania and Massachusetts sites the errors were fairly significant but well within 50%. Throughout the northeastern region the average error was 19%. In winter the errors were worse. The average over the same region was 25% but at the Michigan, Vermont and Pennsylvania sites it was close to 50%. In upstate New York and northern Ontario the errors were around 40%. One reason the estimates were worse in the winter (for $SO_4^=$ and NO_3^-) is that the actual depositions were generally less. Therefore, a relatively small departure, that made little difference on an annual basis, appeared significant.

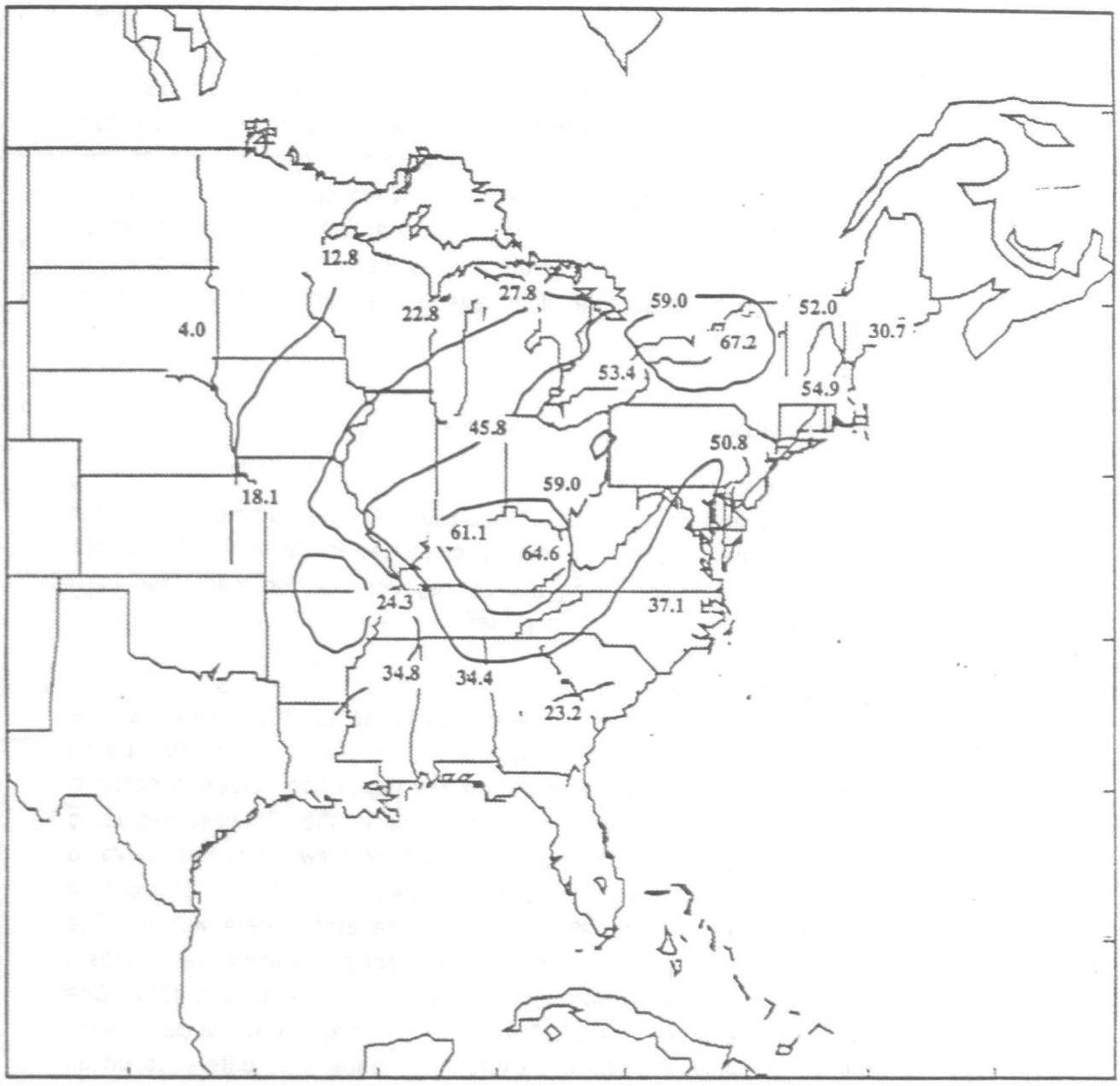

Figure 23a The mean annual wet acidity (H^+) deposition pattern across eastern North America during 1982-1985. (Units=mgm^{-2}). Contours correspond to 15, 30, 45 and 60 mgm^{-2}.

Figure 23b The aggregate estimate of the mean annual wet acidity (H^+) deposition pattern across eastern North America for 1982-1985. (Units=mgm^{-2}). Contours correspond to 15, 30, 45 and 60 mgm^{-2}.

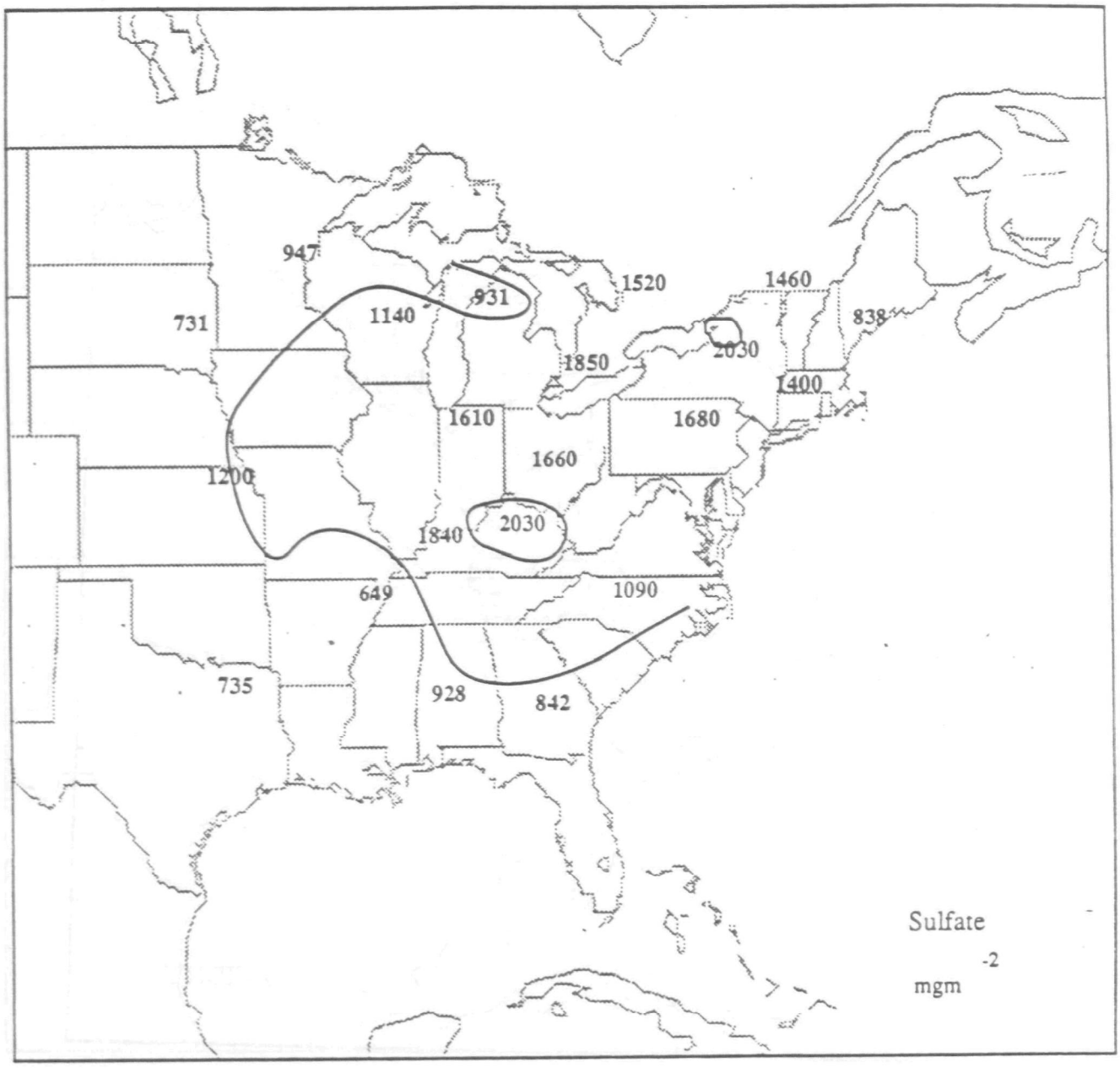

Figure 24a The mean summer $SO_4^=$ wet deposition pattern across eastern North America for 1982-1985. Summer corresponds to the period from April through October. (Units=mgm^{-2}). Contours correspond to 1000 and 2000 mgm^{-2}.

Figure 24b The aggregate estimate of the mean summer $SO_4^=$ wet deposition pattern across eastern North America for 1982-1985. (Units=mgm^{-2}). Contours correspond to 1000 and 2000 mgm^{-2}.

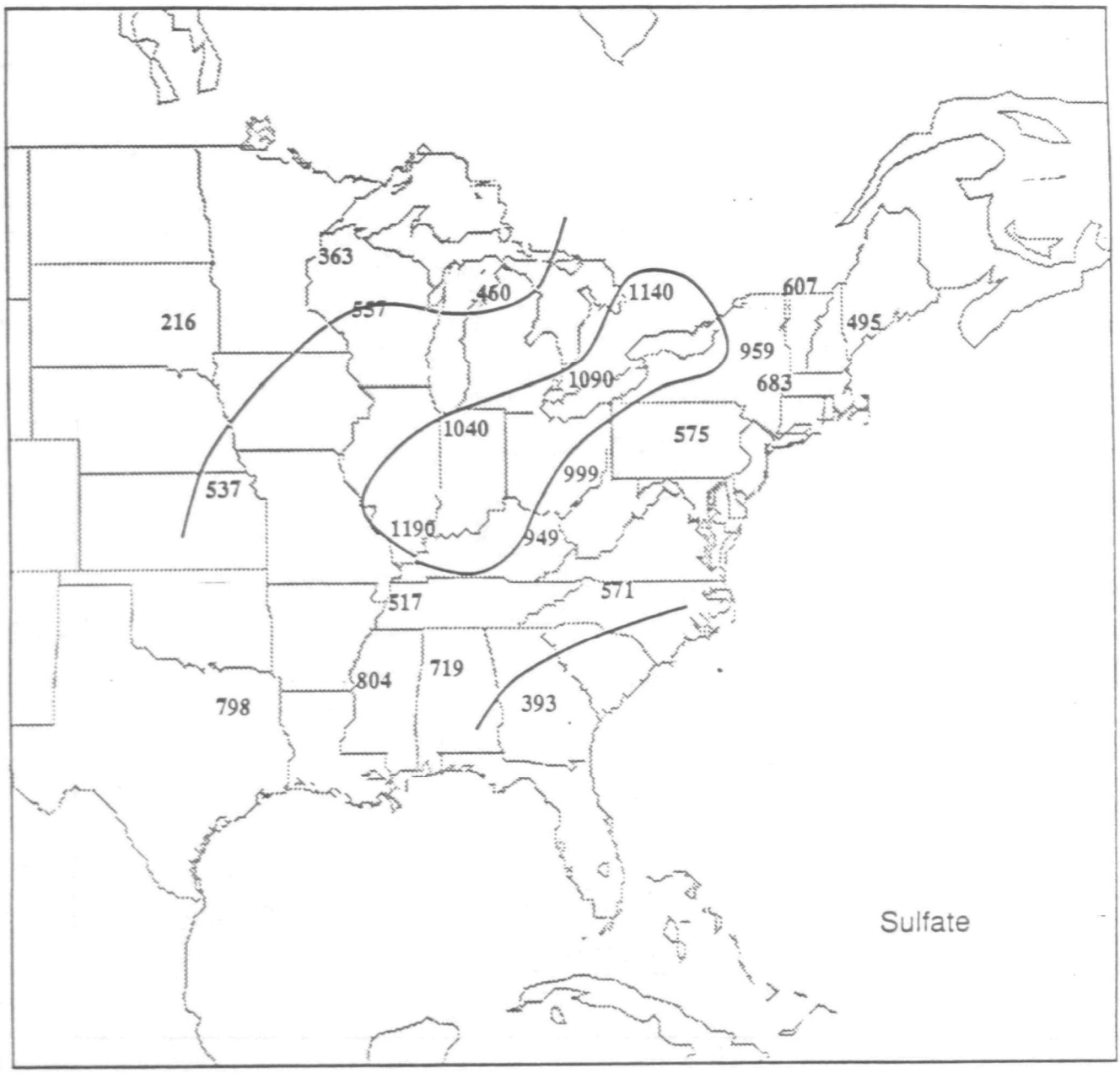

Figure 24c The mean winter $SO_4^=$ wet deposition pattern across eastern North America for 1982-1985. Winter corresponds to the period from November through March. (Units=mgm^{-2}). Contours correspond to 500 and 1000 mgm^{-2}.

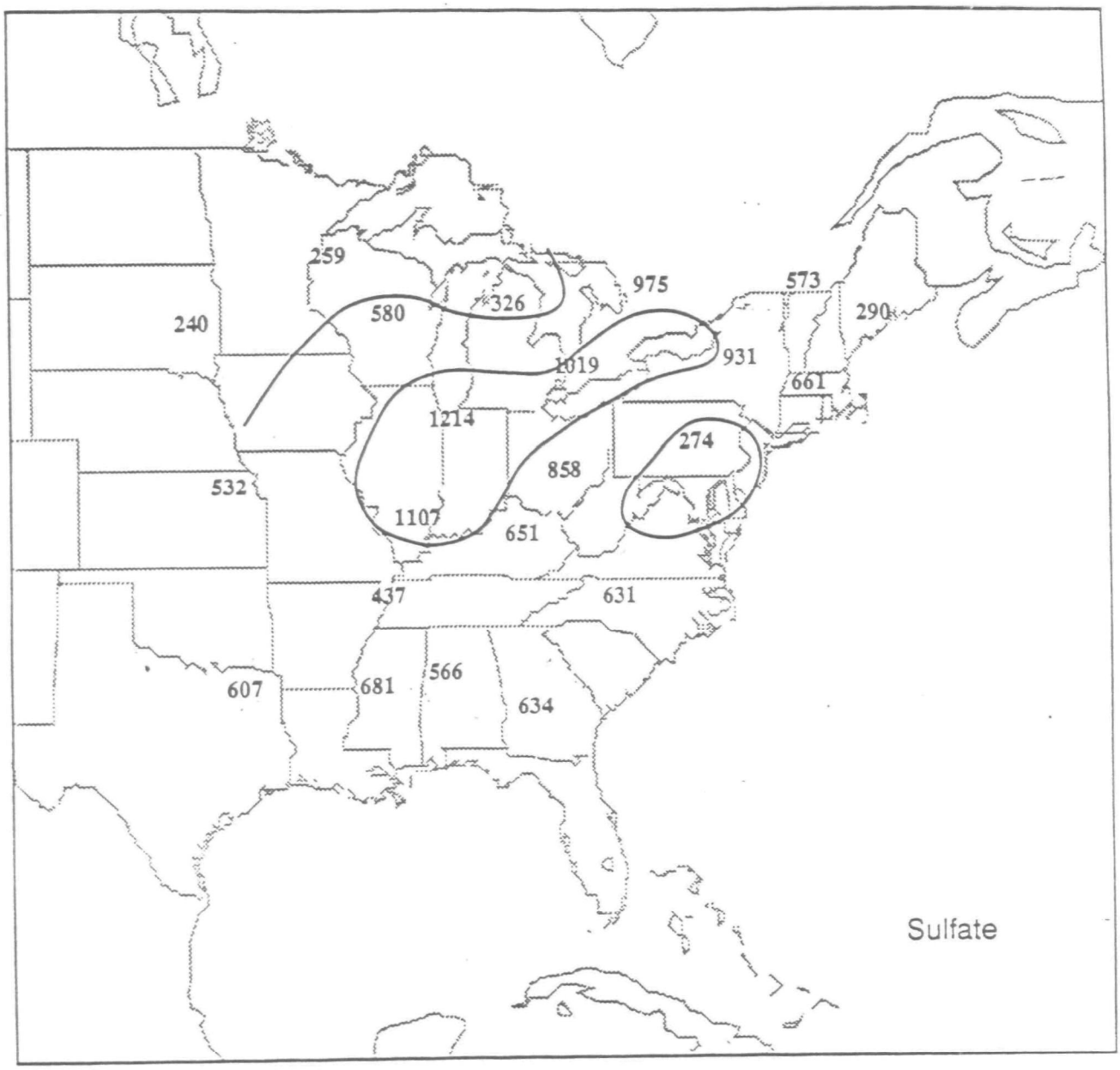

Figure 24d The aggregate estimate of the mean winter $SO_4^{=}$ wet deposition pattern across eastern North America for 1982-1985. (Units=mgm^{-2}). Contours correspond to 500 and 1000 mgm^{-2}.

Figure 25a The mean summer NO_3^- wet deposition pattern across eastern North America for 1982-1985. Summer corresponds to the period from April through October. (Units=mgm^{-2}). Contours correspond to 500 and 1000 mgm^{-2}.

Figure 25b The aggregate estimate of the mean summer NO_3^- wet deposition pattern across eastern North America for 1982-1985. (Units=mgm^{-2}). Contours correspond to 500 and 1000 mgm^{-2}.

Figure 25c The mean winter NO_3^- wet deposition pattern across eastern North America for 1982-1985. Winter corresponds to the period from November through March. (Units=mgm^{-2}). Contours correspond to 500 and 1000 mgm^{-2}.

Figure 25d The aggregate estimate of the mean winter NO_3^- wet deposition pattern across eastern North America for 1982-1985. (Units=mgm^{-2}). Contours correspond to 500 and 1000 mgm^{-2}.

3.3.2.3. Acidity Wet Deposition—

The seasonal estimates of H^+ wet deposition behaved similarly to those for $SO_4^=$ wet deposition. Maps of the actual and aggregate estimates are included in Figures 26 a and b, respectively. In summer, the errors ranged from 3% to 34% with the average over the northeastern region being 16%. For the winter estimates the results were similar, ranging from 0% to 45%. The average was also 16%. For all three analytes the tendencies for over and underestimation were not as consistent for the seasonal depositions. As well there were a number of sites where the bias changed direction between seasons. This further highlights the influence a few slightly atypical episodes had on the aggregate estimates of deposition. In reality these episodes were not atypical since the long-term patterns that were observed and that the aggregate estimates were measured against were a compilation of a large set of highly variable episodes.

3.3.3. Uncertainties in the Aggregate Estimates-

The estimates of seasonal and annual wet deposition were based upon the categories identified for event selection and their mean frequency of occurrence and deposition to precipitation ratio. How well the specific 30 events represented the categories they were selected from ultimately governed the accuracy of the aggregate estimates. Events that had uncharacteristic pollutant concentrations, relative to their categories, caused the long-term estimates to deviate from the actual value. This can be inferred from the aggregation equation (see *equation 7*). The actual deposition (D_{annual}) is scaled by the ratio of the total amount contributed by the events selected, weighted by category frequency, to the total amount expected due to the categories chosen, weighted by their frequencies, and assuming the same precipitation amount as the events selected. Mis-representation of the categories that occurred more frequently and/or had large mean deposition to precipitation ratios had the greatest effect on the accuracy of the estimates. Thus, the real goal of the events selected was to match the mean behavior of the collection of categories chosen to represent the long-term deposition.

The certainty of the estimates basically rests with the relationship between the actual long-term depositions and the categories represented. Since events were selected from those categories containing the meteorological situations contributing the largest percentage of the annual deposition, the relationship should be relatively strong (i.e. Changes in the total annual deposition should be similar to changes in the total amount deposited by the sample of categories). Roughly 75 percent of the mean annual 13-site deposition during 1982-1985 occurred with events in the meteorological categories used. On a site by site basis and from year to year, however, this percentage varied. Values below 50 would imply that the relationship between the actual long-term depositions and the categories represented was weak. In this case the certainty of the annual deposition estimates would be diminished. During 1982-1985 this situation did not arise, the mean percents accounted for varied from 60 to over 80. For three of the sites (Big Moose, Gaylord and Zanesville) Figure 27 shows the amount of variation in the

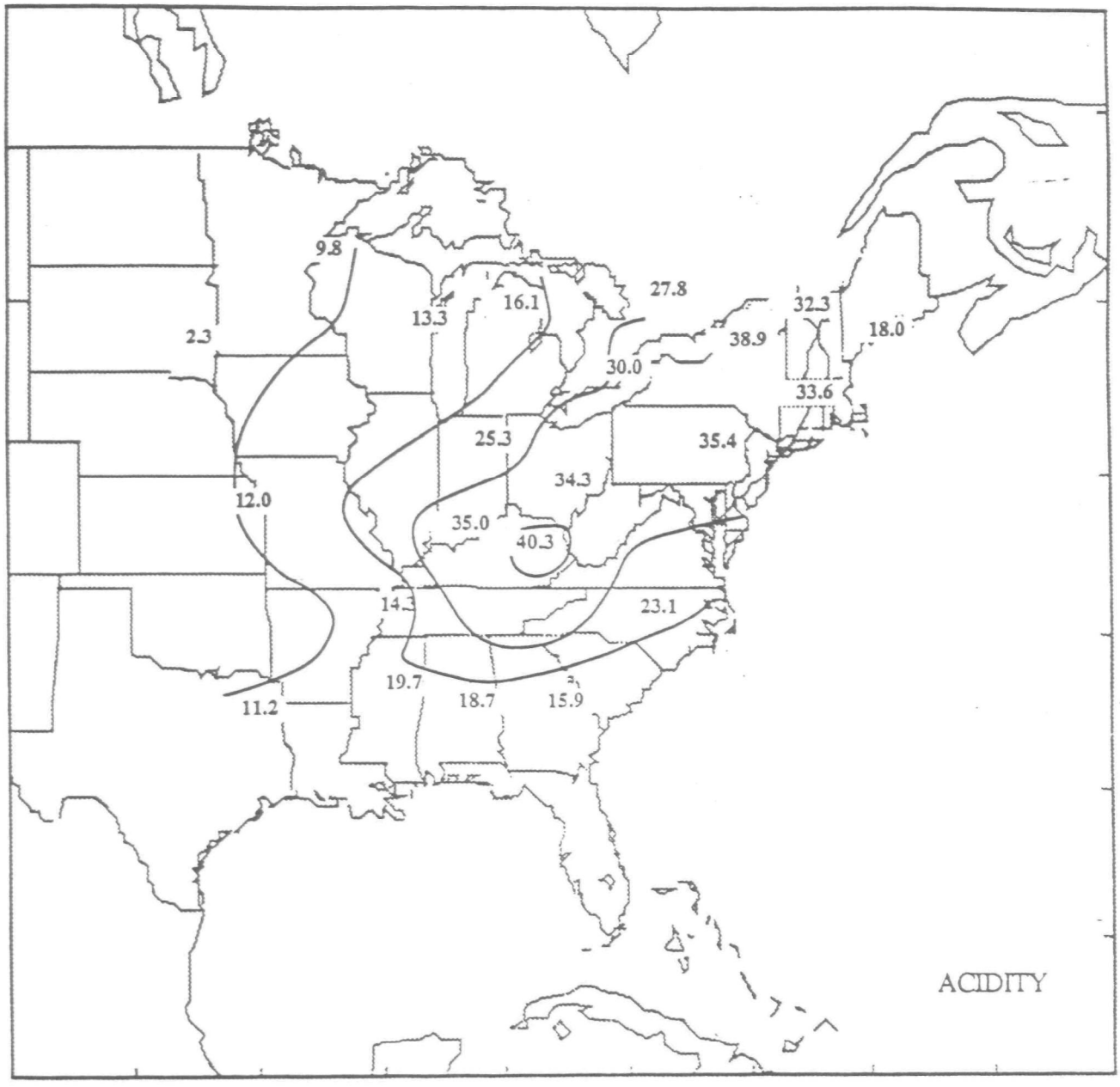

Figure 26a The mean summer wet acid (H^+) deposition pattern across eastern North America for 1982-1985. Summer corresponds to the period from April through October. (Units=mgm^{-2}). Contours correspond to 10, 20, 30 and 40 mgm^{-2}.

Figure 26b The aggregate estimate of the mean summer wet acid (H^+) deposition pattern across eastern North America for 1982-1985. (Units=mgm^{-2}). Contours correspond to 10, 20 and 30 mgm^{-2}.

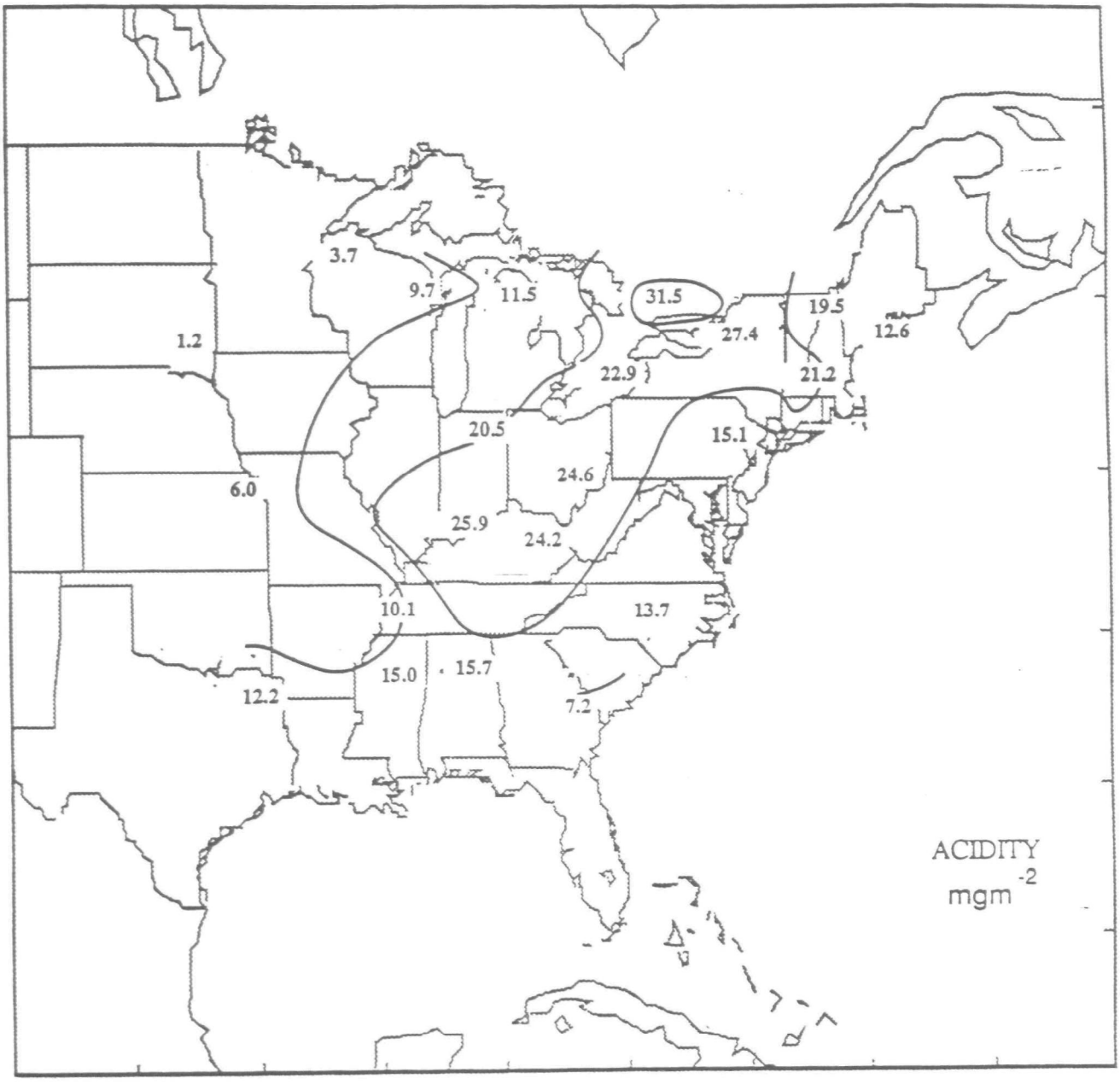

Figure 26c The mean winter wet acid (H^+) deposition pattern across eastern North America for 1982-1985. Winter corresponds to the period from November through March. (Units=mgm^{-2}). Contours correspond to 10, 20 and 30 mgm^{-2}.

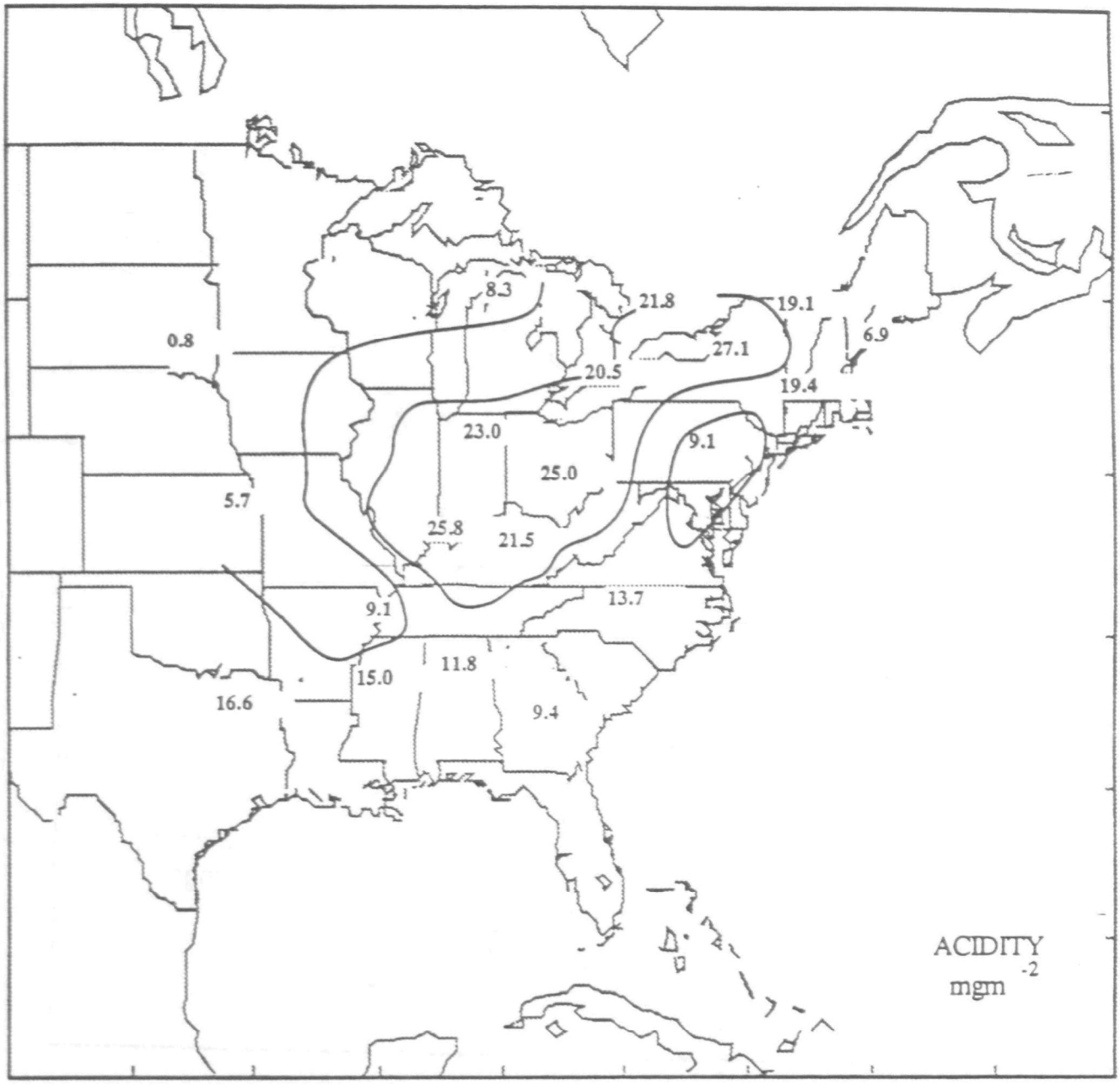

Figure 26d The aggregate estimate of the mean winter wet acid (H^+) deposition pattern across eastern North America for 1982-1985. (Units=mgm^{-2}) Contours correspond to 10 and 20 mgm^{-2}.

percentages from year to year. In general, the meteorological situations represented did not contribute as much during the earlier years as they did in the later years. The reason for the increase is not certain, however, one possible cause is that during the earlier years there was more meteorological data missing (850 mb u-v). More of the deposition events were therefore classified as missing at the expense of the amount of deposition falling within the categories. Across all sites and all years, however, the percent accounted for rarely dropped below 50 and consistently stayed above 60.

In Figures 28 and 29 the total amount of wet $SO_4^=$ deposition by year is compared to the total amount in each year associated with the set of categories represented. Similar temporal variations between the two would suggest that deposition from the categories is related to the annual total. Comparisons were made at two Midwestern sites and at two northeastern sites. At Zanesville, OH the annual amount and the category totals were closely related. At Rockport, IN the relationship is masked by the greater frequency of missing categories during the earlier years but the amounts do vary similarly. In the northeast, there is also some agreement with increases tracking similarly but again the larger number of missing categories during the earlier period caused some discrepancies. The effect of the missing category frequency has not been examined in terms of these results to conclusively say it was causing the problem. This will be studied in the future. The deposition amounts due only to the collection of categories was correlated with the total annual amounts. Thus, when the specific events (30) properly portrayed the behavior of the categories they were selected from, the aggregation technique produced estimates of long-term deposition with a relatively high level of certainty.

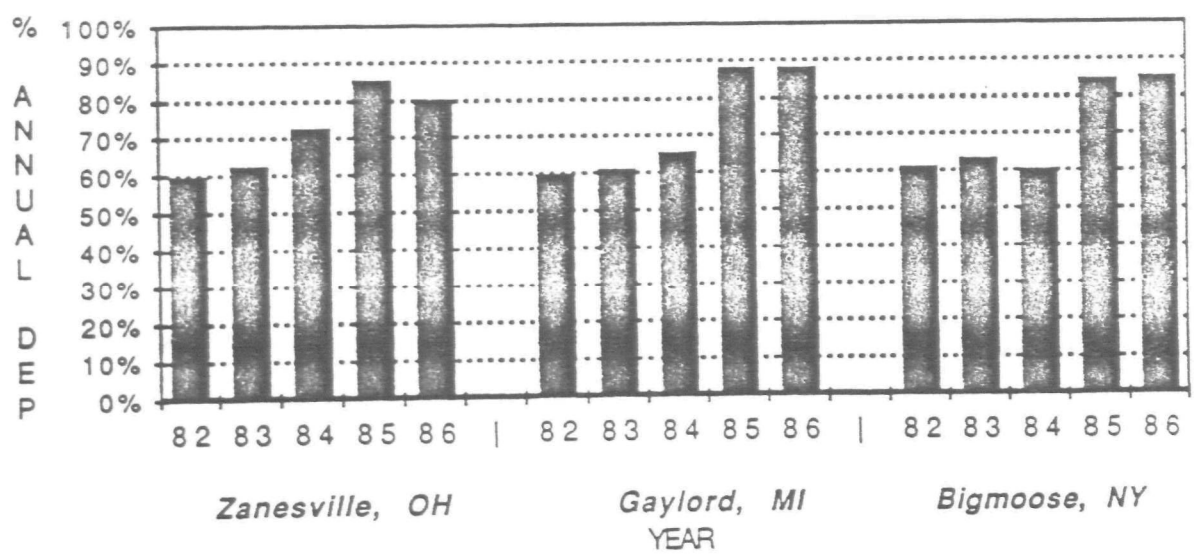

Figure 27. The spatial and temporal variation in the percent of annual $SO_4^=$ deposition accounted for by the meteorological categories selected for representation.

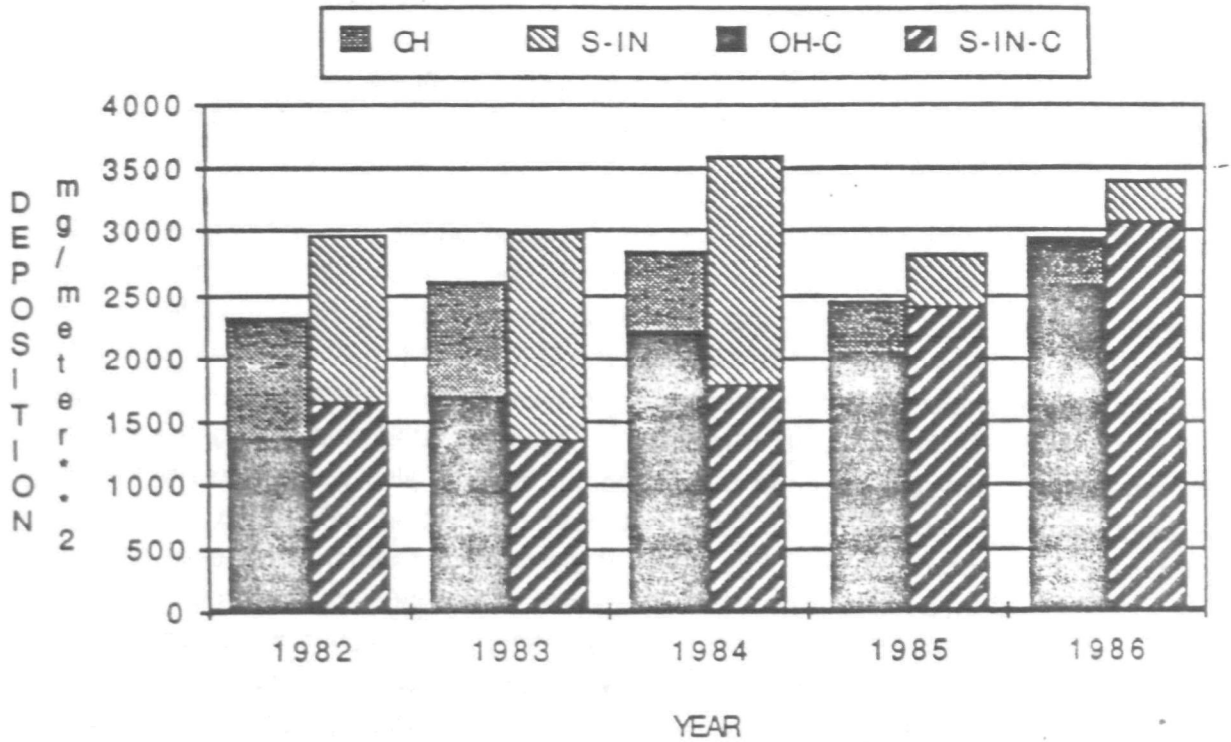

Figure 28. Comparison between the year to year variation in annual $SO_4^{=}$ deposition and the year to year variation in the total amount of deposition accounted for by the categories selected for representation. S-IN = annual total at Rockport and S-IN-C = category total at Rockport. OH = annual total at Zanesville and OH-C = category total at Zanesville.

The aggregate estimates of deposition were sensitive to the frequency of occurrence of the categories, the mean deposition to precipitation ratio of the categories and to the concentrations associated with each event. As mentioned above in reference to *equation 7*, the estimates were most sensitive to events from the frequently occurring, "wet" categories. To insure that these situations were represented properly more than one event was chosen from these categories. This measure reduced the possibility of one non-representative event being selected and drastically altering the estimates. As the number of events selected from each category is increased the estimates will approach the actual deposition. Using all four years of data to determine the category frequencies and the deposition to precipitation ratios insured that the most reliable values were used. Since these factors and the 30 episodes were constant, the values of the aggregate estimates at each site did not vary. Given that the long-term depositions were correlated with the amount of deposition resulting from events within these categories, the

uncertainty ranges associated with the estimated values were expected to be relatively small. The deviation between the estimated and observed depositions supplied an indication of the level of certainty to which long-term deposition could be reproduced.

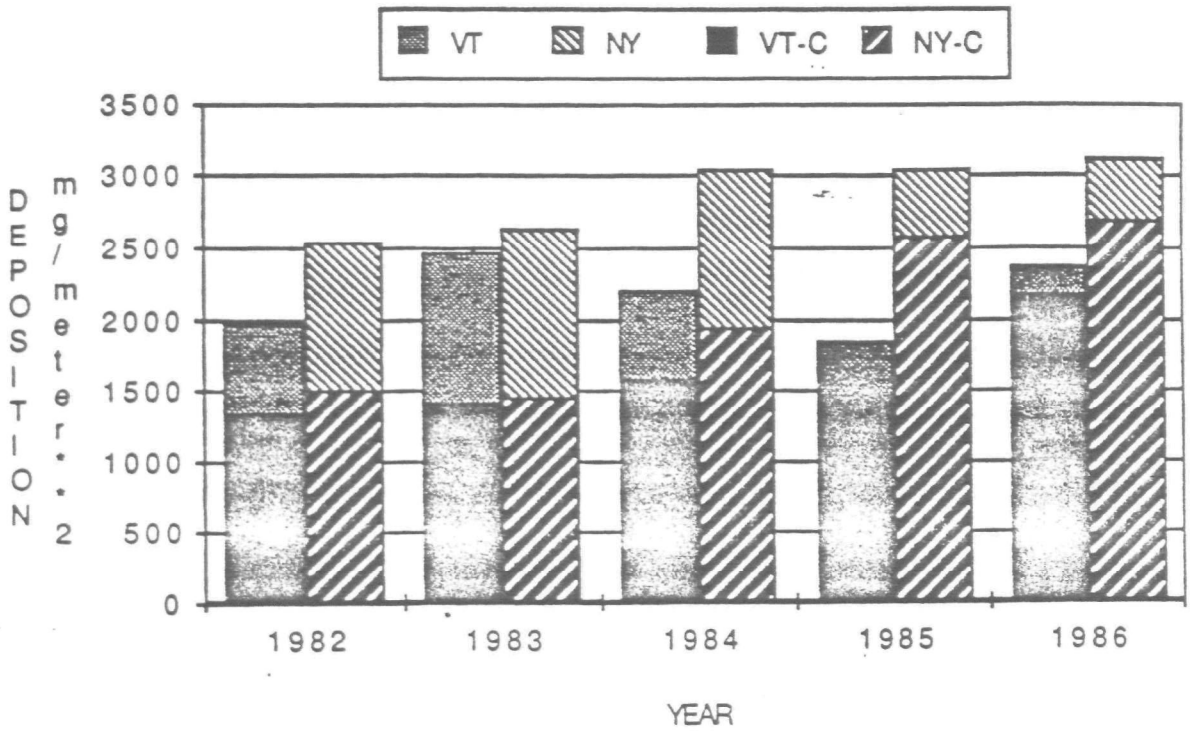

Figure 29. Comparison between the year to year variation in annual $SO_4^=$ deposition and the year to year variation in the total amount of deposition accounted for by the categories selected for representation. NY = annual total at Big Moose and NY-C = category total at Big Moose. VT = annual total at Underhill and VT-C = category total at Underhill.

The actual and aggregate maps of annual and seasonal deposition were discussed in a previous section. The 30 events reproduced the depositions well enough at each site to yield spatial patterns similar to the observed depositions. The magnitude of the differences (uncertainty) between estimated and actual were calculated as a percent of the actual deposition for all of the sites. These were summarized above in Table 9. Expressed as a percent of the mean deposition across all sites, the RMS errors were smallest for the annual estimates. Overall, estimates were closest for wet sulfate deposition with smaller annual and seasonal percent errors as compared to the wet deposition of NO_3^- and H^+.

It was most important to estimate the wet deposition over the smaller thirteen site domain accurately. For each of these sites the estimates were compared to the actual deposition. As with the mean error across all sites, the aggregation technique usually yielded better results for the annual estimates at individual sites. Reasons for this were suggested in the discussion concerning the spatial plots of wet deposition. The percent errors for wet $SO_4^=$ deposition are shown in Figure 30. Positive values indicate an over-estimate and negative ones under-estimation. On an annual basis the error was within 20 percent at all thirteen sites. The estimates were most uncertain at Big Moose, NY and Fort Wayne, IN with errors of -17 and 18 percent respectively. At the other locations uncertainty was less than 11 percent. The most uncertain aggregate estimate occurred at Tunkhannock, PA during the winter half of the year. The percent error was 54 percent. In general, the seasonal estimates were within 30 percent across the thirteen-site region with the exception of Clearfield, KY in both seasons and Winterport, ME in the winter. The uncertainty in the seasonal estimates at Clearfield and Tunkhannock appear to balance during an annual time frame so that the longer-term estimates are more certain. The most consistent bias in uncertainty occurred at Fort Wayne where for both seasons and for the annual period the estimates were high. The aggregate estimates contained the smallest amount of uncertainty in Ontario, Ohio, southern Indiana, Massachusetts and Vermont.

Figure 31 shows the level of uncertainty associated with the aggregate estimates of wet nitrate deposition. Errors appear to be somewhat more variable from region to region and the amount of uncertainty is greater than it was for sulfate. Biases towards over or under prediction were also more consistent across seasons. At Tunkhannock and Turner Falls, MA the uncertainty was skewed towards under-estimation. While at Zanesville and Fort Wayne deposition was over-estimated by around 20 percent. At Big Moose the uncertainty changed sign from winter to summer as it did at Underhill, VT and Dorset, ON. At these sites the altering direction in uncertainty resulted in more stable annual estimates but a Big Moose the annual estimate remained relatively uncertain. In Kentucky, Michigan, North Carolina, Maine and southern Indiana and southern Ontario the aggregate estimates contained relatively little uncertainty for wet nitrate deposition.

Levels of uncertainty in estimates of total acidity deposition were generally between those of nitrate and sulfate. This was shown in Table 9 and is also apparent in Figure 32. In Ohio, Indiana, North Carolina, Michigan, Vermont and Ontario the degree of uncertainty was relatively small (generally within 20 percent). Confidence in acidity deposition was somewhat less and biased low over Massachusetts, Pennsylvania, Maine and New York. Overall the aggregate estimates of wet acid deposition were most uncertain at Tunkhannock.

Compared to the observed depositions the level of certainty in the aggregate estimates varied between sites and seasons. The magnitude of the uncertainty indicated how well the 30 episodes reproduced the mean behavior of the categories they were chosen to represent. The

larger values indicated that the concentration of pollutants in the precipitation for some of the episodes selected were significantly different than the mean volume-weighted concentration of the categories used. In general, it only required a couple of unusual events to noticeable effect the aggregate estimate. Considering that the same 30 episodes were used to estimate deposition at all locations across eastern North America the results were quite good. Certainly it would be possible to produce better estimates if separate events were used for each site. This would significantly increase the number of RADM runs necessary and is therefore not an option. The real root of uncertainty lies not in the accuracy of the specific predictions but in the choice of categories or meteorological situations represented. To place confidence in the outcome of the aggregation study and in the long-term estimates of deposition derived through the RADM project the episodes selected must vary meteorologically and chemically. They must also represent the types of situations that contribute a reasonable portion of the total deposition at any given location. These aspects have been continually tested throughout this study to insure confidence in the estimates and in the reaction of the estimates to altered emission scenarios.

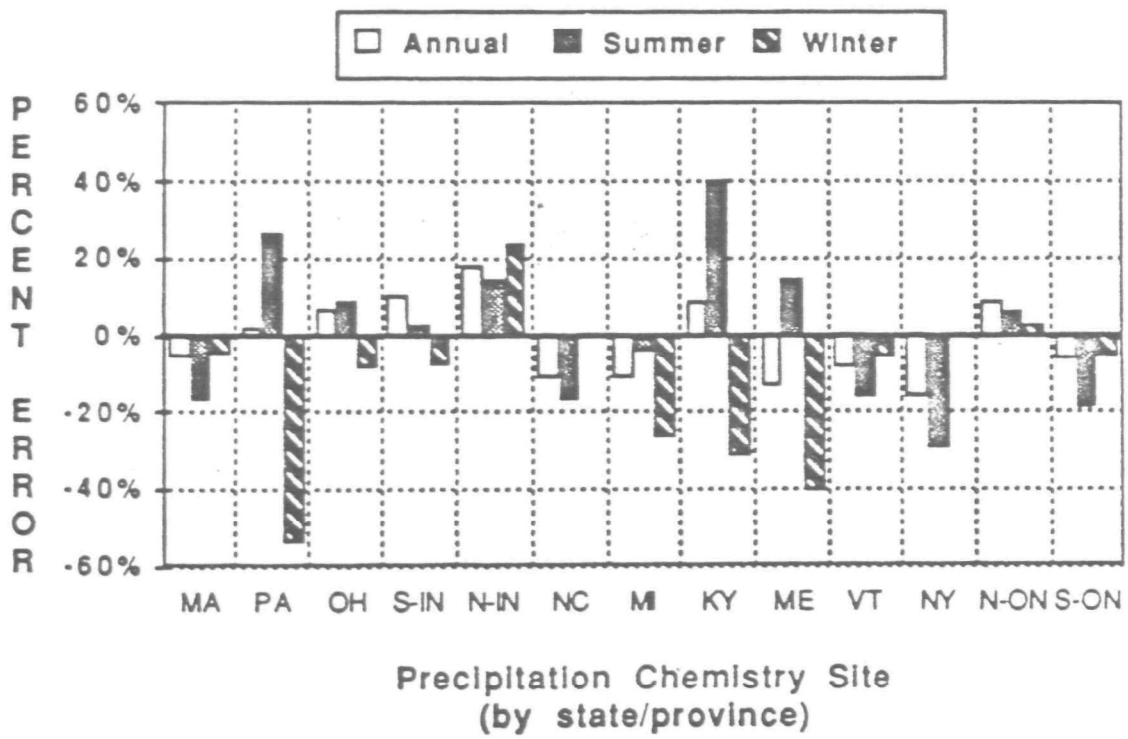

Figure 30. The uncertainty ranges for annual and seasonal wet $SO_4^=$ deposition due to estimation using the aggregation technique.

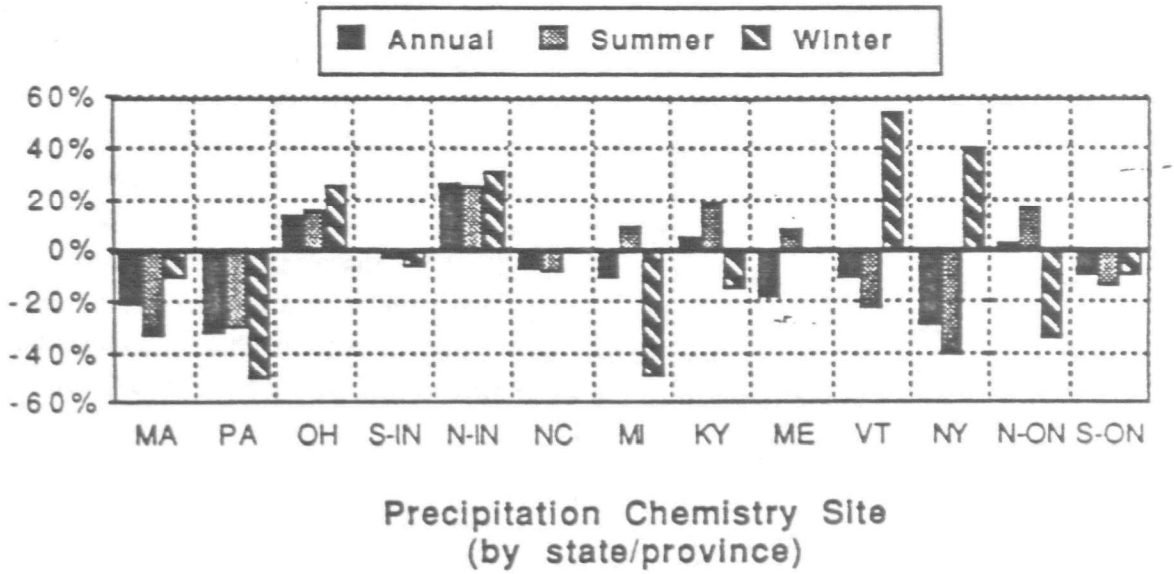

Figure 31. The uncertainty ranges for annual and seasonal wet NO_3^- deposition due to estimation using the aggregation technique.

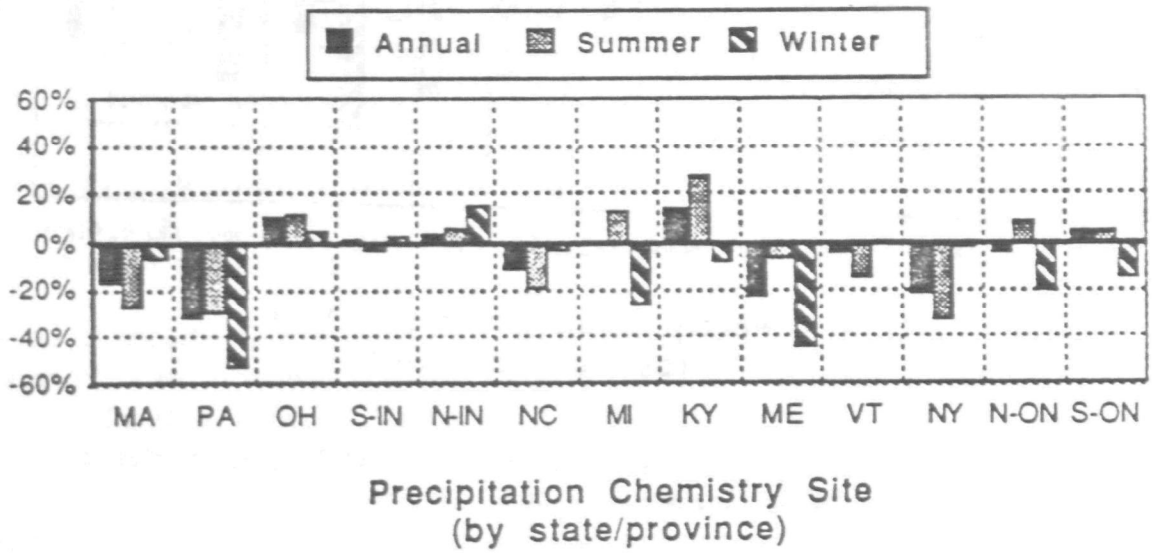

Figure 32. The uncertainty ranges for annual and seasonal wet H^+ deposition due to estimation using the aggregation technique.

3.4. SOURCE-RECEPTOR RELATIONSHIPS

The use of the meteorological categories was a key step in the aggregation project. In addition to providing accurate estimates of deposition it was also assumed that sampling from the dominant categories (in terms of total amount of wet deposition contributed) would insure that the important source-receptor relationships were represented. The category-based method of event selection and the specific 30 selected episodes have thus far only been evaluated in terms of observed wet deposition. The use of these categories, the behavior of which were quantified in terms of deposition and seasonality, also allowed for the application of scaling and weighting factors during aggregation. The actual episodes selected from the categories were also shown to provide good estimates of annual and seasonal wet deposition at a majority of the sites and to reproduce the spatial patterns well.

This section focuses on the differences in source-receptor relationships between categories, the benefits of event selection by category and on the actual source-receptor relationships represented by the 30 episodes. It was initially anticipated that because the categories represent different 850 mb wind-flow patterns they should also be associated with different source-receptor relationships. This implies that the winds at 850 mb (~1500 meters) were related to the winds responsible for transporting and dispersing pollutants in the atmospheric boundary layer (surface to 1500 meters). Evidence to support this hypothesis was uncovered in the testing of the wet deposition behavior of the categories. A possible explanation for their differences in terms of wet deposition is that they were associated with different source-receptor relationships. This should result in different depositions between categories because the chemical composition of precipitation depended upon transport. To investigate this, mixed-layer back-trajectories and Q-fields for three of the monitoring sites; Big Moose, New York; Gaylord, Michigan; and Raleigh, North Carolina were analyzed to provide a more direct measure of source-receptor relationships.

3.4.1. Climatological Wind Flow Patterns during Precipitation

Over eastern North America the air generally moves from west to east advecting airbourne pollutants along with it. At any particular time and place, however, the flow deviates markedly from this pattern. Over the course of a year or longer certain upwind areas will have a stronger influence upon each location. It is these long-term tendencies that play an key role in the spatial pattern of seasonal and annual deposition of $SO_4^{=}$, NO_3^{-} and H^+ and in the specific amount that any given receptor experiences. In terms of long-term wet deposition it is the wind flow during and shortly before each event that is important.

To identify which areas have the greatest tendency to affect Big Moose, Gaylord and Raleigh the trajectories associated with all of the precipitation events during 1982-1986 were

combined into overall Q-fields for each site. Figures 33 to 35 show the mean probability of transport to Big Moose, Gaylord and Raleigh, respectively (units are 10^{-8} km^{-2}). The air arriving at each location had the highest probability of passing over areas immediately adjacent to the receptor and the probability decreases with distance. The rate of decrease depends upon direction and as expected the gradient is somewhat sharper toward the east. This is because the winds from the east were less common than those from the west. At Raleigh, however, a part of the reason for the rapid decrease towards that east was probably due to the lack of data over the ocean. Compared to Big Moose, the boundary layer winds during precipitation events at Gaylord and Raleigh had a greater tendency to come from the north and south and did not favor a westerly direction as much. At Raleigh, northeast and southeast winds were more common than at the other sites and in general, the wind appears to be lighter there. This behavior was indicated by the size of the area encompassed by the 25×10^{-8} contour. The Q-field for Gaylord shows that northwest and southwest winds were relatively more prominent. Relatively close to the receptors (within about 500 km) it appears that any sources to west and east would contribute more at Big Moose and Gaylord while at Raleigh no such tendency was apparent. In general, the probability fields for all events (with and without precipitation - not shown) tended to be more skewed towards the west because non-precipitating events were even less often associated with easterly and southerly winds.

3.4.2. Wind Flow Associated with Sulfate Wet Deposition

To obtain an idea of where the air originated during events with higher levels of $SO_4^=$ in precipitation the Q-fields were re-calculated using the same set of trajectories but with deposition-related weights attached. The weighted Q-fields are shown in Figures 36 to 38. Subtle differences between these fields and the non-weighted fields were discernable by comparing the figures.

At Big Moose the weighting appeared to have resulted in increased probabilities towards the south to southwest and locally. The values decreased to the west, northwest and east. The effect of the weighting for Gaylord showed up as slight increases to the south and north and decreases to the west to northwest. At Raleigh the probabilities increased very slightly to the north and it is more noticeable over Virginia. There were decreases in probabilities to the southwest, west and northeast. These changes suggested a possible relationship to the spatial distribution of SO_2 emissions across the Northeast. To highlight the differences between the weighted and non-weighted fields the potential source contribution functions (PSCF) were determined. These new fields clearly show which regions were most often affiliated with high and low deposition amounts and can be more easily compared to the emissions field.

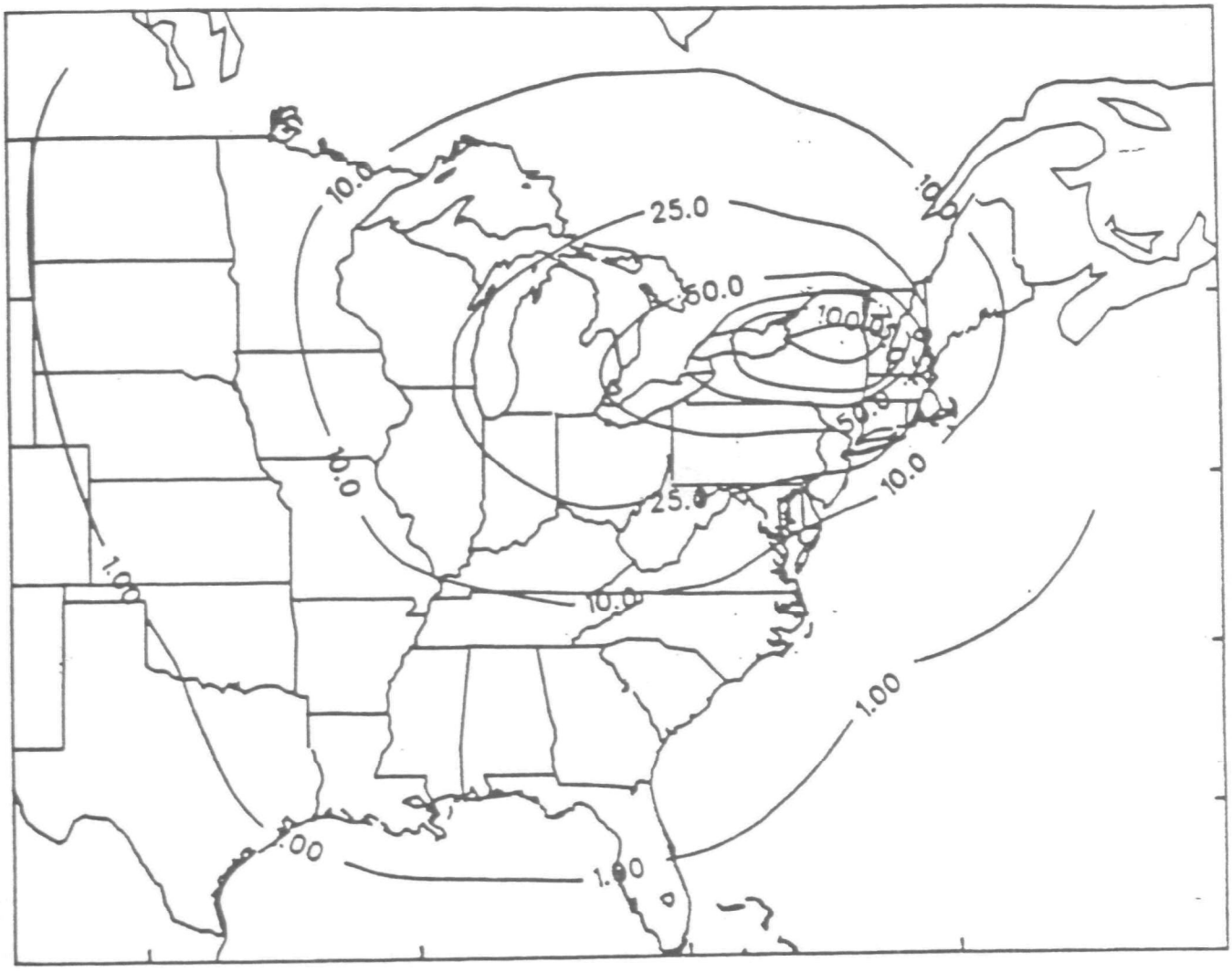

Figure 33. The mean probability (10^{-8} km^{-2}) for transport on precipitation days to Big Moose, NY, during the period 1982-1985.

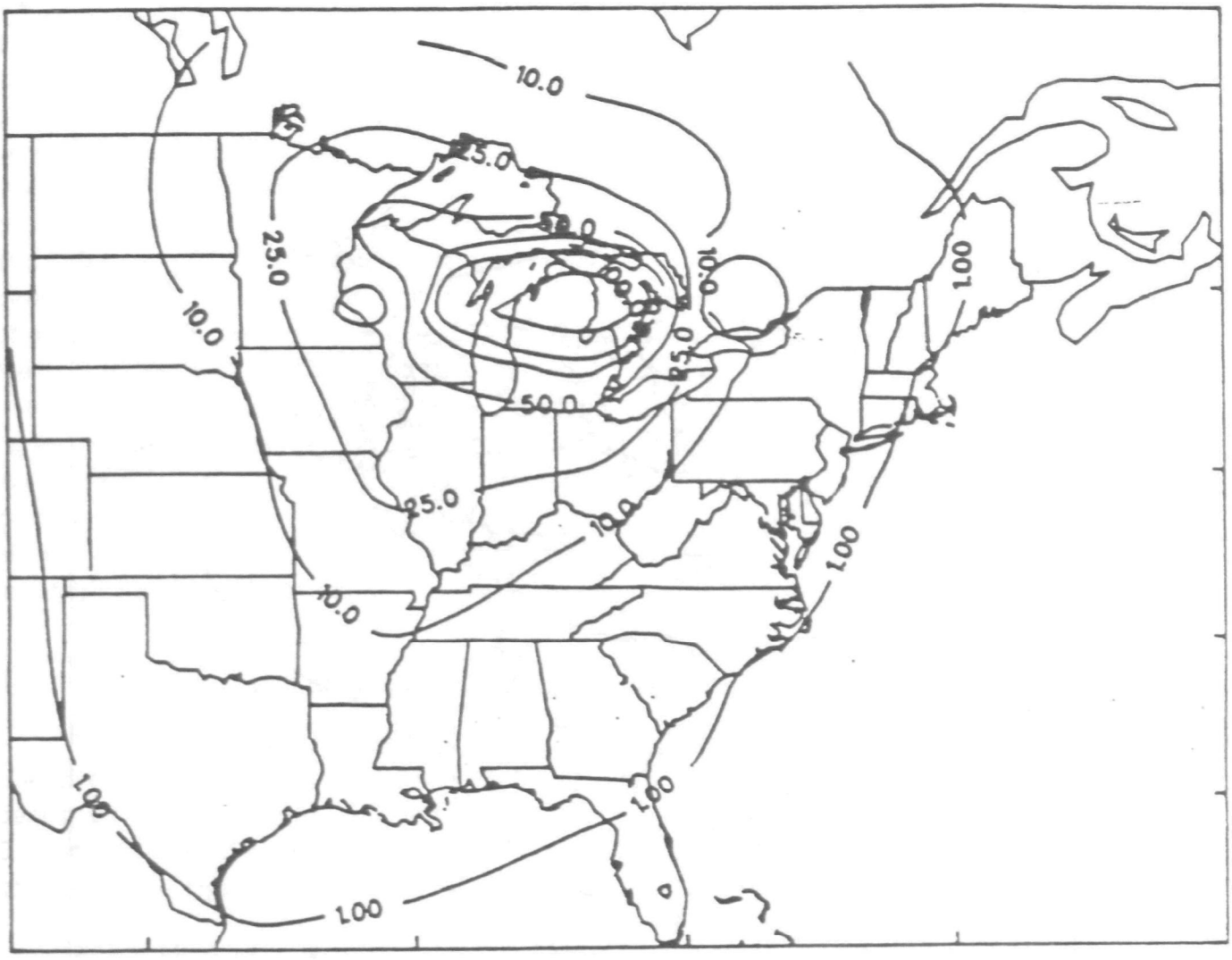

Figure 34. The mean probability (10^{-8} km^{-2}) for transport on precipitation days to Gaylord, MI, during the period 1982-1985.

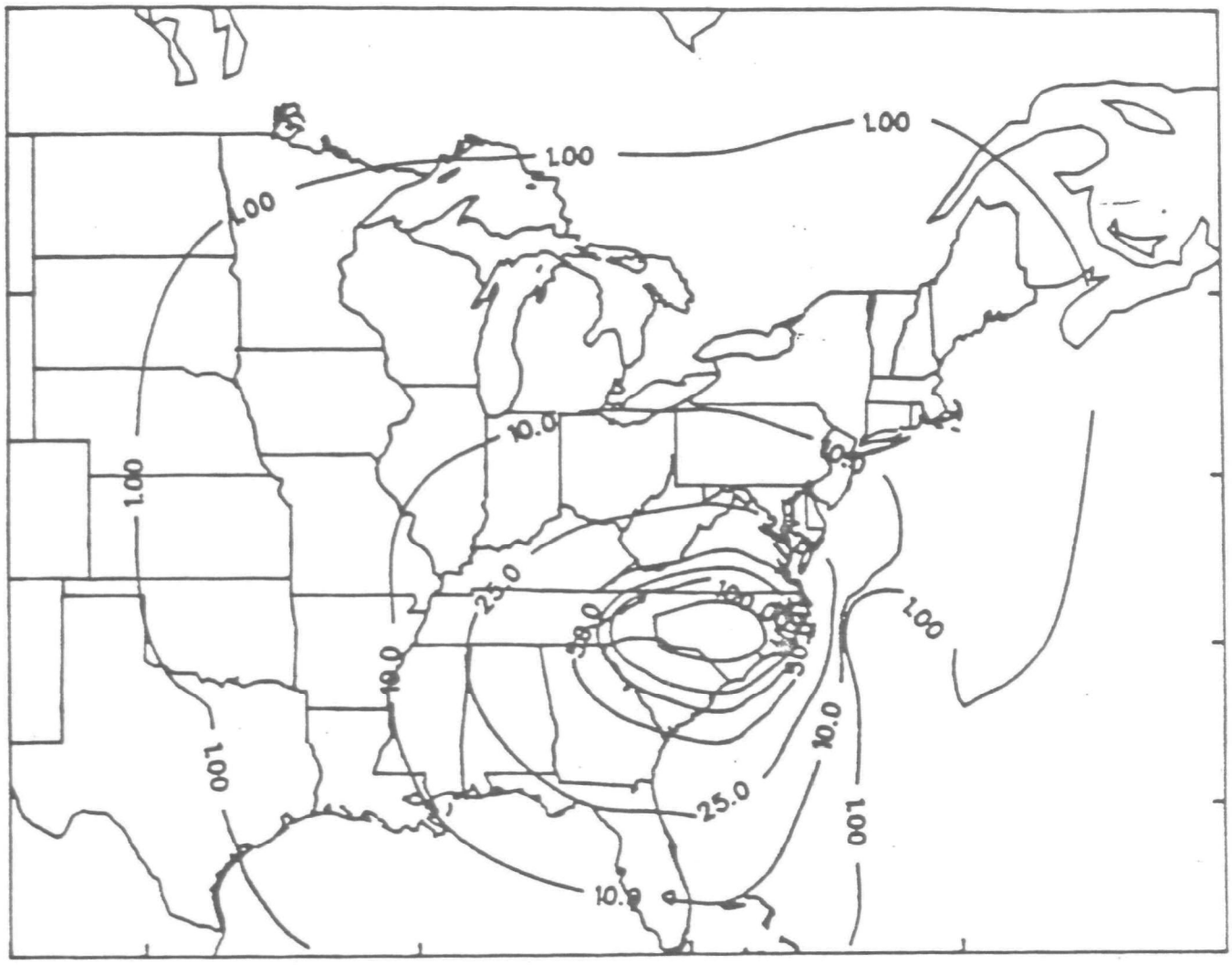

Figure 35. The mean probability (10^{-8} km^{-2}) for transport on precipitation days to Raleigh, NC, during the period 1982-1985.

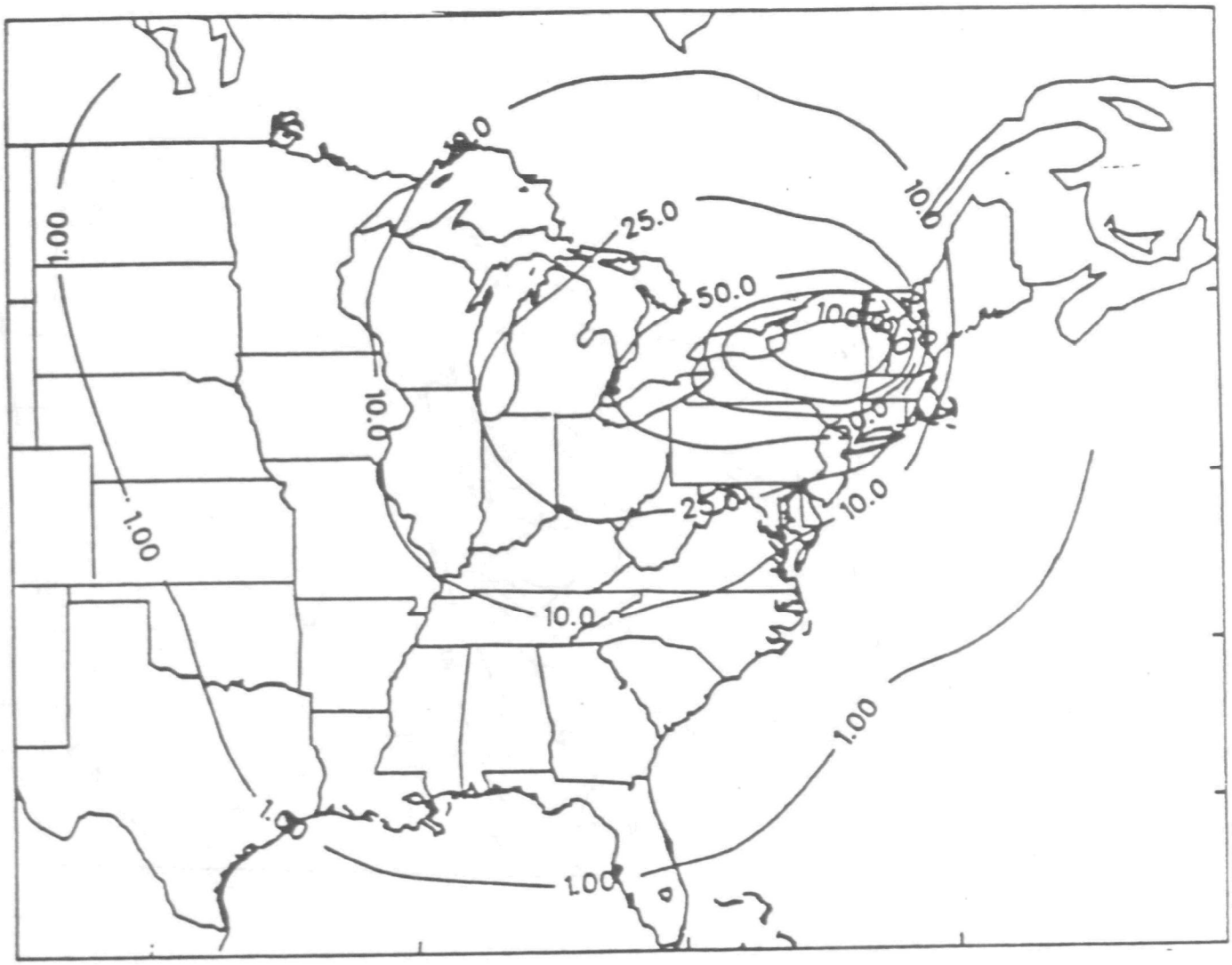

Figure 36. The $SO_4^{=}$ wet deposition weighted probability (10^{-8} km^{-2}) for transport to Big Moose, NY during the period 1982-1985.

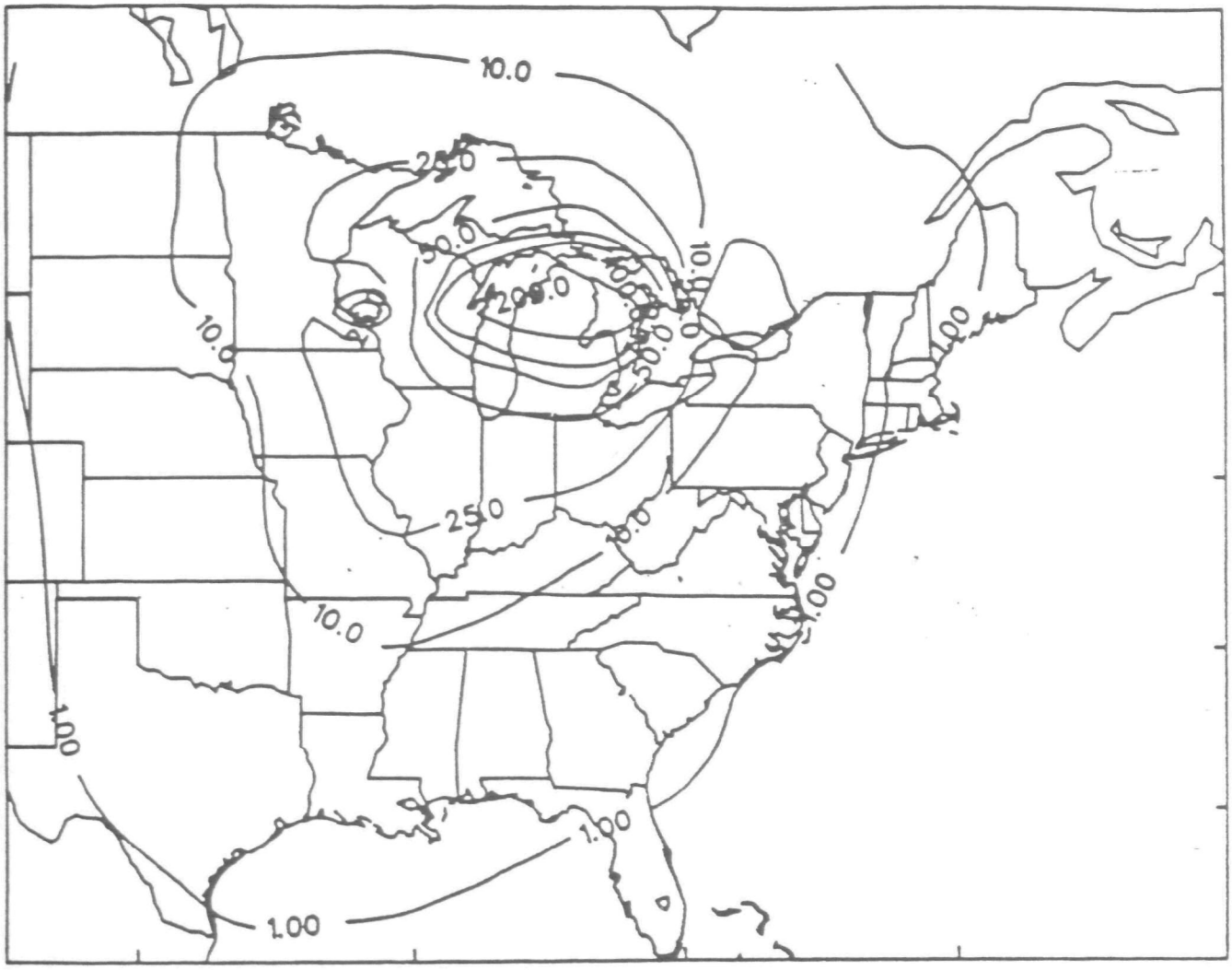

Figure 37. The $SO_4^=$ wet deposition weighted probability (10^{-8} km^{-2}) for transport to Gaylord, MI, during the period 1982-1985.

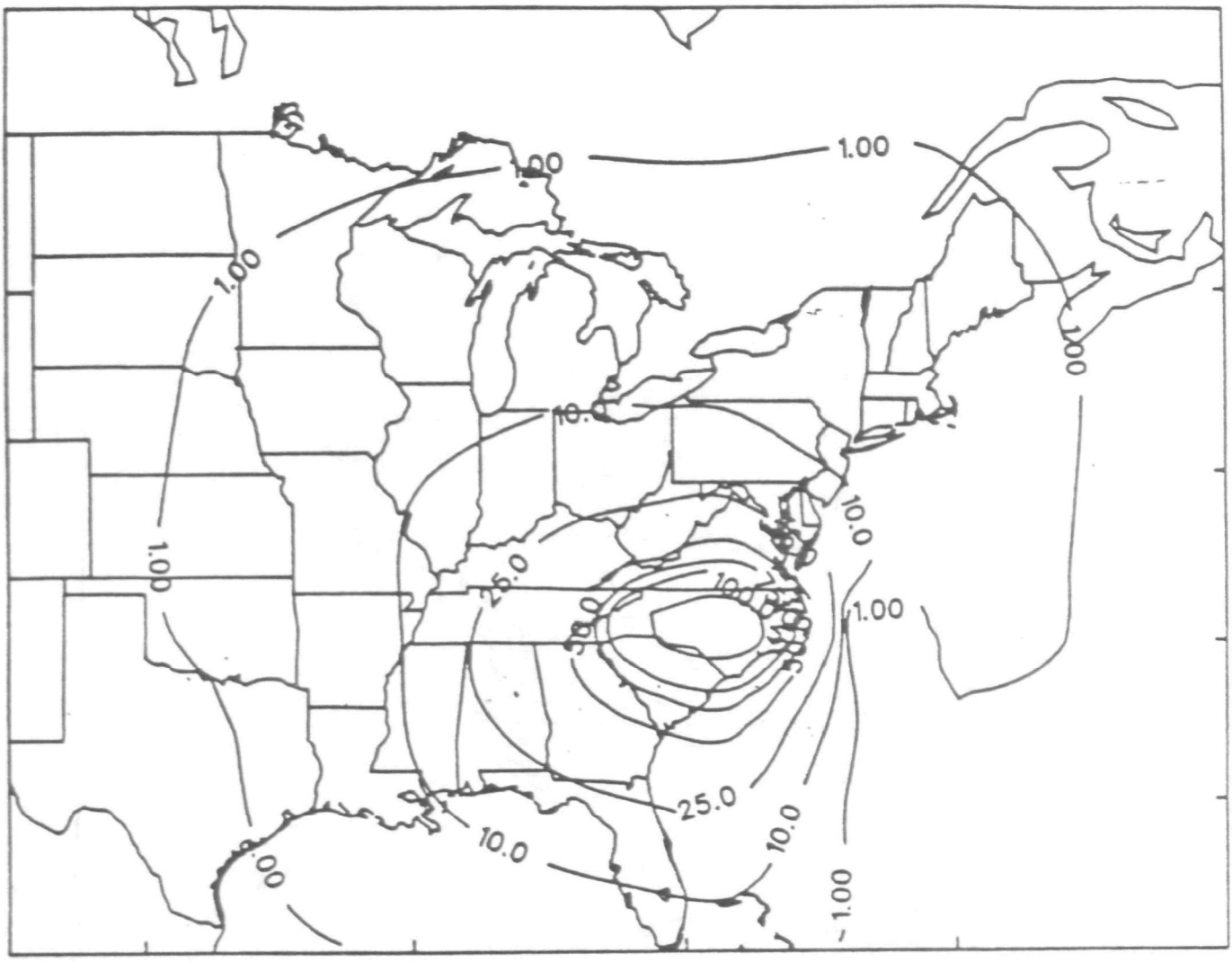

Figure 38. The $SO_4^{=}$ wet deposition weighted probability (10^{-8} km^{-2}) for transport to Raleigh, NC, during the period 1982-1985.

3.4.3. Potential Source Contribution Functions

Figure 39 illustrates the transport bias field for Big Moose, NY. Values are positive (more often associated with above average $SO_4^=$ wet deposition) to the south to southwest and to the northwest to north-northwest. When airmasses originated over Big Moose and over areas immediately to the south extending across Pennsylvania to southeast Ohio the resulting depositions were most likely to be large. Large positive values close to Big Moose are indicative of high depositions during stagnant conditions when the ambient SO_2 and $SO_4^=$ levels were likely to be rather homogeneous over large areas. In general the regions with positive PSCF values agreed with locations of known SO_2 emissions. The main exception is off the coast of Virginia where the PSCF is large. It is possible that this area was linked to above average depositions because of synoptic situation or because of the importance of precipitation amount in determining wet deposition amount there. In Figure 39 it can be seen that when the air was from the east, northeast, northwest and west depositions were more often below average at Big Moose.

Sulfate wet deposition amounts were used to weight the Q-fields in the numerator of the PSCF's hence, one could argue that the results were as much a function of large precipitation amounts as they are enhanced $SO_4^=$ concentrations (i.e. more precipitation fell when the winds were from the southwest). To test for this possibility the PSCF field for precipitation (i.e. numerator weighted by precipitation amount) was determined. The result for Big Moose is shown in Figure 40. In this case the largest values were located to the east where values approached a minimum in the $SO_4^=$ weighted PSCF field. There was overlap between the positive areas in the precipitation and $SO_4^=$ weighted fields in the vicinity of Big Moose and to the north and south. However, along the Ohio River valley and over most of Ohio and southeastern Indiana the $SO_4^=$ weighted field indicated above average contribution (positive) and the precipitation weighted field showed below average (negative) contribution. This discrepancy highlights the importance of the large sources of anthropogenic SO_2 in the Midwest to the wet deposition of $SO_4^=$ at Big Moose. These two figures clearly indicate that $SO_4^=$ wet deposition is not driven solely by precipitation amount.

The results of the PSCF analysis for Gaylord, MI are shown in Figures 41 and 42. Over all wet events (Figure 41), wind flow from the southwest and south-southeast were linked with relatively high $SO_4^=$ deposition events. The area most often tied to large events extended from Gaylord across southeastern Michigan, Ohio, Kentucky and western West Virginia and encompassed much of the Ohio River valley. Winds from the north also appeared to have frequently resulted in above average $SO_4^=$ wet deposition. Flow from the southwest to northwest and the east to southeast did not seem to be systematically related to high deposition events.

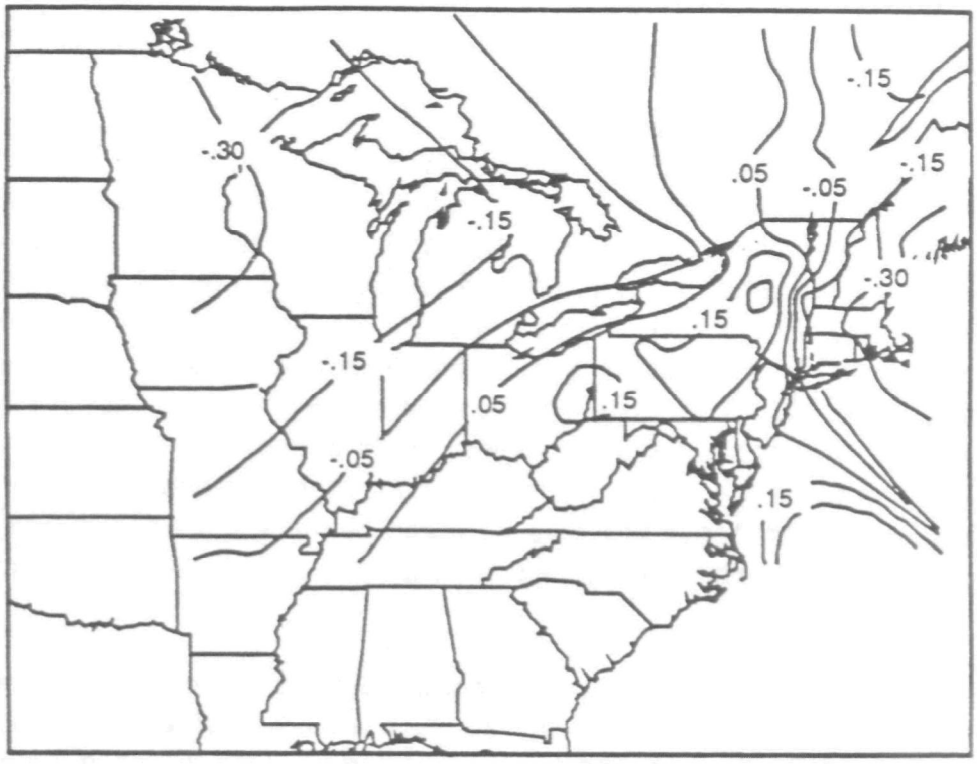

Figure 39. The bias for transport associated with large $SO_4^=$ wet deposition at Big Moose, NY, during the period 1982-1985. Positive values represent regions more often associated with above average $SO_4^=$ wet deposition amounts .

There is better agreement between the $SO_4^=$ weighted and precipitation weighted fields at Gaylord than was seen at Big Moose. As with $SO_4^=$, there was a greater tendency for relatively large precipitation events when the air arrived from the south and north (Figure 42). The magnitudes of the PSCF values over these areas were significantly smaller than those generated with $SO_4^=$ weighting. It is interesting to note that fairly strong winds from the southwest seem to have been associated with high precipitation events more often. As well, winds from the north-northwest across Lake Superior and the Straights of Mackinac were associated with relatively large amounts of water deposition. Some of these events could be associated with cold outbreaks during the winter that pick up large amounts of moisture over the relatively warm lake water.

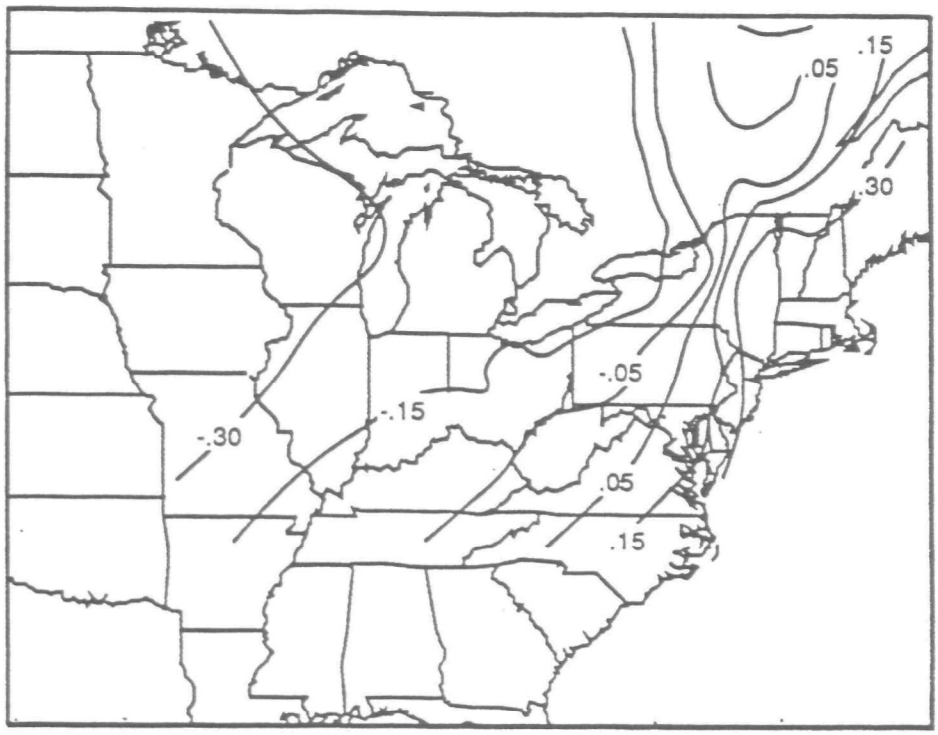

Figure 40. The bias for transport associated with large water deposition at Big Moose, NY, during the period 1982-1985. Positive values represent regions more often associated with above average precipitation .

Similar analyses for Raleigh, NC were hampered by the fact that many of the trajectories from the eastern quadrants ended abruptly over the ocean. It is therefore difficult to assess the relative importance of airmasses approaching from these areas. For all of the wet events during 1982 to 1986 the PSCF field is displayed in Figure 43. The regions most often leading to relatively high wet $SO_4^=$ depositions are to the northwest and towards the east to southeast. The reason for the large values to the east is uncertain. It could be due to a greater influx of moisture and precipitation associated with easterly winds and/or due to polluted airmasses from the northeast that move out over the ocean and then back inland south of anti-cyclones. It could also be partly due to the difficulty discussed above. The region above 0.05 (5%) across Virginia, West Virginia and Ohio is more certain. Flow from this area correlates well with high SO_2 emission regions in the Ohio River valley. This area takes on more significance when compared to the precipitation weighted PSCF fields for Raleigh (Figure 44). Clearly, these areas do not have a tendency to be associated with the large precipitation events. These events usually result with flow from the east and southeast.

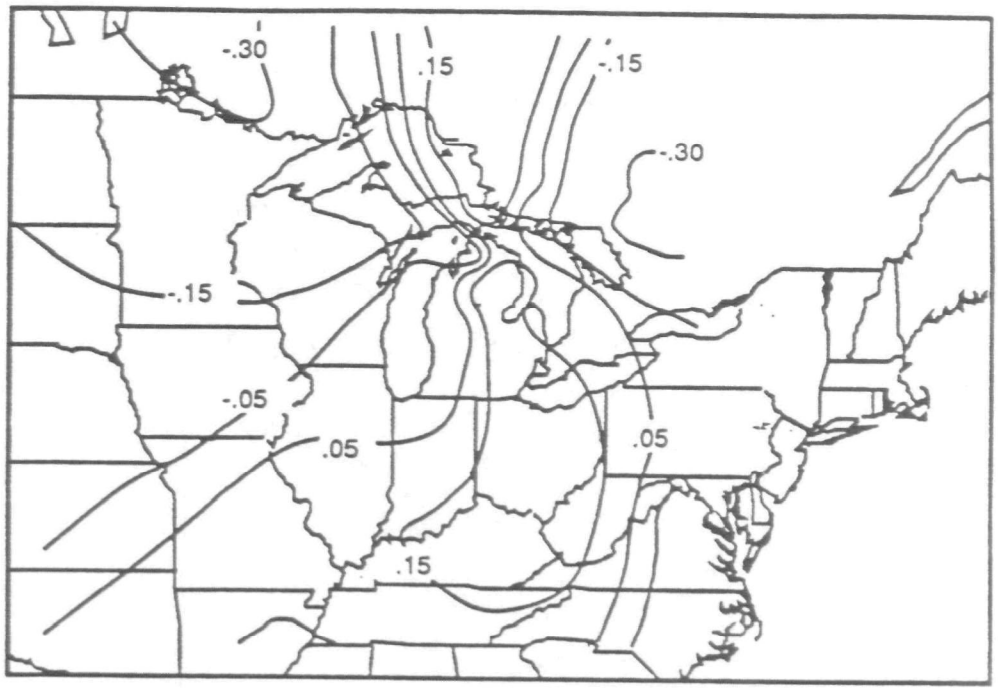

Figure 41. The bias for transport associated with large $SO_4^=$ wet deposition at Gaylord, MI, during the period 1982-1985. Positive values represent regions more often associated with above average precipitation .

To highlight the airmass source regions that were most often associated with high $SO_4^=$ wet deposition events the PSCF fields for Big Moose, Gaylord and Raleigh were combined. This new "product" field is shown in Figure 45. With the individual PSCF fields it is not possible to determine where along the trajectories the $SO_4^=$ has originated. The intersection of the PSCF fields values from these three locations, however, is able to indicate more specifically which regions were consistently associated with relatively large amounts of $SO_4^=$ wet deposition. Areas above 0.25 or below -0.25 are the most significant.

In Figure 45 it can be seen that when the airmasses originated over Ohio, northeastern Kentucky, western Pennsylvania and northwestern West Virginia they lead to relatively large $SO_4^=$ wet depositions at all three sites. This pattern is rather good agreement with the spatial distribution of SO_2 sources. In contrast airflow from the northwest and northeast were not systematically leading to high depositions. Another area of that shows up as being important to wet $SO_4^=$ deposition is located off the coasts of North Carolina and Virginia. This could have been due to the availability of moisture over the Atlantic and/or the easterly flow on the south side of anti-cyclones and north side of cyclones.

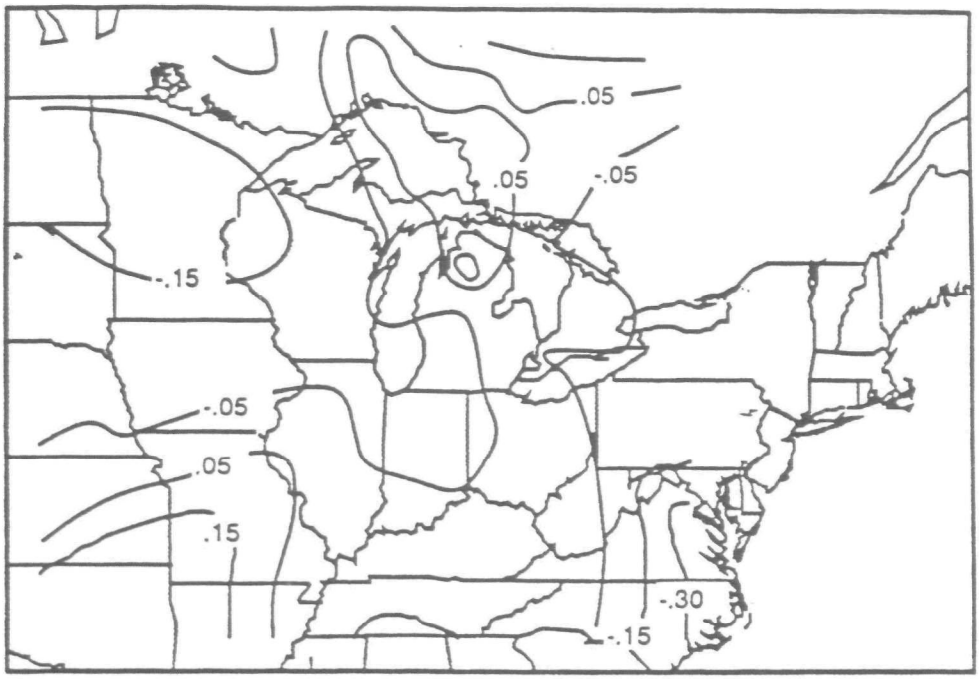

Figure 42. The bias for transport associated with water deposition at Gaylord, MI, during the period 1982-1985. Positive values represent regions more often associated with above average precipitation .

Every location in eastern North America will experience its own unique relationship with the various source regions that contribute pollutants to the atmosphere. From day to day and even year to year these relationships are likely to change. Over the relatively long time period of 5 years the significant short-term variations are essentially smoothed over. These climatological Q-fields were generated and analyzed for three opposing receptors. At each of the three locations studied the upwind regions most often associated with precipitation events were different, however, throughout the five years it was possible for the flow to come from almost any direction regardless of location.

The aggregate estimates of seasonal and annual deposition were compared to the observed values during 1982-1985. Similarly, aggregate Q-fields were compared to the actual wind flow over a longer period of time. Before such comparisons could be made it was necessary to decide which flow pattern should be reproduced. Since wet deposition is of primary interest the precipitation only Q-fields should be the main goal. However, the event selection protocol was designed to identify storms with a high likelihood of producing $SO_4^=$ wet deposition at multiple locations across eastern North America. This implies that flows from areas most often leading to relatively high $SO_4^=$ are desirable. Therefore, an aggregate of the wind flow from the selected storms should most resemble the $SO_4^=$ weighted Q-fields.

Figure 43. The bias for transport associated with large $SO_4^=$ wet deposition at Raleigh, NC, during the period 1982-1985. Positive values represent regions more often associated with above average wet deposition.

3.5. THE VARIATION IN SOURCE-RECEPTOR RELATIONSHIPS BETWEEN CATEGORIES

Over all events (wet and dry) some categories favored flow from the north to northwest (categories 7, 8), others favored the south to southwest (1, 5, 11) and still others showed bias towards the west (6, 10). Category 9 was associated with low wind flow situations and category 10 with higher wind speeds. Wet differential probability fields for these categories are included in Figures 46-54. Figure 46 shows the wet differential field for category 20 (unbiased set of missing days) and illustrates the magnitudes one can expect due to random fluctuations. Close to the site, the differential was as high as 30×10^{-8} km^{-2} but further away the random fluctuations resulted in differentials less than 10^{-8} km^{-2}. Wet differential probabilities seen in Figures 47 to 54 are greater than these values and, hence, can be significant.

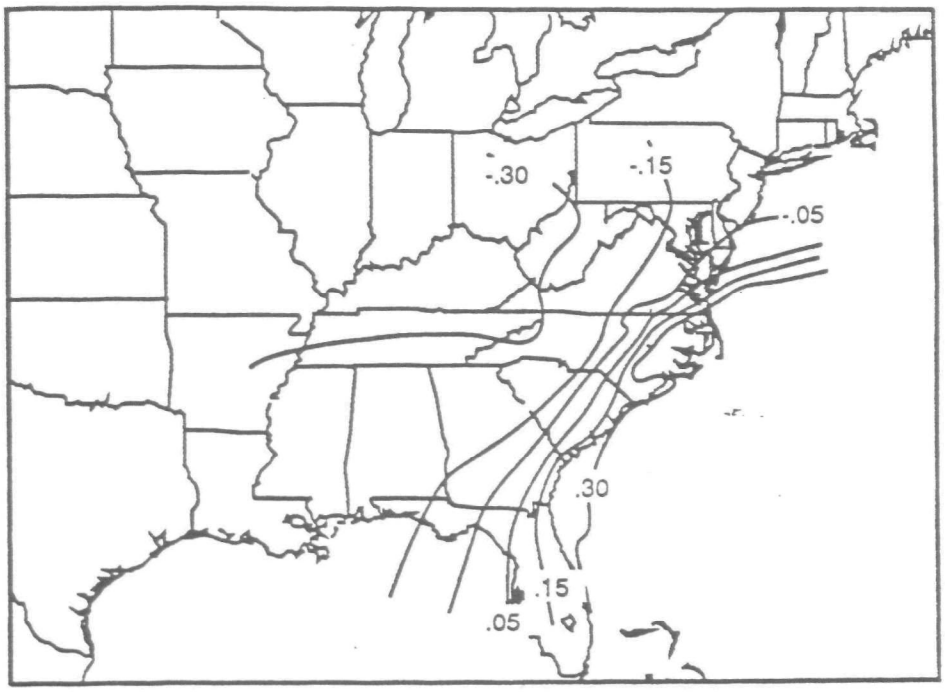

Figure 44. The bias for transport associated with large water deposition at Raleigh, NC, during the period 1982-1985. Positive values represent regions more often associated with above average precipitation .

The wet differential probabilities for these eight categories were similar to those calculated over all events (dry and wet) which were summarized above. The main differences appearing in the wet only cases are outlined in Table 10. In terms of where the air was most and least likely to originate just before and during precipitation there were identifiable differences between categories. Selection from a collection of these categories should help insure that the resulting aggregate estimates of wet deposition are not biased towards a small number of potential source regions.

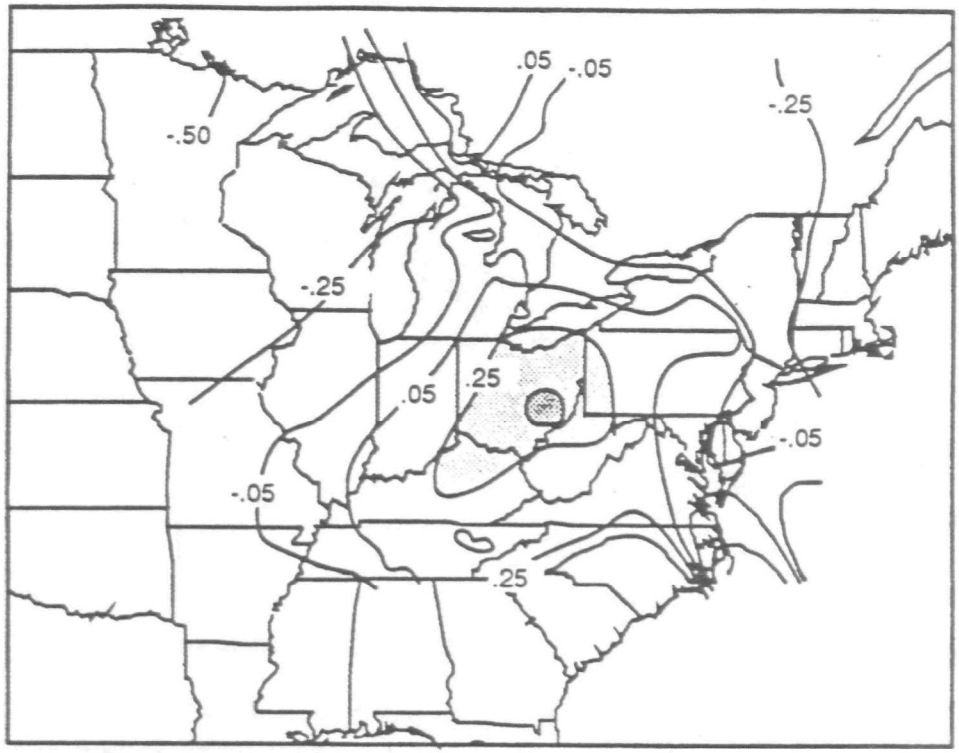

Figure 45. The ensemble bias for transport associated with large $SO_4^=$ wet deposition at Big Moose, NY; Gaylord, MI; and Raleigh, NC, during the period 1982-1985. Positive values represent regions consistently associated with above average $SO_4^=$ deposition amounts.

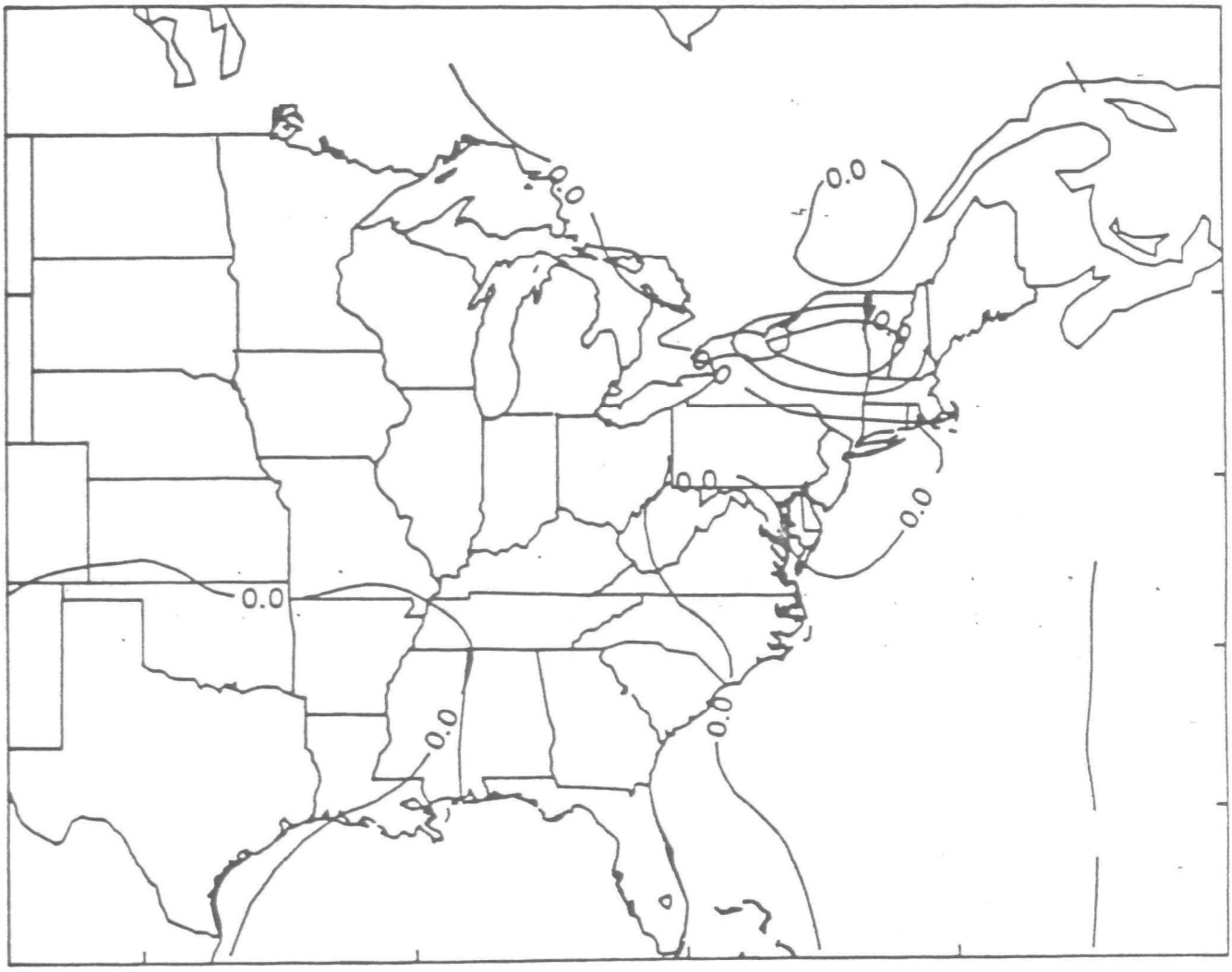

Figure 46. Difference between climatological Q field (1982-1985) and the Q field for category 20 (unbiased set of missing days).

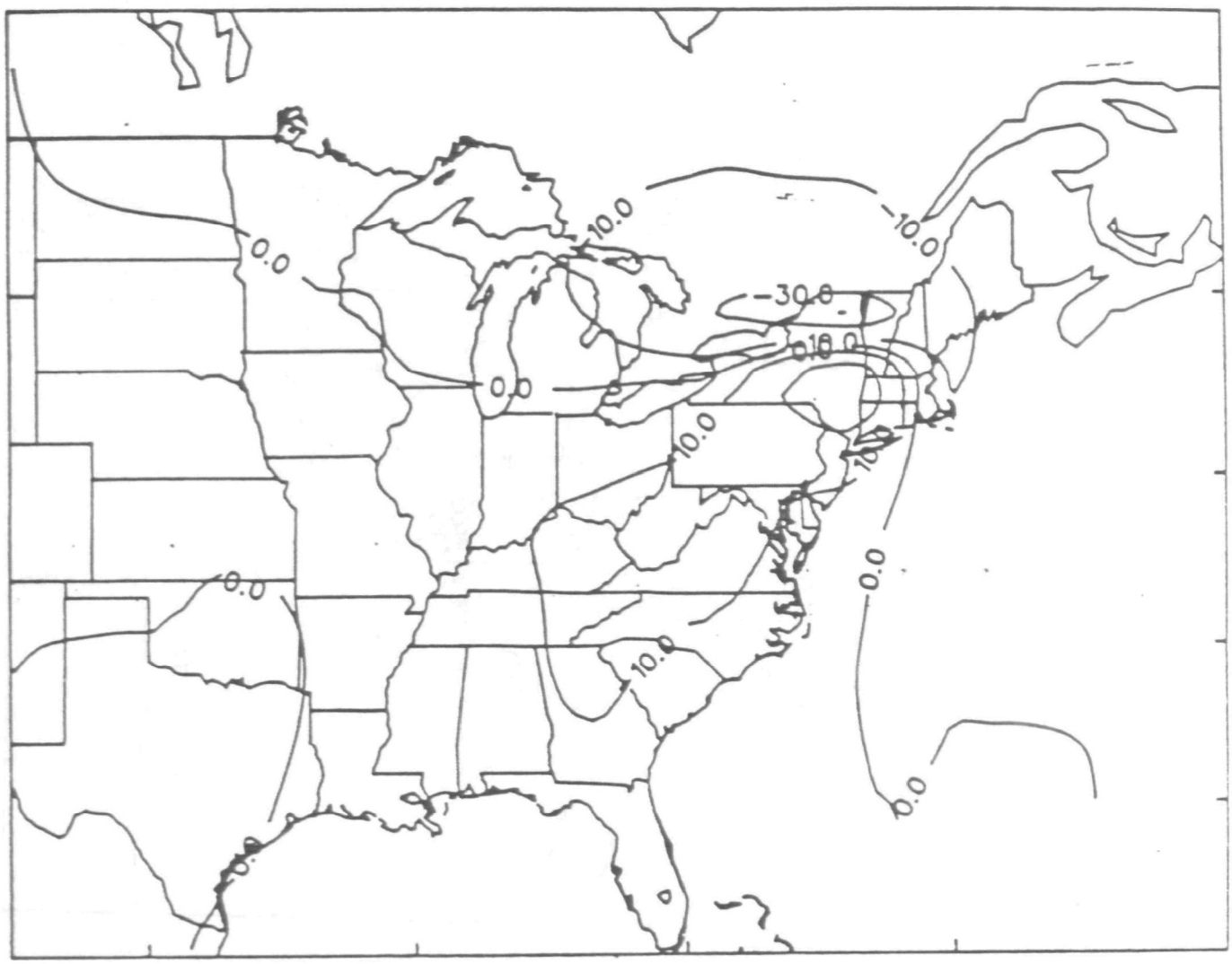

Figure 47. Difference between climatological Q field (1982-1985) and the Q field for category 1.

Figure 48. Difference between climatological Q field (1982-1985) and the Q field for category 5.

Figure 49. Difference between climatological Q field (1982-1985) and the Q field for category 6.

Figure 50. Difference between climatological Q field (1982-1985) and the Q field for category 7.

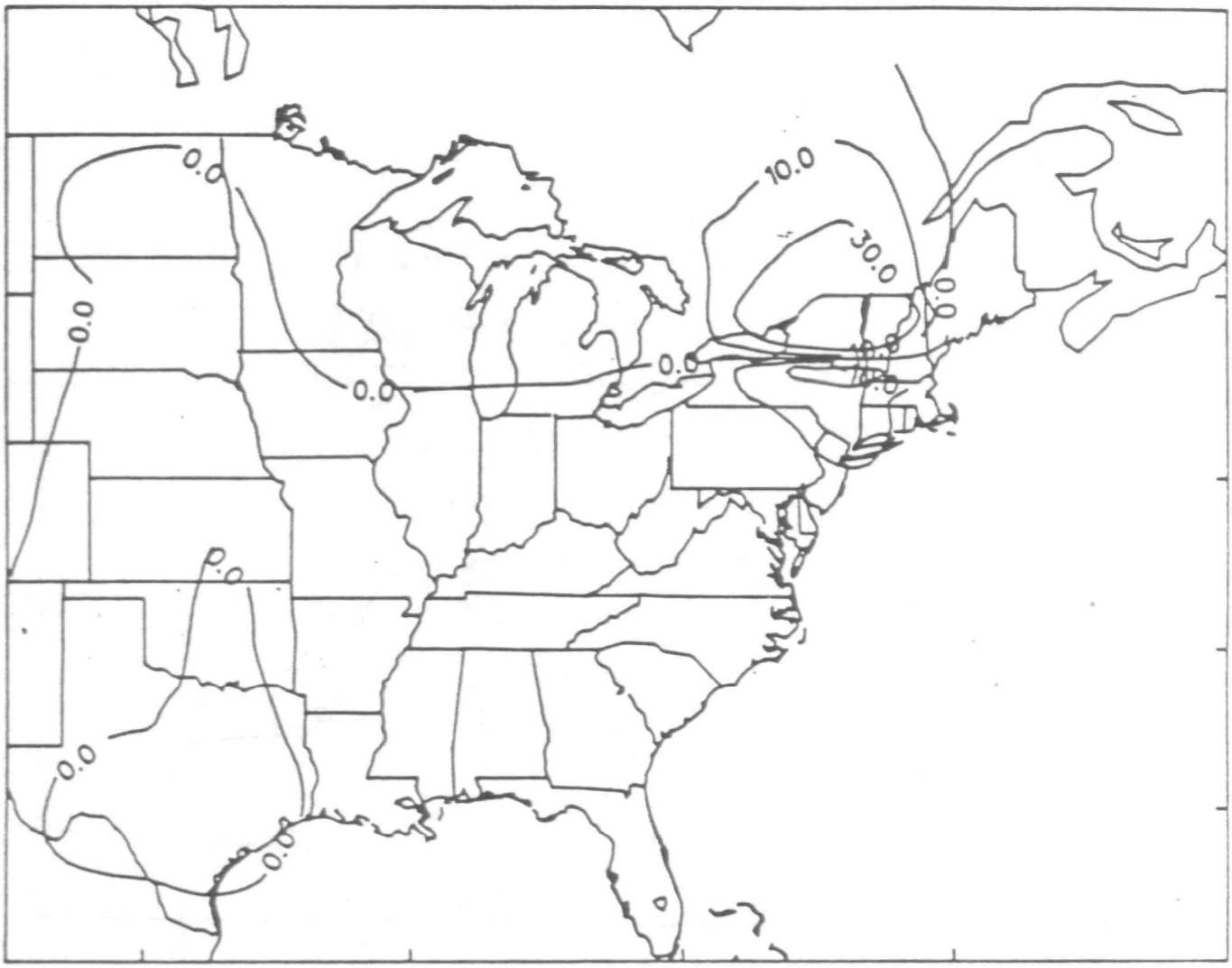

Figure 51. Difference between climatological Q field (1982-1985) and the Q field for category 8.

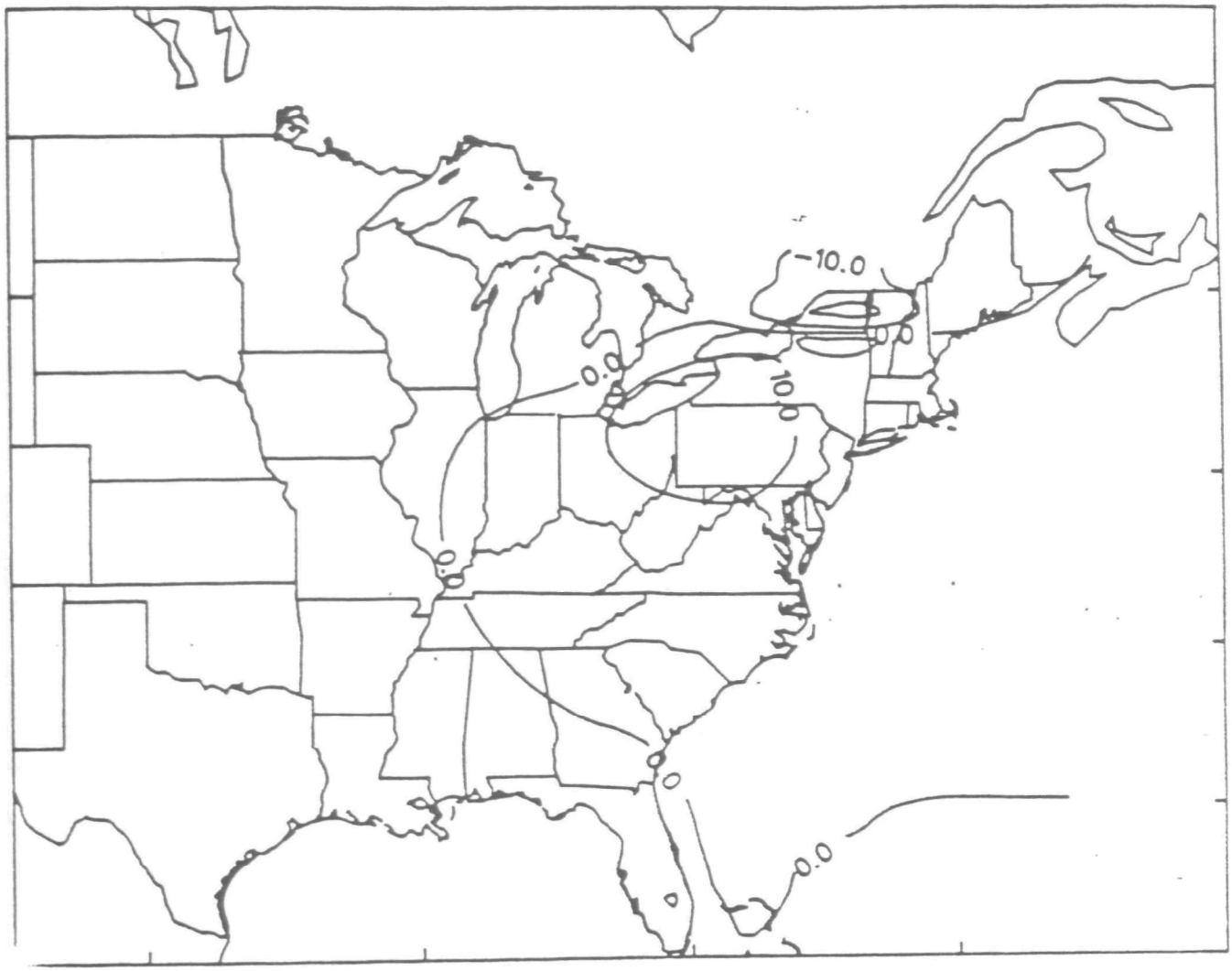

Figure 52. Difference between climatological Q field (1982-1985) and the Q field for category 9.

Figure 53. Difference between climatological Q field (1982-1985) and the Q field for category 10.

Figure 54. Difference between climatological Q field (1982-1985) and the Q field for category 11.

TABLE 10. DESCRIPTION OF SOURCE-RECEPTOR RELATIONSHIPS FOR SELECTED METEOROLOGICAL CATEGORIES.

CATEGORY	DESCRIPTION
Category 1:	There area that the air was more likely to originate from extended to the southwest and south covering the Ohio River Basin and parts of Virginia and North Carolina and did not seem to be associated with Indiana and Ohio. The low-probability region extends a good distance to the west.
Category 5:	This category is different than Category 1 in that the flow bias is stronger and aligned toward the south of the receptor. This category might be more likely to be influenced by east coast sources than would category 1.The region less likely to influence the airmass over Big Moose extends westward to encompass Michigan.
Category 6:	The biases in this pattern are relatively weak with a slight enhancement in probability of wind flow from the west. The area less-likely-to-contribute included a large area around the receptor itself and extends to the south and east slightly. The wind flow was stronger for precipitation events than for dry events.
Category 7:	There is a pronounced positive bias towards the northwest and a little to the west. There is some likelihood of light wind situations during wet events in category 7. This is indicated by a large, positive bias region immediately to the north of Big Moose.
Category 8:	Category 8 has a relatively strong bias toward air flow from the north, though the differences do not extend far from the receptor indicating a weak flow pattern. Category 8 exhibited lower concentrations of $SO_4^=$ than did other predominantly summertime categories.
Category 9:	Category 9, which exhibited a relatively high $SO_4^=$ wet deposition to precipitation ratio, is associated with a moderately pronounced differential probability field. This field decreases fairly fast with distance suggesting a low wind flow associated with the category. There is bias toward transport from the southwest in category 9. For precipitation events the maximum positive area moves further away from the receptor in the southwest. There may therefore be slightly stronger winds associated with precipitation events. A negative bias towards the north is rather pronounced.

TABLE 10 (CONT.). DESCRIPTION OF SOURCE-RECEPTOR RELATIONSHIPS FOR SELECTED METEOROLOGICAL CATEGORIES.

CATEGORY	DESCRIPTION
Category 10:	The relatively large negative bias suggests the transport was less likely to be associated with low wind speed situations. The weak positive bias to the west suggests that air flow to the receptor had a somewhat enhanced chance of arriving from the upper midwestern United States and extreme southern Ontario.
Category 11:	The differences between the overall wet probability field and the wet probability field associated with category 11 were small throughout eastern North America. This suggests that the wind flow pattern common to this category is similar to the wind flow associated with the typical precipitation event at Big Moose.

3.6. SELECTING EPISODES TO ESTIMATE SOURCE-RECEPTOR RELATIONSHIPS

The differences in the wind flow between categories suggests that using them as event selection guidelines should result in a better representation of the long-term $SO_4^=$ weighted source-receptor relationships. In the context of this study better implies relative to selecting events at random. For the estimation of annual depositions category-based selection and weighting was shown to improve upon random and seasonal selection methods. This was demonstrated by selecting and aggregating a number of nineteen-events ensembles using a variety of methods. A similar approach was developed for testing how well categories do in helping to reproduce the expected source-receptor relationships.

The episode selection criteria outlined for estimating deposition were followed. Nineteen were selected from categories 1W, 3W, 5W, 6W, 7W, 8W, 9W and 11W. The random versus strata comparisons were not based upon 30 episodes because it was the original nineteen that were selected to best reproduce deposition and wind flow. The other eleven were included to cover more unusual situations. Random selection of events was limited to those events in the wet halves of the categories. The same episodes were expected to estimate deposition at locations across eastern North America so each ensemble of episodes was tested in terms of its ability to reproduce the wet-weighted fields at Big Moose, Gaylord and Raleigh collectively. Twenty-five individual ensembles were sampled and aggregated using the two techniques (random and strata). For the random case it was assumed that there was no way to weight the various episodes. The only option involved whether or not to use all days or just the wet days. When categories were employed, however, there were a number of potential approaches to weighting the episodes.

- Keep all days or days with reported precipitation only and combine with no weights.
- Keep all days and weight them according to the frequency of occurrence of their respective categories.
- Employ only the days with precipitation and weight them with the amount of deposition on each day and category frequency.
- Employ only the days with precipitation and weight with expected deposition (mean category deposition) and frequency.

The Q-fields against which our selection and aggregation methods were tested were the $SO_4^=$ wet deposition weighted fields shown in Figures 36 to 38. These Q-fields served as the base-line for all comparisons. Two of the above approaches were tested. In the first case both the precipitating and non-precipitating days were retained and both the random and category-based ensembles were aggregated without weights. It was assumed that the way in which the category selections were prescribed implicitly included a weighting since those categories known to produce a large percentage of the deposition across eastern North America were sampled according to importance and frequency. All days were kept because the occurrence or non-occurrence of precipitation at the actual receptor is not indicative of the processes occurring over the surrounding area. The movement of airmasses during the entire evolution of a storm system will effect the chemistry of the resulting precipitation. The results of comparing the random and category-based ensembles in this situation indicated which approach better represented the wind flow associated with long-term regional deposition. Figure 55 shows the percent RMS errors, ranked from smallest to largest, for the random and category-based ensembles.

The Q-fields were compared over all areas with probabilities greater than 10^{-4} km^{-2} and over the Midwest. Figure 55 indicates that selection by category is consistently better than random selection in reproducing the source-receptor relationships important to regional $SO_4^=$ wet deposition. The two methods were compared over the Midwest because flow from this region is frequently associated with significant amounts of $SO_4^=$ wet deposition (Figure 45). Errors are smaller over the Midwest for both selection routines and range from 20 to 45% when categories are used to help select the episodes.

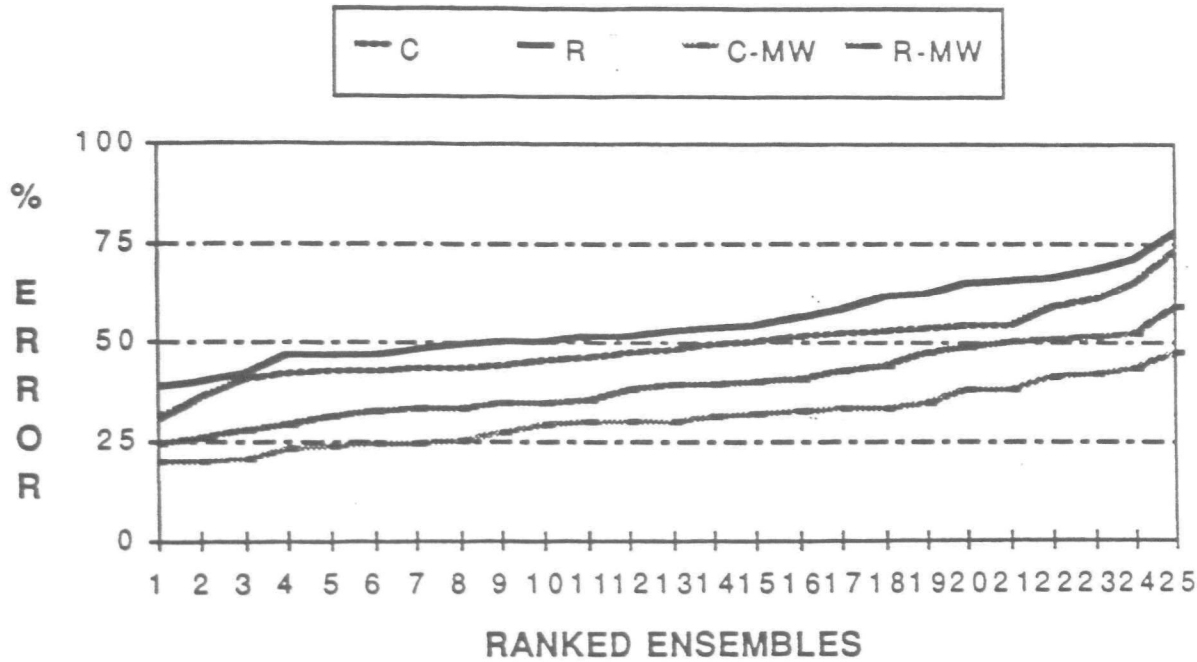

Figure 55. Percent RMS errors, ranked from smallest to largest, for the random and category-based ensembles using trajectories from all days in 30 episode sample.

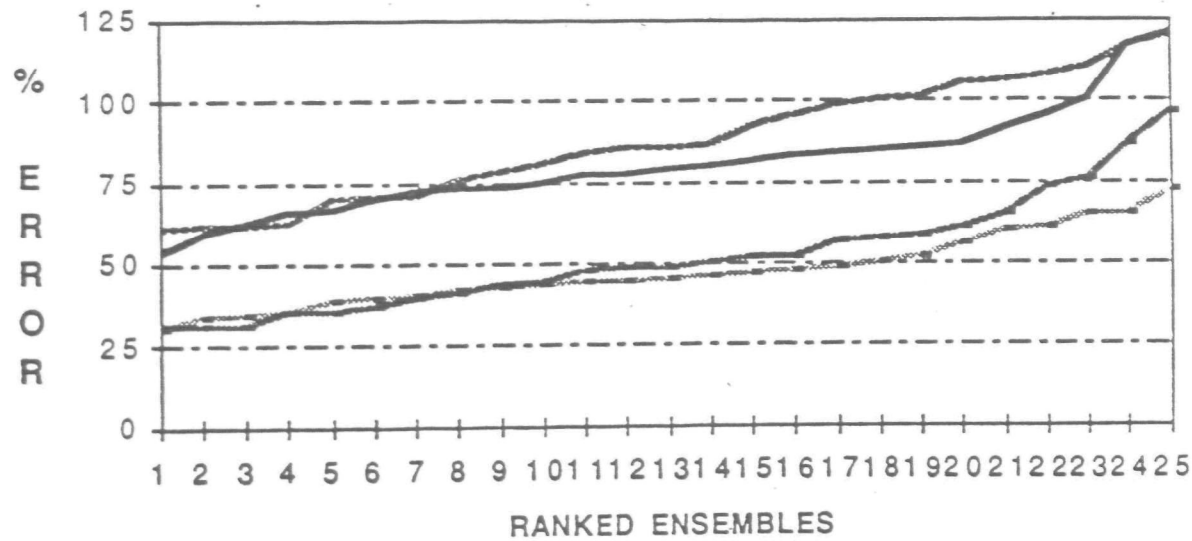

Figure 56. Percent RMS errors, ranked from smallest to largest, for the random and category-based ensembles using trajectories from precipitating days only in 30 episode sample.

In the second case only days with precipitation at the receptors were included when generating the estimated Q-fields (third option listed above). In this approach the comparisons are more specific to each location and not as indicative of the situation over larger areas. The results are also more sensitive to the stochastic nature of precipitation. Each ensemble was selected at random either with or without the guidance of categories and the number of wet days available for source-receptor evaluation varied between ensembles and sites. Weights were applied when aggregating each ensemble to an estimated long-term Q-field. For the category-based ensembles information on the expected deposition and on the frequency of occurrence of the particular categories sampled were used determine the weights. The randomly selected ensembles were weighted according to the amount of deposition occurring with each event selected. The comparison between the random and strata based approaches is shown in Figure 56. Over the high probability areas ($>10^{-4}$ km^{-2}) the method of pure random sampling did slightly better than the category guided selections. Over the Midwest regions, however, the outcome was just the opposite. In general, neglecting the days without precipitation resulted in a decrease in the quality of the estimates of between 10 and 20%. Considering the results of both of the cases tested, the use of the meteorological categories appears to offer improvement when attempting to represent the long-term source-receptor relationships with a finite number of episodes.

3.7. SOURCE-RECEPTOR RELATIONSHIPS ASSOCIATED WITH THE 30 EPISODES

Improvement in source-receptor representation due to category-guided event selection is a fundamental assumption of the aggregation technique developed during this project. The previous section corroborated this assumption. Most important, in terms of applying the outcome of this study to RADM, is the ability of the actual 30 episodes to reproduce the climatological source-receptor relationships. These episodes were recommended for RADM simulation. They were carefully examined for source-receptor representativeness at Big Moose, Gaylord and Raleigh. Mixed-layer trajectories were combined to produce Q-fields for each of these sites. As in the previous section, the long-term wind flow patterns were approximated using all of the days (non-weighted) and with only the wet days (weighted). The resulting fields were compared to the long-term wet sulfate deposition weighted Q-fields.

Of the 30 events selected for RADM simulation two did not have trajectory information. The estimated Q-fields discussed here were generated with up to 28 events instead of 30. The effect of missing this information was not known but it was assumed that with more trajectories the Q-fields would be more accurate. The non-weighted Q-fields for Big Moose, Gaylord and Raleigh are shown in Figures 57 to 59. Qualitatively, they appeared similar to the base-line fields. The probabilities decreased away from the receptors and tended to fall-off quicker to the east. Comparing the actual field to the estimated field for Big Moose it can be seen that the

estimation was not as smooth. This behavior was expected since the number of days included was

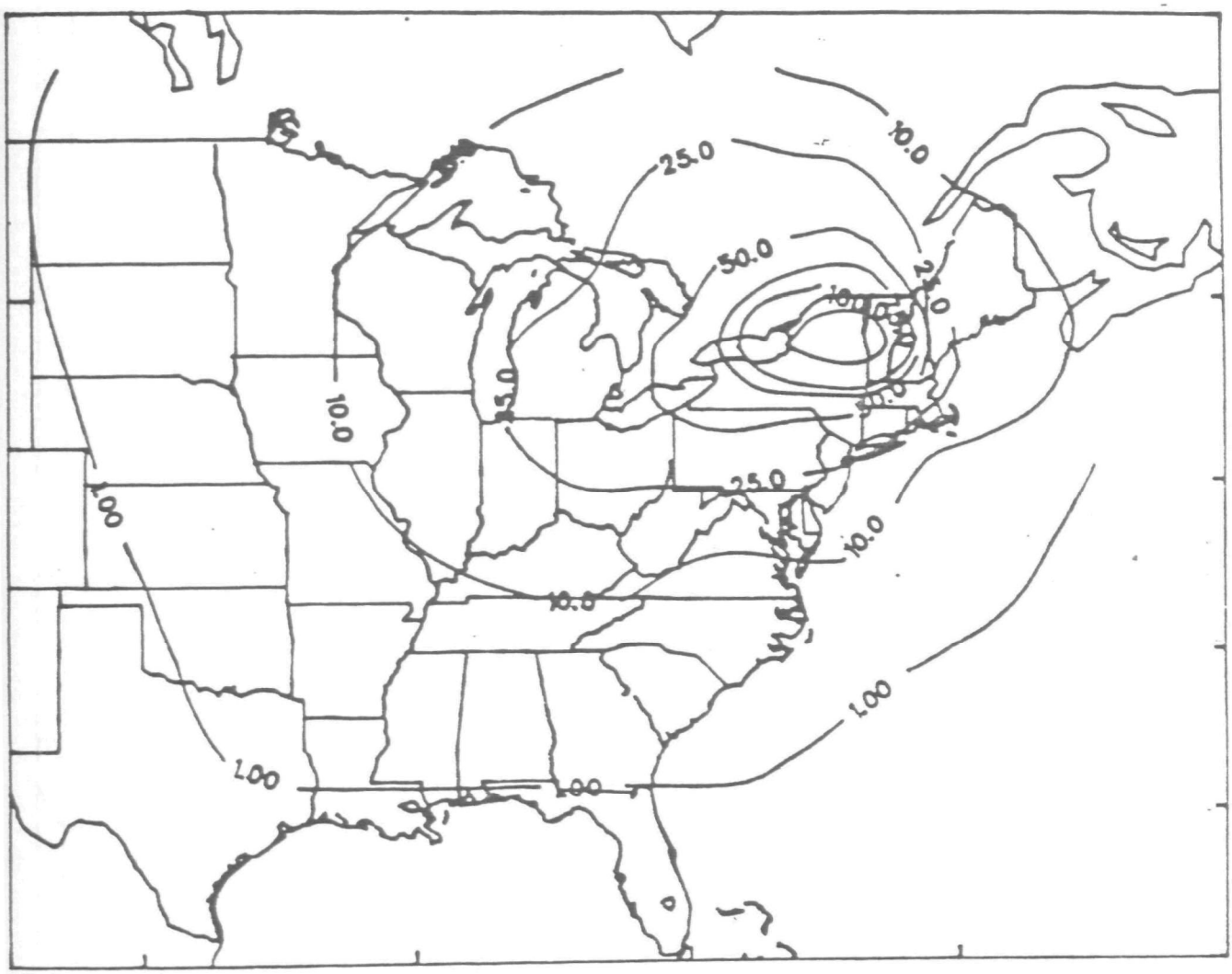

Figure 57. Source-receptor analysis (Q fields) for Big Moose, NY derived from both precipitating and non-precipitating days within the 30 selected episodes.

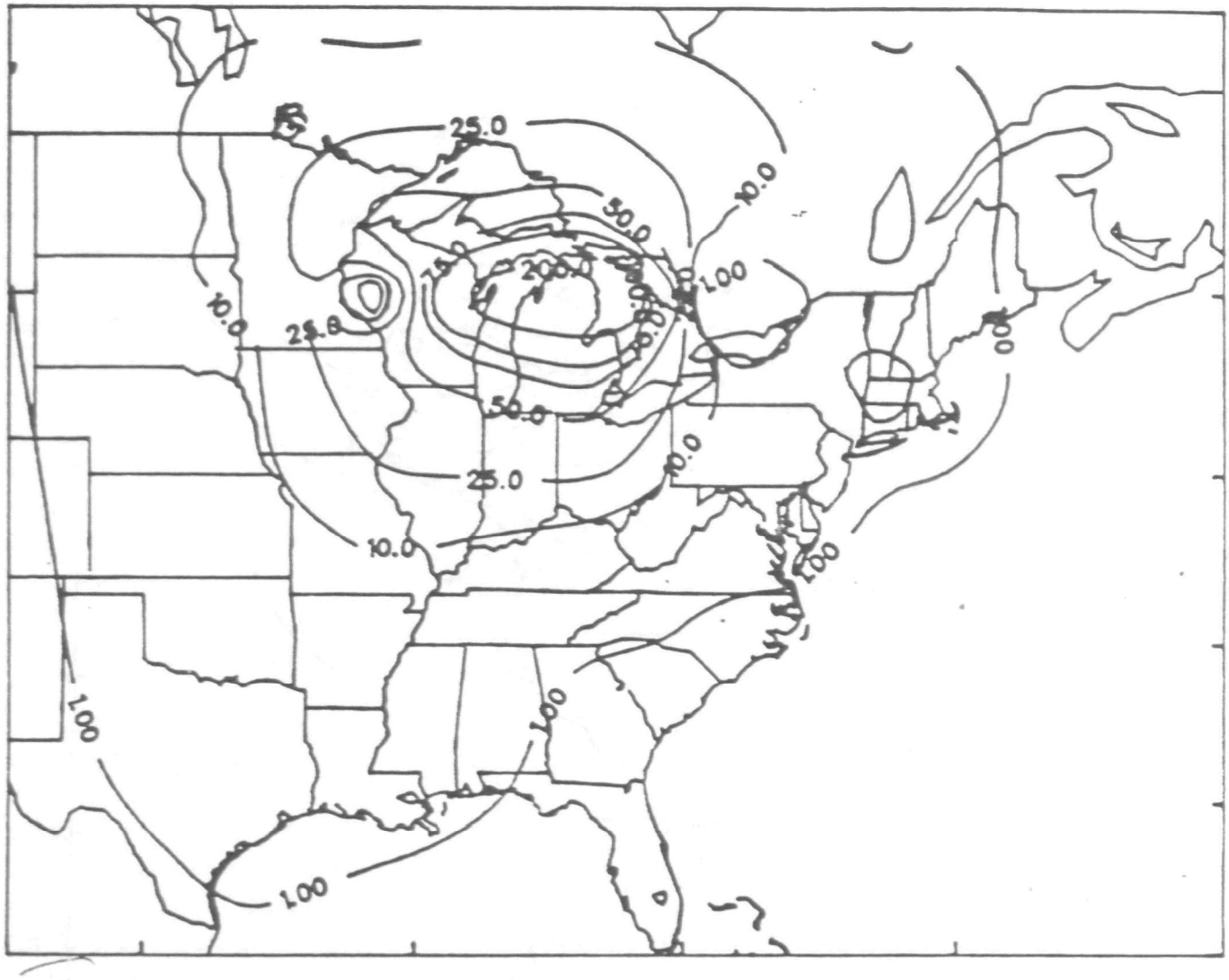

Figure 58. Source-receptor analysis (Q fields) for Gaylord, MI derived from both precipitating and non-precipitating days within the 30 selected episodes.

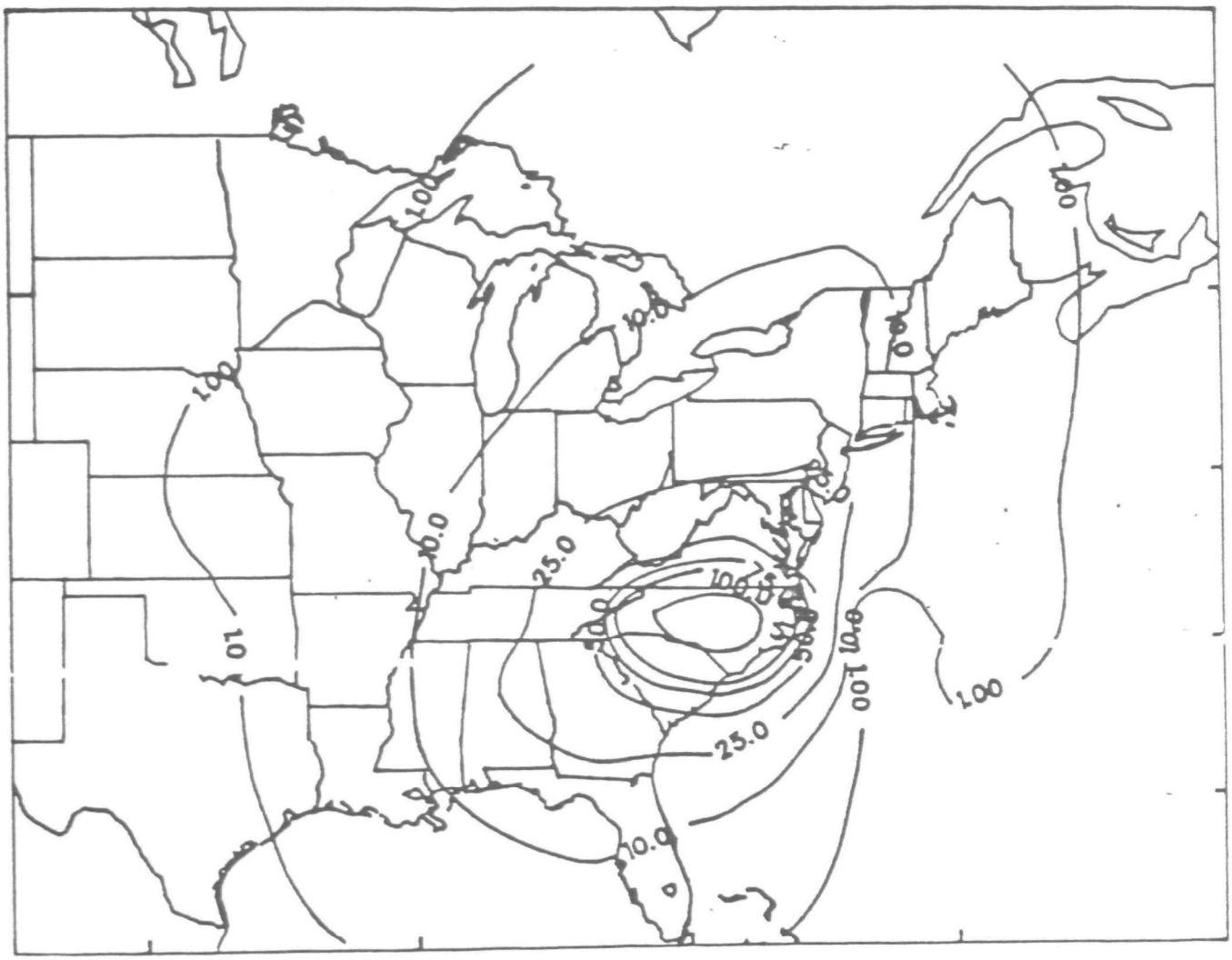

Figure 59. Source-receptor analysis (Q fields) for Raleigh, NC, derived from both precipitating and non-precipitating days within the 30 selected episodes.

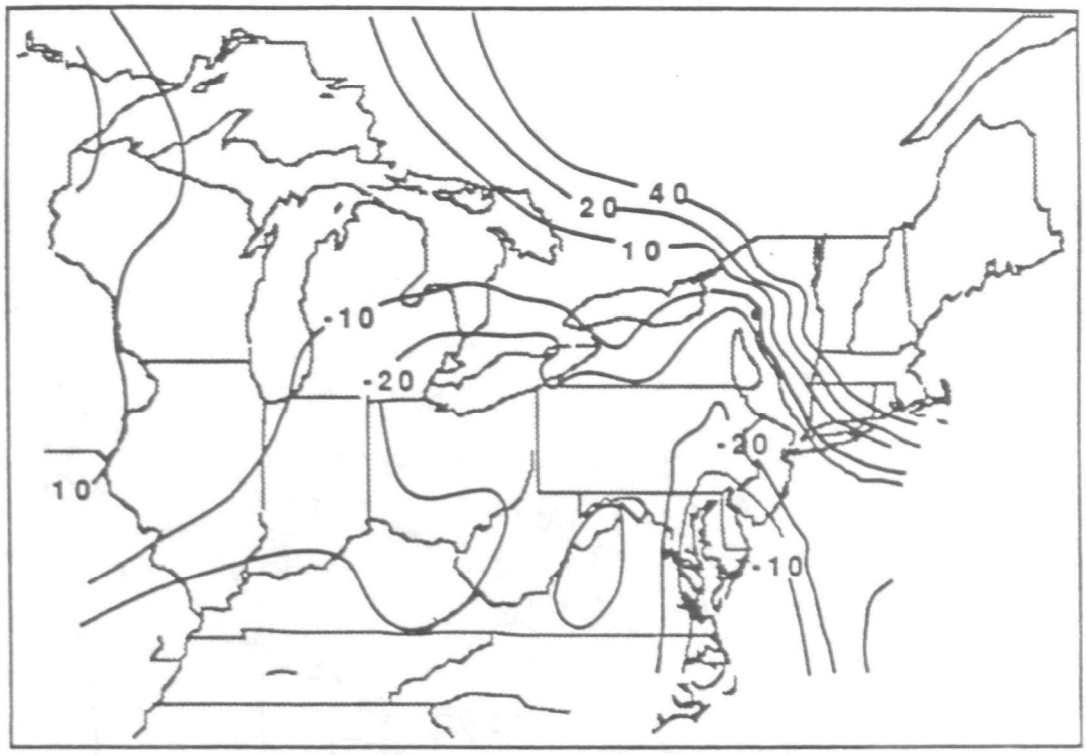

Figure 60. Bias in source-receptor analysis resulting from use of 30-event sample instead of 4-year sample at Big Moose, NY. Bias is expressed as a percent of predicted Q-field from the 4-year analysis. Both precipitating and non-precipitating days during the 30 selected episodes are included in the analysis.

relatively small and it was common to all three sites. To quantitatively compare the actual to the estimated fields the percent difference between the two was determined over all areas with probabilities greater than 10^{-4} km^{-2}. Throughout this area the mean percent RMS error was 46% for Big Moose, 48% for Gaylord and 37% for Raleigh. Contrasting these values to those in Figure 55 we see that the actual episodes selected were reproducing the wind flow patterns about as well as can be expected.

Figure 60 shows the spatial distribution of errors for Big Moose. Positive values indicate over-representation and negative imply under-representation. The wind flow from the northeast was significantly over-emphasized but throughout the remainder of the region analyzed the flow is represented to within -20%. Along the Ohio River valley the bias was towards under-representation and was generally equal to or less than 20%. Northeast of Big Moose the main source area was southwestern Quebec (Montreal). This area will likely be over-emphasized by RADM simulations using the 30 days. These sources were less important than those in the Midwest where the 30 day estimates were representing the flow well.

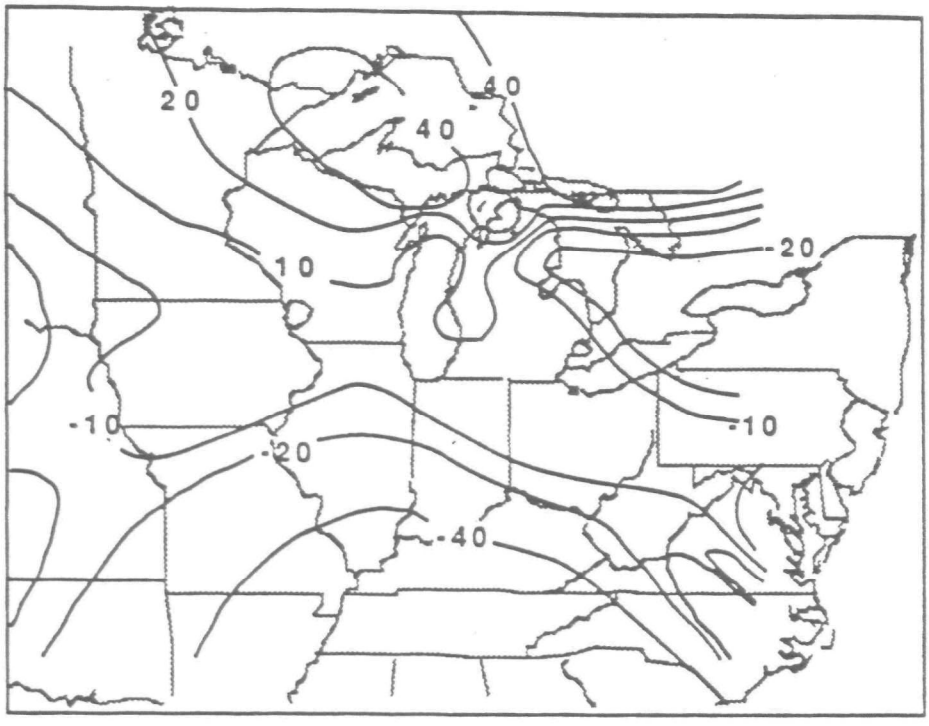

Figure 61. Bias in source receptor analysis resulting from use of 30-event sample instead of 4-year sample at Gaylord, MI. Bias is expressed as a percent of predicted Q-field from the 4-year analysis. Both precipitating and non-precipitating days during the 30 episodes are included in the analysis.

The same type of plot for Gaylord is included in Figure 61. The pattern of over and under representation was more uniform than for Big Moose. The southern section of the midwest including the Ohio River valley was under-emphasized as was southern Ontario and New York. Flow from the north was given more weight. Throughout a rather large area the differences were within 20%. Of the areas shown to be most often related to higher than average depositions (Figure 41) the sources along the western end of the Ohio River valley are most likely to be misrepresented.

The flow resulting from the combination of all 30 days at Raleigh overpredicted towards the north and east and underpredicted to the west and south (Figure 62). Basically, the percent differences were within 20% over much of the continent with the exception of the east coast from east of Raleigh to the north across Pennsylvania. Over the midwest the representation was quite good. RADM simulations using these 30 days will likely give sources from this region proper emphasis while those associated with the eastern seaboard could be significantly over-emphasized.

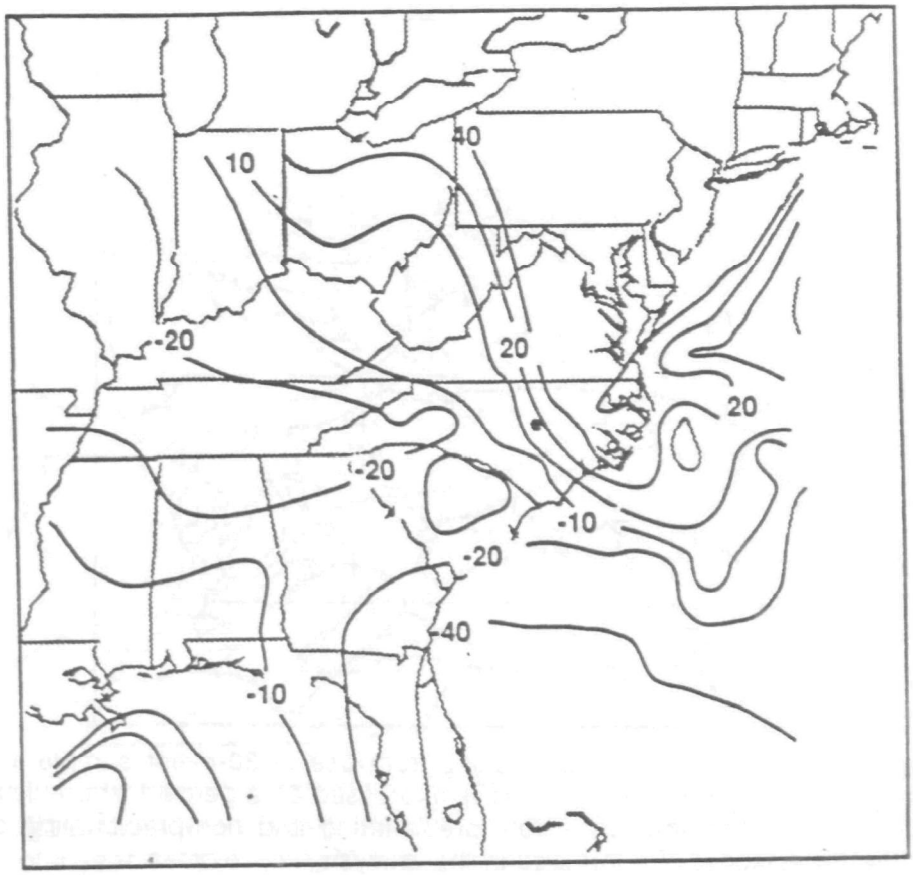

Figure 62. Bias in source receptor analysis resulting from use of 30-event sample instead of 4-year sample at Raleigh, NC. Bias is expressed as a percent of predicted Q-field from the 4-year analysis. Both precipitating and non-precipitating days during the 30 episodes are included in the analysis.

The long-term wind flow at each site was also estimated for precipitation events only. The results of these fields were fairly sensitive to the weighting scheme applied. The estimated fields evaluated here were generated by weighting each of the days with precipitation by the actual amount of $SO_4^=$ deposition reported and by the frequency of occurrence of the category it was selected from. Use of weights may be redundant since they are indirectly accounted for by the breakdown of categories sampled and in some cases neglecting weights and just averaging the trajectories associated with precipitation resulted in a more accurate Q-field. The percent difference fields generated for the wet-only estimates and are shown in Figures 63 to 65. The overall RMS errors attributed the the 30 days were in the same range as those shown in Figure 56. It was 61% for Big Moose, 52% for Gaylord and 76% for Raleigh. As in the previous section the estimates of the flow deteriorated when only precipitation days were included. Of the 28 available episodes at Big Moose 19 resulted in deposition. Thus, only 25 days were used to

produce the estimated Q-field as opposed to 84 days when non-precipitating days were included. At Gaylord, 16 episodes had deposition and at Raleigh only 15. This translated to 25 and 23 wet days at Gaylord and Raleigh respectively.

The estimated flow during precipitation events at Big Moose (Figure 63) indicates that sources to the north were under-represented by up to 60%. Sources in the central Ohio River valley were over-represented by about the same amount. Flows from areas to the west and areas south of Big Moose but north of the Ohio River were portrayed reasonably well considering the number of days included. For Gaylord (Figure 64), the sources to the south to southeast were significantly over-emphasized. Elsewhere the differences were basically less than 30%. At Raleigh, the 23 days used to approximate the long-term wind flow on precipitating days were yielding large positive biases towards the north and northeast (Figure 65). Sources towards the midwest were being under-represented by anywhere from 10 to 60 percent while over the eastern Ohio River valley, an area shown of major importance (Figures 43 and 45) the estimated flow was within 30%.

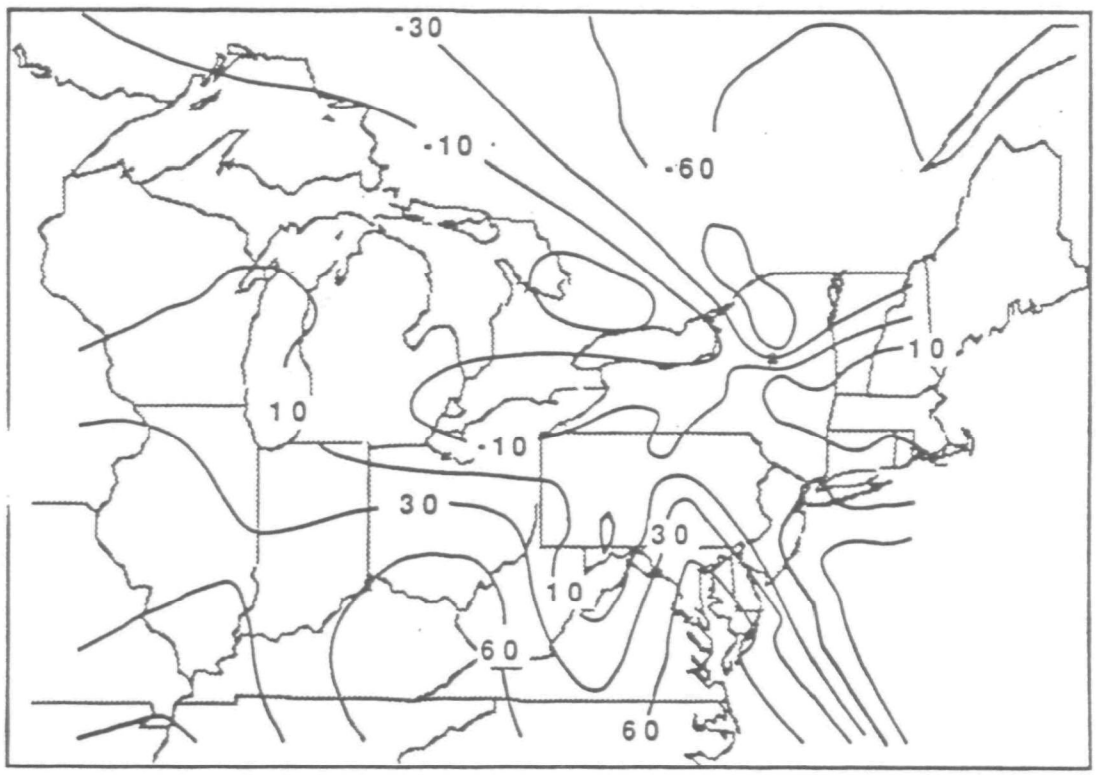

Figure 63. Bias in source receptor analysis resulting from use of 30-event sample instead of 4-year sample at Big Moose, NY. Bias is expressed as a percent of predicted Q-field from the 4-year analysis. Only days with precipitation reported at Big Moose are included in the analysis.

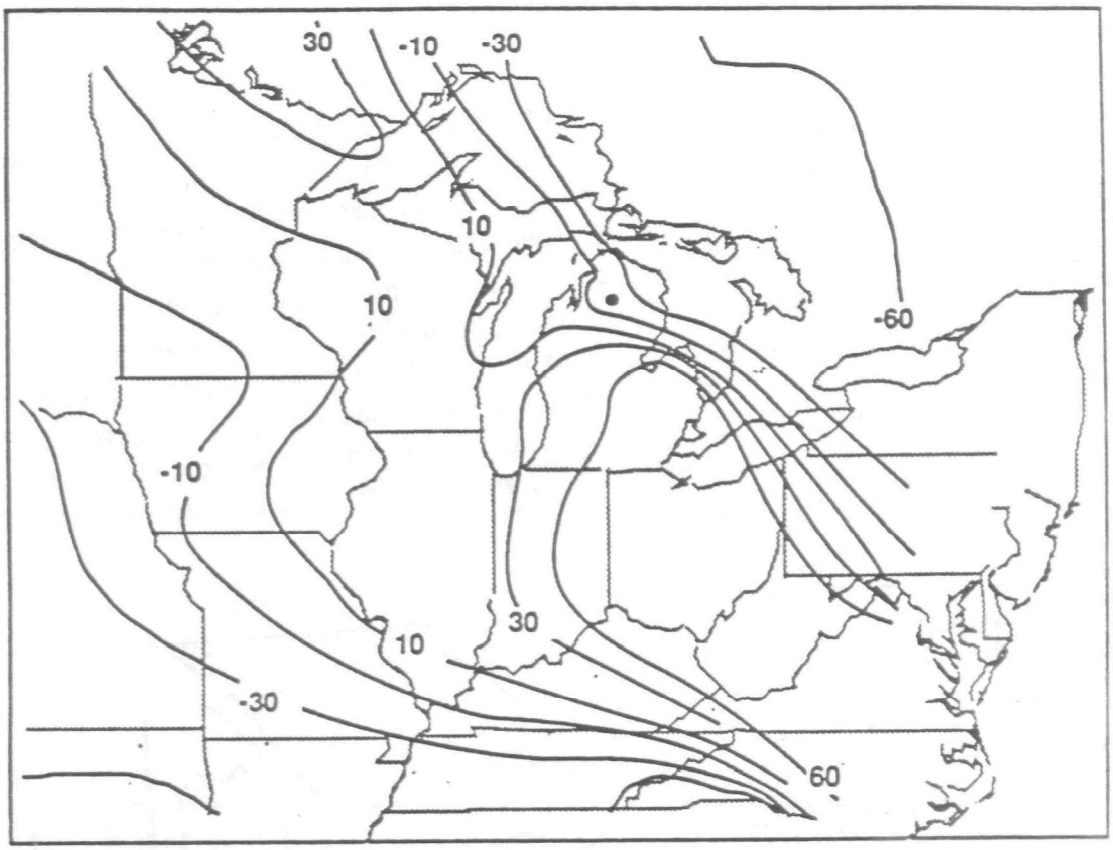

Figure 64. Bias in source receptor analysis resulting from use of 30-event sample instead of 4-year sample at Gaylord, MI. Bias is expressed as a percent of predicted Q-field from the 4-year analysis. Only days with precipitation reported at Gaylord are included in the analysis.

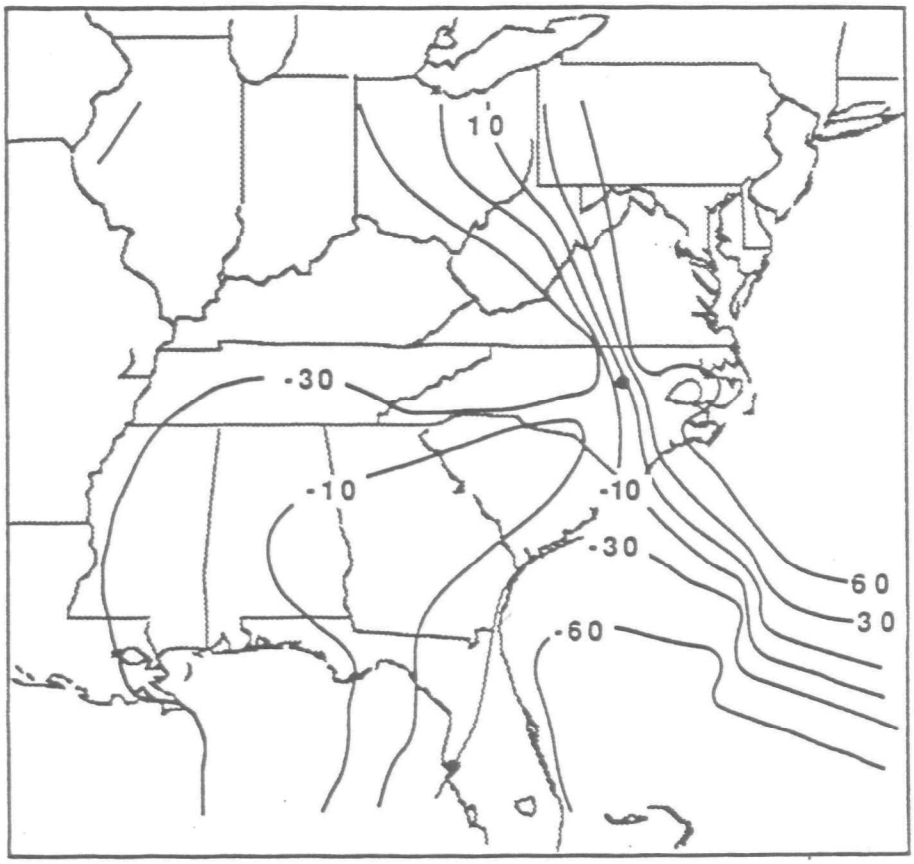

Figure 65. Bias in source receptor analysis resulting from use of 30-event sample instead of 4-year sample at Raleigh, NC. Bias is expressed as a percent of predicted Q-field from the 4-year analysis. Only days with precipitation reported at Raleigh are included in the analysis.

4. SUMMARY

4.1. ACCOMPLISHMENTS

A method for aggregating episodic deposition estimates of the Regional Acid Deposition Model (RADM) has been developed. The method is based upon the stratification of three-day periods into categories of similar wind flow at 850 mb (roughly 1500 meters above mean sea level). The stratification has been used to identify which meteorological situations merit simulation by RADM based on their likelihood of producing sulfur deposition at multiple locations across eastern North America, their frequency of occurrence, and their seasonality. The aggregation technique has been simulated using four years of precipitation chemistry data to demonstrate that uncertainties in estimates of seasonal and annual sulfur deposition using the aggregation technique is significantly less than those obtained from random (non-stratified) sampling of the data.

The following specific tasks have been completed as part of this project:

(1) An extensive data base with daily precipitation and wet deposition of sulfate, nitrate and total H^+ was developed. The data base covered the years 1982-1985 and included 23 sites in the northeastern, southern and midwestern U.S. and southern Canada. Meteorological information to be used in subsequent analysis was also collected.

(2) Techniques of cluster analysis were used to stratify 3-day events over the 4-year period into categories based on the meteorological data described above. Four independent stratification schemes were investigated: stratification by 850 mb wind field, stratification by 850 mb geopotential and mean surface pressure, stratification by 850 mb temperature advection and 500 mb vorticity, and stratification by 500 mb vorticity advection and 850 mb relative humidity. These four stratification schemes were evaluated to find the combination of meteorological parameters which best explained variations in sulfur wet deposition.

(3) A set of 19 meteorological categories was compiled based on similarity in wind flow at 850 mb. These 19 categories were each subdivided into "wet" and "dry" cases, making 38 categories. These 38 categories were used as the basis for selection of individual days and derivation of aggregated estimates for annual deposition.

(4) Accuracy and validity of the 38-category stratification was evaluated based on the ability to predict annual sulfate deposition at eastern and midwestern sites from a finite sample of 3-day events. We compared estimates for annual deposition derived from a random sample of 3-day events with estimates from a cluster-based sample of events. The standard deviation between estimated and actual deposition was lower by 25% with cluster-based selection.

(5) A preliminary selection of 30 individual 3-day events for in-depth study with RADM was made. Selection of individual days was designed to satisfy the following criteria:

(a) representation of the meteorological categories that account for the bulk of dry deposition in the eastern U.S.

(b) Inclusion of days representing a wide variety of circulation patterns, including relatively rare winter circulation patterns.

(c) Inclusion of a number of days with very little wet deposition, to allow for simulation of dry deposition processes.

(d) Selection of individual events within each category by a random process, rather than prescribing specific events.

(e) Accurate representation of total annual deposition at all northeastern and midwestern sites from the ensemble of individual events.

The selected ensemble allows for accurate estimation of summer, winter, and total annual deposition at all sites in the northeast and midwest.

4.2. RECOMMENDATIONS FOR FUTURE WORK

4.2.1. Evaluation of the 30 Episodes and the Meteorological Categories

Meteorological categorization was employed to help select episodes for RADM simulation with the purpose of trying to represent the dominant wind flow situations. Categorization based on the 850 mb wind flow was used because it was assumed that the ensuing categories would best segregate general meteorological situations and the deposition events. These assumptions were tested. The categories were shown to explain a good degree of the variance in wet deposition (95 % confidence level) and in terms of their mean 850 mb wind flow they were seen to differ systematically from each other and resemble common meteorological patterns. In the context of offering improved aggregate estimates the categorization by 850 mb wind flow was shown to be

warranted. Nonetheless, within categories there exist large variations from the mean flow and the mean deposition pattern. The following tasks investigate the magnitude and causes of those variations.

4.2.1.1. Source-Receptor Relationships

The hypothesis that the categories would differ chemically (at any given site) was based upon the assumption that the categories represented systematically different wind flow patterns and hence would differ with respect to source-receptor relationships. This concept is very important to the overall RADM project. The collection of events selected from the various categories should adequately represent the potential influence of all the major source regions effecting eastern North America. In addition, the frequency with which a particular source region impacts upon any given receptor must be as is in nature. If the overall source-receptor behavior represented by the collection of events is biased then the aggregate of RADM runs resulting from various emission change scenarios will also be biased.

The source-receptor relationships associated with the categories and with the 30 days selected for simulation were tested during the past year of research. Results indicated that for Big Moose, NY; Raleigh, NC; and Gaylord, MI the categories did favor different upwind regions and the 30 three-day episodes also differed in terms of where the air was most likely to have originated. How well the wind flow over the 30 days represented the expected wind flow was also tested, however, results of these comparisons are still being investigated.

During the next year a new method for evaluating the various approaches (30 day aggregate vs. actual vs. random 30 days) will be applied to aid in this aspect of the source-receptor testing. This new method will be based on a slightly modified version of the "threat score" (Anthes 1983) and should supply a more meaningful gauge for assessing the effectiveness of the selected days.

In terms of the source-receptor relationships and whether the specific source regions are given proper weight, the categories and the 30 days have yet to be evaluated. This aspect, which will require a more detailed look at the meteorology associated with the episodes and categories, will be explored in the upcoming year. In studying the 30 days the approach will be to examine the winter and summer situations separately. The flow patterns are more distinct in the winter and thus the source receptor relationships for the associated categories should be more clear-cut. As a result, it is hypothesized that the wind flow for the days selected to represent this time of year should do a better job at reproducing the overall pattern (as compared to the reproduction of the summer half). If this is shown to be the case then it will only be necessary to concentrate on improving the categorization and selection of warm season events.

4.2.1.2. Chemical and Meteorological Behavior of the Categories

In general, the categories were shown to differ chemically and meteorologically.

However, as it was pointed out earlier there remains a large amount of variability. While the current methodology has been shown to improve upon a random selection of episodes, the ability of our specific events to represent the expected range of situations is still clouded by the within category variability. This variability is great enough to allow some overlap. Events from different categories can be more similar than different and also not resemble the mean category pattern at all. These effects can lead to selecting events which do not possess the desired pollutant transport paths and the under or over representation of certain meteorological situations.

The within category variability is most notable in the summer when just a few categories are predominant. There are clearly other mechanisms previously not accounted for that govern the precipitation and pollutant deposition behavior. To understand and include these effects the meteorology of these situations needs to be examined in more detail. The goal will be to better understand what differentiates the events in these more ubiquitous categories. This knowledge could be used to further stratify some categories leading to better weighting factors for some of our selected days. It will also identify any key situations that are not presently being modeled.

In the process of testing the nineteen categories for their ability to explain the variation in wet deposition a number of regression models were developed. These models are capable of relating depositions and concentrations to specific parameters in quantitative terms. The importance of a variety of meteorological factors, in terms of their influence on precipitation chemistry, can be quantitatively assessed in this way. This approach can be used in conjunction with additional stratification to uncover the other dominant mechanisms controlling deposition and to improve the aggregate estimates. Using the results of the regression models alternate aggregation schemes can also be explored and techniques that can better account for the effects of meteorological variability can be incorporated. As discussed above, specific knowledge of the source-receptor relationships associated with the categories and the 30 events have not been determined. This information is especially lacking for the light wind categories which are associated with high deposition to precipitation ratios and relatively large numbers of events. The regression studies and sub-stratification along with careful meteorological analysis will add more to our knowledge of the source receptor relationships under these types of situations.

4.2.2. Application of aggregation to other atmospheric phenomena

4.2.2.1. Dry Deposition

A method for aggregating dry deposition estimates from the RADM simulations has not been developed. This problem is difficult to tackle because the amount of suitable dry deposition data is very limited. In addition, the mechanisms associated with dry deposition processes are not completely understood. A variety of factors such as boundary layer turbulence and surface characteristics are known to influence the amount of pollutants that are dry deposited. In order to apply similar aggregation methods to dry deposition it will be necessary to study the behavior

of the various contributing mechanisms and the ambient levels of $SO_4^=$, SO_2 and NO_x with respect to the meteorological categories.

The data gathered during the RADM intensive evaluation period (Summer, 1988) can provide some of the information needed to address the dry deposition issue. With a better understanding of the within versus between category variation in ambient concentrations it will be possible to evaluate the suitability of estimating the long-term patterns of dry deposition using a small subset of episodes.

In the present selection six of thirty episodes were selected to enhance dry deposition representation. The only criteria used in selecting these episodes was that they be associated with a small amount of wet deposition across the Northeast as a whole (< 50 mgm^{-2}). However, with no dry deposition or ambient concentration data it has been very difficult to evaluate the days chosen. The information gained through the ideas mentioned above will help test these days and also indicate whether or not more episodes need to be selected to estimate dry deposition patterns.

4.2.2.2. Visibility

Visibility in the eastern United States is known to be largely governed by the concentrations of $SO_4^=$. Therefore, the methods developed thus far could be applied to visibility. Specific aspects of the problem that need to be addressed include:

- Identification of the sources of visibility data across eastern North America;
- Examination of methods for reducing meteorological variability in visibility data due to humidity;
- Examination of the behavior of visibility associated with the different meteorological categories;
- Evaluate need for additional meteorological categories based on differences in visibility;
- Identification of some of the conditions (categories) that are conducive to good/poor visibilities. Study of the specific relationships existing between these conditions and visibility.
- Test performance of the current 30 days in predicting visibility behavior over seasonal and annual time periods.
- Selection of specific episodes useful in predicting long-term visibility behavior through an aggregate technique. This could include:

— Episodes to supplement the existing 30 days, or

— An independent set of episodes,

4.2.3. Quantification of Aggregation Sensitivity

There are a number of factors that influence the aggregate estimates. In particular, the variability of deposition-to-precipitation ratios within categories, between categories and between years can affect the estimate. The variation in the frequency and amount of precipitation associated with the categories and variation in the frequency of occurrence of the actual categories also affects the estimates. The sensitivity of the aggregate estimates to these types of factors needs to be quantified and the factors that have the most impact on the results need to be highlighted. This will also enable us to determine what time scale the aggregation scheme handles best (i.e. one year averages, four year averages) and the amount of inter-annual variability associated with the average estimates.

5. REFERENCES

Anderberg, M.R. 1973. *Cluster Analysis for Applications.* Academic Press, New York, 359 p.

Beale, E. M. L. 1969. Euclidean cluster analysis. *Bull. Intrnl. Statist. Inst.*, **43**, p. 92-94.Berge, E. 1988. Time-trends of sulfate and nitrate in precipitation in Norway (1972-1982). *Atmospheric Environment*, 22: 333-338.

Buishand T.A., G.T. Kempen, A.J. Frantzen, H.F.R. Reignders and A.J. Van Den Eshof. 1988. Trend and seasonal variation of precipitation chemistry in the Netherlands. *Atmospheric Environment*, 22:339-348.

Calinski, T. and Harabasz, J. 1974. A dendral method for cluster analysis. *Communications in Statistics.*, **3**, p. 1-27.

Cass, G.R., 1981, Sulfate air quality control design. *Atmospheric Environment*, 15, 1227-1249.

Chang, J. S., Brost, R. A., Isaksen, I. S. A., Madronich, S., Middleton, P., Stockwell, W. R., and Walcek, C. J. 1987. A three-dimensional Eulerian acid deposition model: physical concepts and formulation. *J. Geophys. Res.*, 92, 14681-14700.

Davies, T.D., G. Farmer and R.J. Barthelmie. 1990. Use of simple daily atmospheric circulation types for the interpretation of precipitation composition at a site (Eskdalemuir) in Scotalnd, 1978-1984. *Atmospheric Environment*, 24A: 63-72.

Draxler, R.R., 1987, Sensitivity of a trajectory model to the spatial and temporal resolution of the meteorological data during CAPTEX. *J. Climate Appl. Meteor.*, 26, 1577-1588.

Endlich, R.M., B.P. Eynon, R.J. Ferek, A.D. Valdes and C. Maxwell. 1986. Statistical Analysis of Precipitation Chemistry Measurements over the Eastern United States. UAPSP 112, Utility Acid Precipitation Study Program, Washington, D.C., Available from UAPSP Report Center, P.O. Box 599, Damascus, MD, 20872.

Fernau, M.E. 1988. *Use of Cluster Analysis to Define Periods of Similar Meteorology and Precipitation Chemistry in Eastern North America.* Ph.D. Thesis, University of Michigan, University Microfilms, Ann Arbor, MI, pp. 330, 1988.

Finkelstein, P.L. and S.K. Seilkop. 1986. Changing patterns in acid rain. Extended Abstracts, 5th Joint Conference on Applications of Air Pollution Meteorology, Nov. 18-21, 1986, Amer. Meteor. Society, Boston, MA, p. 79-82.

Freund, R. J., R. C. Littell and P. C. Spector. 1986. *SAS System for Linear Models*, SAS Institute Inc., Cary, NC.

Heffter, J. L. 1980. Air Resources Laboratories Atmospheric Transport and Dispersion Model (ARL-ATAD). NOAA Tech. Memo. ERL ARL-81; Rockville, MD, 1980; p. 17.

Hidy, G.M., Mueller, P.K. and E.Y. Tong, 1978, Spatial and temporal distributions of airborne sulfate in parts of the U.S. *Atmospheric Environment*, **12**: 735-752.

Hooper, R. P. and N. E. Peters. 1989. The applicability of principal components analysis for determining sources of wet deposition, presented at the Joint International Association of Hydrological Sciences/American Geophysical Union Symposium on Atmospheric Deposition, Baltimore, MD., May 10-11, 1989.

Johnson, R. A. and D. W. Wichern. 1982. *Applied Multivariate Statistical Analysis*, Prentice-Hall, Inc., Englewood Cliffs, NY.

Kahl J.D. and Samson P.J. 1986: Uncertainty in trajectory calculations due to low resolution meteorological data, *J. Climate Appl. Meteor.* **25**: 1816-1831.

Kahl J.D. and Samson P.J. 1988: Trajectory sensitivity to rawinsonde data resoltuion. *Atmospheric Environment*, **22**: 1291-1299.

Kalkstein L.S. and P. Corrigan, 1986: A synoptic climatological approach for geographic analusis: Assessment of sulfur dioxide concentrations. *Anal. Assoc. Amer. Geographers*, **76**: 381-195.

Kalkstein L.S., G. Tan and J.A. Skindlov. 1987. An evaluation of three clustering procedures for use in synoptic climatological classification. *J. Climate Appl. Meteor.*, **26**: 717-730.

Keeler G.J., and P.J. Samson, 1989. Spatial Representativeness of trace element ratios. *Environ. Sci. and Technol.*, **23**: 1358-1364.

Lamb R.G. and J.H. Seinfeld, 1973, Mathematical modeling of urban air pollution - general theory, *Environ. Sci. and Technol.*, **7**: 253.

MAP3S/RAINE Research Community. 1982. The MAP3S/RAINE precipitation chemistry network: statistical overview for the period 1976-1980. Atmospheric Environment, 16:1603-1632.

Moody J.L. and Galloway J.N. 1988: Quantifying the relationship between atmospheric transport and the chemical composition of precipitation on Bermuda, *Tellus*, **40B**: 446-462.

Moody J.L. and Samson P.J. 1986: The Influence of Meteorological Factors on Precipitation Chemistry. UAPSP 111, Contract U101-4. University of Michigan final report for Utility Acid Precipitation Study Program, Washington D.C. and Electric Power Research Institute, Palo Alto, CA. Available from UAPSP Report Center, P.O. Box 599, Damascuc, MD, 20872.

Moody, J.L. and P.J. Samson. 1989. The influence of atmospheric transport on precipitation chemistry at two sites in the midwestern United States. *Atmospheric Environment*, **23**: 2117-2132.

Mueller, P. K. and M. A. Allan. 1987. Utility Acid Precipitation Study Program, Third Summary Report. UAPSP 114, Utility Acid Precipitation Study Program, Washington, D.C., Available from UAPSP Report Center, P.O. Box 599, Damascus, MD, 20872.

Samson, P.J., and M.J. Small. 1984. Atmospheric trajectory models for diagnosing the sources of acid precipitation. in *Modeling of Total Acid Precipitation Impacts*, J. L. Schnoor, ed., Butterworth Publishers, Boston, 1984.

Samson, P.J. 1980. Trajectory analysis of summertime sulfate concentrations in the north-eastern United States. *J. Appl. Meteor.*,**19**: 1382-1394.

Samson P.J. 1989a. Aggregation Pollutant Deposition Episodes into Seasonal and Annual Estimates. EPA Cooperative Agreement CR-814854-01. Prepared for the United States Environmental Protection Agency, Meteorology and Assessment Division, Research Triangle Park, NC. January, 1989.

Stein, M. S. and X Niu. 1989. "Analysis of Precipitation and Deposition Data", personnal communication.

Summers Peter W. 1987: Empirical source-receptor relationships in eastern Canada determined from monitoring data and airmass trajectory climatologies: In EMEP - Workshop in data analysis and presentation, Cologne, FRG 15-17 June 1987, EMEP/CCC-Report 7/87.

The Sulfate Regional Experiment: Report of Findings. EA-1901, Volume 1, Electric Power Research Institute, Palo Alto, CA, March, 1983.

Trenberth, K.E. and J.G. Olson. 1988. Evaluation of NMC Global Analyses: 1979-1987. NCAR Technical Note NCAR/TN-299+STR, National Center for Atmospheric Research, Boulder, CO.

Vukovich, F.M. and J. Fishman: 1986. The climatology of summertime ozone and sulfur dioxide (1977-1981). *Atmospheric Environment*, **20**:

Ward, J. H. 1963. Hierarchical grouping to optimize an objective function. *J. Am. Statist. Assoc.*, **58**: 236-244.

Wilson J.W., Mohnen, V.A. and J.A. Kadlecek, 1982, Wet deposition variability as observed by MAP3S. *Atmospheric Environment*, **16**: 1667-1676.

Zemba, S.G., D. Golomb and J.A. Fay. 1988 Wet sulfate and nitrate deposition patterns in eastern North America, *Atmospheric Environment*, **22**: 2751-2761.

Zeng Y. and P.K. Hopke. 1989. A study of the sources of acid precipitation in Ontario, Canada, *Atmospheric Environment*, **23**: 1499-1509.

APPENDIX A

Mean 850 mb Wind Flow Patterns
for the 19 Categories

EASTERN NORTH AMERICAN MEAN 850MB WIND FIELD - 19 CLUSTERS

TRAJECTORY CLUSTER 1 3.6%, N= 13

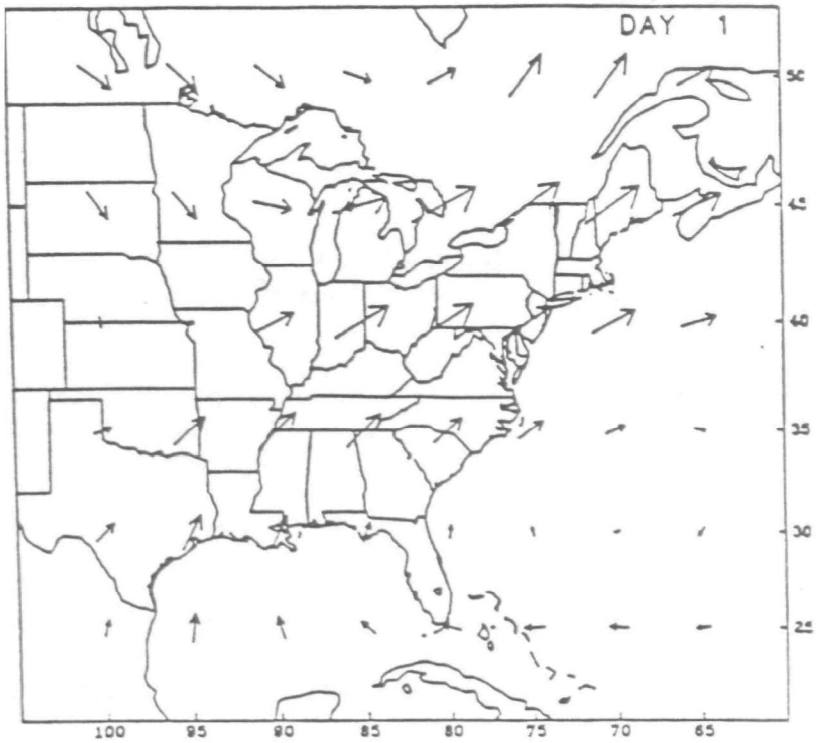

EASTERN NORTH AMERICAN MEAN 850MB WIND FIELD - 19 CLUSTERS

TRAJECTORY CLUSTER 1 3.6%, N= 13

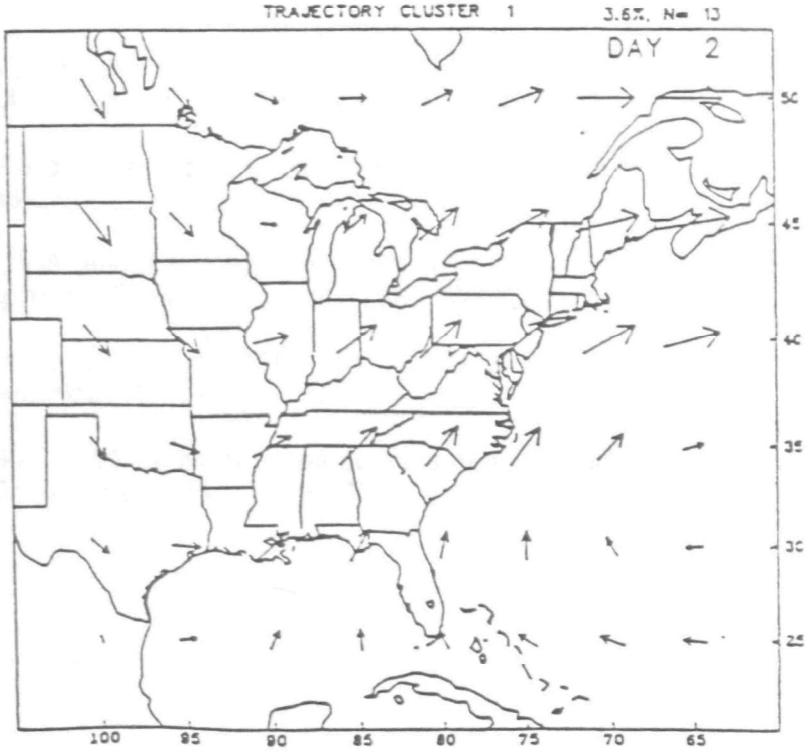

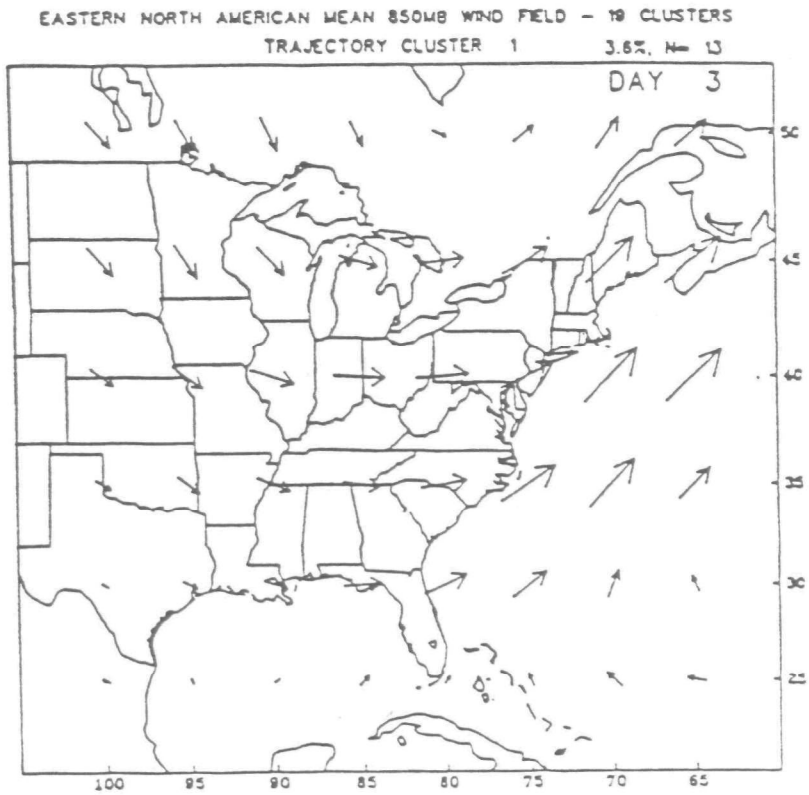

Figure A1 - Mean 850 mb wind flow patterns for the three days in Cluster 1. The clusters were extracted from a set of consecutive three-day periods during 1979, 1981 and 1983. N corresponds to the number of occurrences of cluster 1 during that period. The percent of time (out of all cases) the cluster occurred is also shown in the upper right. Wind vectors represent six hours of motion at reported wind speed.

EASTERN NORTH AMERICAN MEAN 850MB WIND FIELD – 19 CLUSTERS

TRAJECTORY CLUSTER 2 3.3%, N= 12

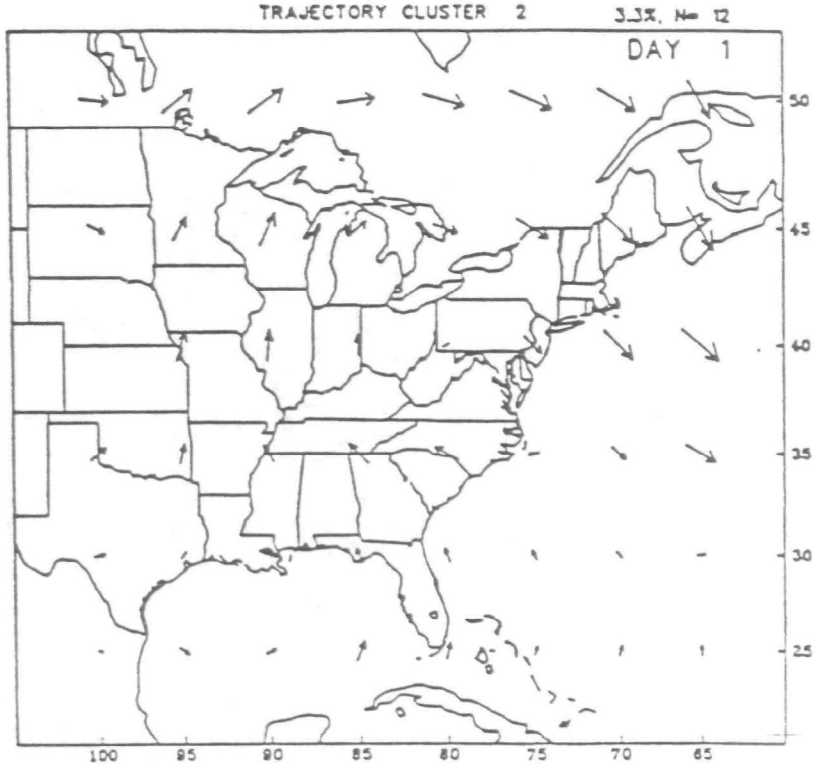

EASTERN NORTH AMERICAN MEAN 850MB WIND FIELD – 19 CLUSTERS

TRAJECTORY CLUSTER 2 3.3%, N= 12

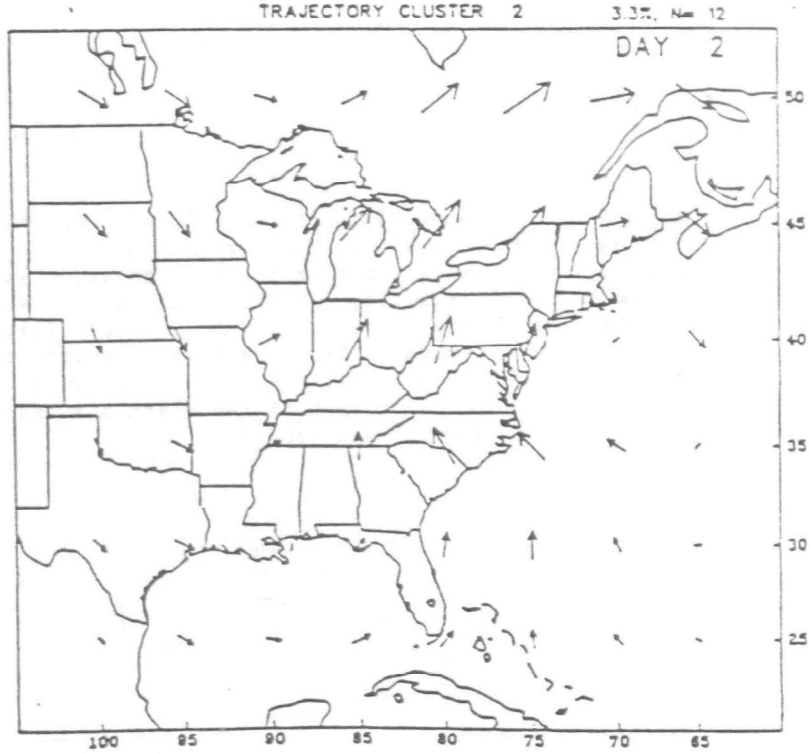

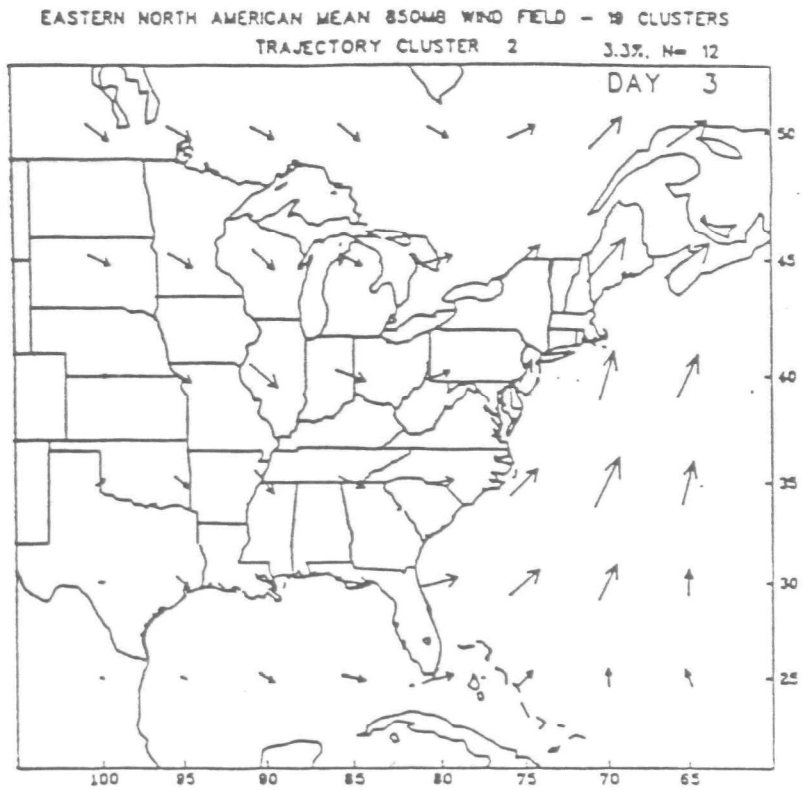

Figure A2 - Mean 850 mb wind flow patterns for the three days in Cluster 2. The clusters were extracted from a set of consecutive three-day periods during 1979, 1981 and 1983. N corresponds to the number of occurrences of cluster 2 during that period. The percent of time (out of all cases) the cluster occurred is also shown in the upper right. Wind vectors represent six hours of motion at reported wind speed.

EASTERN NORTH AMERICAN MEAN 850MB WIND FIELD - 19 CLUSTERS
TRAJECTORY CLUSTER 3 17%, N= 6

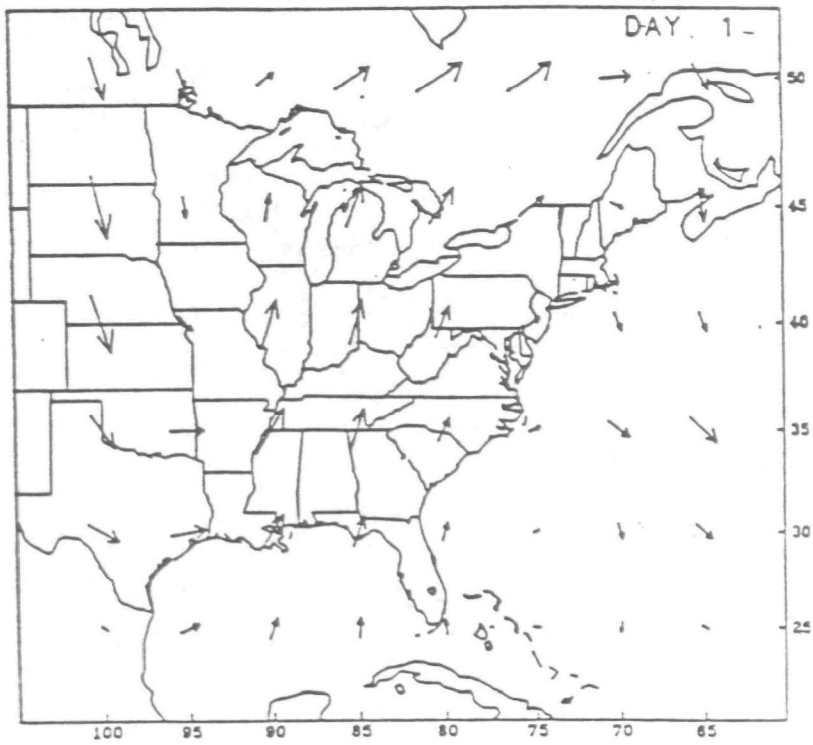

EASTERN NORTH AMERICAN MEAN 850MB WIND FIELD - 19 CLUSTERS
TRAJECTORY CLUSTER 3 17%, N= 6

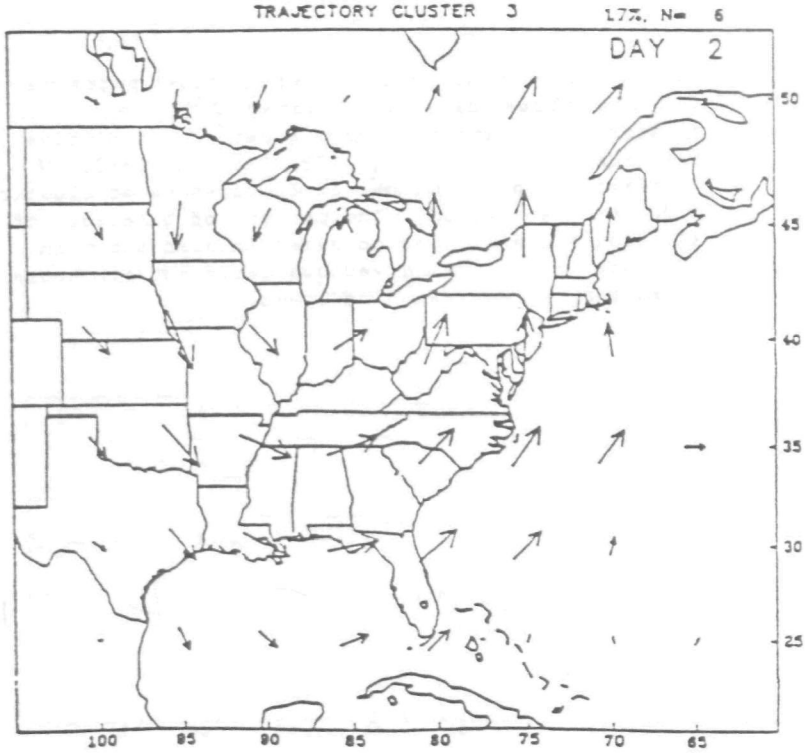

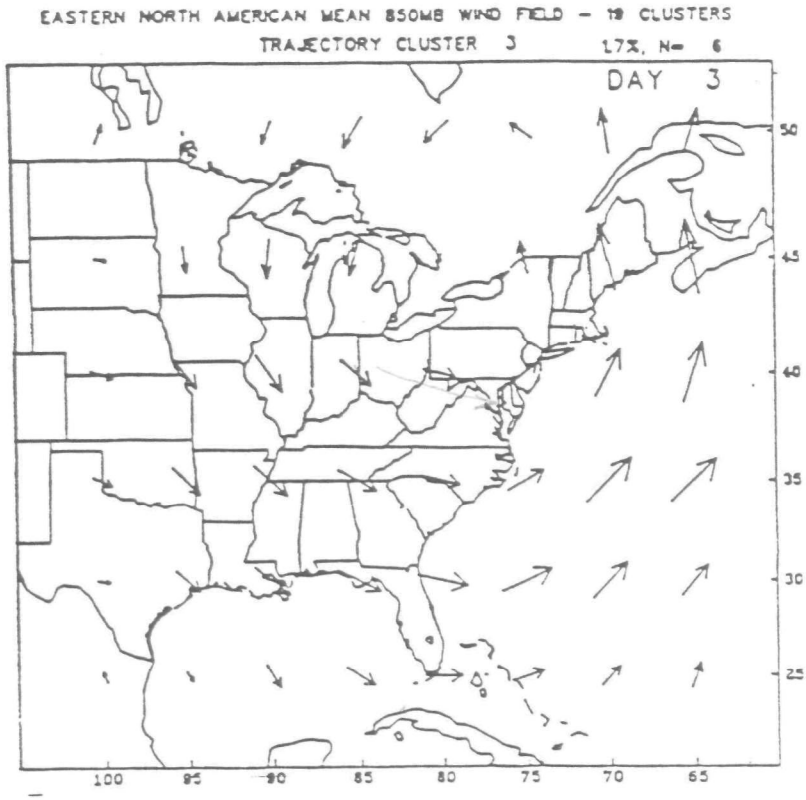

Figure A3 - Mean 850 mb wind flow patterns for the three days in Cluster 3. The clusters were extracted from a set of consecutive three-day periods during 1979, 1981 and 1983. N corresponds to the number of occurrences of cluster 3 during that period. The percent of time (out of all cases) the cluster occurred is also shown in the upper right. Wind vectors represent six hours of motion at reported wind speed.

EASTERN NORTH AMERICAN MEAN 850MB WIND FIELD – 19 CLUSTERS

TRAJECTORY CLUSTER 4 2.2%, N= 8

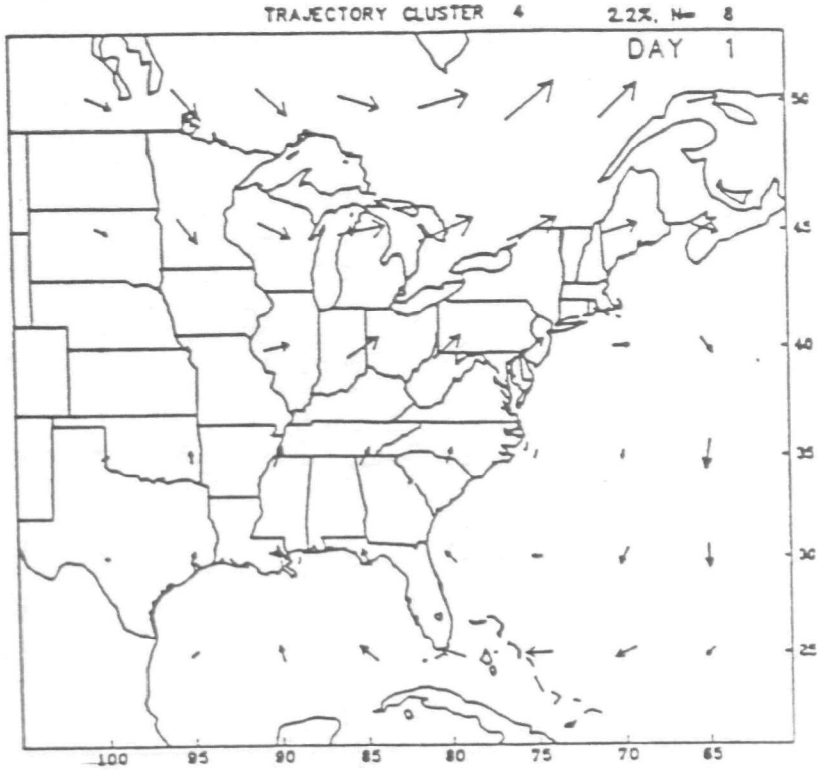

EASTERN NORTH AMERICAN MEAN 850MB WIND FIELD – 19 CLUSTERS

TRAJECTORY CLUSTER 4 2.2%, N= 8

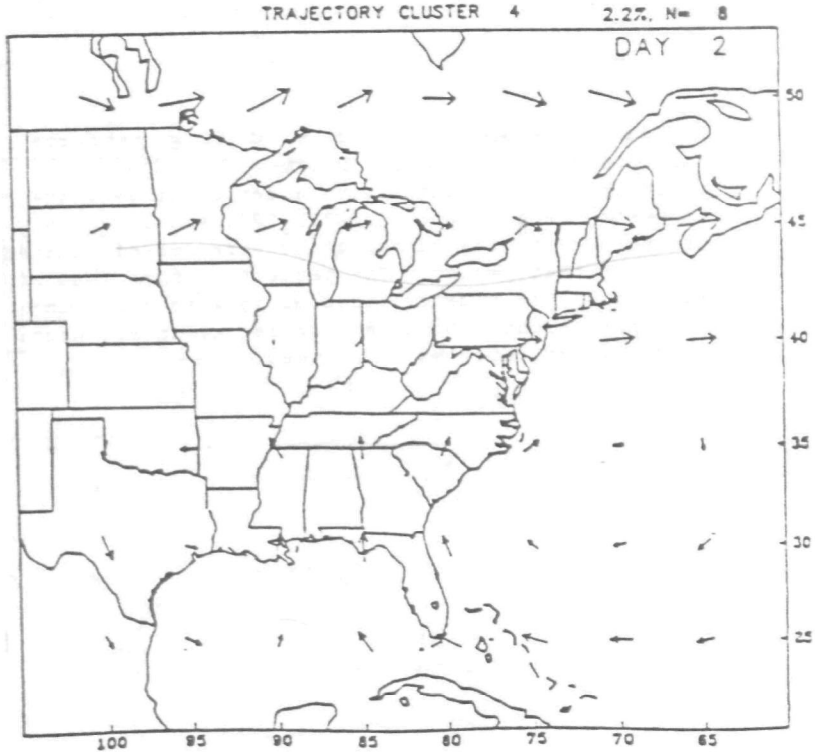

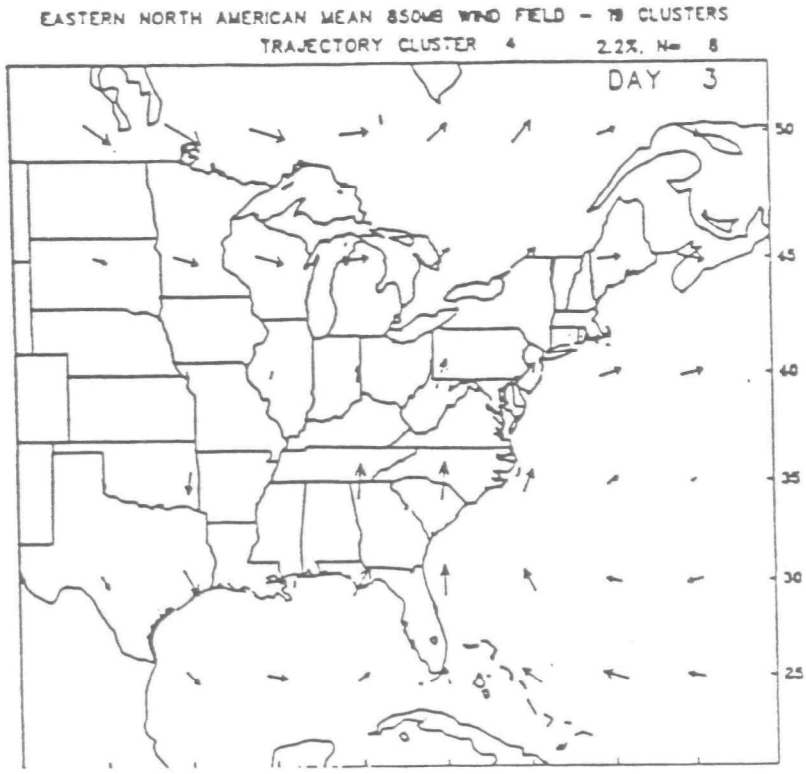

Figure A4 - Mean 850 mb wind flow patterns for the three days in Cluster 4. The clusters were extracted from a set of consecutive three-day periods during 1979, 1981 and 1983. N corresponds to the number of occurrences of cluster 4 during that period. The percent of time (out of all cases) the cluster occurred is also shown in the upper right. Wind vectors represent six hours of motion at reported wind speed.

EASTERN NORTH AMERICAN MEAN 850MB WIND FIELD - 19 CLUSTERS
TRAJECTORY CLUSTER 5 6.9%, N= 25

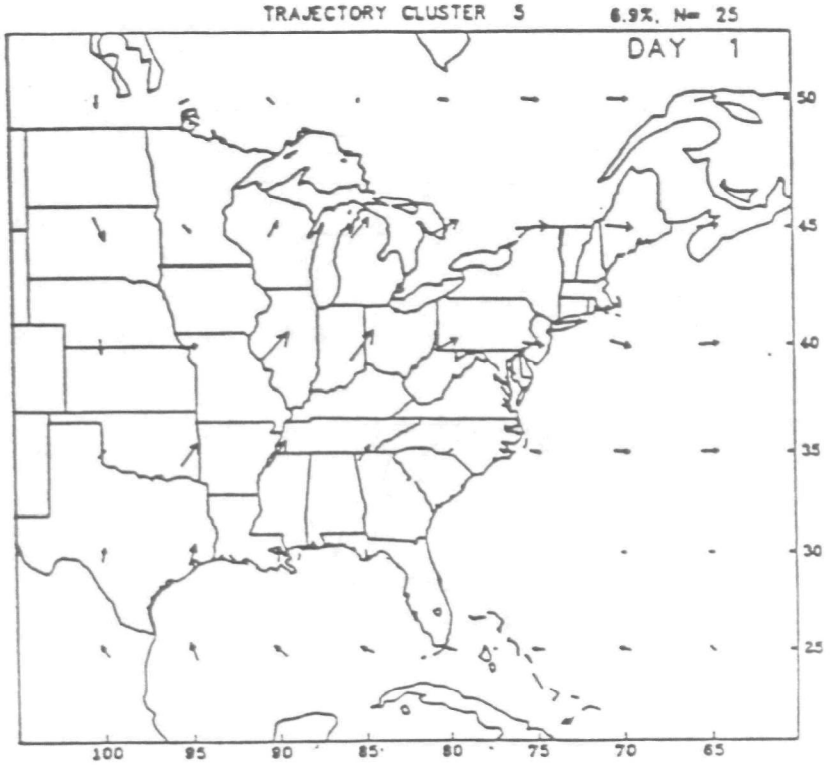

EASTERN NORTH AMERICAN MEAN 850MB WIND FIELD - 19 CLUSTERS
TRAJECTORY CLUSTER 5 6.9%, N= 25

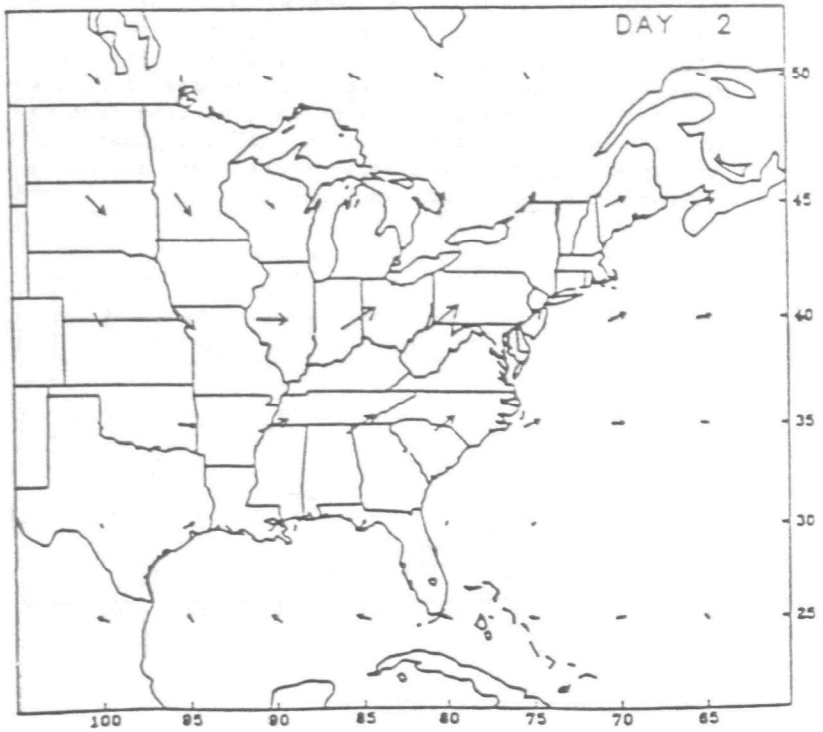

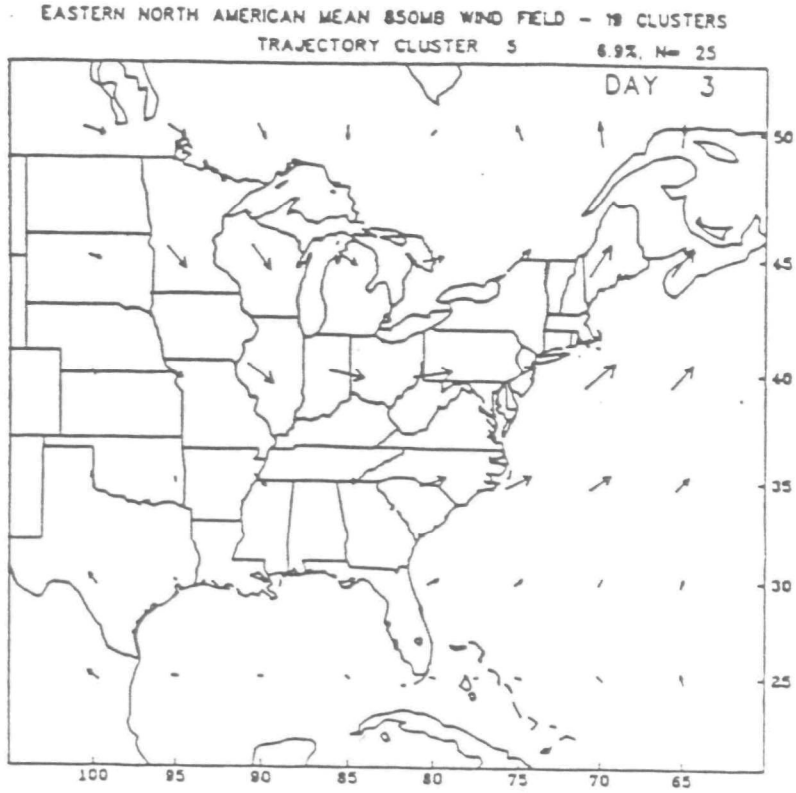

Figure A5 - Mean 850 mb wind flow patterns for the three days in Cluster 5. The clusters were extracted from a set of consecutive three-day periods during 1979, 1981 and 1983. N corresponds to the number of occurrences of cluster 5 during that period. The percent of time (out of all cases) the cluster occurred is also shown in the upper right. Wind vectors represent six hours of motion at reported wind speed.

EASTERN NORTH AMERICAN MEAN 850MB WIND FIELD - 19 CLUSTERS

TRAJECTORY CLUSTER 6 8.0%, N= 29

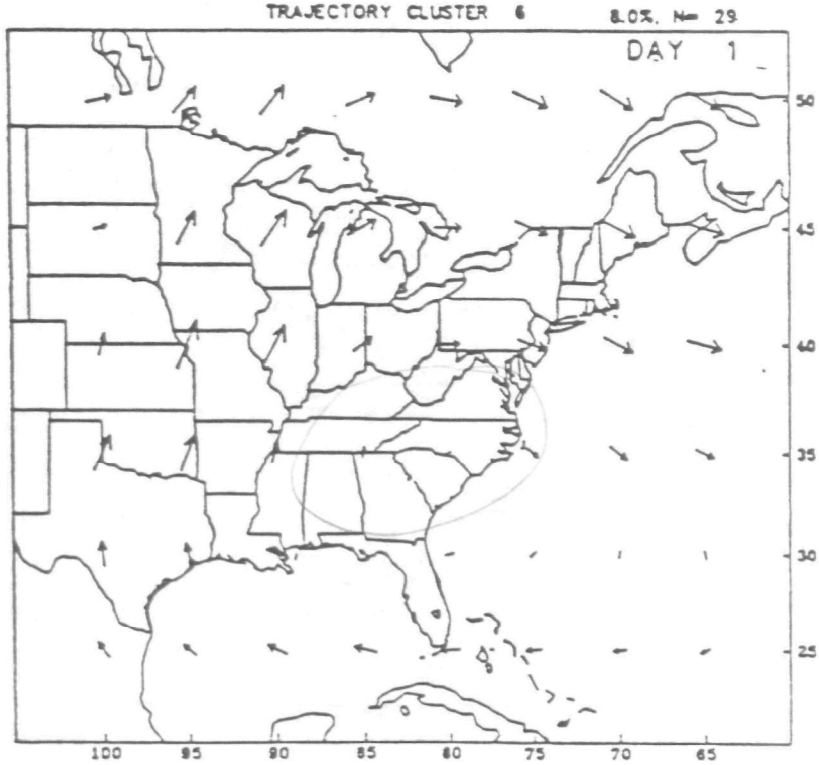

EASTERN NORTH AMERICAN MEAN 850MB WIND FIELD - 19 CLUSTERS

TRAJECTORY CLUSTER 6 8.0%, N= 29

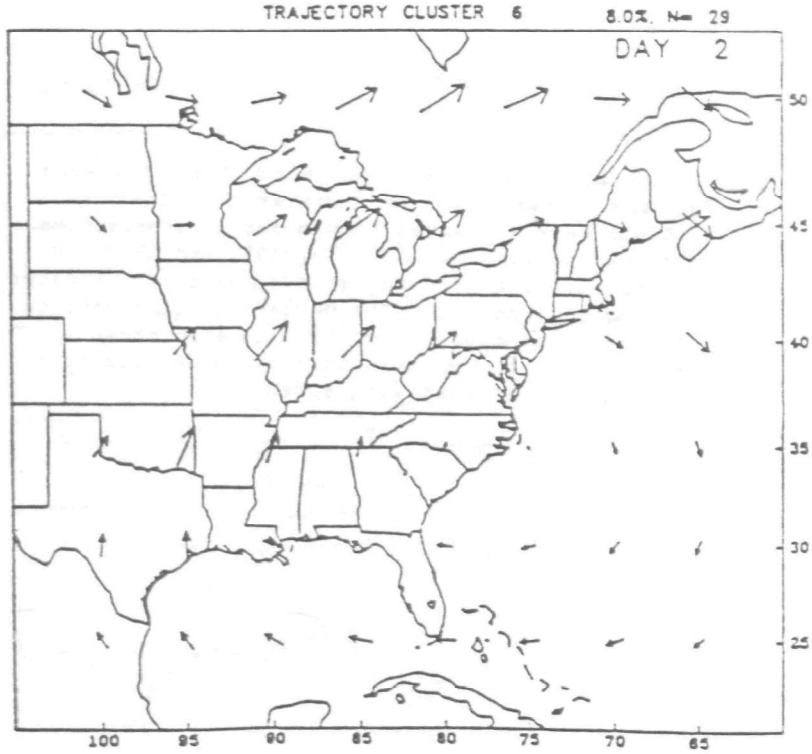

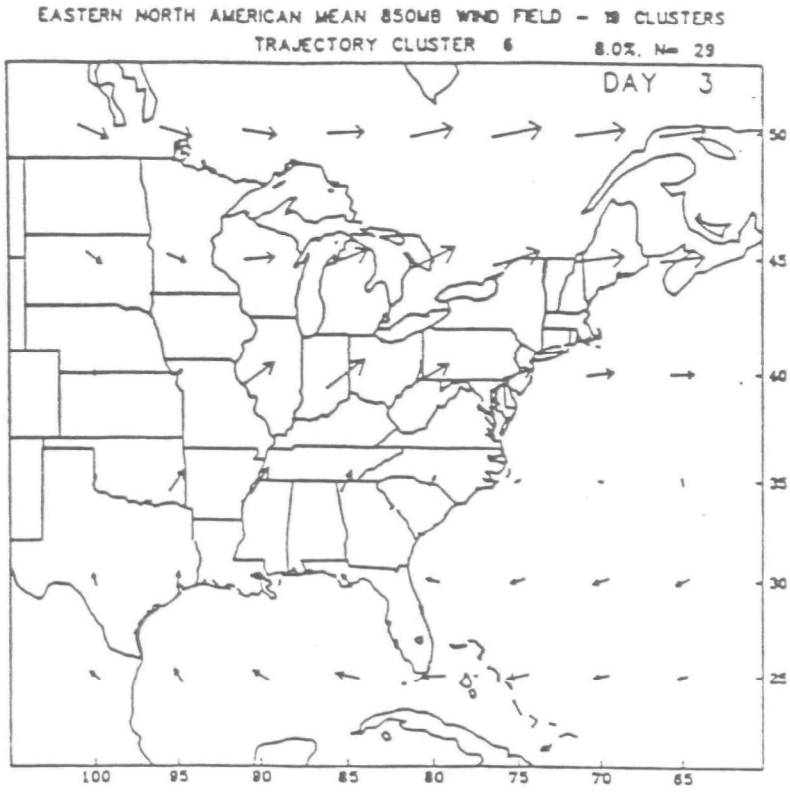

Figure A6 - Mean 850 mb wind flow patterns for the three days in Cluster 6. The clusters were extracted from a set of consecutive three-day periods during 1979, 1981 and 1983. N corresponds to the number of occurrences of cluster 6 during that period. The percent of time (out of all cases) the cluster occurred is also shown in the upper right. Wind vectors represent six hours of motion at reported wind speed.

EASTERN NORTH AMERICAN MEAN 850MB WIND FIELD – 19 CLUSTERS
TRAJECTORY CLUSTER 7 8.8%, N= 32

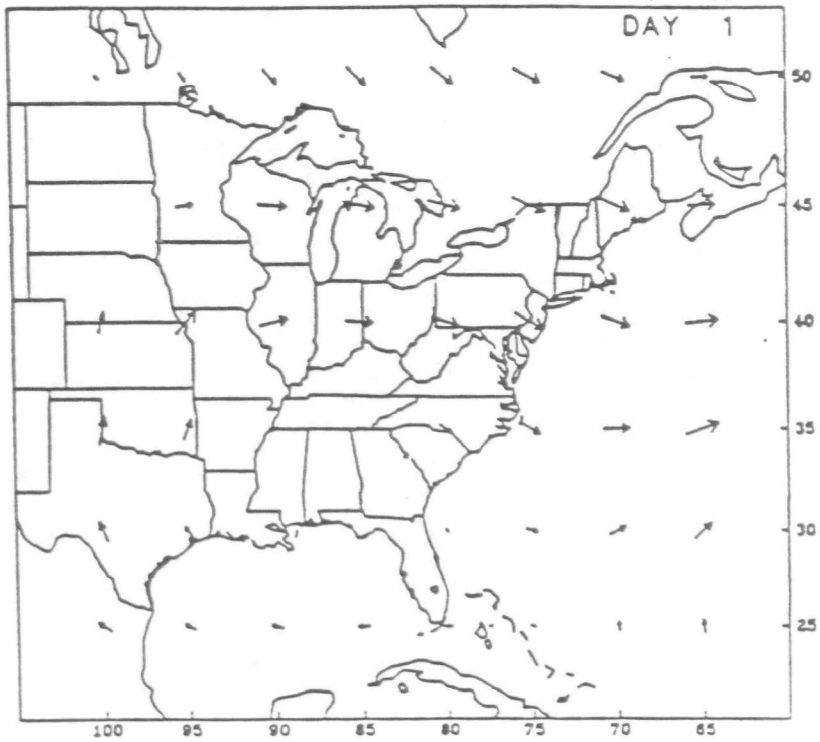

EASTERN NORTH AMERICAN MEAN 850MB WIND FIELD – 19 CLUSTERS
TRAJECTORY CLUSTER 7 8.8%, N= 32

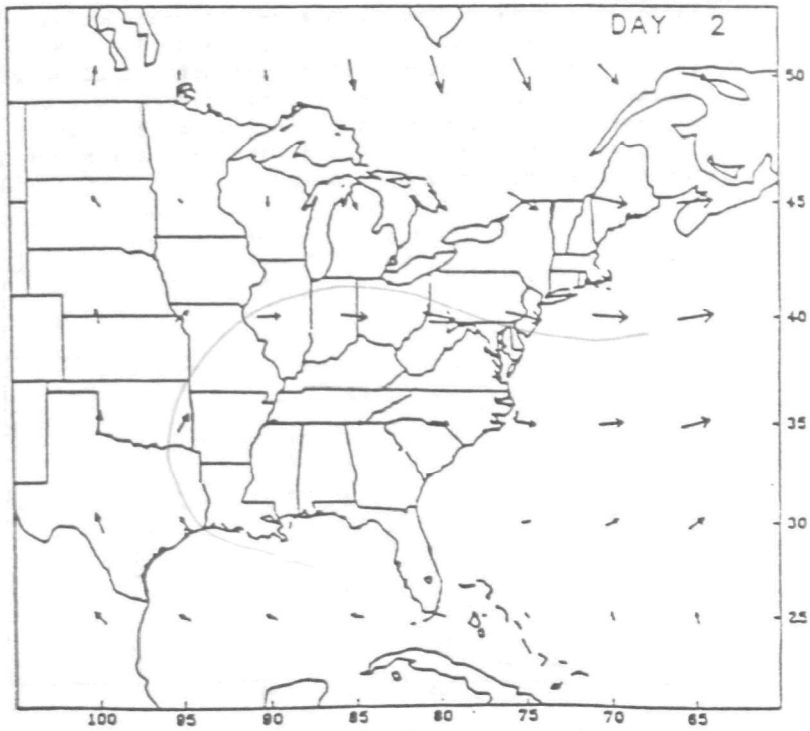

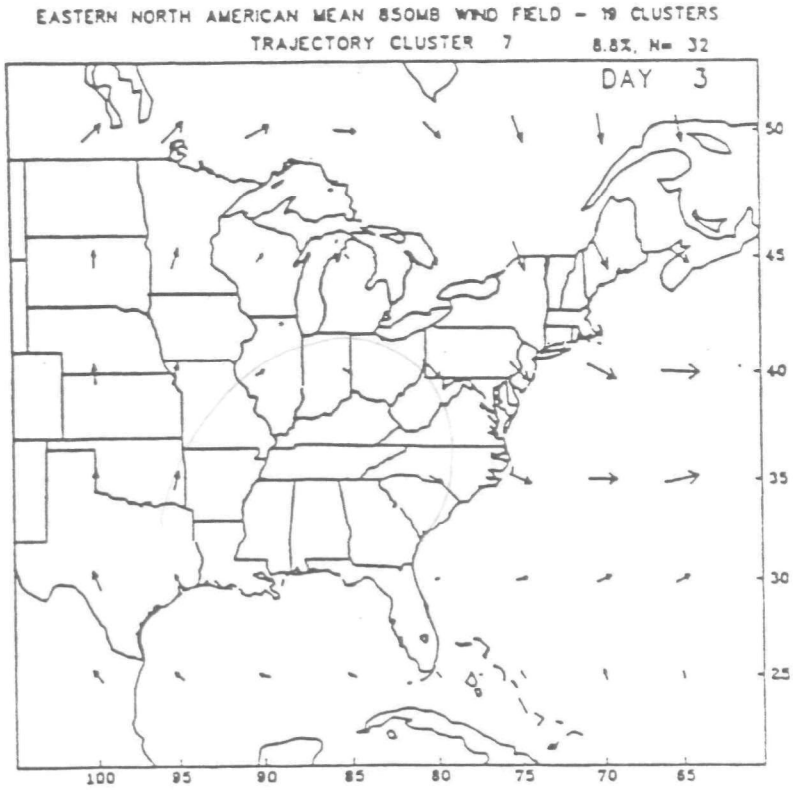

Figure A7 - Mean 850 mb wind flow patterns for the three days in Cluster 7. The clusters were extracted from a set of consecutive three-day periods during 1979, 1981 and 1983. N corresponds to the number of occurrences of cluster 7 during that period. The percent of time (out of all cases) the cluster occurred is also shown in the upper right. Wind vectors represent six hours of motion at reported wind speed.

EASTERN NORTH AMERICAN MEAN 850MB WIND FIELD - 19 CLUSTERS

TRAJECTORY CLUSTER 8 5.0%, N= 18

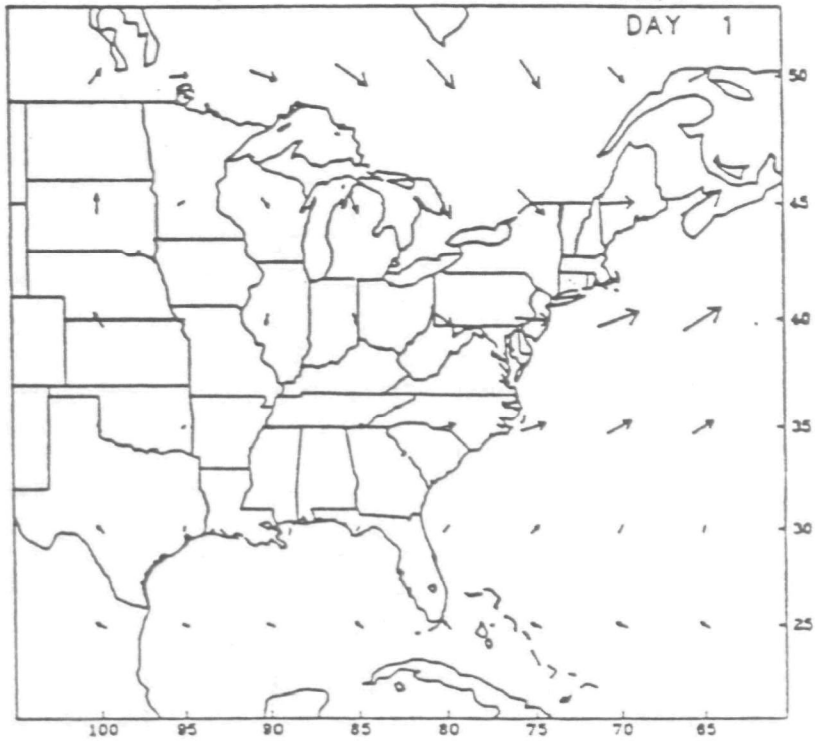

EASTERN NORTH AMERICAN MEAN 850MB WIND FIELD - 19 CLUSTERS

TRAJECTORY CLUSTER 8 5.0%, N= 18

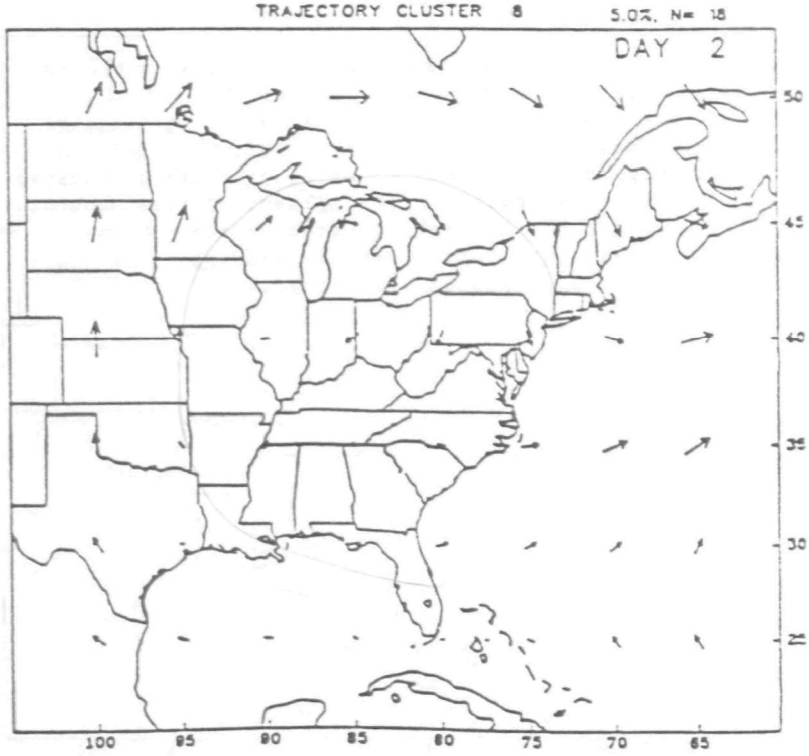

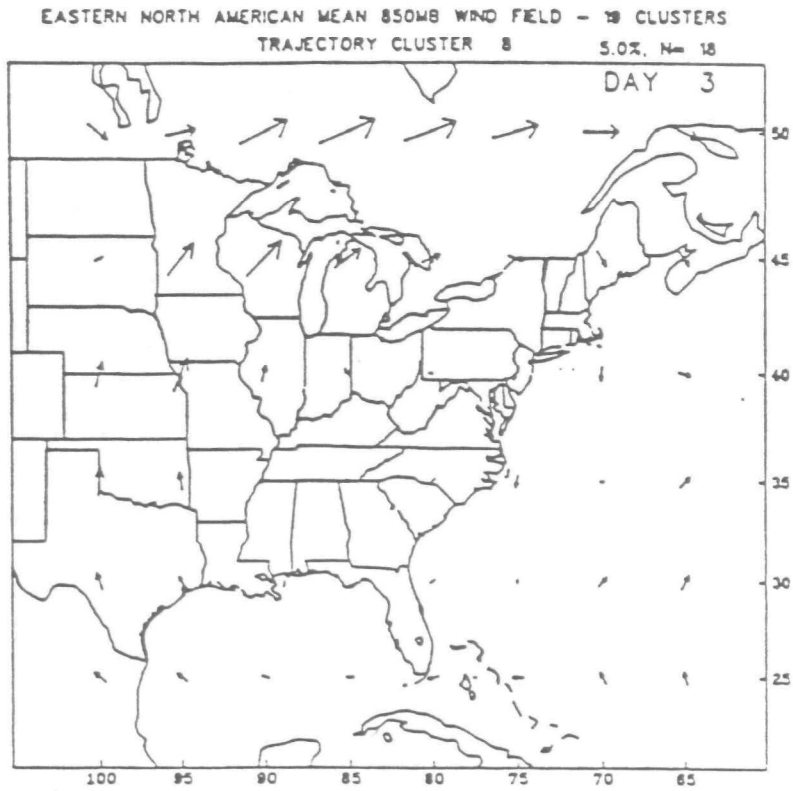

Figure A8 - Mean 850 mb wind flow patterns for the three days in Cluster 8. The clusters were extracted from a set of consecutive three-day periods during 1979, 1981 and 1983. N corresponds to the number of occurrences of cluster 8 during that period. The percent of time (out of all cases) the cluster occurred is also shown in the upper right. Wind vectors represent six hours of motion at reported wind speed.

EASTERN NORTH AMERICAN MEAN 850MB WIND FIELD - 19 CLUSTERS

TRAJECTORY CLUSTER 9 9.1%, N= 33

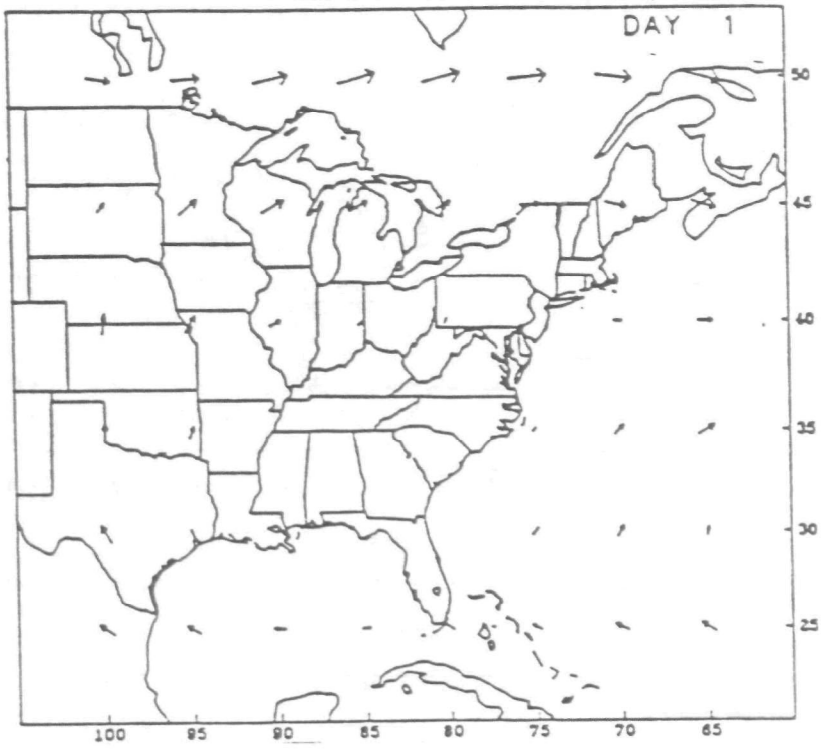

EASTERN NORTH AMERICAN MEAN 850MB WIND FIELD - 19 CLUSTERS

TRAJECTORY CLUSTER 9 9.1%, N= 33

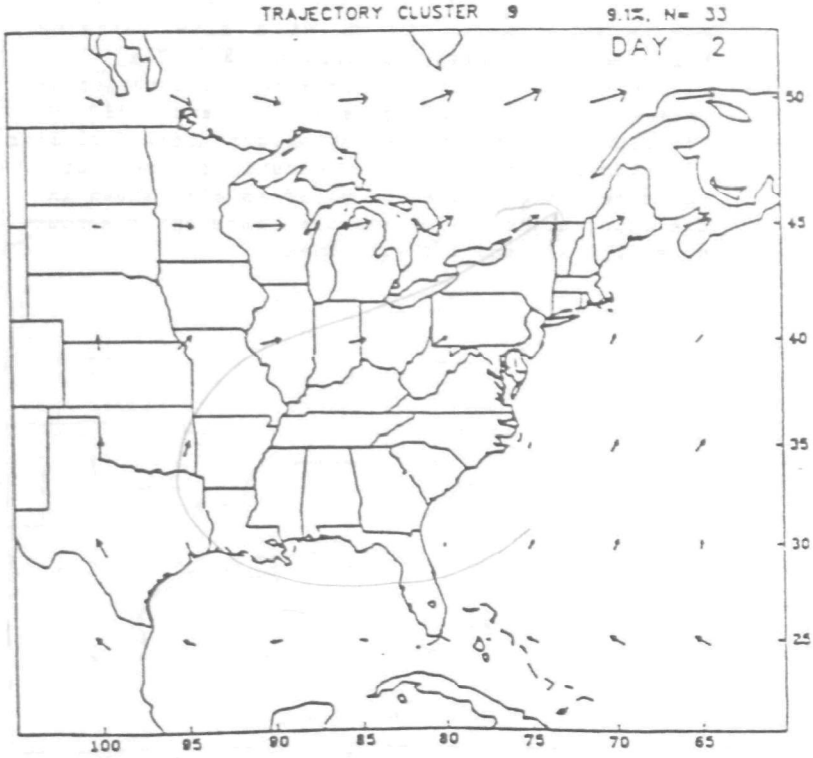

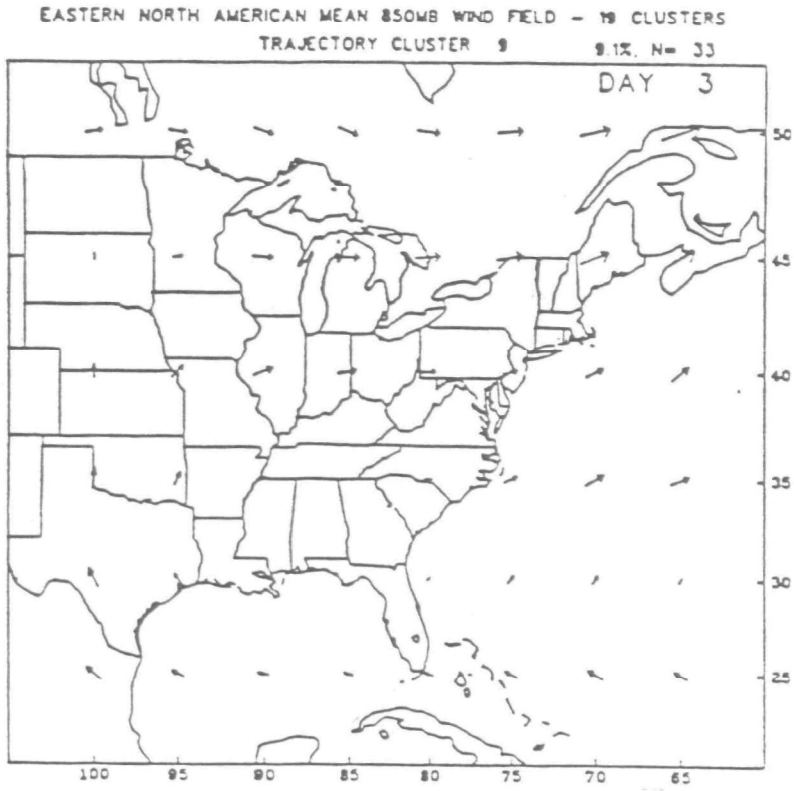

Figure A9 - Mean 850 mb wind flow patterns for the three days in Cluster 9. The clusters were extracted from a set of consecutive three-day periods during 1979, 1981 and 1983. N corresponds to the number of occurrences of cluster 9 during that period. The percent of time (out of all cases) the cluster occurred is also shown in the upper right. Wind vectors represent six hours of motion at reported wind speed.

EASTERN NORTH AMERICAN MEAN 850MB WIND FIELD - 19 CLUSTERS
TRAJECTORY CLUSTER 10 2.2%, N= 8

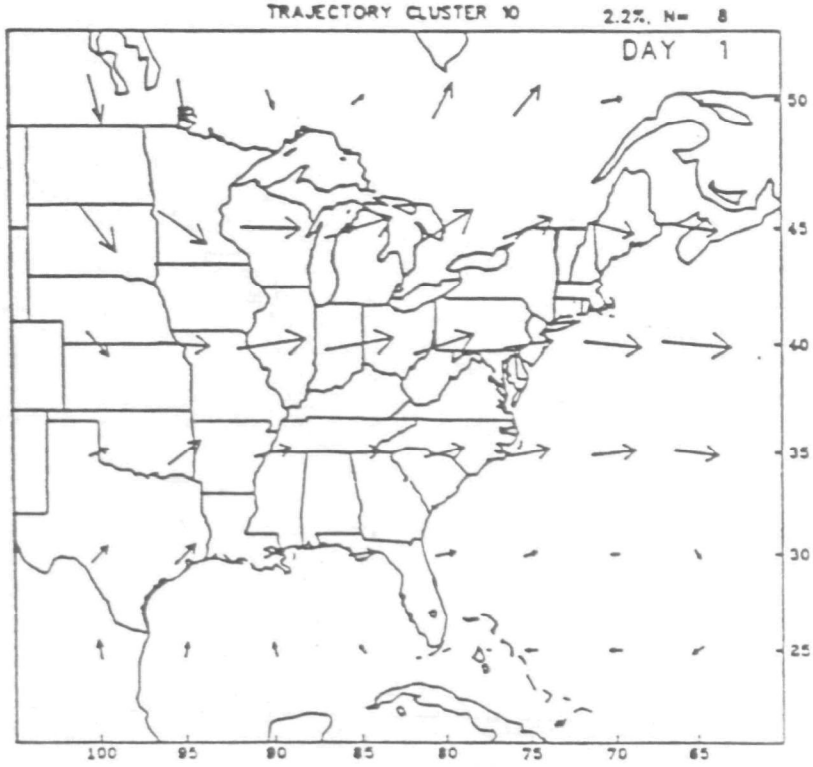

EASTERN NORTH AMERICAN MEAN 850MB WIND FIELD - 19 CLUSTERS
TRAJECTORY CLUSTER 10 2.2%, N= 8

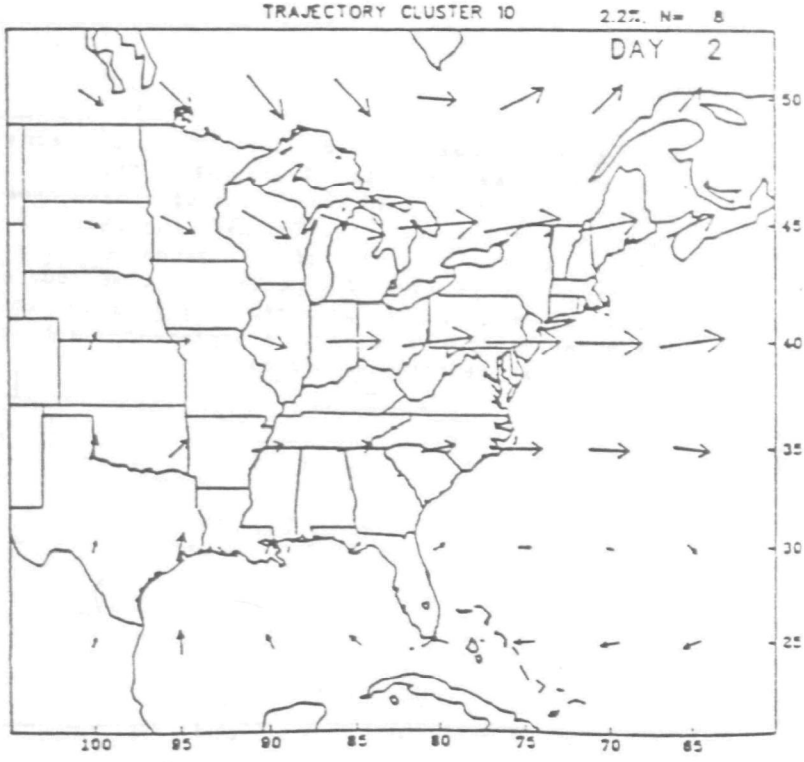

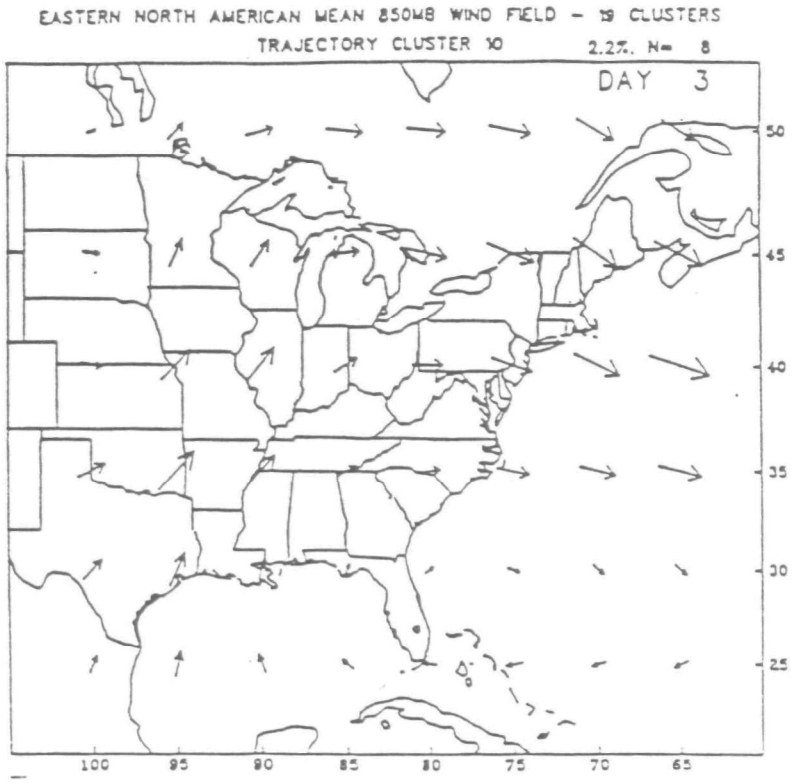

Figure A10 - Mean 850 mb wind flow patterns for the three days in Cluster 10. The clusters were extracted from a set of consecutive three-day periods during 1979, 1981 and 1983. N corresponds to the number of occurrences of cluster 10 during that period. The percent of time (out of all cases) the cluster occurred is also shown in the upper right. Wind vectors represent six hours of motion at reported wind speed.

EASTERN NORTH AMERICAN MEAN 850MB WIND FIELD - 19 CLUSTERS
TRAJECTORY CLUSTER 11 7.4%, N= 27

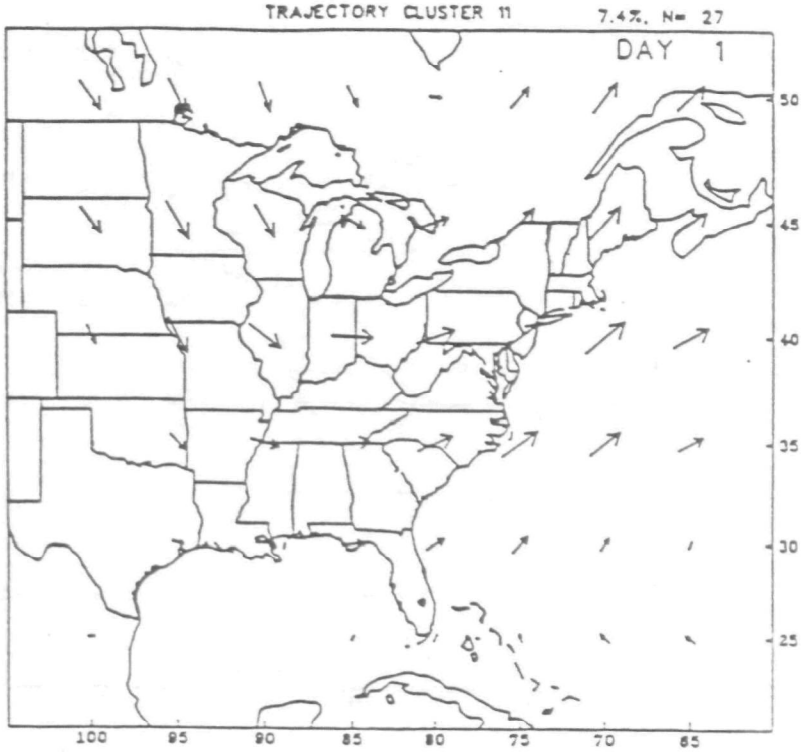

EASTERN NORTH AMERICAN MEAN 850MB WIND FIELD - 19 CLUSTERS
TRAJECTORY CLUSTER 11 7.4%, N= 27

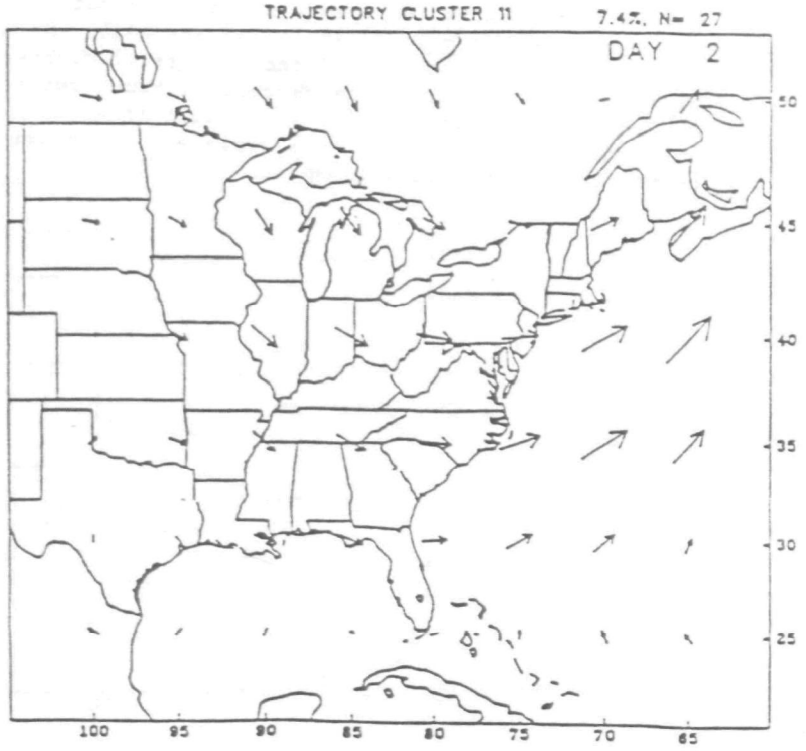

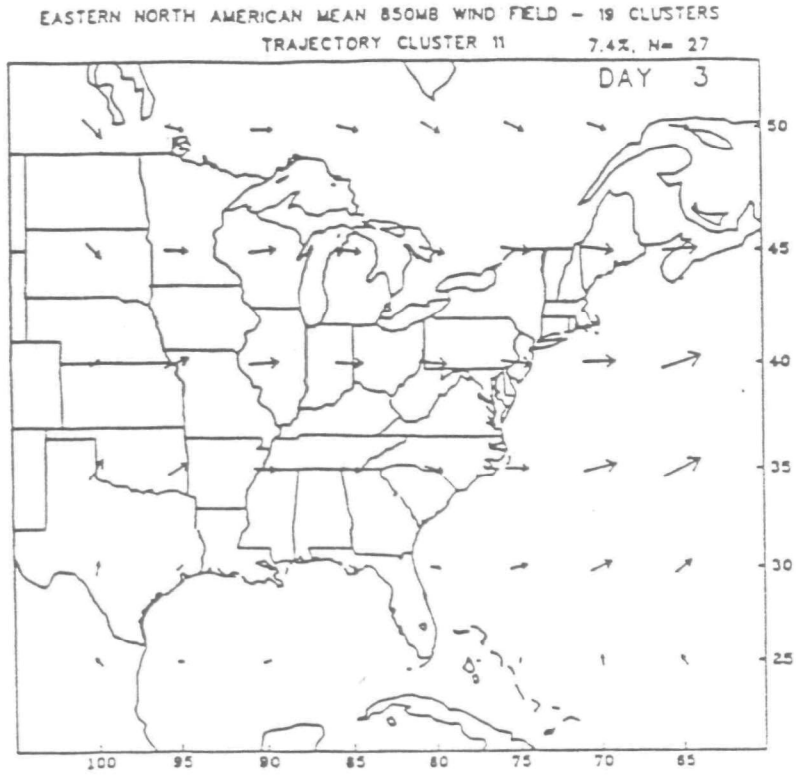

Figure A11 - Mean 850 mb wind flow patterns for the three days in Cluster 11. The clusters were extracted from a set of consecutive three-day periods during 1979, 1981 and 1983. N corresponds to the number of occurrences of cluster 11 during that period. The percent of time (out of all cases) the cluster occurred is also shown in the upper right. Wind vectors represent six hours of motion at reported wind speed.

EASTERN NORTH AMERICAN MEAN 850MB WIND FIELD – 19 CLUSTERS

TRAJECTORY CLUSTER 12 4.1%, N= 15

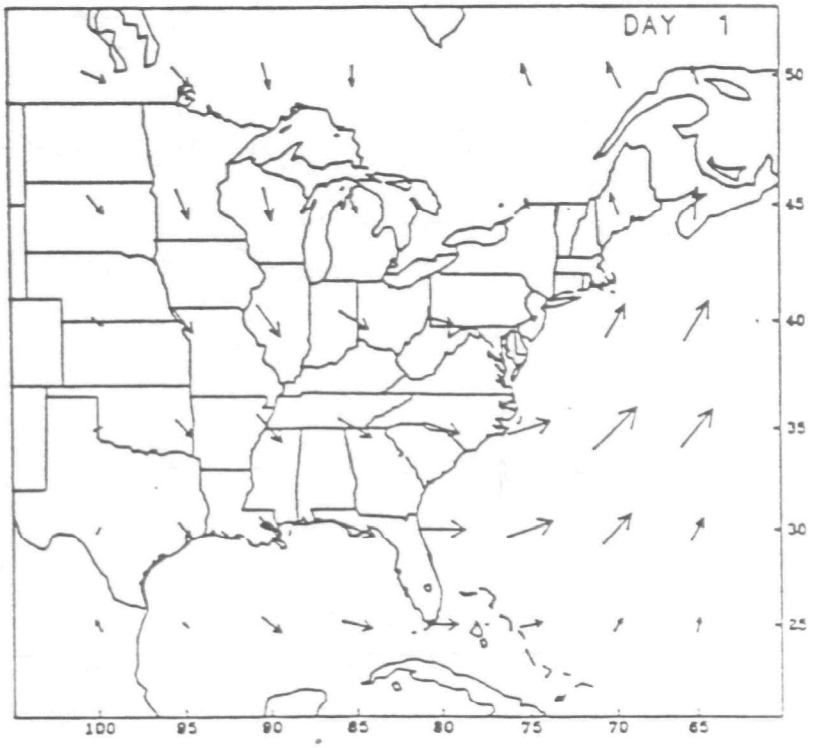

EASTERN NORTH AMERICAN MEAN 850MB WIND FIELD – 19 CLUSTERS

TRAJECTORY CLUSTER 12 4.1%, N= 15

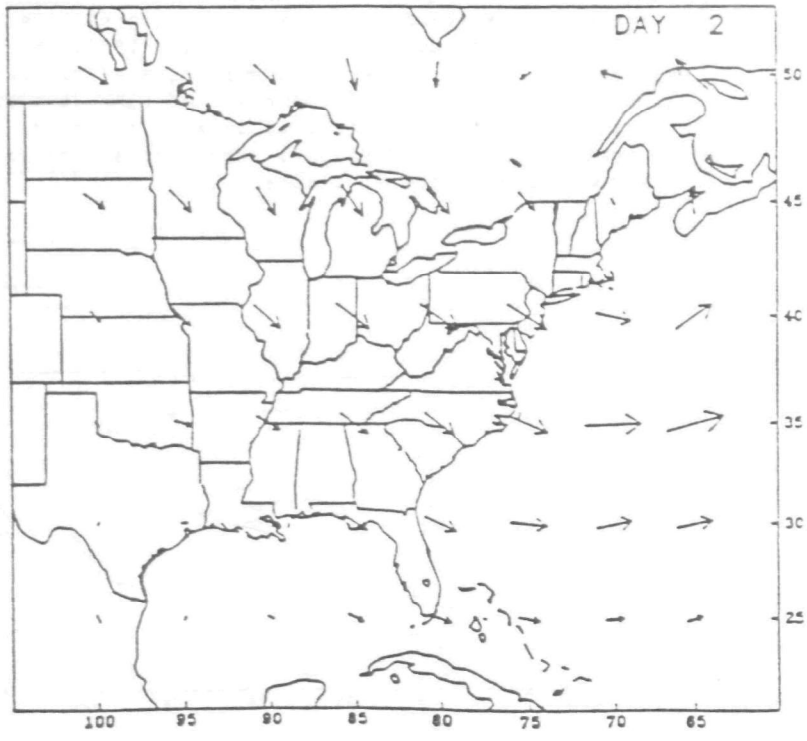

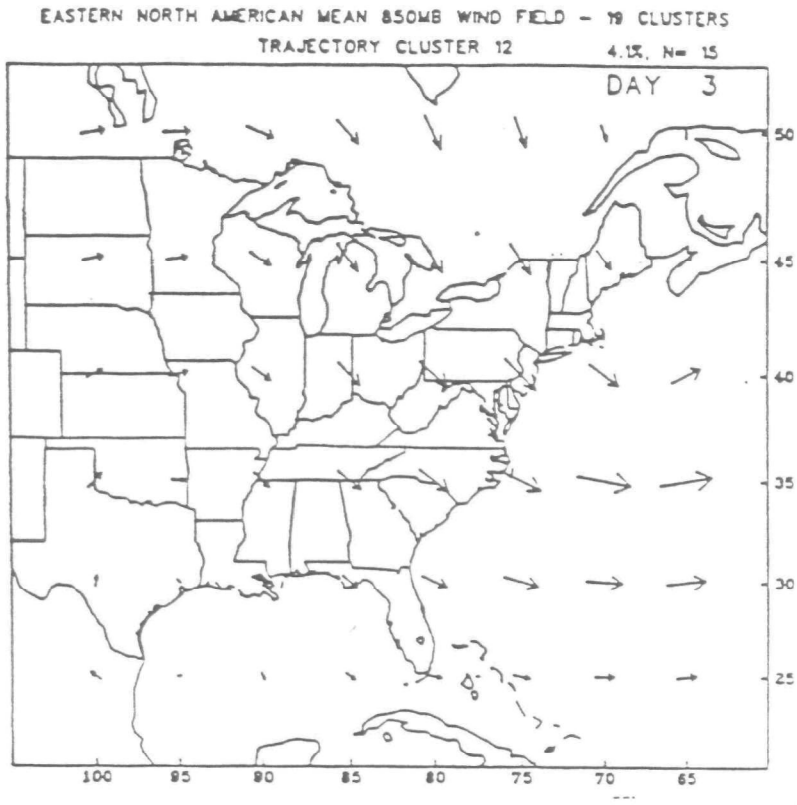

Figure A12 - Mean 850 mb wind flow patterns for the three days in Cluster 12. The clusters were extracted from a set of consecutive three-day periods during 1979, 1981 and 1983. N corresponds to the number of occurrences of cluster 12 during that period. The percent of time (out of all cases) the cluster occurred is also shown in the upper right. Wind vectors represent six hours of motion at reported wind speed.

EASTERN NORTH AMERICAN MEAN 850MB WIND FIELD - 19 CLUSTERS
TRAJECTORY CLUSTER 13 2.2%, N= 8

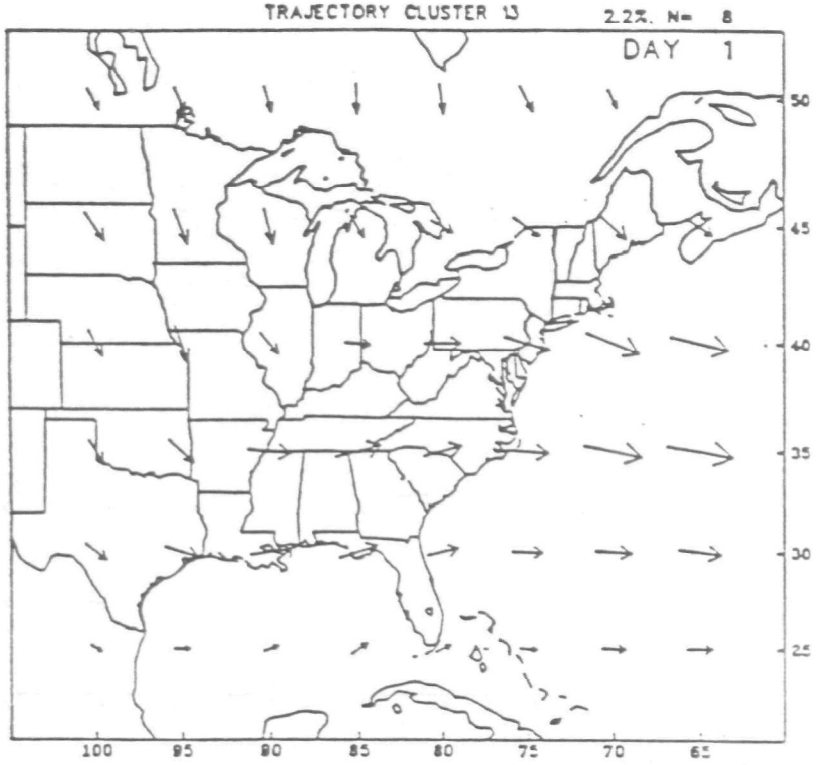

EASTERN NORTH AMERICAN MEAN 850MB WIND FIELD - 19 CLUSTERS
TRAJECTORY CLUSTER 13 2.2%, N= 8

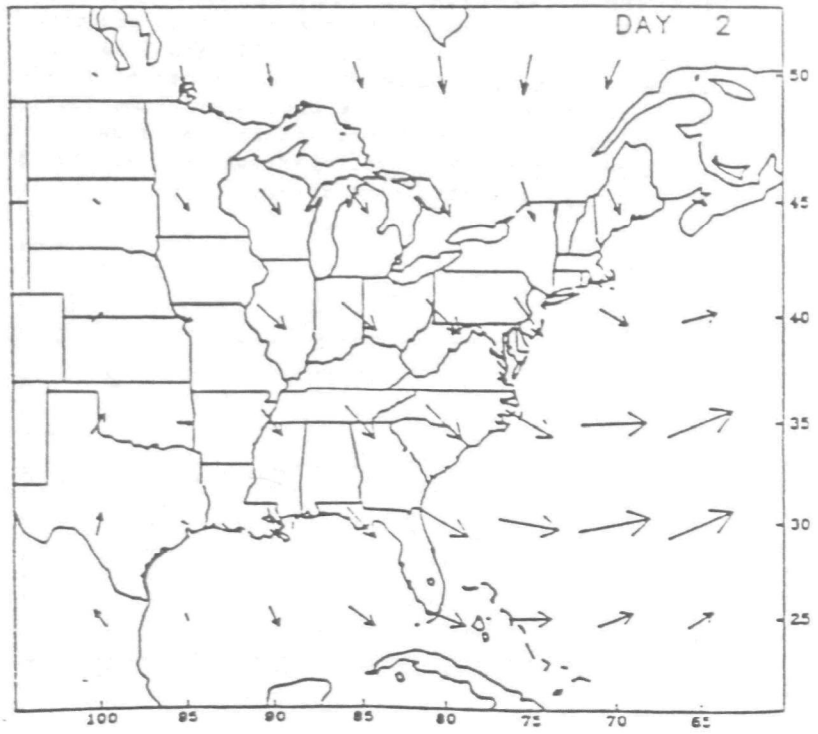

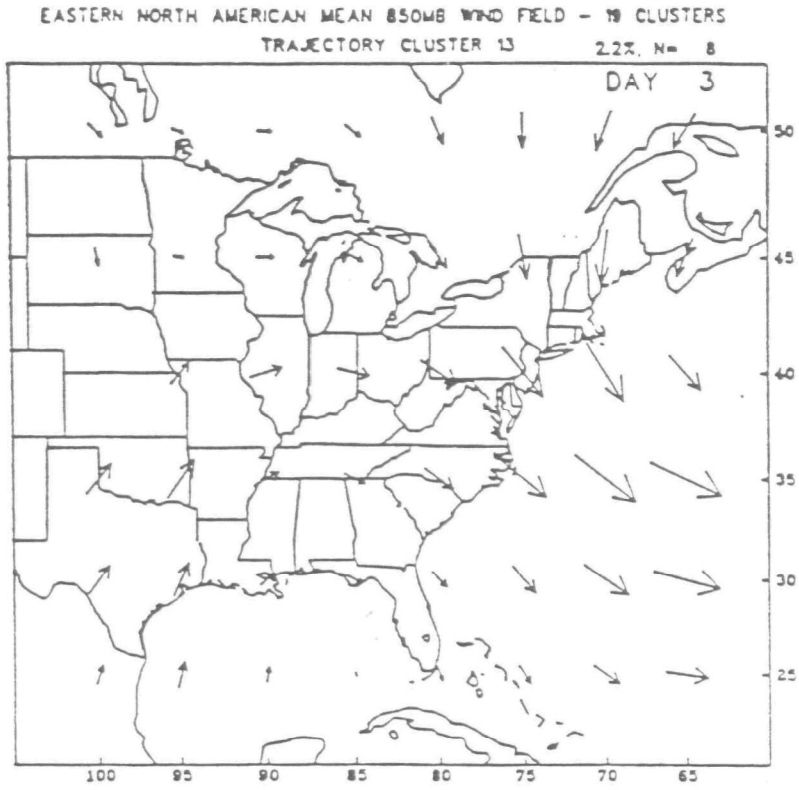

Figure A13 - Mean 850 mb wind flow patterns for the three days in Cluster 13. The clusters were extracted from a set of consecutive three-day periods during 1979, 1981 and 1983. N corresponds to the number of occurrences of cluster 13 during that period. The percent of time (out of all cases) the cluster occurred is also shown in the upper right. Wind vectors represent six hours of motion at reported wind speed.

EASTERN NORTH AMERICAN MEAN 850MB WIND FIELD – 19 CLUSTERS

TRAJECTORY CLUSTER 14 1.4%, N= 5

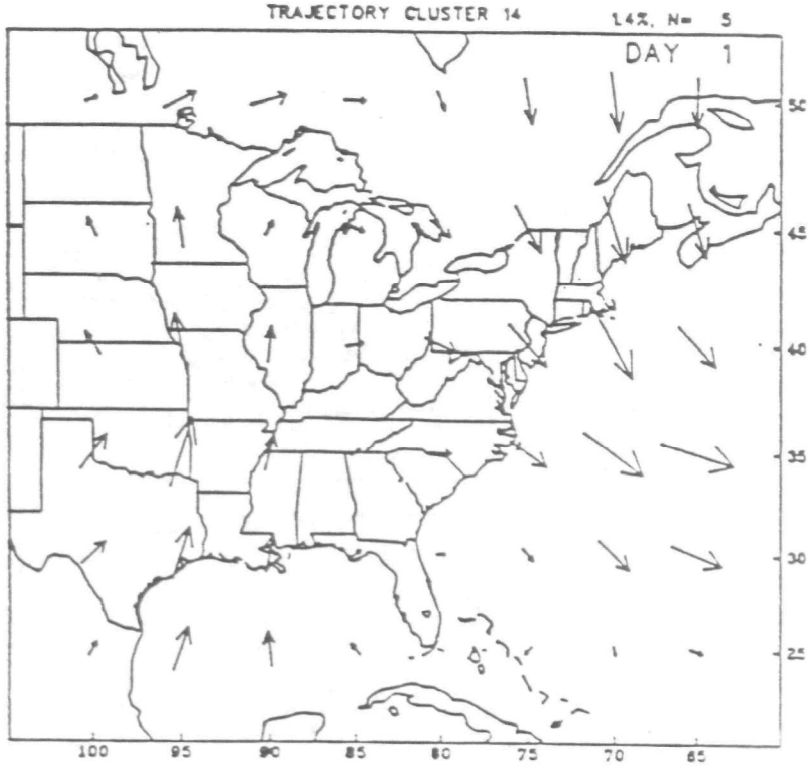

EASTERN NORTH AMERICAN MEAN 850MB WIND FIELD – 19 CLUSTERS

TRAJECTORY CLUSTER 14 1.4%, N= 5

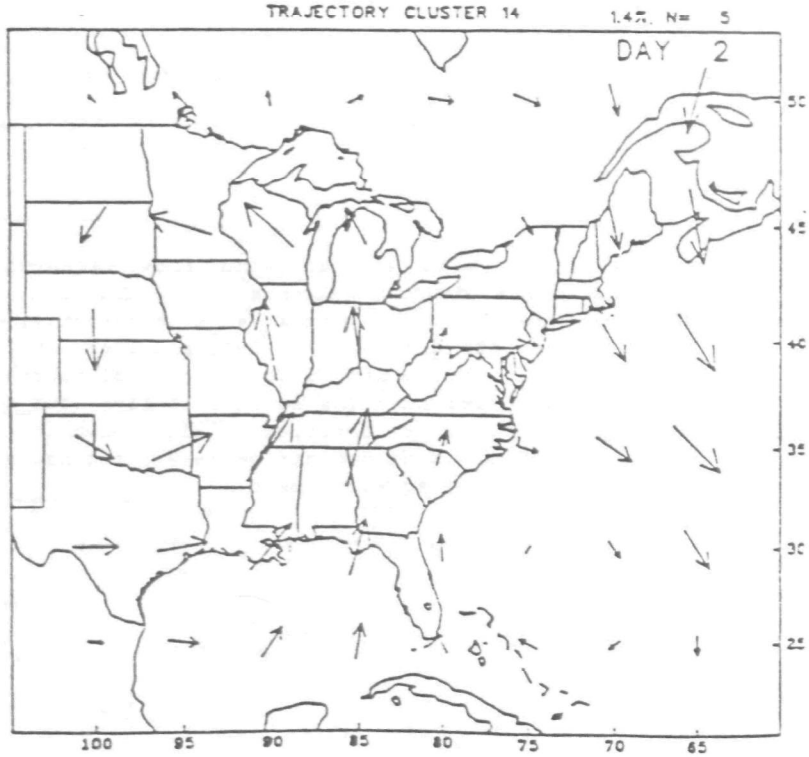

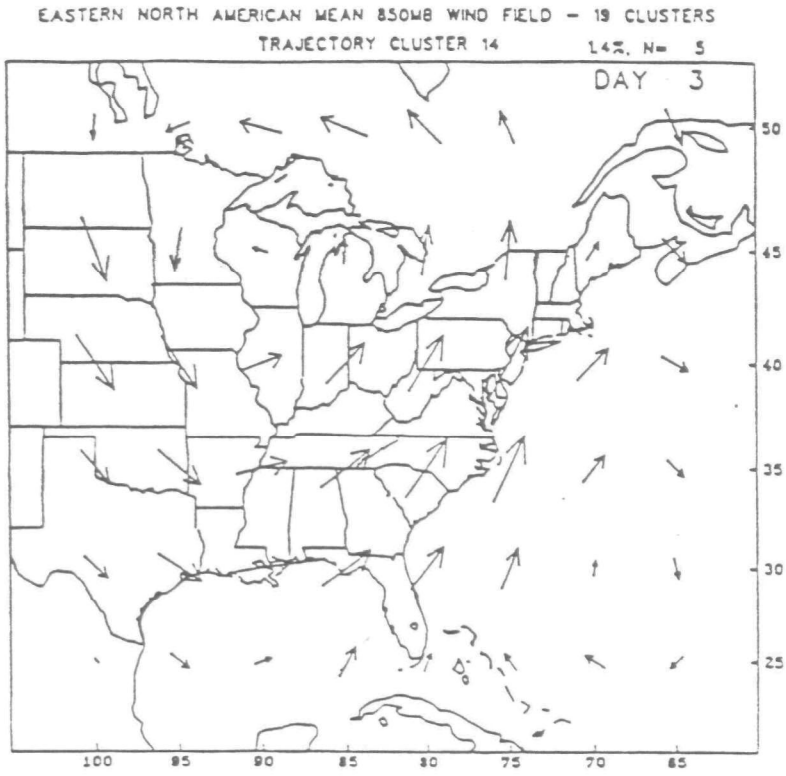

Figure A14 - Mean 850 mb wind flow patterns for the three days in Cluster 14. The clusters were extracted from a set of consecutive three-day periods during 1979, 1981 and 1983. N corresponds to the number of occurrences of cluster 14 during that period. The percent of time (out of all cases) the cluster occurred is also shown in the upper right. Wind vectors represent six hours of motion at reported wind speed.

EASTERN NORTH AMERICAN MEAN 850MB WIND FIELD - 19 CLUSTERS
TRAJECTORY CLUSTER 15 14%, N= 5

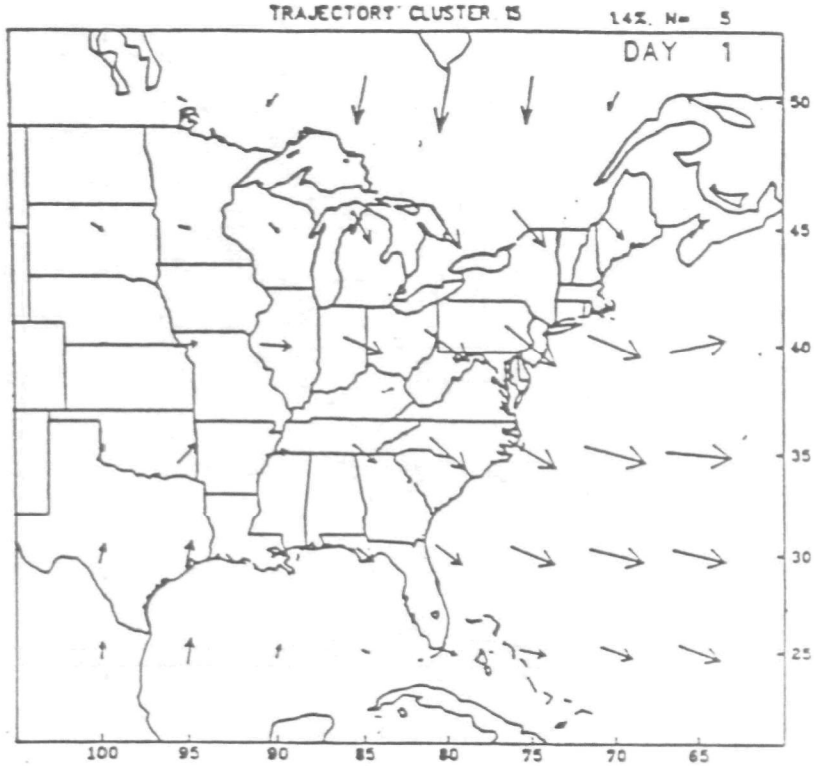

EASTERN NORTH AMERICAN MEAN 850MB WIND FIELD - 19 CLUSTERS
TRAJECTORY CLUSTER 15 14%, N= 5

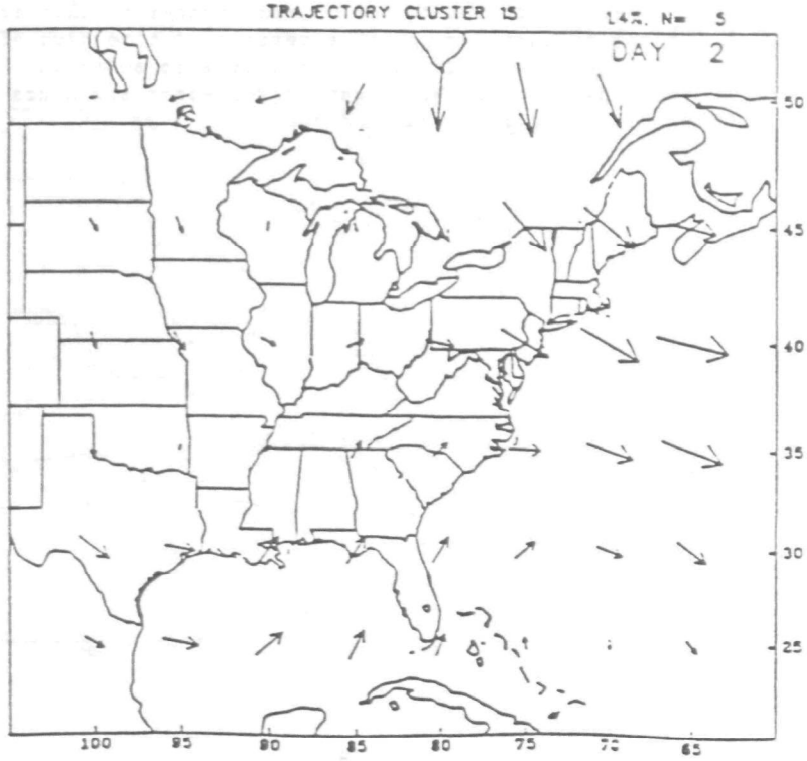

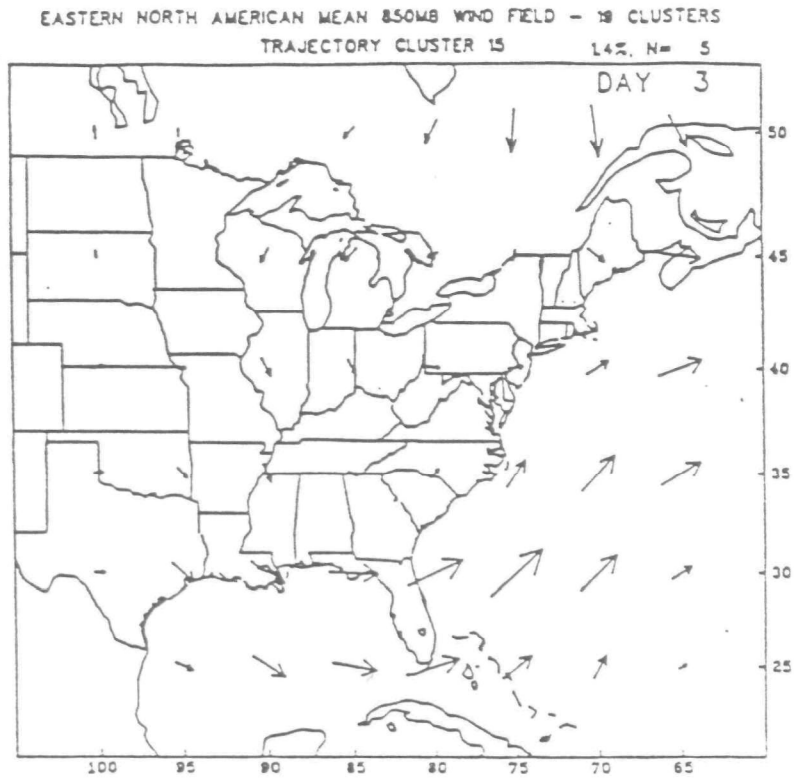

Figure A15 - Mean 850 mb wind flow patterns for the three days in Cluster 15. The clusters were extracted from a set of consecutive three-day periods during 1979, 1981 and 1983. N corresponds to the number of occurrences of cluster 15 during that period. The percent of time (out of all cases) the cluster occurred is also shown in the upper right. Wind vectors represent six hours of motion at reported wind speed.

EASTERN NORTH AMERICAN MEAN 850MB WIND FIELD – 19 CLUSTERS
TRAJECTORY CLUSTER 16 1.7%, N= 6

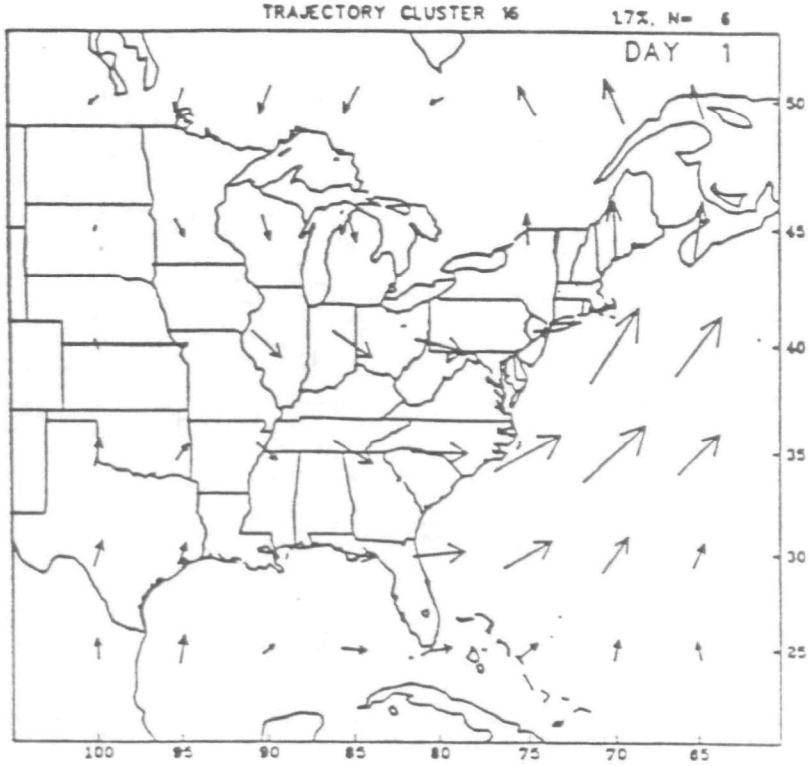

EASTERN NORTH AMERICAN MEAN 850MB WIND FIELD – 19 CLUSTERS
TRAJECTORY CLUSTER 16 1.7%, N= 6

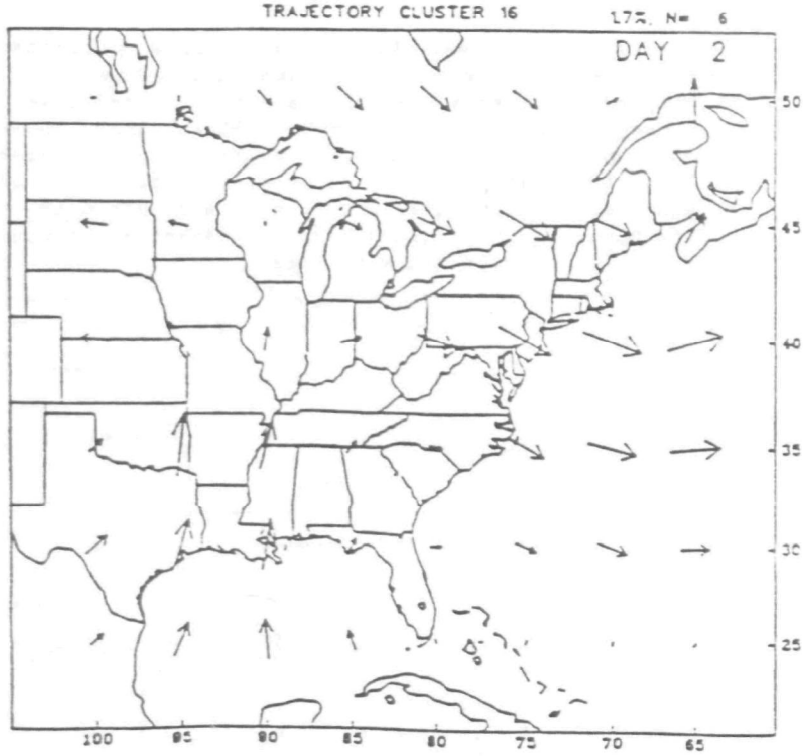

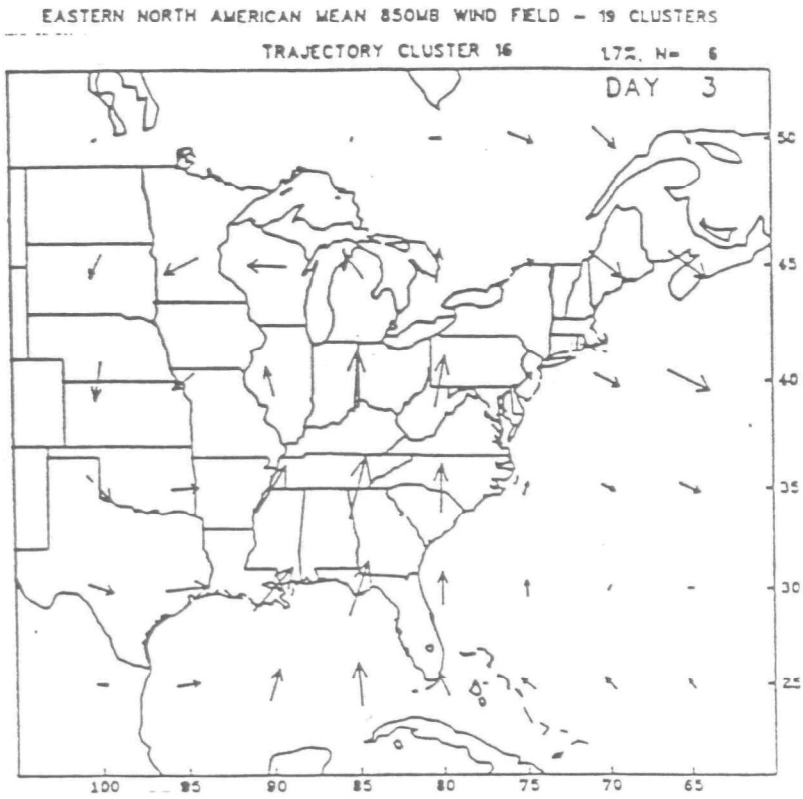

Figure A16 - Mean 850 mb wind flow patterns for the three days in Cluster 16. The clusters were extracted from a set of consecutive three-day periods during 1979, 1981 and 1983. N corresponds to the number of occurrences of cluster 16 during that period. The percent of time (out of all cases) the cluster occurred is also shown in the upper right. Wind vectors represent six hours of motion at reported wind speed.

EASTERN NORTH AMERICAN MEAN 850MB WIND FIELD – 19 CLUSTERS

TRAJECTORY CLUSTER 17 3.6%, N= 13

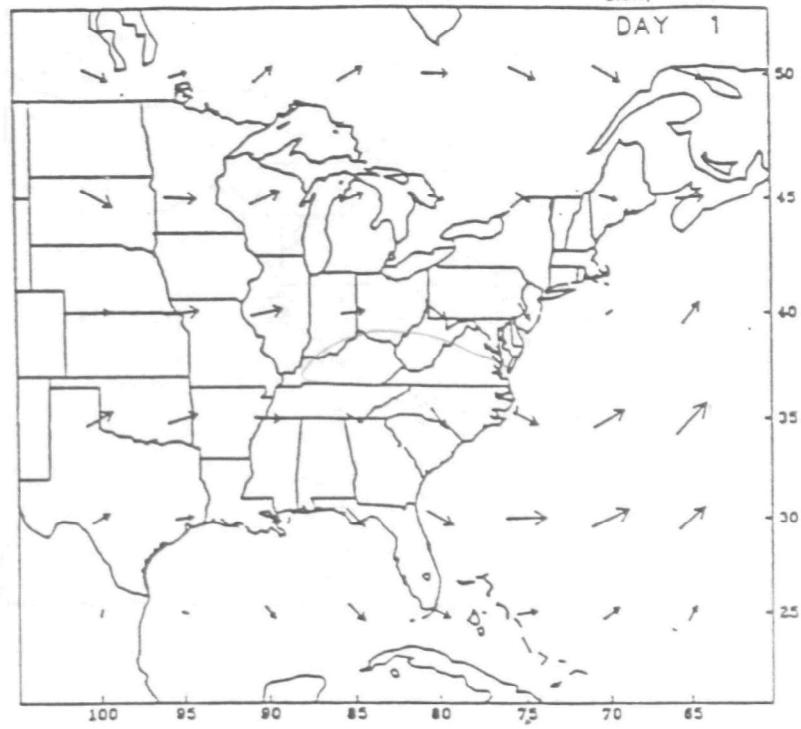

EASTERN NORTH AMERICAN MEAN 850MB WIND FIELD – 19 CLUSTERS

TRAJECTORY CLUSTER 17 3.6%, N= 13

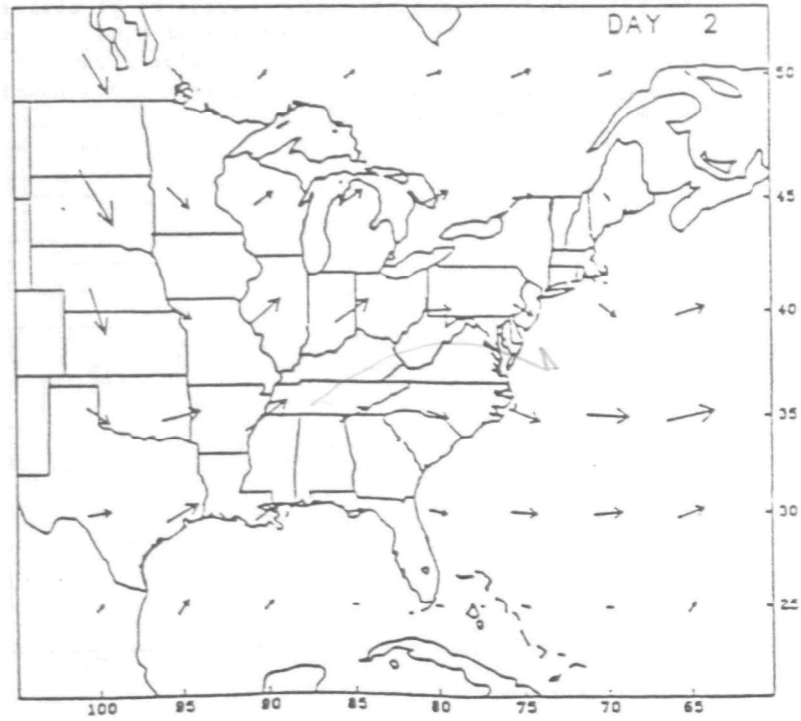

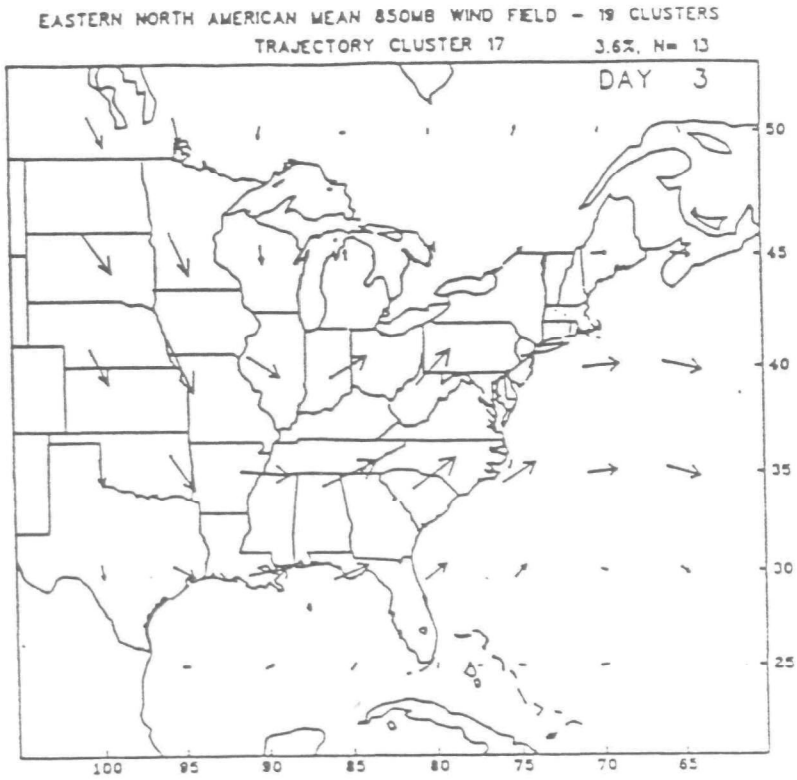

Figure A17 - Mean 850 mb wind flow patterns for the three days in Cluster 17. The clusters were extracted from a set of consecutive three-day periods during 1979, 1981 and 1983. N corresponds to the number of occurrences of cluster 17 during that period. The percent of time (out of all cases) the cluster occurred is also shown in the upper right. Wind vectors represent six hours of motion at reported wind speed.

EASTERN NORTH AMERICAN MEAN 850MB WIND FIELD - 19 CLUSTERS

TRAJECTORY CLUSTER 18 3.6%, N= 13

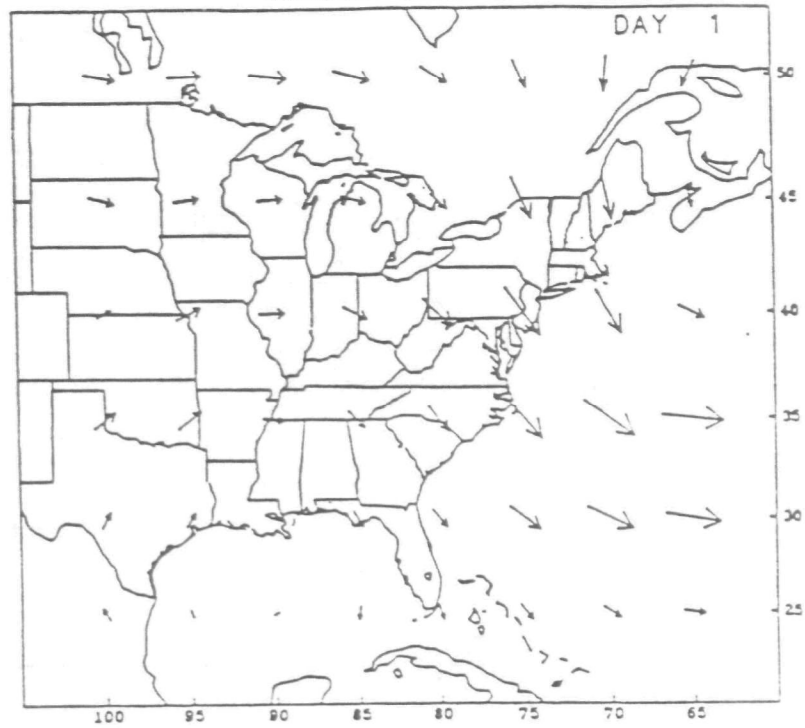

EASTERN NORTH AMERICAN MEAN 850MB WIND FIELD - 19 CLUSTERS

TRAJECTORY CLUSTER 18 3.6%, N= 13

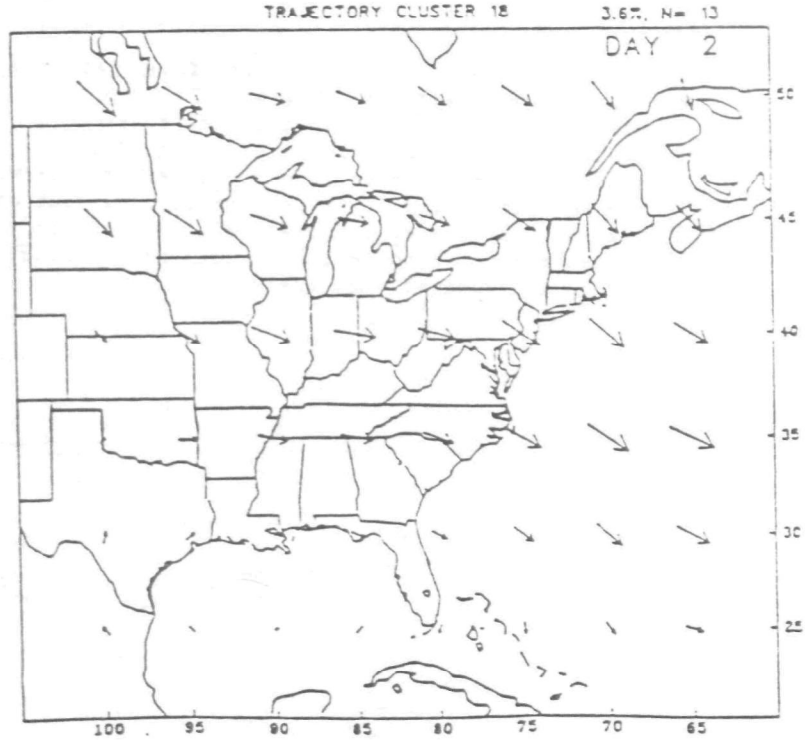

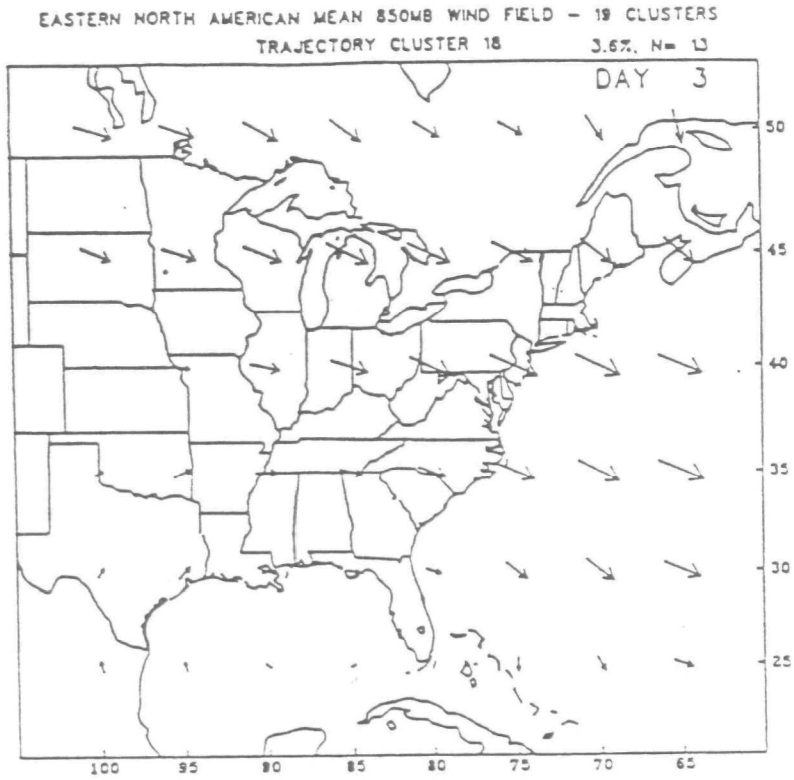

Figure A18 - Mean 850 mb wind flow patterns for the three days in Cluster 18. The clusters were extracted from a set of consecutive three-day periods during 1979, 1981 and 1983. N corresponds to the number of occurrences of cluster 18 during that period. The percent of time (out of all cases) the cluster occurred is also shown in the upper right. Wind vectors represent six hours of motion at reported wind speed.

EASTERN NORTH AMERICAN MEAN 850MB WIND FIELD - 19 CLUSTERS
TRAJECTORY CLUSTER 19 2.8%, N= 10

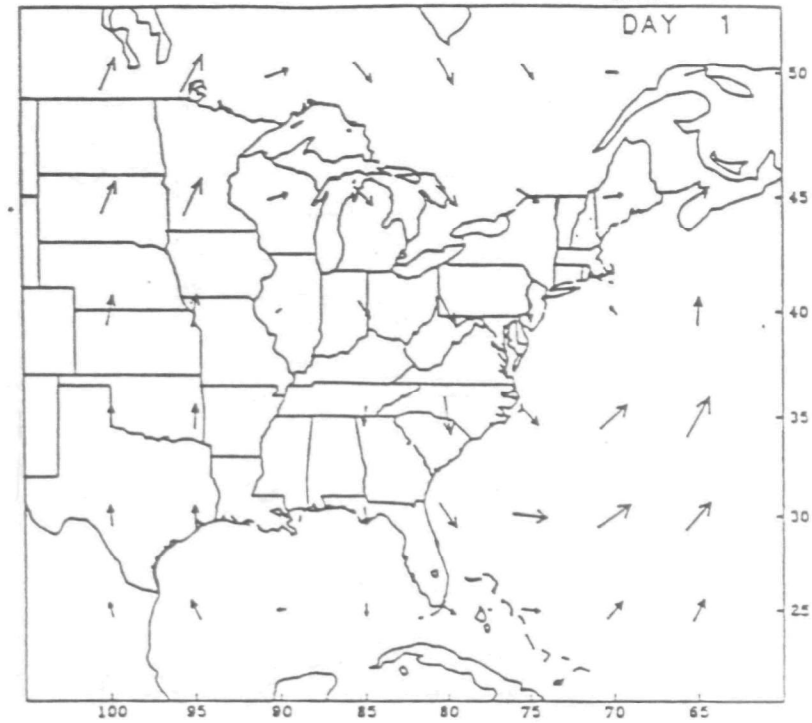

EASTERN NORTH AMERICAN MEAN 850MB WIND FIELD - 19 CLUSTERS
TRAJECTORY CLUSTER 19 2.8%, N= 10

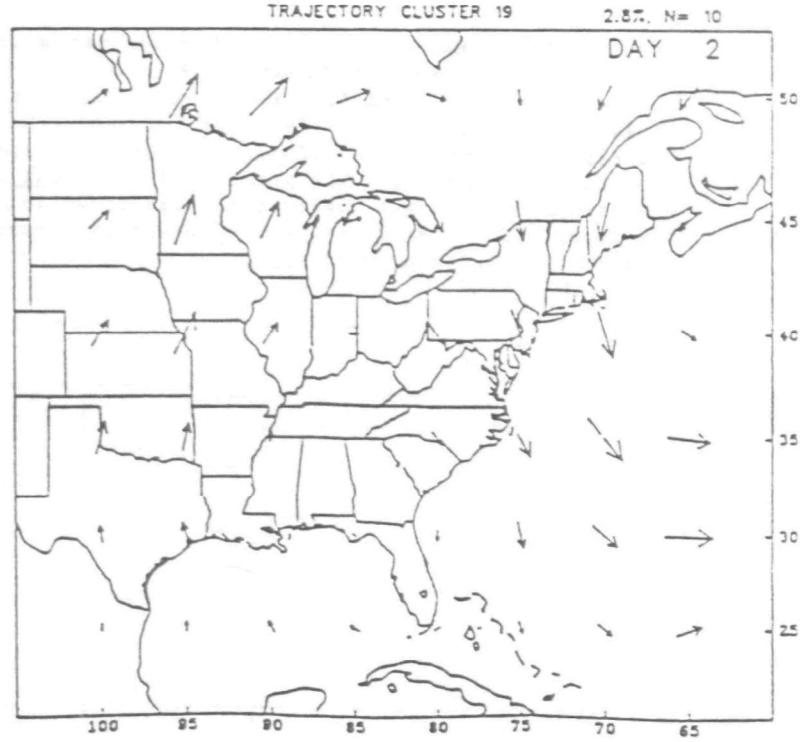

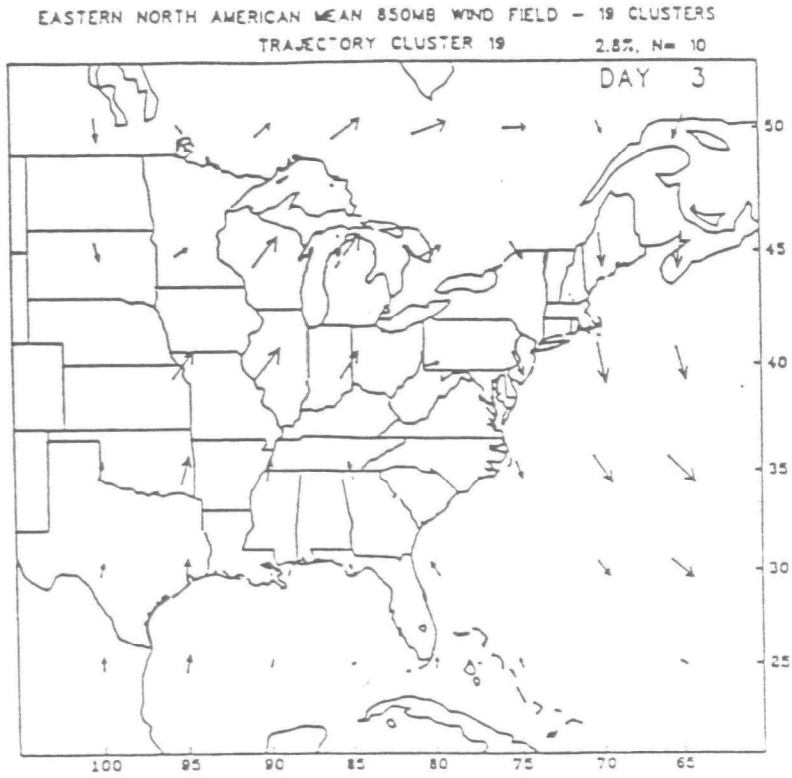

Figure A19 - Mean 850 mb wind flow patterns for the three days in Cluster 19. The clusters were extracted from a set of consecutive three-day periods during 1979, 1981 and 1983. N corresponds to the number of occurrences of cluster 19 during that period. The percent of time (out of all cases) the cluster occurred is also shown in the upper right. Wind vectors represent six hours of motion at reported wind speed.

APPENDIX B

85th Percentile Wet Sulfate
Deposition Plots for the
19 Categories

85th Percentile SO4= Deposition (STEP 19) - CLUSTER 1

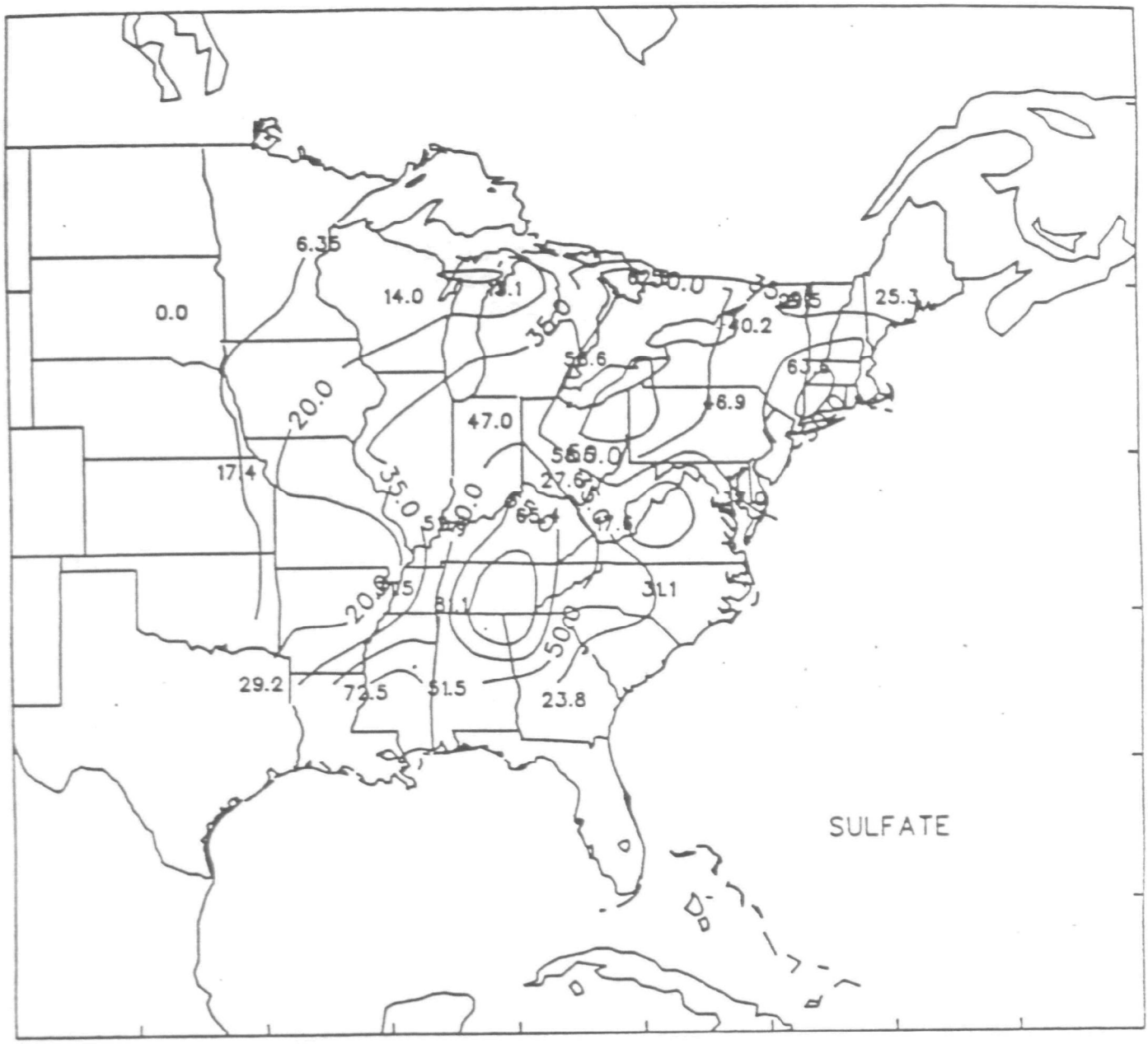

Figure B1 - 85th Percentile Three-day Total Deposition Pattern due to Cluster 1 Cases. The 85th percentile at each site was derived from the distribution of all available three-day total deposition cases within the cluster.

85th Percentile SO4= Deposition (STEP 19) - CLUSTER 2

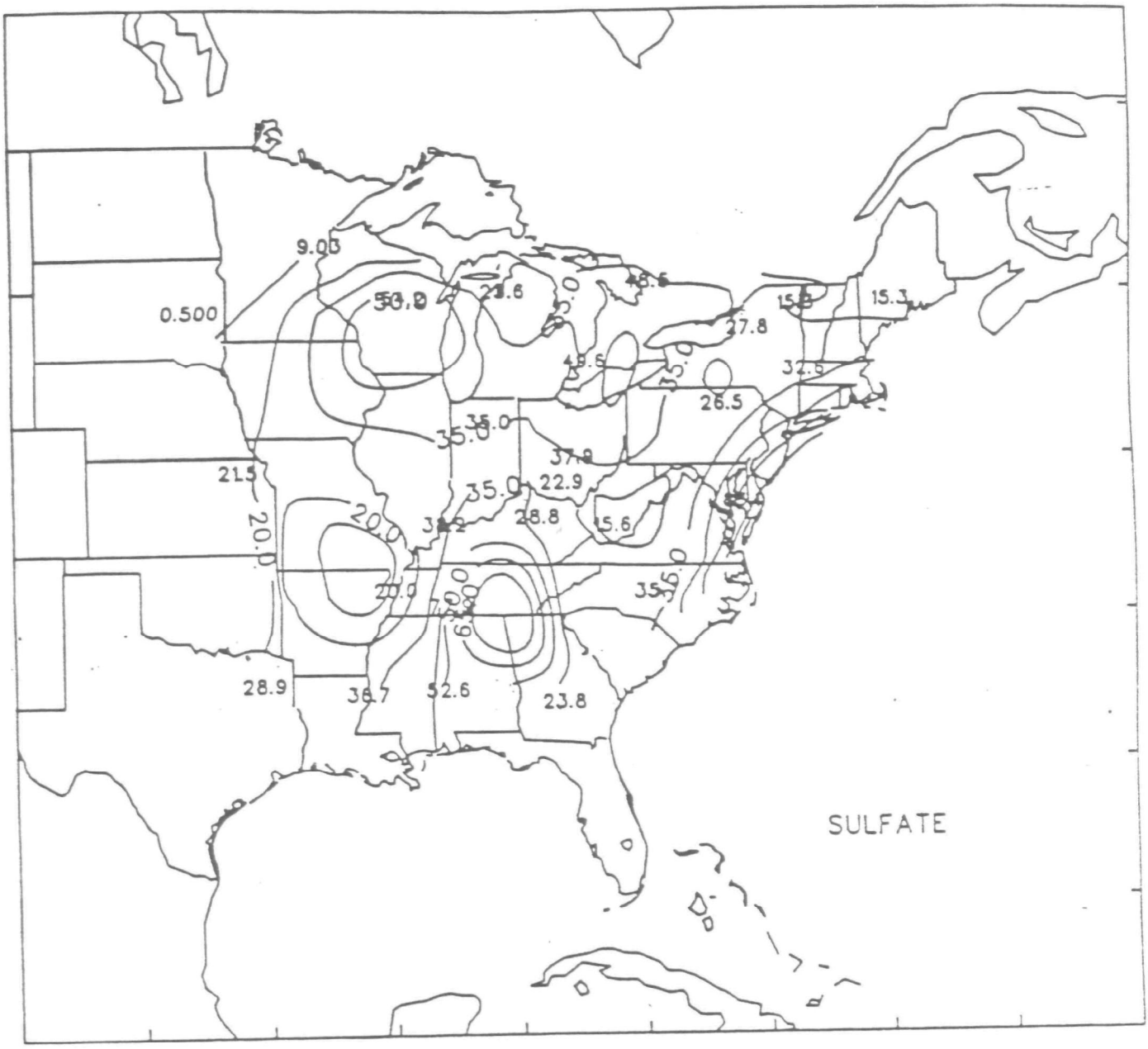

Figure B2 - 85th Percentile Three-day Total Deposition Pattern due to Cluster 2 Cases. The 85th percentile at each site was derived from the distribution of all available three-day total deposition cases within the cluster.

85th Percentile SO4= Deposition (STEP 19) - CLUSTER 3

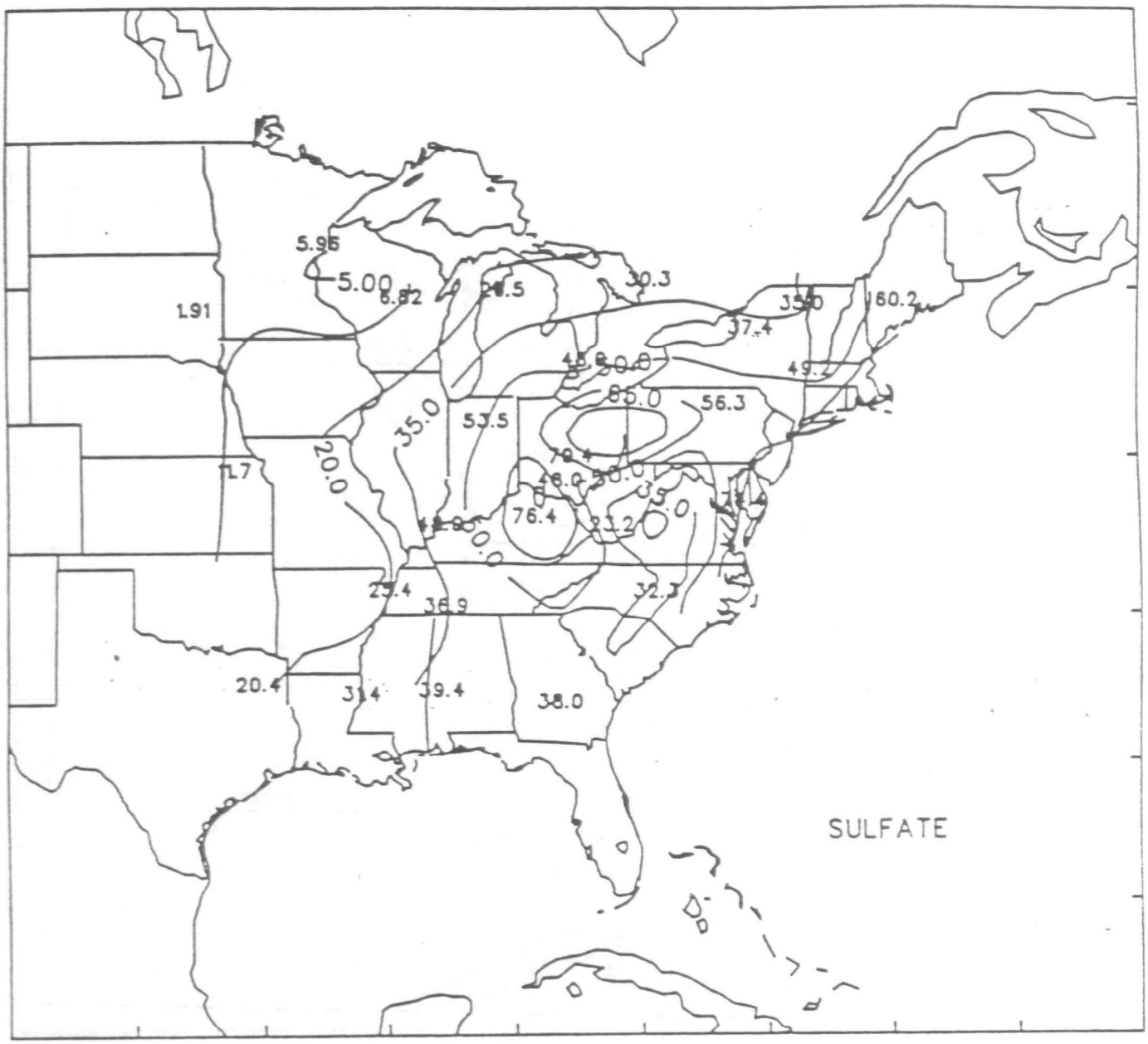

Figure B3 - 85th Percentile Three-day Total Deposition Pattern due to Cluster 3 Cases. The 85th percentile at each site was derived from the distribution of all available three-day total deposition cases within the cluster.

85th Percentile SO4= Deposition (STEP 19) - CLUSTER 4

Figure B4 - 85th Percentile Three-day Total Deposition Pattern due to Cluster 4 Cases. The 85th percentile at each site was derived from the distribution of all available three-day total deposition cases within the cluster.

85th Percentile SO4= Deposition (STEP 19) - CLUSTER 5

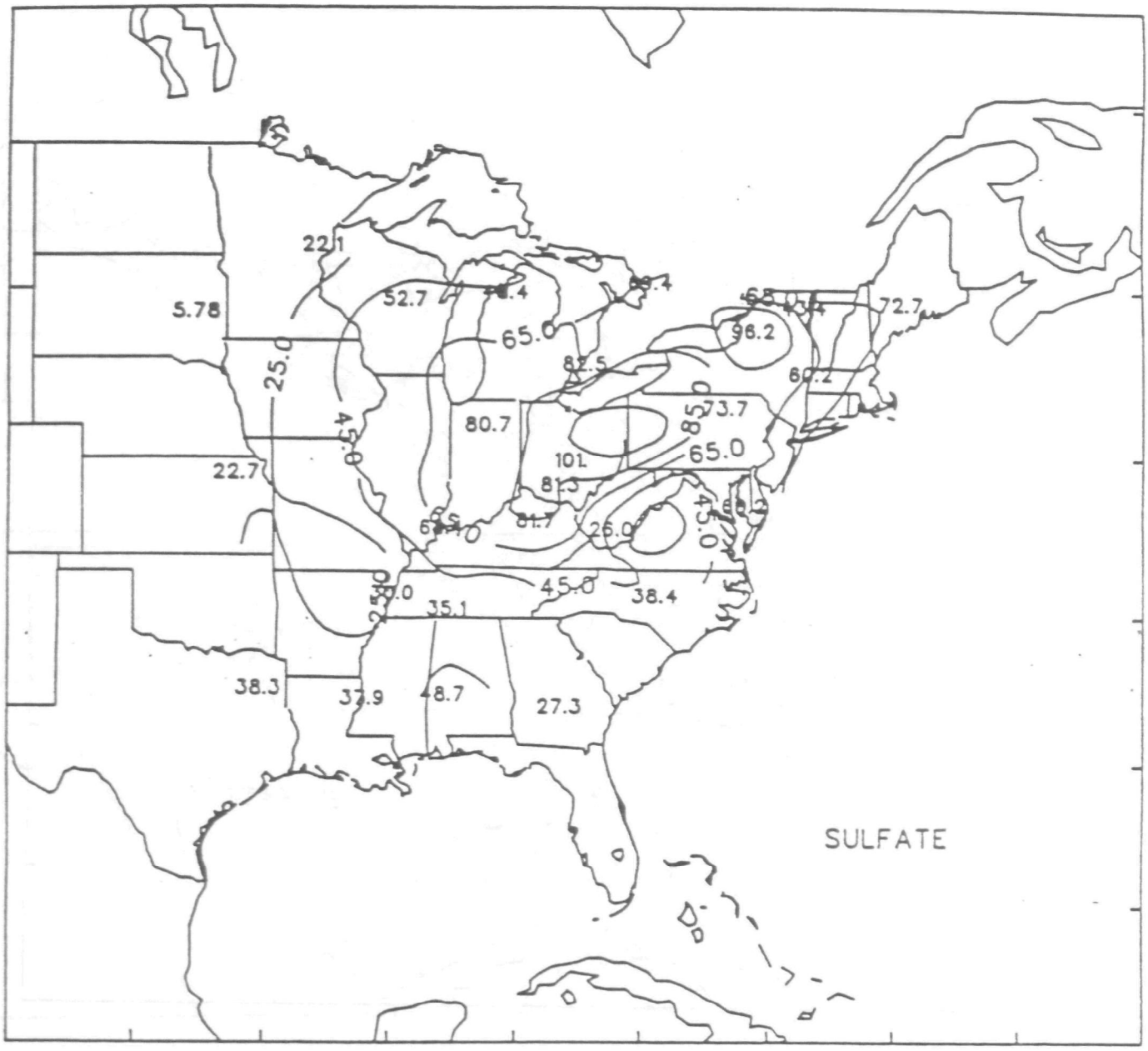

Figure B5 - 85th Percentile Three-day Total Deposition Pattern due to Cluster 5 Cases. The 85th percentile at each site was derived from the distribution of all available three-day total deposition cases within the cluster.

85th Percentile SO4= Deposition (STEP 19) - CLUSTER 6

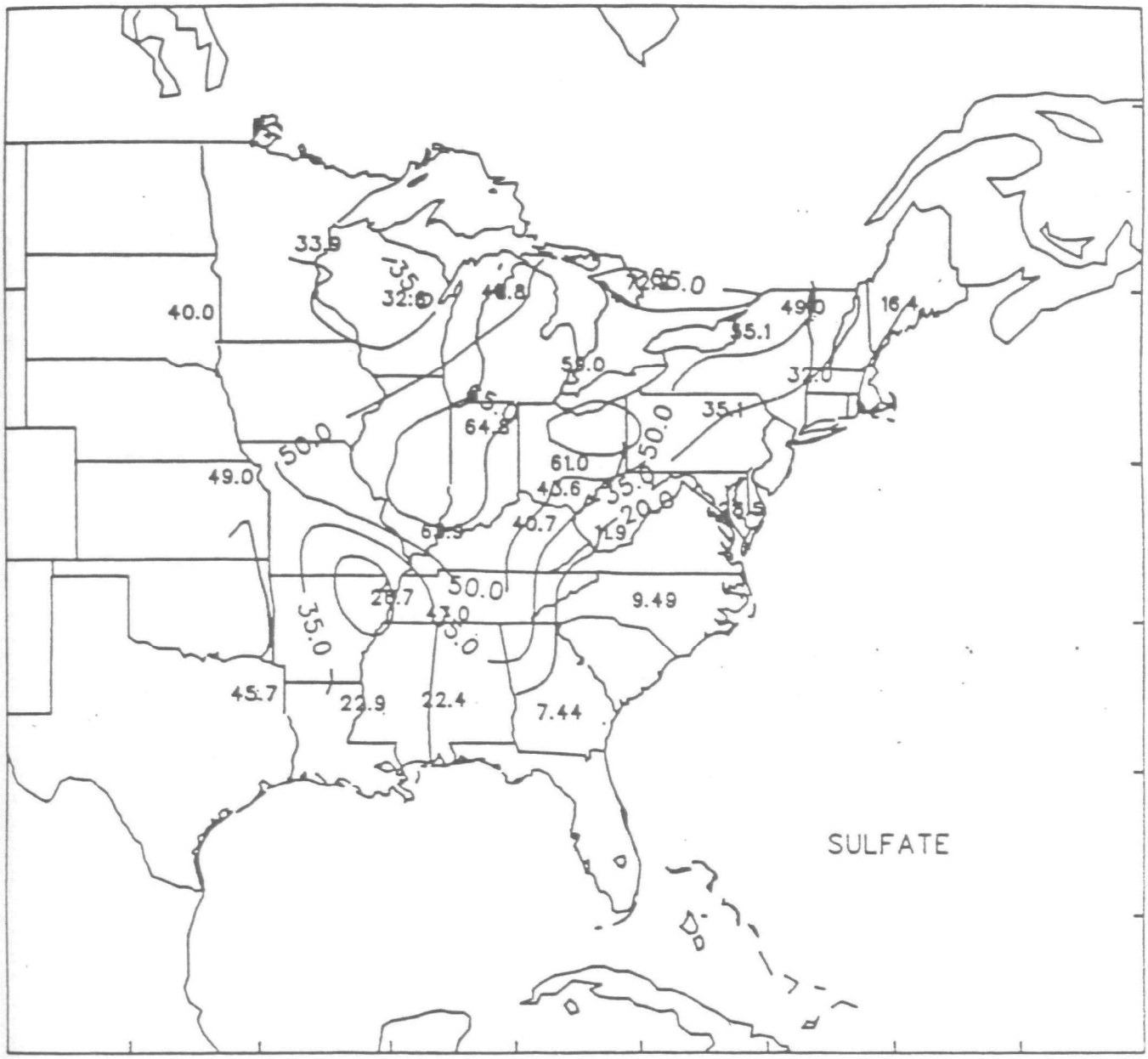

Figure B6 - 85th Percentile Three-day Total Deposition Pattern due to Cluster 6 Cases. The 85th percentile at each site was derived from the distribution of all available three-day total deposition cases within the cluster.

85th Percentile SO4= Deposition (STEP 19) - CLUSTER 7

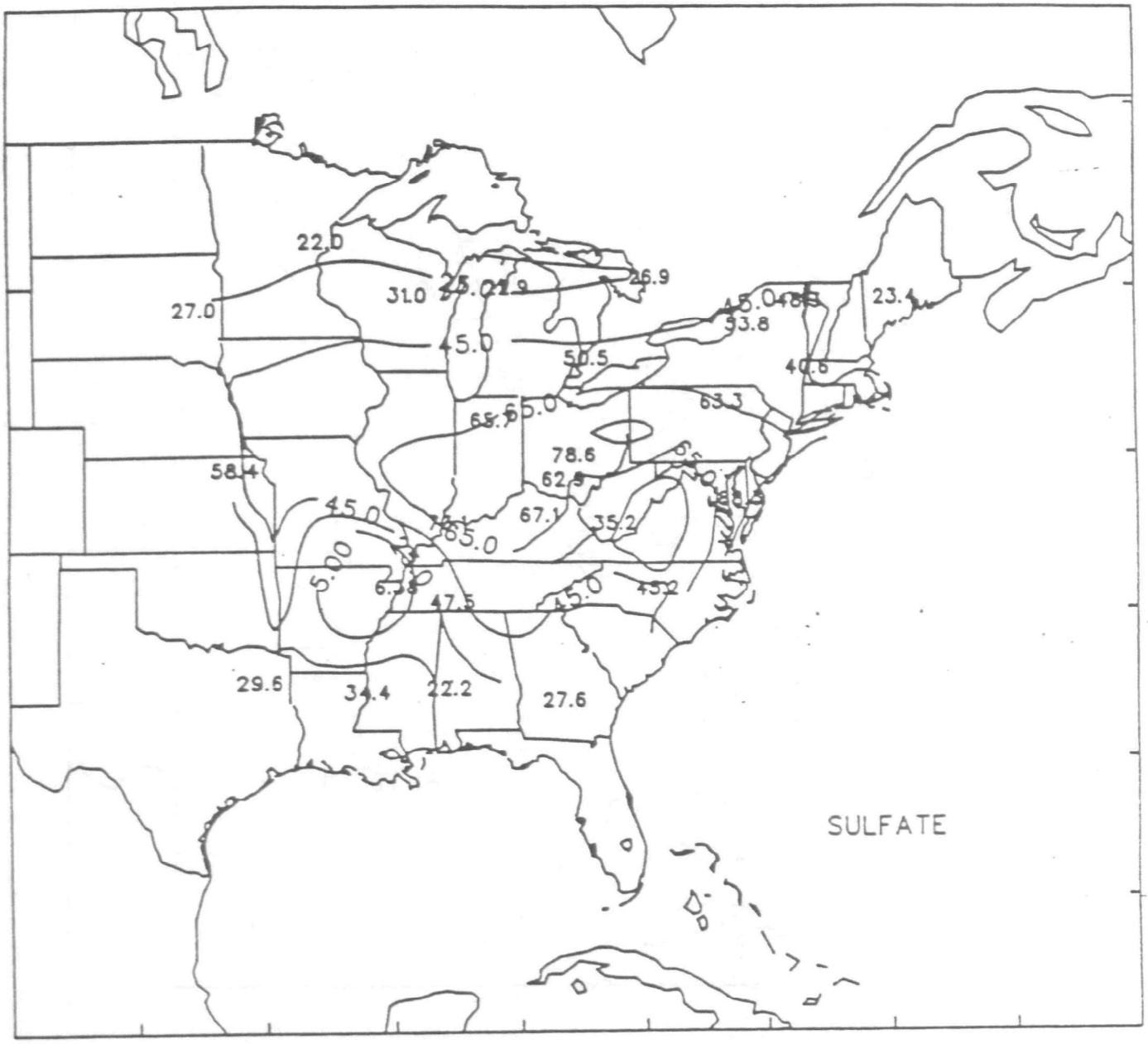

Figure B7 - 85th Percentile Three-day Total Deposition Pattern due to Cluster 7 Cases. The 85th percentile at each site was derived from the distribution of all available three-day total deposition cases within the cluster.

85th Percentile SO4= Deposition (STEP 19) - CLUSTER 8

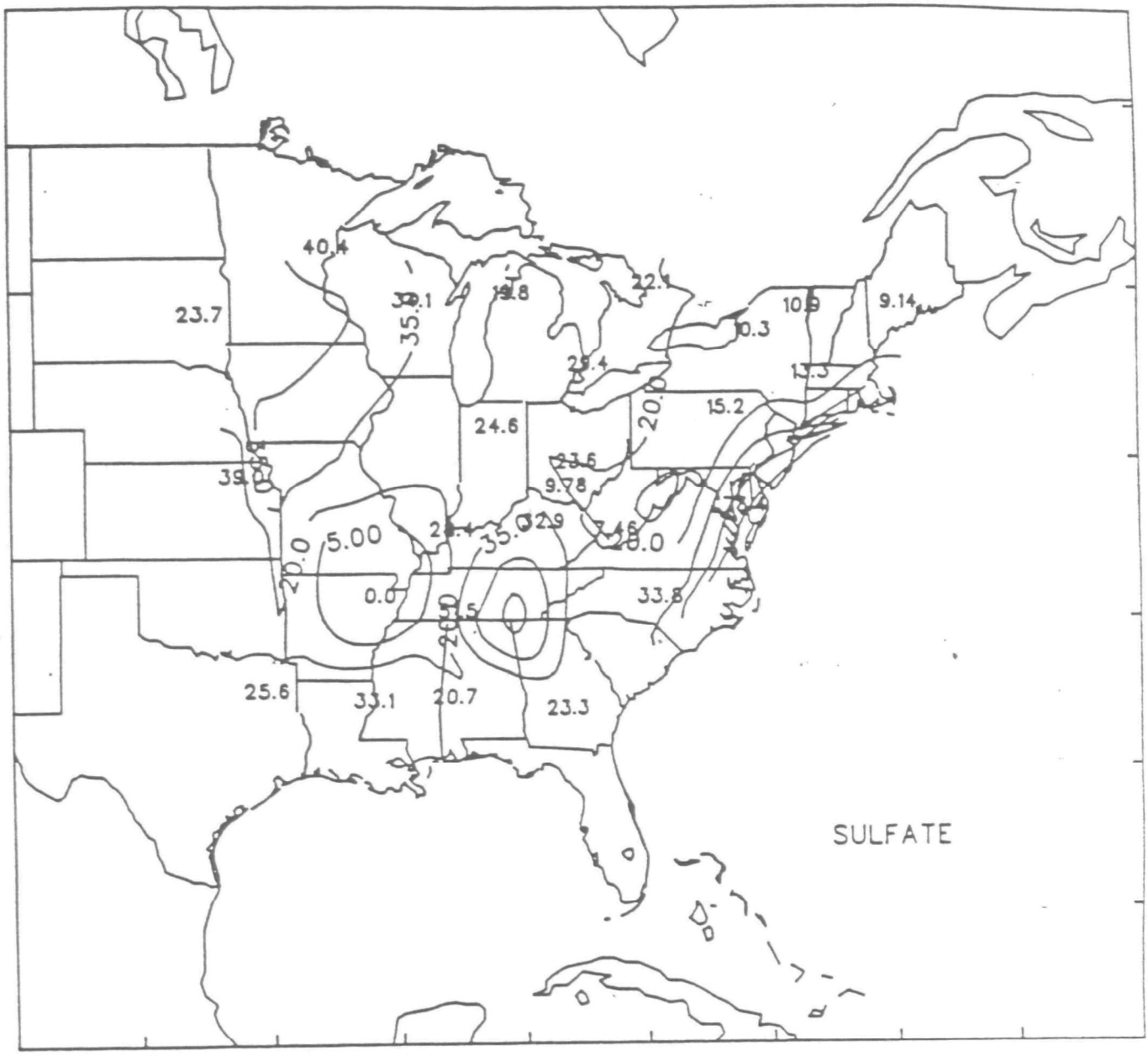

Figure B8 - 85th Percentile Three-day Total Deposition Pattern due to Cluster 8 Cases. The 85th percentile at each site was derived from the distribution of all available three-day total deposition cases within the cluster.

85th Percentile SO4= Deposition (STEP 19) - CLUSTER 9

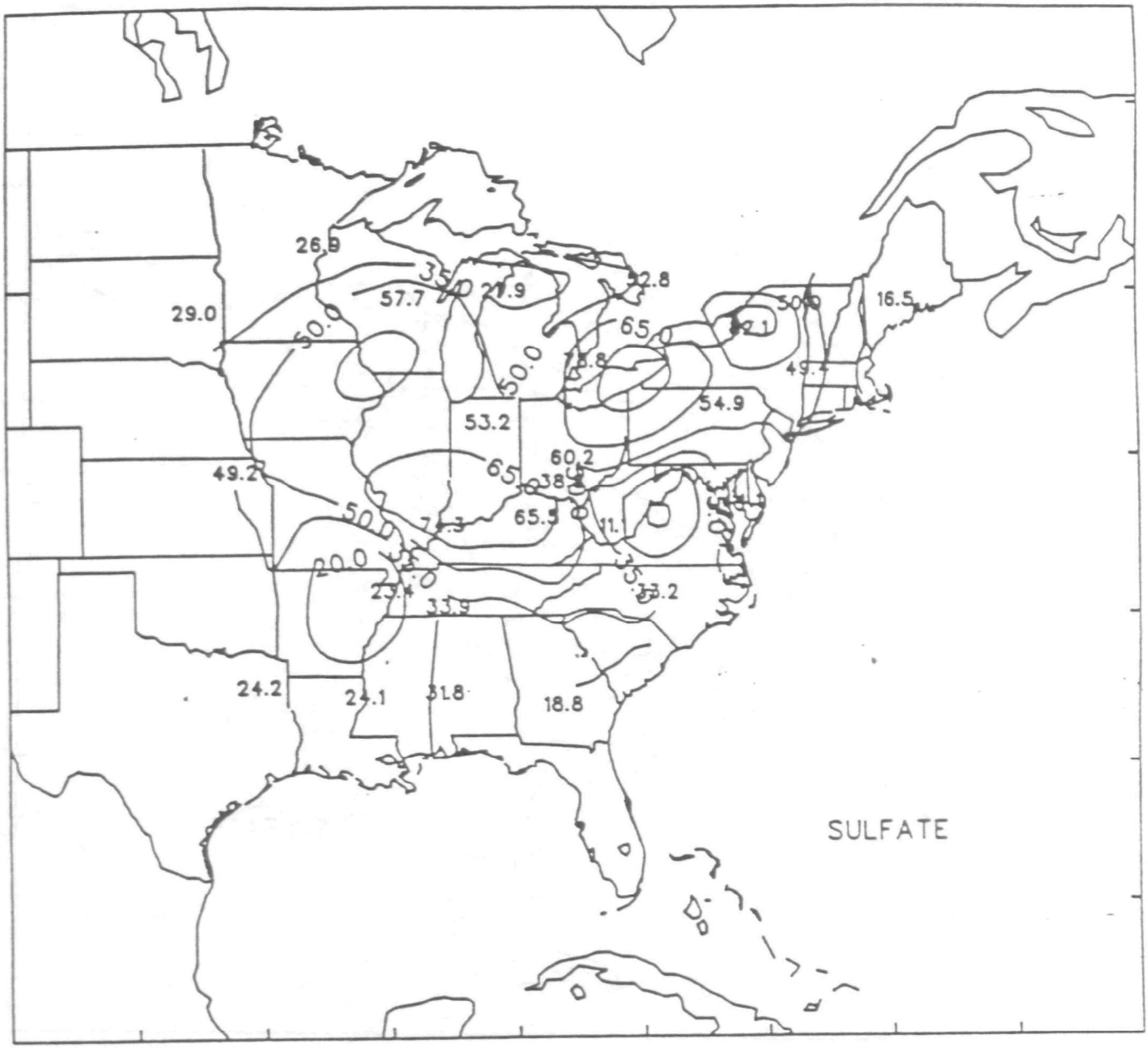

Figure B9 - 85th Percentile Three-day Total Deposition Pattern due to Cluster 9 Cases. The 85th percentile at each site was derived from the distribution of all available three-day total deposition cases within the cluster.

85th Percentile SO4= Deposition (STEP 19) - CLUSTER 10

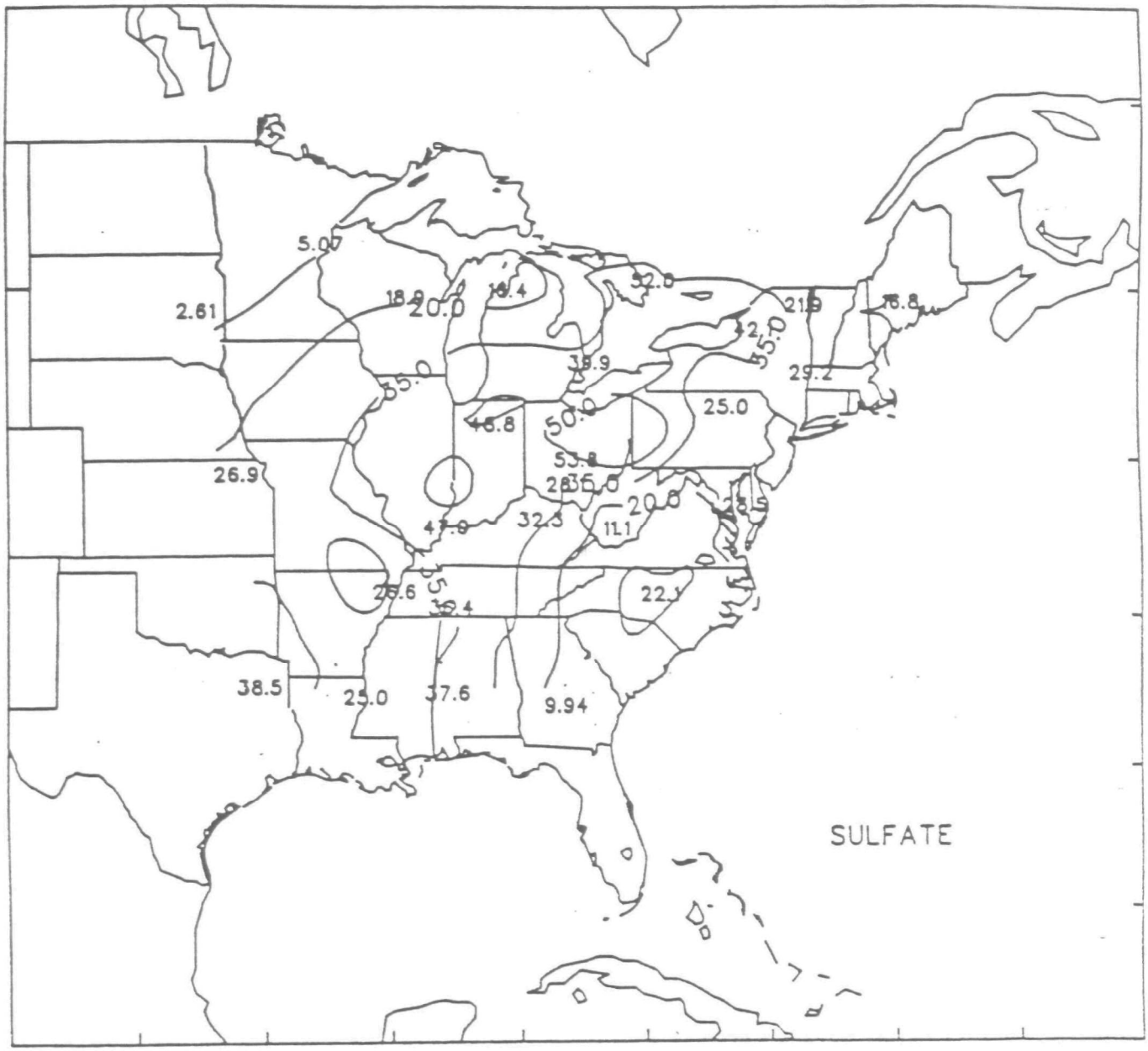

Figure B10 - 85th Percentile Three-day Total Deposition Pattern due to Cluster 10. The 85th percentile at each site was derived from the distribution of all available three-day total deposition cases within the cluster.

85th Percentile SO4= Deposition (STEP 19) - CLUSTER 11

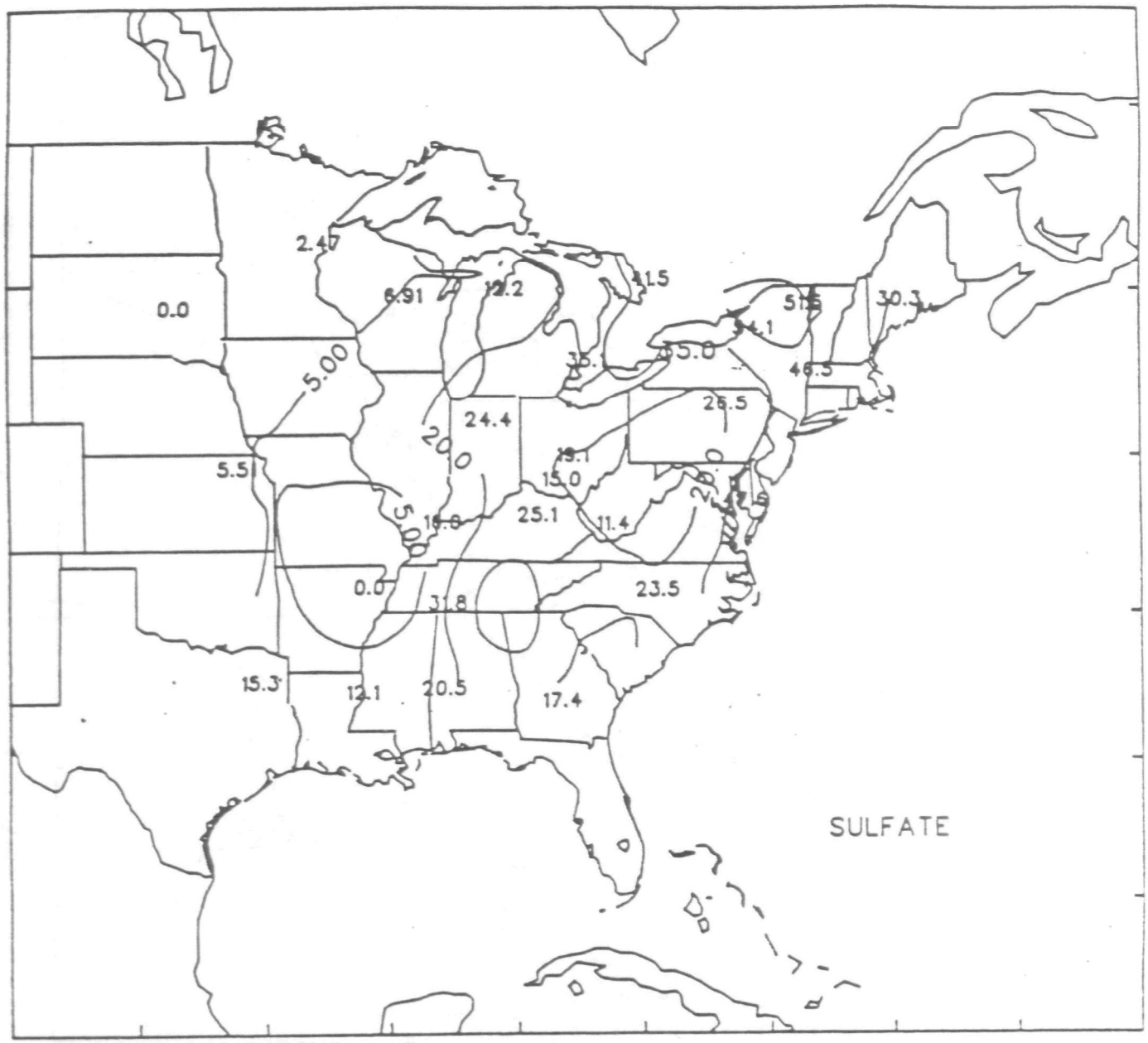

Figure B11 - 85th Percentile Three-day Total Deposition Pattern due to Cluster 11. The 85th percentile at each site was derived from the distribution of all available three-day total deposition cases within the cluster.

85th Percentile SO4= Deposition (STEP 19) - CLUSTER 12

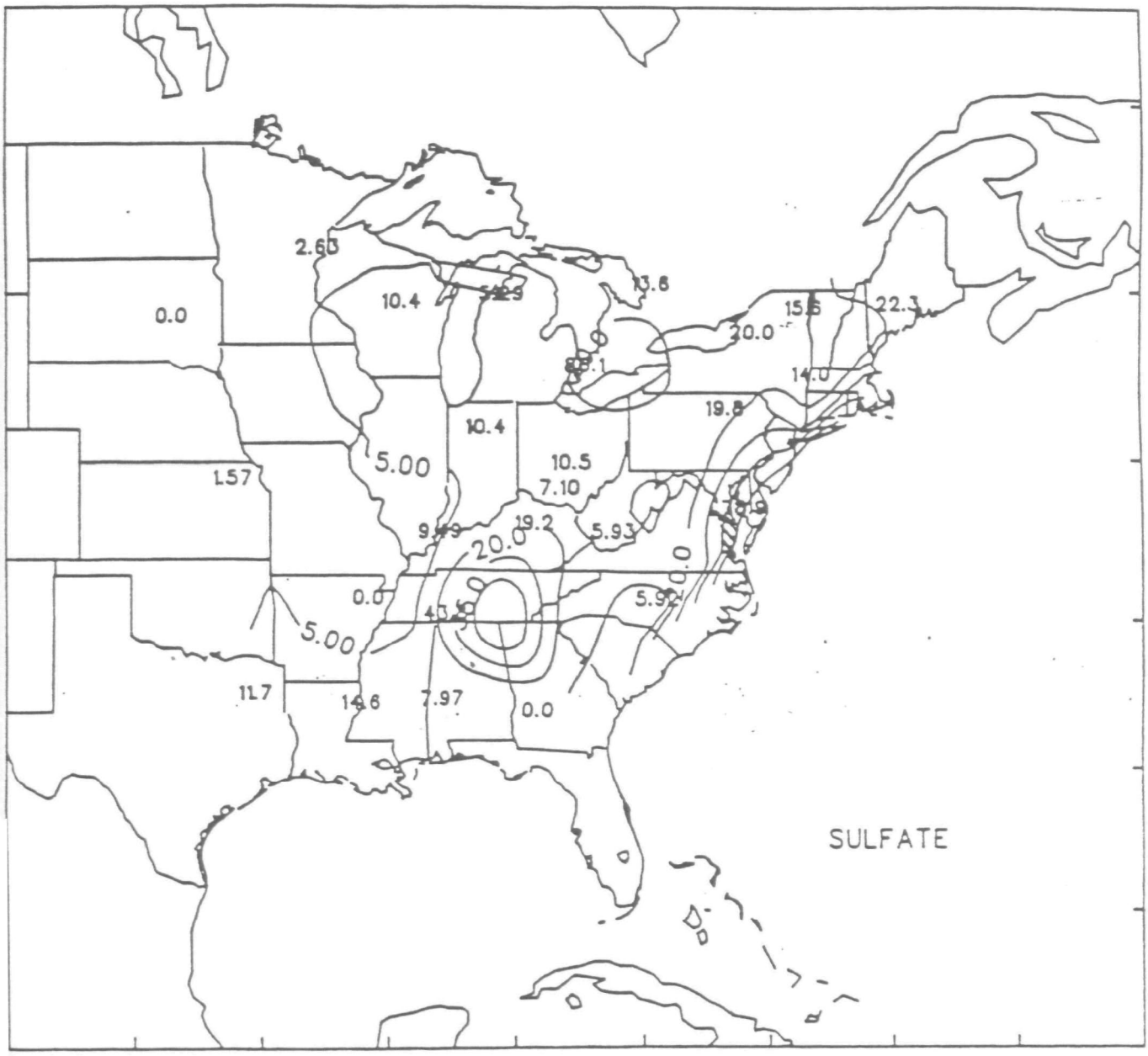

Figure B12 - 85th Percentile Three-day Total Deposition Pattern due to Cluster 12. The 85th percentile at each site was derived from the distribution of all available three-day total deposition cases within the cluster.

85th Percentile SO4= Deposition (STEP 19) - CLUSTER 13

Figure B13 - 85th Percentile Three-day Total Deposition Pattern due to Cluster 13. The 85th percentile at each site was derived from the distribution of all available three-day total deposition cases within the cluster.

85th Percentile SO4= Deposition (STEP 19) – CLUSTER 14

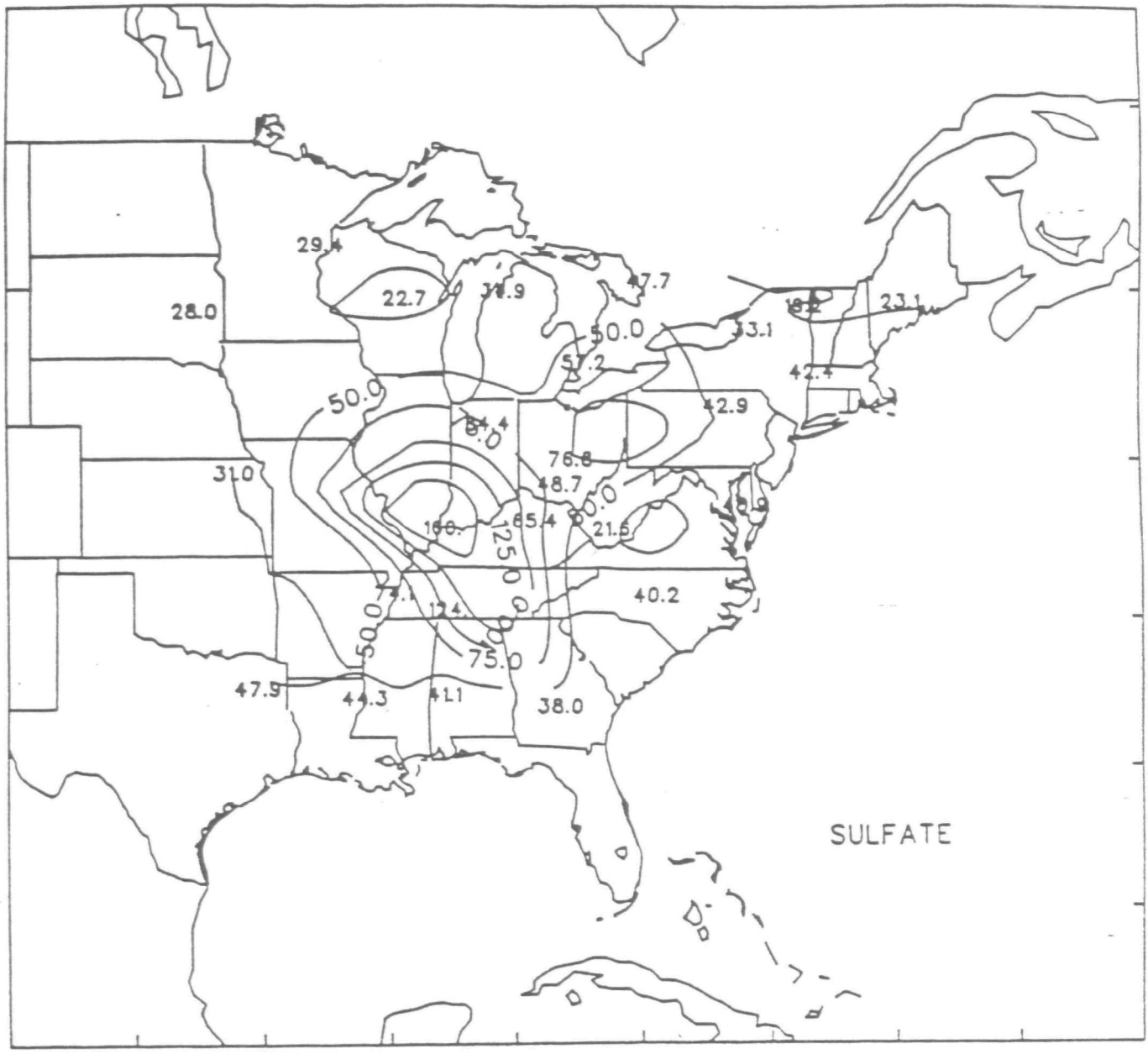

Figure B14 - 85th Percentile Three-day Total Deposition Pattern due to Cluster 14. The 85th percentile at each site was derived from the distribution of all available three-day total deposition cases within the cluster.

85th Percentile SO4= Deposition (STEP 19) - CLUSTER 15

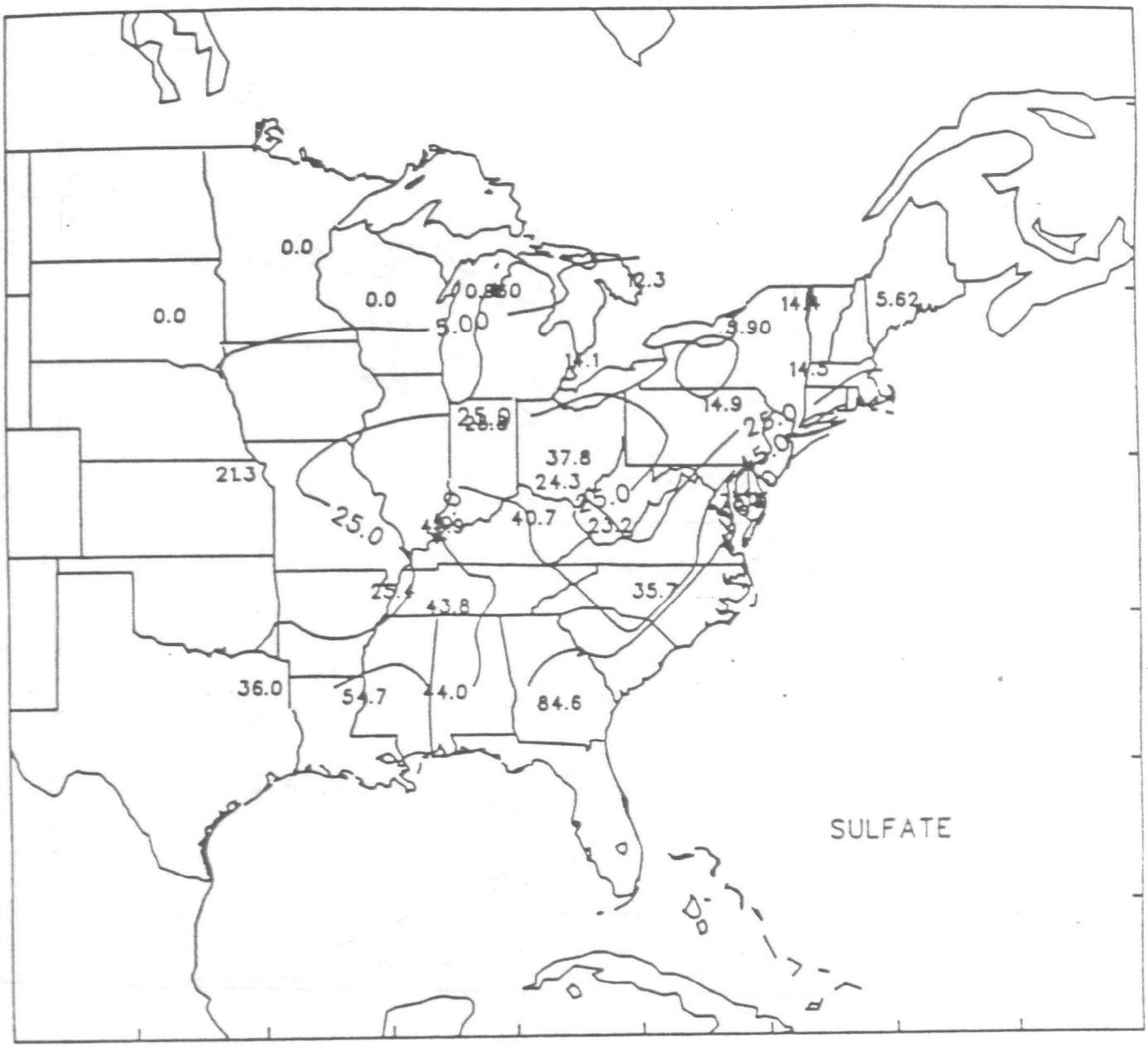

Figure B15 - 85th Percentile Three-day Total Deposition Pattern due to Cluster 15. The 85th percentile at each site was derived from the distribution of all available three-day total deposition cases within the cluster.

85th Percentile SO4= Deposition (STEP 19) - CLUSTER 16

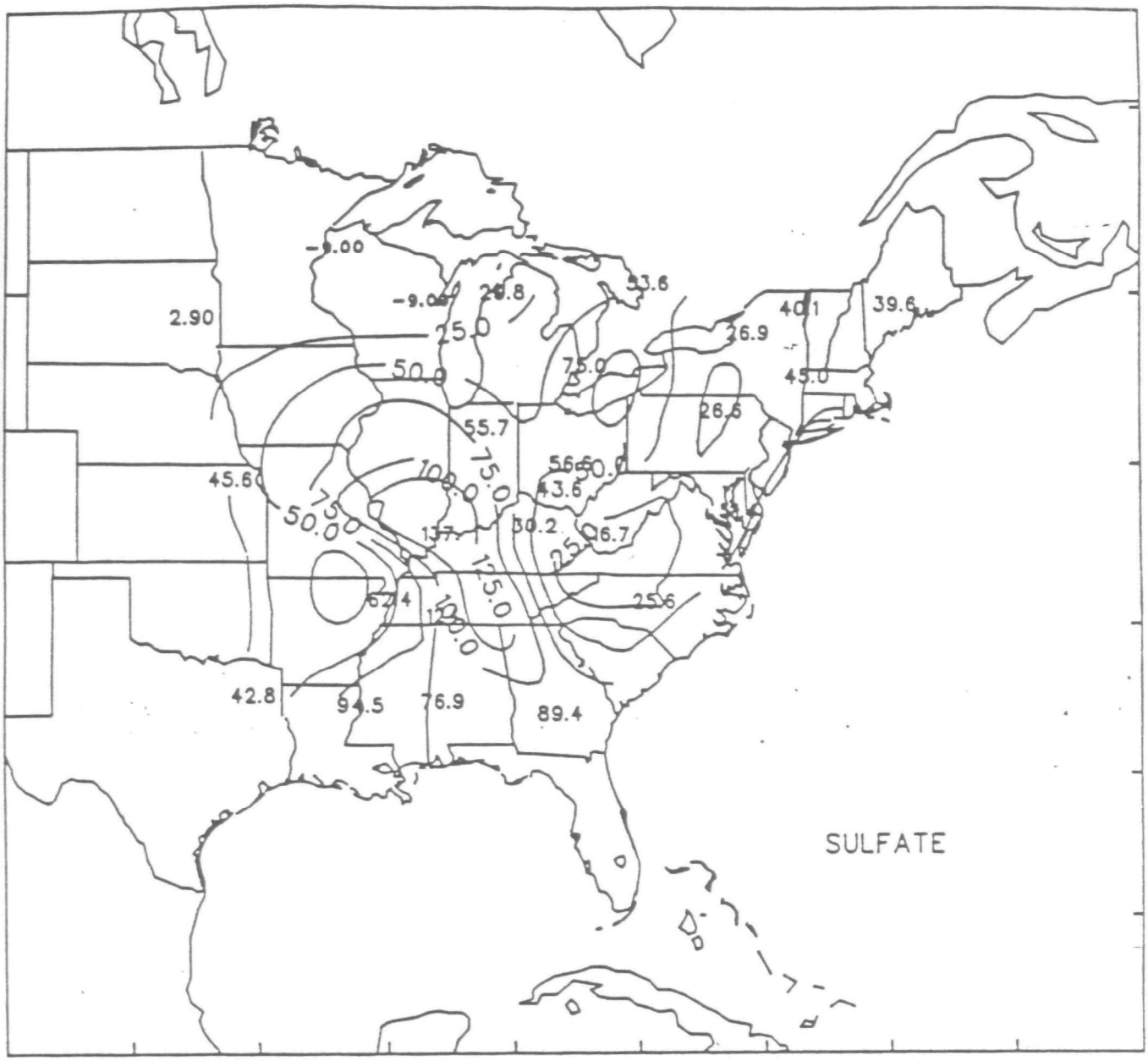

Figure B16 - 85th Percentile Three-day Total Deposition Pattern due to Cluster 16. The 85th percentile at each site was derived from the distribution of all available three-day total deposition cases within the cluster.

85th Percentile SO4= Deposition (STEP 19) – CLUSTER 17

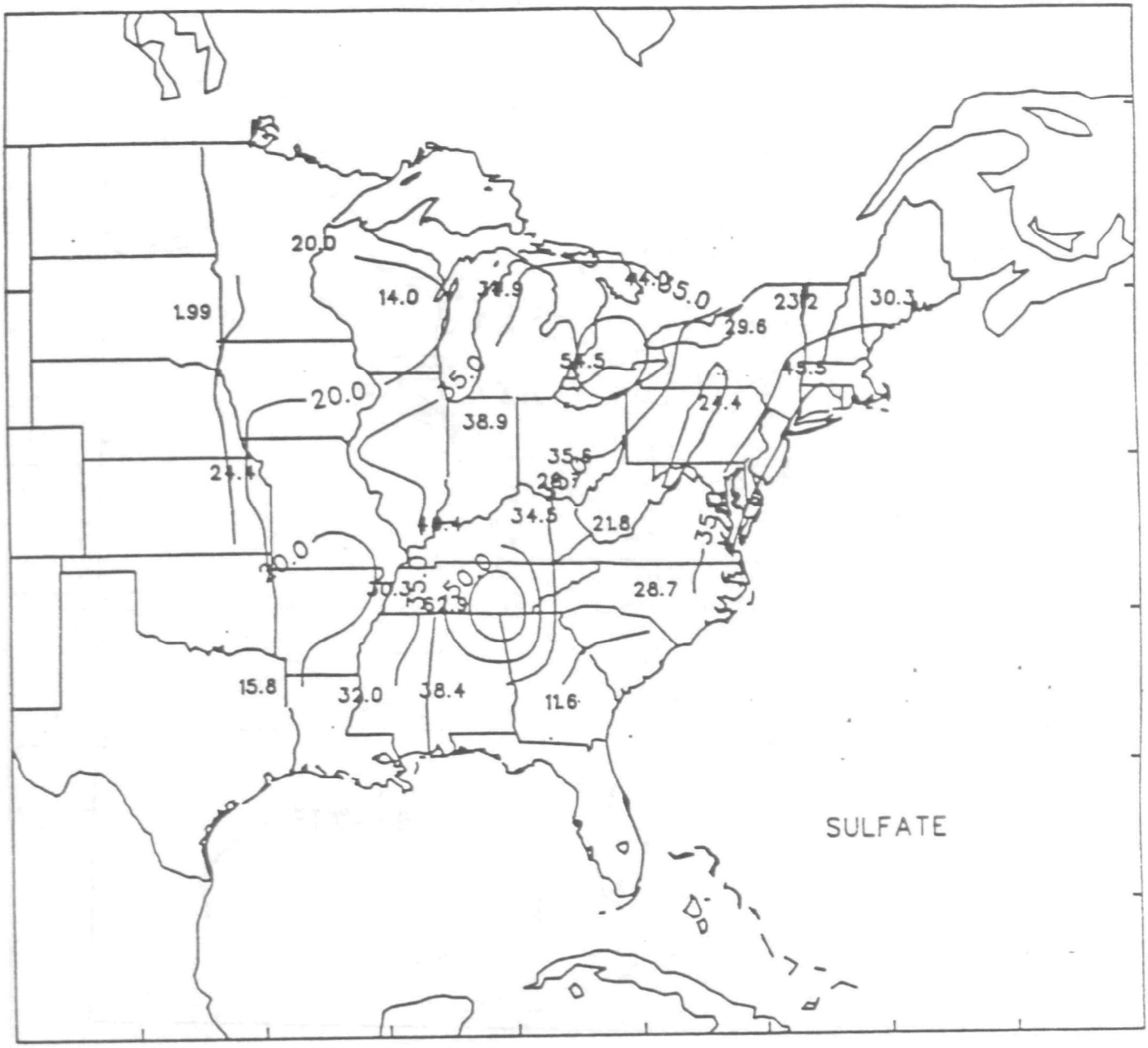

Figure B17 - 85th Percentile Three-day Total Deposition Pattern due to Cluster 17. The 85th percentile at each site was derived from the distribution of all available three-day total deposition cases within the cluster.

85th Percentile SO4= Deposition (STEP 19) - CLUSTER 18

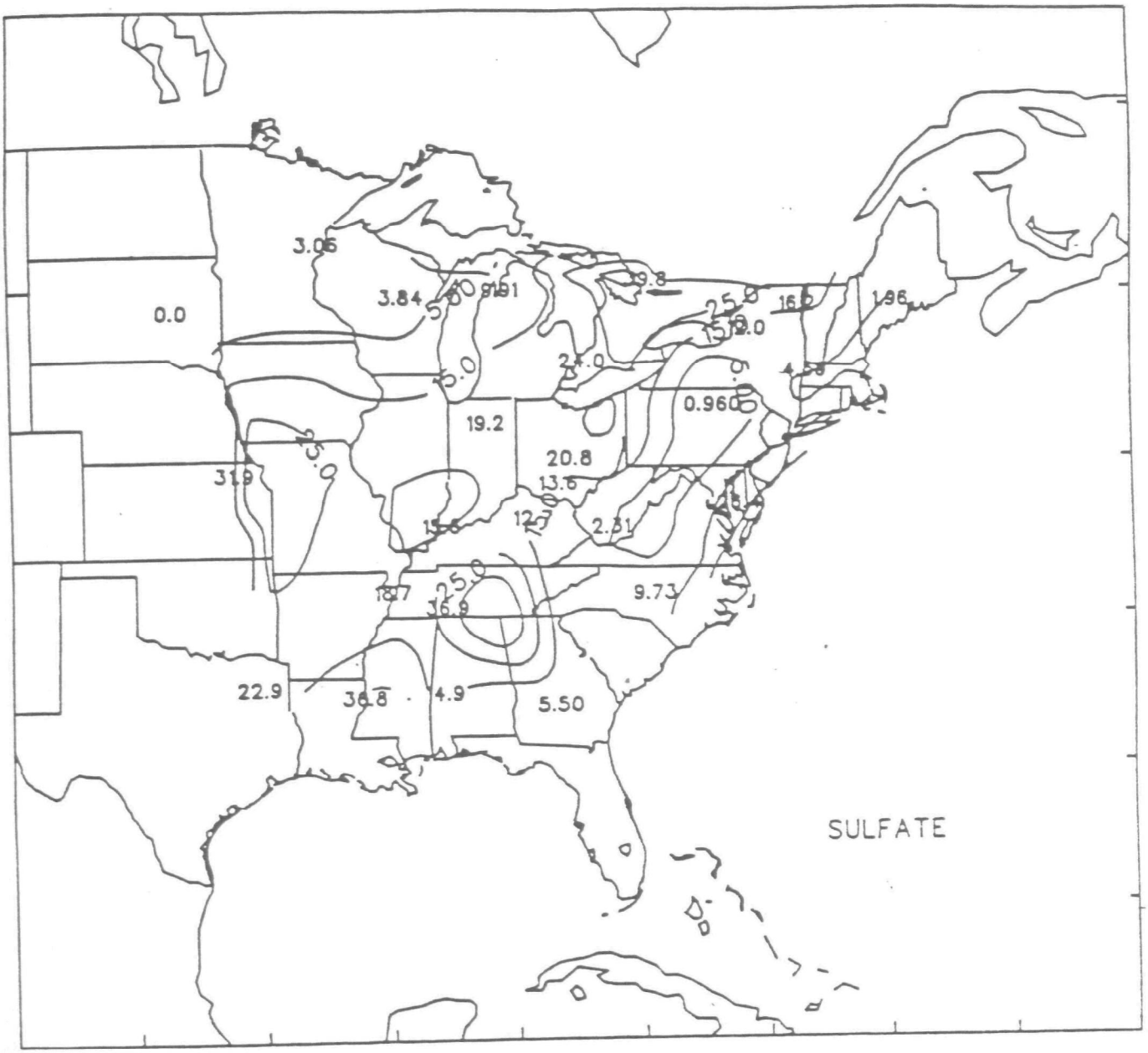

Figure B18 - 85th Percentile Three-day Total Deposition Pattern due to Cluster 18. The 85th percentile at each site was derived from the distribution of all available three-day total deposition cases within the cluster.

85th Percentile SO4= Deposition (STEP 19) - CLUSTER 19

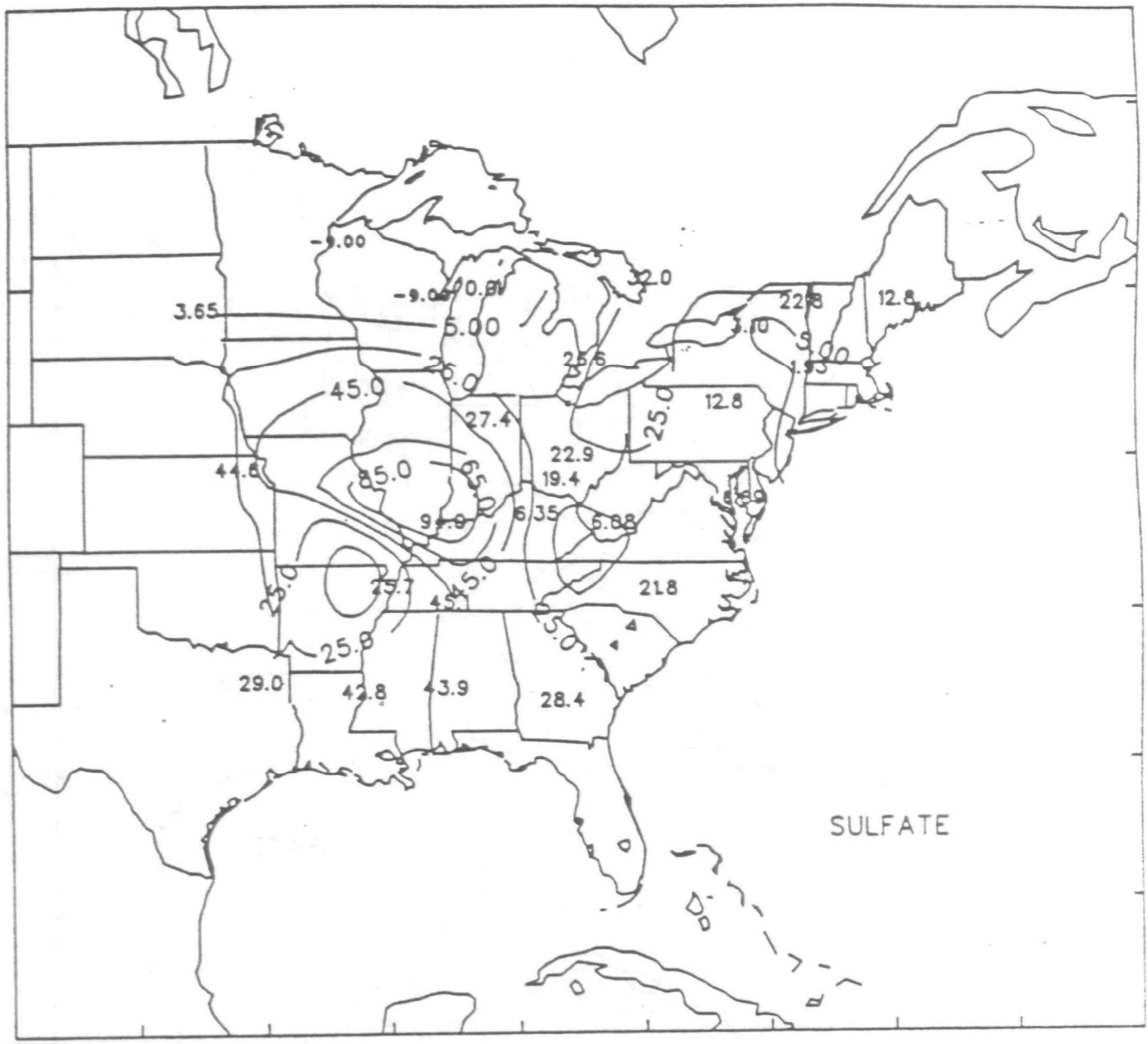

Figure B19 - 85th Percentile Three-day Total Deposition Pattern due to Cluster 19. The 85th percentile at each site was derived from the distribution of all available three-day total deposition cases within the cluster.

85th Percentile SO4= Deposition (STEP 19) - CLUSTER 20

Figure B20 - 85th Percentile Three-day Total Deposition Pattern due to Cluster 20. The 85th percentile at each site was derived from the distribution of all available three-day total deposition cases within the cluster.

APPENDIX C

Site Specific Tables of Total and Percent of Total Wet Sulfate Deposition

KEY

No. - Number of times cluster had precipitation
%ofDep - Percent of total deposition
Total - Total wet sulfate deposition (mgm^{-2})
AVG - Average deposition of wet events only (mgm^{-2})
Max - Maximum deposition value reported (mgm^{-2})
S.D. - Standard deviation of the wet events (mgm^{-2})

SITE	1					
CL	No.	%ofDep	TOTAL	AVG	MAX	S.D.
9	68	16.7	2612.81	38.424	230.09	45.458
11	90	16.13	2523.21	28.036	150.78	24.801
7	58	9.78	1529.61	26.373	192.73	35.594
6	53	9.63	1505.99	28.415	117.5	29.668
5	47	9.38	1467.35	31.22	150.78	27.58
8	45	8.4	1314.23	29.205	192.73	37.178
12	41	5.51	861.36	21.009	80.43	20.564
1	28	5.36	838.47	29.945	117.24	28.932
3	25	4.45	696.54	27.862	102.3	26.133
10	29	3.08	481.18	16.592	83.5	16.24
19	26	2.63	410.67	15.795	125.49	23.99
2	12	1.75	273.63	22.802	50.62	14.462
17	14	1.67	261.53	18.681	66.97	18.981
16	10	1.62	253.94	25.394	80.43	23.95
14	7	1.59	248.1	35.443	46.37	10.67
4	8	1.1	171.88	21.485	52.67	20.802
15	4	0.99	154.12	38.53	71.35	36.021
18	8	0.18	28.34	3.543	8.82	2.692
13	4	0.07	10.87	2.717	4.76	1.838
20	150	0	7160.86	47.739	230.09	44.174

SITE	2					
CL	No.	%ofDep	TOTAL	AVG	MAX	S.D.
7	58	20.66	3460.22	59.659	328.08	73.296
9	55	16.76	2807.97	51.054	328.08	66.853
11	67	12.43	2082.47	31.082	146.87	33.437
5	40	10.06	1685.34	42.133	143.16	37.464
8	35	9.42	1578.31	45.095	327.9	62.082
6	53	8.42	1410.03	26.604	140.77	26.044
12	23	4.43	741.24	32.228	145.56	33.533
1	19	4.38	734.31	38.648	124.61	28.209
3	24	3.43	574.71	23.946	81.33	19.565
10	24	2.55	426.5	17.771	65.91	14.666
4	12	1.45	243.19	20.266	47.28	14.797
14	12	1.39	232.36	19.363	74.05	21.394
17	12	1.18	197.68	16.473	46.18	14.973
16	6	1.08	181.06	30.177	68.69	21.668
2	12	0.91	153.12	12.76	37.61	10.356
18	13	0.55	92.29	7.099	39.51	12.576
15	9	0.53	89.26	9.918	29.68	11.151
19	12	0.35	58.67	4.889	14.4	5.047
13	1	0	0.5	0.5	0.5	0
20	160	0	6288.38	39.302	204.37	38.606

SITE	4					
CL	No.	%ofDep	TOTAL	AVG	MAX	S.D.
6	75	15.9	3451.02	46.014	180.65	50.758
7	61	14.15	3071.06	50.345	164.53	35.461
9	68	13.91	3018.09	44.384	402.37	63.322
5	60	11.7	2538.01	42.3	170.36	40.517
11	78	9.44	2049.42	26.275	152.91	29.947
8	29	7.51	1629.42	56.187	448.26	92.825
1	32	4.51	978.58	30.581	123.21	32.238
3	23	4.47	969.31	42.144	143.25	38.152
10	41	4.11	892.98	21.78	173.74	35.657
4	11	2.77	601.1	54.645	204.13	75.285
14	16	2.49	541.44	33.84	108.21	29.263
12	29	1.93	417.97	14.413	50.52	13.329
2	23	1.91	414.33	18.014	53.99	13.387
17	18	1.62	351.88	19.549	68.09	16.237
19	8	1.25	271.91	33.989	87.3	28.051
16	8	0.66	144.18	18.023	58.71	18.838
18	14	0.62	135.39	9.671	51.49	14.986
13	9	0.53	113.97	12.663	43.51	13.57
15	8	0.51	111.29	13.911	56.64	18.098
20	193	0	7266.73	37.651	230.92	39.294

SITE	5					
CL	No.	%ofDep	TOTAL	AVG	MAX	S.D.
6	79	15.36	3695.48	46.778	190.27	45.879
7	57	13.25	3187.9	55.928	333.5	58.679
9	58	11.88	2858.47	49.284	170.22	35.692
5	50	11.26	2710.61	54.212	333.5	57.408
11	56	6.91	1663.57	29.707	134.91	30.691
10	36	6.59	1584.97	44.027	233.66	54.861
14	16	5.76	1385.26	86.579	233.66	72.276
1	25	5.59	1346.05	53.842	169.1	51.079
2	27	3.85	927.13	34.338	103.4	32.208
8	29	3.72	895.62	30.883	79.03	26.83
3	18	3.35	805.53	44.752	233.66	53.201
19	13	2.76	663.97	51.075	137.41	42.757
17	15	2.32	559.47	37.298	164.68	39.479
4	14	2.15	518.18	37.013	103.3	32.082
16	9	1.86	447.4	49.711	175.01	50.53
15	10	1.4	337.53	33.753	92.98	29.485
12	14	1.03	248.24	17.731	38.87	12.266
13	5	0.61	146.07	29.214	64.08	29.275
18	10	0.35	84	8.4	17.09	6.463
20	161	0	9042.69	56.166	280.62	55.165

SITE	7					
CL	No.	%ofDep	TOTAL	AVG	MAX	S.D.
6	71	18.06	3466.08	48.818	234.88	47.94
7	57	16.97	3256.63	57.134	186.23	51.377
9	61	12.74	2445.27	40.086	160.3	38.462
5	43	9.18	1761.87	40.974	226.18	46.933
11	48	8.26	1584.62	33.013	128.68	34.104
1	28	7.24	1389.6	49.629	160.55	50.764
10	33	4.97	953.38	28.89	135.39	30.708
8	20	4.09	784.8	39.24	172.58	44.462
14	15	3.43	658.39	43.893	125.11	30.774
3	17	3.34	640.67	37.686	128.68	31.792
17	17	2.91	557.85	32.815	124.29	32.953
4	11	1.58	302.99	27.545	84.28	22.565
12	15	1.53	293.78	19.585	40.84	12.401
2	13	1.43	273.72	21.055	56.61	14.023
16	7	1.36	261	37.286	105.01	35.182
18	8	1.02	196.31	24.539	91.2	28.441
19	4	0.85	163.77	40.943	91.2	34.082
15	5	0.83	160.2	32.04	86.54	32.164
13	4	0.21	40.45	10.113	19.6	7.256
20	152	0	6801.45	44.746	353.82	52.32

SITE	8					
CL	No.	%ofDep	TOTAL	AVG	MAX	S.D.
11	75	16.51	2037.28	27.164	124.37	26.377
9	66	13.11	1618.52	24.523	101.64	24.459
8	39	11.1	1369.53	35.116	105.13	27.159
7	30	10.95	1351.92	45.064	330.62	59.368
5	31	9.22	1138.2	36.716	123.42	29.691
3	22	6.25	771.6	35.073	112.16	29.844
2	25	4.73	584.13	23.365	112.16	28.098
19	16	3.74	461.26	28.829	62.02	20.264
12	19	3.59	443.45	23.339	75.76	21.268
1	23	3.5	432.04	18.784	63.92	15.175
10	20	3.03	373.63	18.682	45.93	13.447
17	16	2.95	364.34	22.771	61.99	16.072
4	11	2.85	352.28	32.025	103.14	37.131
14	10	2.49	307.79	30.779	75.56	22.365
6	20	2.15	264.98	13.249	73.78	18.247
15	9	1.4	172.63	19.181	35.14	12.736
18	6	1.39	171.63	28.605	136.16	52.909
13	6	0.77	95.06	15.843	54.55	19.654
16	5	0.27	32.76	6.552	15	4.992
20	143	0	4870.14	34.057	330.62	44.688

SITE	10					
CL	No.	%ofDep	TOTAL	AVG	MAX	S.D.
6	93	23.97	2674.48	28.758	202.95	31.137
5	46	15.87	1770.82	38.496	215.16	39.804
9	65	14.7	1640.54	25.239	117.38	21.807
7	48	10.38	1158.78	24.141	96.74	23.902
11	66	8.82	983.93	14.908	151.13	24.766
3	18	4.25	474.72	26.373	65.66	21.203
10	31	3.78	421.28	13.59	48.57	14.06
1	25	3.65	407.08	16.283	75.59	18.354
2	18	2.67	297.98	16.554	99.25	24.162
8	16	2.55	284.06	17.754	64.03	18.385
14	12	2.21	246.12	20.51	58.59	17.665
17	19	1.98	220.8	11.621	44.05	11.439
19	11	1.88	209.94	19.085	31.49	8.189
4	7	1.09	121.72	17.389	70.31	24.737
12	9	0.94	104.67	11.63	47.83	13.886
16	4	0.7	78.44	19.61	46.9	21.357
18	6	0.39	44.07	7.345	31.49	12.028
13	2	0.11	12.56	6.28	6.28	0
15	2	0.06	7.24	3.62	6.28	3.762
20	161	0	3949.21	24.529	105.14	24.977

SITE	11					
CL	No.	%ofDep	TOTAL	AVG	MAX	S.D.
9	73	17.89	3886.21	53.236	362.37	75.088
11	91	13.94	3028.78	33.283	359.07	50.239
7	57	13.61	2957.89	51.893	289.71	71.324
5	50	10.21	2219.3	44.386	279.55	46.443
8	41	8.83	1918.94	46.803	236.63	56.984
6	75	7.36	1598.49	21.313	93.49	18.214
10	50	5.09	1105.56	22.111	93.49	21.848
3	24	4.01	870.54	36.273	90.24	30.889
12	30	3.37	732.01	24.4	93.54	24.753
1	29	3.28	712.52	24.57	76.11	19.603
17	21	2.66	578.51	27.548	82.38	21.964
14	15	1.63	354.81	23.654	78.63	19.039
4	15	1.42	307.72	20.515	54.35	14.127
15	14	1.41	306.08	21.863	75.48	20.465
18	13	1.25	272.34	20.949	164.14	43.535
19	13	1.25	271.42	20.878	73.09	23.808
2	22	1.22	265.21	12.055	40.05	10.796
16	8	1	218.25	27.281	97.6	30.673
13	8	0.57	123.28	15.41	49.06	15.586
20	198	0	9651.78	48.746	313.13	55.283

SITE	12					
CL	No.	%ofDep	TOTAL	AVG	MAX	S.D.
9	36	19.65	1912.42	53.123	214.56	58.198
6	51	16.24	1581.01	31	214.56	42.681
5	22	9.84	957.66	43.53	227.57	61.717
11	32	9.46	920.71	28.772	73.69	21.99
1	26	8.17	795.02	30.578	84.84	20.35
10	25	6.09	592.33	23.693	84.84	19.899
3	15	5.01	487.85	32.523	75.55	23.784
16	8	3.94	383.85	47.981	93.06	30.95
14	11	3.64	353.87	32.17	74.14	21.456
2	13	3.47	337.6	25.969	74.14	19.253
7	12	2.95	287.46	23.955	64.49	21.179
17	8	2.67	259.54	32.443	75.55	22.86
8	11	2.2	214.54	19.504	33.13	11.063
4	10	1.95	189.99	18.999	44.03	12.719
15	6	1.27	123.5	20.583	40.1	10.577
12	5	1.19	116.29	23.258	46.81	13.994
19	4	1.09	105.76	26.44	30.25	2.62
13	4	0.75	73.45	18.363	28.6	7.363
18	3	0.41	39.87	13.29	18.67	5.845
20	112	0	2898.22	25.877	206.37	25.283

SITE	13					
CL	No.	%ofDep	TOTAL	AVG	MAX	S.D.
11	89	19.04	1917.71	21.547	107.33	21.749
6	56	12.14	1222.67	21.833	112.77	32.428
5	41	11.26	1133.82	27.654	104.32	29.015
9	56	9.6	966.99	17.268	94.55	21.437
7	52	8.41	847.03	16.289	122.59	20.237
8	46	7.36	740.93	16.107	65.45	15.538
12	37	7.19	723.62	19.557	80.42	18.167
1	30	5.87	590.96	19.699	127.76	24.29
19	25	3.92	394.69	15.788	38.82	11.868
10	39	3.62	364.35	9.342	47.87	10.592
3	17	2.95	297.27	17.486	54.33	13.803
16	10	2.62	263.89	26.389	85.68	24.807
17	16	2.13	214.96	13.435	50.05	14.212
15	2	1.03	103.33	51.665	67.85	22.889
2	10	0.88	88.78	8.878	29.01	7.996
4	11	0.77	77.51	7.046	16.35	5.668
18	12	0.61	61.07	5.089	17.7	6.087
14	5	0.51	51.12	10.224	24.77	10.329
13	2	0.09	9.37	4.685	8.9	5.961
20	159	0	3853.9	24.238	112.46	25.997

SITE	14					
CL	No.	%ofDep	TOTAL	AVG	MAX	S.D.
7	49	15.59	1598.28	32.618	382.37	66.725
8	46	13.99	1434.15	31.177	382.37	56.898
9	57	13.09	1342.66	23.555	401.1	52.593
11	71	11.32	1160.97	16.352	161.9	21.579
3	20	5.42	555.53	27.776	161.9	39.317
6	29	5.1	523.48	18.051	93.55	23.803
1	28	5.06	518.41	18.515	161.9	29.578
19	10	4.71	482.62	48.262	117.5	43.327
5	26	4.58	469.58	18.061	60.93	16.052
2	27	4.12	422.42	15.645	50.64	11.834
15	11	3.44	352.46	32.042	76.61	26.095
13	6	2.86	293.4	48.9	94.1	34.743
17	18	2.63	269.72	14.984	40.49	11.928
14	10	2.16	221.58	22.158	38.68	14.754
12	14	2.14	219.61	15.686	66.54	15.969
10	15	1.89	194.26	12.951	50.04	14.347
4	9	1.15	118.1	13.122	28.88	8.866
16	5	0.56	57.42	11.484	25.72	9.526
18	4	0.19	19.9	4.975	7.97	2.451
20	145	0	3632.68	25.053	192.41	35.95

SITE	15					
CL	No.	%ofDep	TOTAL	AVG	MAX	S.D.
9	55	15.53	2178.93	39.617	195.3	44.448
11	71	15.19	2131.73	30.024	97.09	24.506
5	39	8.45	1185.32	30.393	104	21.955
8	41	7.05	989.22	24.127	191.73	32.844
6	48	6.93	972.52	20.261	113.1	21.555
7	45	6.34	889.8	19.773	138.24	28.245
1	27	6.09	854.55	31.65	97.09	21.717
2	30	5.69	798.5	26.617	66.67	17.771
3	19	4.93	691.84	36.413	97.09	26.502
10	29	4.45	624.59	21.538	51.98	17.231
17	17	3.74	525.45	30.909	77.28	20.933
4	16	3.14	440.56	27.535	113.1	29.693
14	13	2.81	394.43	30.341	76.88	21.75
15	12	2.38	334.41	27.868	46.53	17.51
16	9	2.29	321.8	35.756	58.85	14.836
13	9	1.79	250.59	27.843	67.05	20.709
19	11	1.28	179.86	16.351	47.86	13.35
12	9	1.19	167.03	18.559	57.18	17.234
18	7	0.72	100.4	14.343	51.98	18.208
20	163	0	4457.37	27.346	195.3	29.072

SITE	16					
CL	No.	%ofDep	TOTAL	AVG	MAX	S.D.
7	58	14.59	2236.6	38.562	254.14	55.72
9	61	11.1	1701.24	27.889	216.22	43.099
11	68	10.87	1665.93	24.499	123.19	27.446
1	31	7.71	1181.38	38.109	155.75	38.107
6	64	7.62	1168.07	18.251	127.33	20.374
5	47	7.22	1105.85	23.529	123.19	33.177
8	37	5.92	907.18	24.518	159.77	28.676
10	36	5.14	788.44	21.901	103.09	20.814
4	17	4.79	733.61	43.154	107.48	33.154
2	29	4.32	662.34	22.839	59.58	14.161
3	17	3.67	563.11	33.124	94.51	31.03
19	17	3.13	480.13	28.243	79.63	26.77
16	10	2.61	399.33	39.933	94.51	26.184
17	13	2.39	366.08	28.16	78.89	26.887
15	9	2.36	362.03	40.226	78.27	26.732
14	11	2.3	352.22	32.02	94.51	26.869
12	16	1.81	276.97	17.311	77.96	21.343
13	7	1.4	213.98	30.569	61.08	22.702
18	7	1.05	161.42	23.06	61.08	19.623
20	165	0	5373.42	32.566	254.14	41.579

SITE	17					
CL	No.	%ofDep	TOTAL	AVG	MAX	S.D.
6	74	17.93	2403.38	32.478	135.2	28.669
7	47	10.53	1411.58	30.034	88.33	29.137
9	52	9.88	1324.33	25.468	84.72	21.505
11	52	8.32	1114.81	21.439	76.86	17.428
10	30	6.96	932.88	31.096	113.02	27.888
5	38	6.92	927.35	24.404	97.46	22.599
8	35	6.61	885.78	25.308	80.94	23.077
1	27	5.23	700.9	25.959	85	17.977
4	14	5.01	670.91	47.922	126.04	32.045
2	17	3.78	506.34	29.785	94.17	26.456
19	21	3.57	479.05	22.812	81.57	18.538
14	12	3.15	422.86	35.238	68.46	19.949
16	11	2.39	320.54	29.14	59.97	14.742
15	12	2.31	310.12	25.843	59.97	14.612
17	12	2.28	305.41	25.451	97.46	30.809
3	12	2.01	269.08	22.423	47.9	13.533
13	8	1.21	162.12	20.265	46.63	12.927
18	9	1.17	156.65	17.406	30.33	8.119
12	10	0.75	100.12	10.012	29.57	9.429
20	151	0	3893.04	25.782	96.17	22.375

SITE	18					
CL	No.	%ofDep	TOTAL	AVG	MAX	S.D.
9	68	17.95	2504.82	36.836	145.26	35.551
6	74	16.62	2319.08	31.339	126.02	27.616
7	57	16.35	2281.78	40.031	135.46	34.781
8	35	9.54	1331.78	38.051	156.28	39.16
5	38	7.42	1035.05	27.238	106.03	26.236
19	26	7.11	992.43	38.17	130.02	30.397
14	16	3.68	512.95	32.059	87.08	23.176
10	28	2.9	404.95	14.463	51.92	13.294
11	29	2.75	384.26	13.25	75.89	15.53
4	10	2.72	379.44	37.944	72.39	27.4
1	19	2.33	324.57	17.083	40.79	13.605
16	10	2.16	301.18	30.118	73.88	20.043
3	16	1.67	233.3	14.581	31.03	9.34
2	13	1.63	227.7	17.515	53.45	12.952
15	8	1.33	185.1	23.138	44.68	12.481
17	12	1.31	183.29	15.274	33.01	10.35
18	4	1.18	164.09	41.022	111.19	47.472
13	7	0.82	114.54	16.363	56.06	18.794
12	5	0.53	73.43	14.686	57.11	23.794
20	160	0	5132.71	32.079	159.37	33.882

SITE	19					
CL	No.	%ofDep	TOTAL	AVG	MAX	S.D.
6	63	27.16	1999.28	31.735	106.62	27.301
9	57	23.11	1701.4	29.849	145.26	33.868
7	44	14.57	1073.04	24.387	135.46	29.394
8	29	10.61	781.02	26.932	120.28	35.05
5	21	7	515.66	24.555	69.57	22.898
19	18	5.86	431.7	23.983	74.16	20.769
11	11	1.96	144.45	13.132	75.89	21.185
4	6	1.88	138.05	23.008	57.03	23.856
14	3	1.56	115.15	38.383	85.03	42.413
10	11	1.27	93.14	8.467	24.41	8.068
1	4	1.1	81.24	20.31	26.5	11.031
2	7	1.06	78.12	11.16	28.29	11.871
3	7	0.86	62.95	8.993	32.17	11.389
17	6	0.74	54.73	9.122	24.41	8.495
16	2	0.71	52.2	26.1	27.98	2.659
12	2	0.26	19.29	9.645	17.38	10.939
18	2	0.18	12.99	6.495	11.38	6.908
13	2	0.06	4.33	2.165	3.51	1.902
15	1	0.05	3.65	3.65	3.65	0
20	99	0	1859.52	18.783	121.66	21.779

SITE	20					
CL	No.	%ofDep	TOTAL	AVG	MAX	S.D.
7	71	16.44	2670.1	37.607	151.18	39.701
11	86	16.3	2647.88	30.789	233.2	40.89
6	74	15.08	2448.57	33.089	264.74	54.4
9	66	11.92	1935.92	29.332	150.27	28.83
5	43	8.17	1326.61	30.851	227.74	42.302
8	49	7.52	1221.64	24.931	125.36	29.064
10	44	4.91	796.83	18.11	93.31	20.992
1	34	4.21	683.04	20.089	106.27	26.842
12	35	4.19	680.22	19.435	67.84	21.604
19	21	3.1	504.25	24.012	110.01	27.256
17	17	1.67	270.79	15.929	61.67	20.752
16	10	1.34	217.95	21.795	93.31	28.287
3	21	1.29	209.74	9.988	63.72	13.247
4	14	1.22	198.46	14.176	69.39	19.714
2	12	0.98	159.63	13.303	40.12	11.309
14	9	0.56	90.68	10.076	19.16	6.289
18	12	0.47	75.75	6.313	22.72	6.762
15	8	0.42	68.73	8.591	14.44	3.954
13	8	0.21	33.62	4.203	9.53	3.26
20	181	0	4810.84	26.579	151.18	28.728

SITE	21					
CL	No.	%ofDep	TOTAL	AVG	MAX	S.D.
7	65	16.18	3248.21	49.972	255.09	60.174
9	74	14.25	2861.77	38.673	255.09	42.096
11	79	13.26	2662.01	33.696	216.03	32.821
6	78	12.78	2566.08	32.898	255.09	42.433
5	45	11.41	2289.95	50.888	230.9	52.327
1	33	6.91	1386.54	42.016	174.88	42.662
8	44	5.71	1145.87	26.043	124.7	32.513
10	38	5.43	1089.85	28.68	174.88	30.082
4	13	3.55	713.23	54.864	295.54	83.919
12	29	2.38	478.23	16.491	51.43	14.245
16	9	1.63	328.14	36.46	174.88	52.703
3	21	1.52	305.31	14.539	52.3	13.961
17	14	1.27	254.97	18.212	63.81	18.442
2	17	1.07	215.81	12.695	40.27	12.085
19	17	0.92	184.28	10.84	28.88	9.371
14	9	0.69	139.14	15.46	42.07	13.354
18	12	0.64	128.25	10.687	62.94	16.918
15	5	0.28	56.02	11.204	26.95	10.719
13	5	0.11	22.93	4.586	9.24	3.384
20	185	0	8019.24	43.347	419.5	61.703

SITE	27					
CL	No.	%ofDep	TOTAL	AVG	MAX	S.D.
6	83	21.07	3502.05	42.193	257.77	42.839
9	67	14.94	2483.48	37.067	265.19	40.573
11	63	14.22	2363.91	37.522	265.19	46.135
5	47	14.21	2361.19	50.238	178.57	45.409
7	53	6.98	1160.56	21.897	90	18.766
10	38	6.19	1029.34	27.088	142.58	29.25
1	25	6.14	1020.29	40.812	142.58	38.687
8	32	3.23	536.45	16.764	78.21	18.639
3	20	2.47	410.71	20.536	69.39	17.61
2	15	2.21	367.11	24.474	58.46	19.959
17	13	1.92	319.38	24.568	72.1	26.25
4	14	1.91	317.73	22.695	68.71	21.186
12	16	1.35	225.07	14.067	58.87	15.713
18	11	0.85	140.45	12.768	38.91	14.1
14	9	0.75	125.06	13.896	24.1	9.052
16	5	0.56	92.95	18.59	56.63	21.37
19	5	0.45	75.51	15.102	31.5	12.733
13	6	0.29	48.35	8.058	13.58	5.453
15	4	0.25	41.09	10.273	13.84	6.233
20	147	0	4906.59	33.378	169.36	28.888

SITE	28					
CL	No.	%ofDep	TOTAL	AVG	MAX	S.D.
9	65	18.9	3940.1	60.617	458.42	75.112
5	48	14.12	2943.62	61.325	391.45	76.565
6	78	12.93	2696.28	34.568	117.02	26.926
7	41	12.55	2616.8	63.824	193.36	58.354
11	68	9.74	2031.65	29.877	180.94	30.52
1	28	5.61	1169.49	41.767	157.2	42.594
10	43	5.31	1106.47	25.732	88.17	22.646
4	14	3.69	769.66	54.976	141.18	41.308
17	18	3.52	733.6	40.756	183.09	47.878
8	19	2.88	599.67	31.562	103.26	32.445
2	15	2.43	507.3	33.82	73.43	19.221
14	14	2.25	469.98	33.57	78.65	20.795
3	12	2.16	451.01	37.584	125.6	32.21
12	8	1.38	286.76	35.845	86.81	35.788
18	9	0.8	166.97	18.552	61.57	18.304
16	6	0.63	130.32	21.72	33.65	11.754
13	8	0.53	110.64	13.83	32.66	9.201
19	4	0.35	73.38	18.345	32.55	9.569
15	5	0.23	47.08	9.416	15.73	6.67
20	138	0	6274.74	45.469	458.42	60.823

APPENDIX D

Site Specific Tables of Total and Percent of Total Precipitation

KEY

No. - Number of times cluster had precipitation
%of Pre - Percent of total precipitation
Total - Total precipitation (cm)
AVG - Average precipitation for wet events only (mgm^{-2})
Max - Maximum precipitation reported (mgm^{-2})
S.D. - Standard deviation of precipitation
the wet events only(mgm^{-2})

SITE	1					
CL	No.	%of Pre	TOTAL	AVG	MAX	S.D.
11	104	18.95	179.41	1.725	16.13	1.986
9	75	12.02	113.74	1.517	5.58	1.411
5	55	8.88	84.06	1.528	6.09	1.393
12	43	8.21	77.67	1.806	4.55	1.411
6	66	6.78	64.19	0.973	4.06	1.027
3	27	6.46	61.17	2.266	4.58	1.265
7	69	6.31	59.74	0.866	5.05	0.897
8	47	5.89	55.78	1.187	5	1.217
1	33	5.06	47.87	1.451	4.39	0.975
10	41	3.92	37.06	0.904	3.55	0.994
19	28	3.77	35.73	1.276	8.38	1.776
2	18	3.52	33.28	1.849	8.25	1.973
16	11	2.69	25.47	2.315	3.81	1.35
17	18	2.57	24.35	1.353	4.11	1.322
14	9	1.88	17.83	1.981	3.35	0.741
15	5	1.02	9.61	1.922	4.19	1.609
4	12	0.74	7	0.583	1.52	0.584
18	12	0.74	6.99	0.582	2.39	0.783
13	6	0.59	5.62	0.937	2.74	0.92
20	179	0	428.41	2.393	19.82	2.478

SITE	2					
CL	No.	%of Pre	TOTAL	AVG	MAX	S.D.
11	79	14.34	105.79	1.339	11.63	1.633
9	80	12.98	95.81	1.198	11.63	1.693
7	70	11.6	85.59	1.223	5.07	1.293
6	67	9.31	68.72	1.026	11.63	1.588
5	48	8.79	64.84	1.351	4.01	1.183
8	43	6.78	50.02	1.163	5.07	1.223
3	27	6.23	45.96	1.702	5.08	1.178
12	30	5.94	43.81	1.46	4.06	1.162
1	28	5.93	43.76	1.563	6.38	1.556
10	37	3.94	29.11	0.787	4.27	0.905
2	16	3.32	24.5	1.531	7.49	1.835
14	14	2.48	18.29	1.306	4.83	1.401
17	14	1.85	13.67	0.976	3.13	0.941
16	10	1.76	13.02	1.302	3.43	1.262
4	13	1.41	10.38	0.798	2.49	0.708
18	16	1.04	7.64	0.478	1.52	0.53
19	23	0.98	7.26	0.316	1.48	0.423
13	4	0.77	5.65	1.413	3.76	1.66
15	9	0.56	4.16	0.462	1.37	0.393
20	207	0	321.48	1.553	13.28	2.195

SITE	4					
CL	No.	%of Pre	TOTAL	AVG	MAX	S.D.
6	83	14.63	117.48	1.415	7.69	1.94
5	66	11.01	88.43	1.34	4.65	1.308
7	73	10.8	86.71	1.188	8.24	1.248
11	92	9.88	79.35	0.863	5.16	1.013
9	77	9.42	75.66	0.983	8.44	1.331
3	28	6.79	54.49	1.946	4.79	1.333
8	38	6.28	50.46	1.328	8.85	1.708
1	35	5.97	47.96	1.37	4.54	1.221
10	47	5.69	45.72	0.973	7.95	1.567
12	34	3.35	26.91	0.791	3.16	0.828
4	16	3.27	26.28	1.642	4.5	1.382
14	18	3.06	24.6	1.367	4.43	1.311
17	23	2.77	22.25	0.967	3.16	0.915
2	25	2.57	20.65	0.826	1.91	0.557
18	18	1.11	8.93	0.496	2.62	0.606
15	10	1.01	8.1	0.81	2.34	0.613
19	10	0.95	7.66	0.766	2.16	0.746
13	12	0.77	6.17	0.514	2.29	0.593
16	9	0.63	5.08	0.564	1.5	0.492
20	205	0	264.87	1.292	6	1.249

SITE	5					
CL	No.	%of Pre	TOTAL	AVG	MAX	S.D.
6	91	17.88	185.49	2.038	11.23	1.947
5	57	10.11	104.84	1.839	9.07	1.838
7	63	9.13	94.75	1.504	9.07	1.452
9	70	7.86	81.51	1.164	5.92	1.112
11	68	7.61	78.98	1.161	4.83	1.235
10	43	7.41	76.86	1.787	7.29	1.778
1	31	7.15	74.16	2.392	8.58	2.025
14	19	6.49	67.28	3.541	7.38	1.807
2	30	4.86	50.39	1.68	4.78	1.509
4	18	3.8	39.45	2.192	9.19	2.201
3	22	3.58	37.16	1.689	4.62	1.251
19	15	3.19	33.13	2.209	4.32	1.576
8	31	3.09	32.01	1.033	3.81	1.081
16	10	2.26	23.45	2.345	5.86	1.628
17	20	2.06	21.38	1.069	5.16	1.177
15	11	1.38	14.34	1.304	2.59	0.954
12	15	0.78	8.1	0.54	2.39	0.573
18	11	0.77	8	0.727	4.09	1.153
13	7	0.58	6.03	0.861	2.08	0.686
20	195	0	383.06	1.964	18.56	2.564

SITE	7					
CL	No.	%of Pre	TOTAL	AVG	MAX	S.D.
6	95	19.08	161.69	1.702	8.94	1.82
7	72	13.36	113.27	1.573	6.35	1.632
11	82	10.54	89.38	1.09	6.48	1.25
5	61	9.93	84.18	1.38	11.91	2.091
1	36	8.15	69.07	1.919	7.87	2.104
9	73	7.97	67.52	0.925	5.08	0.962
10	43	5.27	44.69	1.039	3.4	0.96
3	26	4.23	35.89	1.38	4.17	1.257
14	17	3.87	32.79	1.929	4.32	1.182
17	28	3.18	26.99	0.964	3.81	1.108
8	31	2.99	25.35	0.818	8.05	1.646
2	24	2.35	19.95	0.831	3.17	0.947
12	27	2	16.98	0.629	3.28	0.721
4	12	1.98	16.76	1.397	3.56	1.233
16	11	1.4	11.88	1.08	3.68	1.447
18	17	1.15	9.79	0.576	2.67	0.703
19	8	1.03	8.74	1.092	3.35	1.248
15	7	0.94	7.94	1.134	2.49	0.765
13	9	0.56	4.77	0.53	1.65	0.549
20	195	0	258.24	1.324	7.8	1.201

SITE	8					
CL	No.	%of Pre	TOTAL	AVG	MAX	S.D.
11	91	17.75	181.88	1.999	13.76	2.126
9	80	11.85	121.43	1.518	9.04	1.69
8	57	10.94	112.04	1.966	5.03	1.533
2	31	7.62	78.04	2.517	11.66	2.492
5	42	6.96	71.33	1.698	9.3	1.704
7	47	6.16	63.15	1.344	4.17	1.204
3	25	6.09	62.42	2.497	11.66	2.556
1	35	5.37	55.05	1.573	5.74	1.359
12	30	4.06	41.63	1.388	4.42	1.243
17	21	3.84	39.36	1.874	6.1	1.552
10	26	3.71	38	1.462	8.79	1.858
6	30	2.98	30.48	1.016	6.96	1.596
19	19	2.97	30.39	1.599	3.94	1.254
4	11	2.61	26.75	2.432	7.62	2.794
15	13	2.36	24.2	1.862	7.29	1.983
14	13	1.83	18.71	1.439	2.92	0.961
13	12	1.67	17.14	1.428	7.29	1.945
18	9	0.61	6.24	0.693	3.15	0.982
16	6	0.6	6.17	1.028	3.28	1.16
20	188	0	344.87	1.834	18.71	2.14

SITE	10					
CL	No.	%of Pre	TOTAL	AVG	MAX	S.D.
6	99	20.57	133.98	1.353	8.38	1.683
5	53	12.9	84.02	1.585	8.13	1.402
9	74	11.95	77.8	1.051	3.99	0.942
11	91	11.84	77.09	0.847	5.59	0.908
7	53	8.86	57.72	1.089	4.09	1.066
10	46	6.23	40.6	0.883	4.15	0.836
1	31	5.47	35.62	1.149	5.16	1.092
3	22	4.16	27.08	1.231	3.6	1.207
8	22	3.25	21.14	0.961	4.24	1.182
17	23	2.75	17.93	0.78	3.1	0.693
14	15	2.37	15.44	1.029	2.54	0.768
2	22	2.3	14.95	0.68	1.88	0.507
12	19	2.1	13.67	0.719	2.51	0.569
4	10	2.04	13.29	1.329	4.08	1.166
19	15	1.08	7.02	0.468	1.45	0.361
16	6	0.87	5.64	0.94	1.98	0.859
18	10	0.76	4.93	0.493	1.45	0.474
15	4	0.28	1.8	0.45	0.66	0.203
13	3	0.23	1.47	0.49	0.66	0.294
20	185	0	238.42	1.289	5.26	1.168

SITE	11					
CL	No.	%of Pre	TOTAL	AVG	MAX	S.D.
11	108	13.42	130.73	1.21	7.49	1.396
9	82	12.25	119.37	1.456	7.67	1.738
5	63	11.05	107.59	1.708	6.91	1.61
6	81	9.03	87.97	1.086	5.97	1.141
7	72	9.03	87.92	1.221	6.89	1.359
1	37	7.03	68.49	1.851	7.31	1.534
8	52	6.91	67.3	1.294	6.38	1.577
10	60	6.69	65.2	1.087	6.79	1.236
3	28	5.18	50.42	1.801	5.26	1.503
12	38	3.82	37.22	0.979	5.82	1.176
14	18	2.84	27.65	1.536	6.91	1.74
17	22	2.58	25.13	1.142	3.83	0.978
2	30	2.54	24.72	0.824	1.9	0.558
4	16	1.92	18.71	1.169	3.05	0.913
15	14	1.49	14.51	1.036	3.81	1.044
19	17	1.32	12.9	0.759	3.81	0.939
16	10	1.21	11.77	1.177	4.57	1.318
18	15	1.07	10.46	0.697	4.5	1.097
13	13	0.62	6.01	0.462	2.18	0.576
20	242	0	379.43	1.568	7.85	1.717

SITE	12					
CL	No.	%of Pre	TOTAL	AVG	MAX	S.D.
6	70	21.95	222.48	3.178	33.7	5.688
9	43	11.85	120.17	2.795	33.7	5.053
11	52	11.42	115.74	2.226	7.11	1.955
1	31	9.1	92.22	2.975	9.45	2.186
5	33	6.97	70.61	2.14	8.26	2.271
10	32	6.77	68.64	2.145	9.45	2.365
14	16	5.1	51.65	3.228	9.35	2.577
3	17	3.83	38.81	2.283	9.35	2.367
2	17	3.69	37.36	2.198	8.81	2.145
4	14	3.67	37.18	2.656	8.81	2.342
8	16	3.37	34.19	2.137	6.07	1.91
7	21	3.03	30.68	1.461	6.1	1.586
16	9	3.01	30.55	3.394	9.35	3.222
19	6	1.73	17.53	2.922	6.14	2.094
17	10	1.63	16.48	1.648	3.3	1.089
15	9	1.6	16.27	1.808	6.1	1.75
12	10	0.9	9.12	0.912	2.24	0.893
18	3	0.21	2.16	0.72	1.02	0.267
13	4	0.19	1.88	0.47	0.63	0.17
20	132	0	239.07	1.811	7.09	1.698

SITE	13					
CL	No.	%of Pre	TOTAL	AVG	MAX	S.D.
11	110	20.3	185.43	1.686	11.84	1.964
12	44	10.39	94.91	2.157	6.43	1.903
9	69	8.33	76.07	1.102	6.35	1.37
5	48	6.93	63.33	1.319	6.09	1.366
7	70	6.89	62.92	0.899	4.24	0.953
8	55	6.43	58.69	1.067	5.75	1.222
6	70	6.39	58.39	0.834	4.01	0.9
3	22	5.86	53.5	2.432	6.12	1.632
19	31	5.22	47.7	1.539	7.39	1.899
10	55	5.07	46.32	0.842	5.21	1.126
1	36	4.38	39.97	1.11	4.25	0.919
16	12	3.72	34	2.833	10.5	2.959
17	21	3.29	30.09	1.433	6.23	1.738
2	12	1.5	13.69	1.141	5	1.374
14	7	1.5	13.67	1.953	6.12	2.571
15	5	1.33	12.19	2.438	7.19	2.796
4	14	1.13	10.29	0.735	3.32	0.941
18	15	1.06	9.72	0.648	3.89	1.053
13	6	0.26	2.42	0.403	1.22	0.483
20	199	0	412.02	2.07	11.94	2.694

SITE	14					
CL	No.	%of Pre	TOTAL	AVG	MAX	S.D.
11	79	15.72	156.6	1.982	10.03	2.236
9	68	12.16	121.16	1.782	12.3	2.348
7	53	10.87	108.3	2.043	8.1	2.214
8	55	10.75	107.12	1.948	8.1	1.806
2	32	7.19	71.65	2.239	6.99	1.994
1	30	6.76	67.35	2.245	10	2.29
3	24	6.47	64.47	2.686	10.03	2.849
5	34	5.12	51.04	1.501	6.6	1.742
6	32	4.61	45.88	1.434	6.81	1.962
14	11	3.8	37.82	3.438	9.14	2.711
10	19	3.46	34.49	1.815	12.3	3.336
19	13	3.09	30.76	2.366	6.99	2.204
17	20	2.24	22.28	1.114	6.17	1.339
15	12	1.99	19.82	1.652	5.03	1.269
4	10	1.98	19.72	1.972	4.69	1.523
13	7	1.61	16	2.286	5.86	2.187
12	15	1.54	15.38	1.025	5.03	1.327
16	5	0.44	4.42	0.884	1.27	0.245
18	4	0.18	1.81	0.452	1.02	0.386
20	164	0	330.5	2.015	8.74	2.06

SITE	15					
CL	No.	%of Pre	TOTAL	AVG	MAX	S.D.
11	75	15.51	175.13	2.335	11.76	2.118
9	62	8.77	98.99	1.597	5.62	1.505
6	56	8.74	98.68	1.762	6.35	1.741
1	33	8.11	91.63	2.777	7.44	2.121
2	33	7.84	88.54	2.683	11.76	2.542
8	55	7.66	86.51	1.573	10.32	1.985
5	39	7.28	82.26	2.109	6.5	1.913
10	33	5.34	60.29	1.827	5.94	1.997
3	21	5.16	58.33	2.778	11.59	2.622
7	48	4.32	48.83	1.017	5.87	1.202
14	13	3.99	45.04	3.465	11.59	2.974
17	17	3.89	43.91	2.583	7.7	2.114
4	18	3.26	36.8	2.044	6.3	1.569
16	9	3.16	35.64	3.96	10.08	3.534
15	14	1.9	21.46	1.533	4.14	1.459
19	13	1.68	18.94	1.457	8	2.229
12	11	1.33	15.04	1.367	5.51	1.804
13	10	1.27	14.37	1.437	4.6	1.572
18	7	0.8	8.98	1.283	4.29	1.563
20	183	0	383.42	2.095	13.36	2.156

SITE	16					
CL	No.	%of Pre	TOTAL	AVG	MAX	S.D.
6	66	11.84	157.48	2.386	12.56	2.749
11	70	11.04	146.9	2.099	10.61	2.38
9	63	7.72	102.65	1.629	6.07	1.738
7	60	7.71	102.56	1.709	11.61	2.161
1	34	7.68	102.21	3.006	8.15	2.446
5	50	7.55	100.42	2.008	15.12	2.965
4	17	6.83	90.82	5.342	12.56	4.024
10	43	6.29	83.71	1.947	8.15	2.283
8	42	6.29	83.61	1.991	7.82	2.143
2	29	4.68	62.2	2.145	6.35	1.634
14	15	4.44	59.08	3.939	9.66	3.585
3	21	3.67	48.8	2.324	8.84	2.531
19	18	3.2	42.62	2.368	7.87	2.565
16	10	2.72	36.24	3.624	9.02	2.767
17	16	2.72	36.19	2.262	5.79	1.901
15	10	1.99	26.46	2.646	6.45	2.438
12	16	1.34	17.76	1.11	6.35	1.773
18	9	1.27	16.93	1.881	4.9	1.322
13	8	1.02	13.54	1.692	3.79	1.564
20	186	0	462.86	2.488	17.25	3.145

SITE	17					
CL	No.	%of Pre	TOTAL	AVG	MAX	S.D.
6	87	23.11	274.05	3.15	13.09	2.862
10	37	7.96	94.39	2.551	16.7	3.497
11	58	7.82	92.67	1.598	5.33	1.242
9	61	7.46	88.42	1.45	7.72	1.564
4	17	7.24	85.86	5.051	16.7	4.314
7	49	7.13	84.5	1.724	8.35	1.91
5	44	6.47	76.75	1.744	5.82	1.638
1	30	6.42	76.07	2.536	11.68	2.818
8	41	5.08	60.26	1.47	7.62	1.843
2	20	4.42	52.37	2.619	16.7	3.868
19	21	3.19	37.81	1.8	5.39	1.7
14	13	2.71	32.13	2.472	5.54	1.456
17	15	2.46	29.2	1.947	5.46	1.846
3	13	2.22	26.35	2.027	4.52	1.378
15	15	2.07	24.59	1.639	4.11	1.218
16	11	1.55	18.4	1.673	4.11	1.225
13	9	1.1	13	1.444	3.76	1.389
18	9	0.9	10.71	1.19	2.79	0.743
12	10	0.68	8.08	0.808	3.1	1.11
20	162	0	286.63	1.769	9.45	1.913

SITE	18					
CL	No.	%of Pre	TOTAL	AVG	MAX	S.D.
6	96	19.34	208.89	2.176	10.08	2.321
9	71	17.74	191.62	2.699	13.49	2.763
7	63	14.76	159.44	2.531	14.12	2.543
8	40	9.23	99.71	2.493	9.78	2.384
5	47	6.55	70.78	1.506	5.33	1.545
19	29	5.95	64.27	2.216	9.65	2.413
11	41	4.19	45.3	1.105	6.86	1.314
1	27	3.54	38.2	1.415	5.76	1.487
4	11	3.13	33.81	3.074	9.08	2.862
10	36	3.08	33.29	0.925	2.7	0.856
14	17	2.81	30.3	1.782	4.63	1.427
17	21	2.14	23.1	1.1	4.7	1.527
16	12	1.71	18.46	1.538	4.45	1.322
2	19	1.63	17.59	0.926	3.59	0.951
3	18	1.6	17.31	0.962	4.62	1.101
18	7	1.09	11.76	1.68	8.89	3.198
15	10	0.71	7.65	0.765	1.9	0.607
13	7	0.5	5.38	0.769	2.67	0.912
12	8	0.29	3.15	0.394	2.39	0.807
20	188	0	305.3	1.624	9.91	1.672

SITE	19					
CL	No.	%of Pre	TOTAL	AVG	MAX	S.D.
6	90	26.43	217.13	2.413	9.12	2.314
9	82	19.93	163.74	1.997	13.49	2.755
7	73	14.93	122.71	1.681	14.12	2.285
8	41	8.24	67.73	1.652	7.22	2.033
5	39	7.1	58.35	1.496	4.85	1.31
19	24	4.36	35.84	1.493	5.46	1.253
11	33	3.05	25.07	0.76	6.86	1.306
14	10	2.64	21.69	2.169	4.77	1.598
10	29	2.62	21.56	0.743	2.46	0.814
4	8	2.6	21.4	2.675	9.08	3.705
1	15	2.52	20.67	1.378	5.76	1.917
2	14	1.35	11.11	0.794	3.59	0.922
3	11	1.35	11.09	1.008	2.84	0.857
17	17	1.19	9.75	0.574	2.59	0.685
16	4	0.63	5.16	1.29	2.64	0.914
18	6	0.39	3.18	0.53	1.65	0.606
12	8	0.36	2.93	0.366	1.19	0.375
15	3	0.17	1.38	0.46	1.1	0.557
13	5	0.14	1.15	0.23	0.51	0.221
20	149	0	238.39	1.6	8.15	1.894

SITE	20					
CL	No.	%of Pre	TOTAL	AVG	MAX	S.D.
11	114	19.17	188.25	1.651	8.28	1.475
7	87	11.64	114.28	1.314	8.77	1.278
9	83	9.82	96.47	1.162	8.13	1.316
6	94	9.5	93.3	0.993	4.8	1.203
12	45	8.17	80.23	1.783	7.11	1.459
8	59	6.86	67.41	1.143	9.02	1.576
5	51	5.61	55.07	1.08	4.95	1.071
10	50	5.46	53.64	1.073	5.36	1.187
1	39	5.22	51.24	1.314	3.83	1.142
19	27	3.87	37.99	1.407	3.49	1.037
3	26	3.53	34.7	1.335	3.71	0.849
17	22	2.57	25.24	1.147	5.63	1.301
2	17	2.01	19.77	1.163	4.38	1.319
16	12	1.65	16.25	1.354	3.49	1.026
4	16	1.51	14.82	0.926	5.31	1.298
18	18	1.24	12.18	0.677	2.59	0.654
14	10	0.94	9.25	0.925	1.93	0.665
15	12	0.7	6.87	0.572	1.72	0.409
13	12	0.52	5.15	0.429	1.85	0.516
20	232	0	368.04	1.586	9.02	1.801

SITE	21					
CL	No.	%of Pre	TOTAL	AVG	MAX	S.D.
11	122	16.6	190.93	1.565	7.66	1.433
6	112	10.92	125.59	1.121	7.29	1.259
7	92	9.78	112.51	1.223	6.45	1.153
9	91	9.35	107.51	1.181	7.29	1.136
5	62	9.17	105.5	1.702	7.66	1.478
10	69	9.11	104.82	1.519	14.45	1.965
1	39	6.8	78.21	2.005	6.17	1.371
12	47	5.86	67.39	1.434	5.45	1.156
8	57	4.26	49	0.86	3.99	0.926
3	27	3.89	44.7	1.656	5.1	1.118
2	24	2.31	26.62	1.109	6.07	1.456
17	25	2.26	25.97	1.039	5.24	1.215
4	15	2.05	23.6	1.573	6.37	1.584
18	24	1.75	20.14	0.839	3.62	0.954
19	29	1.7	19.53	0.673	1.99	0.609
16	13	1.62	18.68	1.437	3.73	1.287
14	14	1.23	14.17	1.012	3.4	0.899
13	11	0.73	8.36	0.76	1.6	0.515
15	12	0.62	7.12	0.593	1.65	0.476
20	256	0	416.18	1.626	14.4	1.88

SITE	27					
CL	No.	%of Pre	TOTAL	AVG	MAX	S.D.
11	111	16.24	159.66	1.438	6.05	1.277
6	121	14.77	145.19	1.2	5.84	1.291
9	106	11.77	115.73	1.092	5.82	1.173
5	65	9.94	97.69	1.503	5.84	1.142
10	61	8.3	81.6	1.338	5.52	1.142
1	37	6.9	67.84	1.834	5.36	1.539
7	81	6.57	64.62	0.798	4.19	0.854
3	27	3.84	37.78	1.399	4.11	0.996
12	43	3.78	37.2	0.865	3.27	0.761
2	27	3.49	34.29	1.27	3.82	1.252
17	27	2.84	27.91	1.034	4.06	0.983
8	51	2.84	27.88	0.547	3.13	0.62
4	17	2.37	23.32	1.372	3.83	1.161
14	16	1.82	17.91	1.119	4.51	1.251
18	21	1.58	15.54	0.74	2.82	0.75
16	12	0.99	9.77	0.814	1.71	0.611
19	17	0.82	8.05	0.474	2.44	0.652
15	6	0.65	6.41	1.068	3.21	1.167
13	8	0.48	4.71	0.589	1.53	0.44
20	248	0	281.27	1.134	5.86	1.053

SITE	28					
CL	No.	%of Pre	TOTAL	AVG	MAX	S.D.
6	111	15.33	130.86	1.179	5.17	1.143
9	78	13	111	1.423	9.42	1.622
11	90	11.17	95.38	1.06	5.36	0.95
5	62	10.74	91.66	1.478	8.36	1.505
7	63	9.82	83.79	1.33	6.56	1.465
10	54	6.92	59.04	1.093	4.29	0.964
1	34	6.09	51.97	1.529	6.6	1.622
3	24	4.75	40.54	1.689	5.16	1.198
17	28	3.52	30.07	1.074	5.46	1.131
4	15	3.27	27.89	1.859	4.18	1.245
2	23	3.2	27.34	1.189	3.32	0.853
12	34	2.77	23.67	0.696	2.12	0.626
8	30	2.67	22.79	0.76	3.22	0.933
14	15	2.27	19.34	1.289	2.86	0.823
19	15	1.12	9.52	0.635	2.54	0.802
18	13	1.11	9.44	0.726	1.63	0.422
13	12	1.01	8.64	0.72	1.76	0.569
16	10	0.7	5.94	0.594	1.25	0.547
15	10	0.56	4.78	0.478	2.3	0.675
20	198	0	261.51	1.321	9.42	1.391